

Functions and interactions of homeodomain proteins during development of the spinal cord

Dissertation
zur Erlangung des Doktorgrades
der Mathematisch-Naturwissenschaftlichen Fakultäten
der Georg-August-Universität zu Göttingen

vorgelegt von
Sonja Kriks

aus
Hamel

Göttingen 2006

Die vorliegende Arbeit wurde in der Arbeitsgruppe von Prof. Dr. Martyn Goulding in der Abteilung Molecular Neurobiology des Salk Institutes For Biological Studies in La Jolla, USA angefertigt.

D7

Referent: Prof. Dr. Michael Kessel

Korreferent: Prof. Dr. Sigrid Hoyer-Fender

Tag der mündlichen Prüfung:

Table of Contents

List of abbreviations	VII
1 Introduction	1
1.1 Basic anatomy and function of the spinal cord.....	1
1.2 The dorsal horn of the spinal cord	2
1.3 Early development of the spinal cord.....	3
1.4 The Notch signaling pathway of lateral inhibition in neural development.....	6
1.5 Dorso-ventral patterning.....	8
1.5.1 Ventral patterning	8
1.5.2 Dorsal patterning	11
1.5.2.1 Early patterning of the dorsal neural tube.....	11
1.5.2.2 The molecular basis of dorsal cell type specification.....	12
1.5.2.3 Interneuron development in the dorsal spinal cord (early phase)	14
1.5.2.4 Interneuron development in the dorsal spinal cord (late phase)	16
1.6 The role of transcription factors expressed in neuronal progenitors in the dorsal spinal cord.....	18
1.6.1 basic Helix-Loop-Helix (bHLH) proteins.....	18
1.6.2 Homeodomain proteins	21
1.6.2.1 The role of Gsh1/2 in neuronal development	21
1.6.2.1.1 The role of Ind, the Drosophila homolog of Gsh1/2, in neuronal development.....	21
1.6.2.1.2 Gsh1/2 function in the brain	22
1.6.2.1.3 The role of Gsh1/2 in the embryonic spinal cord	23
1.7 Aim.....	25
2 Material and Methods	27
2.1 Material.....	27
2.1.1 Equipment.....	27
2.1.2 Chemicals.....	27

2.1.3	Supplies	28
2.1.4	Detergents.....	28
2.1.5	Enzymes, antibiotics.....	28
2.1.6	Commercial kits.....	28
2.1.7	Antibodies	29
2.1.7.1	Primary antibodies	29
2.1.7.2	Secondary antibodies.....	30
2.1.8	Vectors	30
2.1.9	DNA molecular weight marker.....	30
2.1.10	Buffers and stock solutions	30
2.1.11	Cultures to grow bacteria	31
2.1.12	Organisms	32
2.1.12.1	Bacteria.....	32
2.1.12.2	Chicken eggs	32
2.1.12.3	Mice.....	32
2.2	Molecular biology methods	33
2.2.1	General methods for working with DNA	33
2.2.2	Concentration measurement of nucleic acids	33
2.2.3	Restriction digest of DNA	33
2.2.4	Dephosphorylation of plasmid DNA	34
2.2.5	Agarose gel electrophoresis.....	35
2.2.6	Isolation of DNA fragments from agarose gels.....	36
2.2.7	Ligation of DNA fragments into plasmids	36
2.2.8	Amplification of plasmid DNA in bacteria	37
2.2.8.1	Production of competent <i>E.coli</i> cells	37
2.2.8.2	Transformation of competent XL1-Blue <i>E.coli</i> bacteria with plasmid DNA	37
2.2.8.3	Blue-white selection	38
2.2.8.4	Mini-preparation of plasmid DNA	38
2.2.8.5	Midi-preparation of plasmid DNA	39
2.2.9	Preparation of genomic DNA.....	40
2.2.10	Preparation of total RNA from spinal cord tissue	41
2.2.11	Ethanol precipitation of DNA	41
2.2.12	Phenol/chloroform extraction of DNA.....	41
2.2.13	Making cDNA using reverse transcriptase	42

2.2.14	Polymerase chain reaction (PCR)	43
2.2.14.1	Designing of primers	43
2.2.14.2	PCR to amplify from cDNA.....	44
2.2.14.3	Genotyping of knock-out mice.....	45
2.2.15	Sequencing of DNA.....	46
2.3	Developmental and analytical methods	46
2.3.1	<i>In vivo</i> electroporation of chick embryos	46
2.3.1.1	Electroporation at E3.....	46
2.3.1.2	Electroporation at E6.....	47
2.3.2	Anterograde labeling of primary afferent fibers using Dil	47
2.3.3	Injection of 5-bromo2'-deoxy-uridine (BrdU) into pregnant mice.....	48
2.3.4	Preparation of mice embryos	48
2.3.5	Embedding of embryos	48
2.3.6	Dissecting out spinal cords.....	49
2.3.7	Sectioning of tissue using a cryostat	49
2.3.8	Sectioning of tissue using a vibratome	49
2.3.9	Preparation of hybridoma supernatant	50
2.3.9.1	Initiation and maintenance of cell culture	50
2.3.9.2	Getting the supernatant.....	50
2.3.9.3	Making cell stocks	50
2.3.10	Immunohistochemical staining of tissue sections	51
2.3.11	Alternative staining procedures for some antibodies	51
2.3.11.1	Staining using an antibody against BrdU	52
2.3.11.2	Staining using an antibody against NICD	52
2.3.12	<i>In situ</i> hybridization	53
2.3.12.1	<i>In situ</i> hybridization using digoxigenin-labeled antisense probes	53
2.3.12.1.1	Labeling of antisense probes with digoxigenin	53
2.3.12.1.2	Pretreatment and hybridization.....	54
2.3.12.1.3	Incubation of anti-DIG antibody	55
2.3.12.1.4	Color reaction	55
2.3.12.2	<i>In situ</i> hybridization using radioactive-labeled antisense probes	56
2.3.12.2.1	Labeling of antisense probes with S-35.....	56

2.3.12.2.2	Pretreatment and hybridization.....	57
2.3.12.2.3	Post-hybridization washes	59
2.3.12.2.4	Exposure and development.....	59
2.3.12.2.5	Photography	60
3	Results.....	61
3.1	Functional analysis of Gsh1	61
3.1.1	Generation of <i>Gsh1</i> ^{-/-} mice embryos.....	61
3.1.2	Analysis of <i>Gsh1</i> ^{-/-} spinal cords	63
3.1.3	Analysis of postmitotic IN populations in the spinal cord of <i>Gsh1/2</i> ^{-/-} embryos	66
3.1.4	Analysis of dorsal IN progenitors in <i>Gsh1/2</i> ^{-/-} embryos.....	69
3.2	Functional analysis of bHLH factors expressed in dorsal interneuron progenitors	72
3.2.1	Functional analysis of Mash1	72
3.2.1.1	Genotyping of <i>Mash1</i> ^{-/-} embryos	73
3.2.1.2	Analysis of <i>Mash1</i> ^{-/-} spinal cords	74
3.2.1.3	Changes in transcription factor expression in dorsal IN progenitors of <i>Mash1</i> ^{-/-} spinal cords	77
3.2.1.4	Gain-of-function analysis of <i>Mash1</i>	79
3.3	Misexpression of Gsh2	83
3.4	Functional analysis of Ngn1	85
3.4.1	Gain-of-function analysis of Ngn1.....	85
3.4.1.1	Cloning of a full-length <i>Ngn1</i> cDNA	85
3.4.1.2	Electroporation of Ngn1 into the chick spinal cord	86
3.4.2	Loss-of-function analysis of <i>Ngn1/2</i>	87
3.5	The two late-born interneuron populations arise from Gsh1/2 positive progenitors.....	89
3.6	Analysis of <i>Gsh1/2</i>^{-/-} spinal cords at E12.5, when late-born INs are being born	91
3.7	<i>Gsh1/2</i>^{-/-} embryos show a respecification from excitatory to inhibitory interneurons in the dorsal horn.....	99
3.8	Expression of Mash1, Ngn1 and Ngn2 in the vz of <i>Gsh1/2</i>^{-/-} spinal cords.....	101

3.9	Functional analysis of <i>Ngn1</i> and <i>Ngn2</i>	103
3.9.1	Overexpression analysis of <i>Ngn1</i> in the chick spinal cord	103
3.9.2	Gain-of-function analysis of <i>Ngn2</i>	105
3.9.3	Gain-of-function analysis of <i>Ngn1/2</i>	107
3.10	Loss-of-function analysis of <i>Mash1</i>	108
3.11	Misexpression analysis of <i>Mash1</i> in E6 chick spinal cords	113
3.12	Overexpression of a transcriptional activator and repressor form of <i>Mash1</i>	115
3.13	Progenitor gene expression during early and late phases of dorsal interneuron development	122
3.14	<i>Ptf1a</i> misexpression analysis	129
3.14.1	Cloning of <i>Ptf1a</i> full-length coding sequence.....	129
3.14.2	Misexpression analysis of <i>Ptf1a</i> in the chick spinal cord	130
3.15	Analysis of Notch signalling in spinal cords of <i>Gsh1/2^{-/-}</i> and <i>Mash1^{-/-}</i> embryos	132
3.16	Analysis of <i>Presenilin1^{-/-}</i> and <i>Delta1^{hypo/-}</i> embryos	136
3.17	Overexpression analysis of <i>Dll1</i>	139
3.18	<i>Gsh1/2^{-/-}</i> embryos show a defect in the anatomy of the dorsal horn	141
4	Discussion	145
4.1	The role of <i>Gsh1</i> and <i>Gsh2</i> in patterning dorsal progenitors in the developing spinal cord	145
4.1.1	<i>Gsh1</i> and <i>Gsh2</i> are necessary for the specification of two types of early-born interneurons.....	146
4.1.1.1	<i>Gsh1</i> and <i>Gsh2</i> are obligate determinants for <i>dl3</i> and <i>dl5</i> neurons	146
4.1.1.2	Cross-repressive interactions between homeodomain transcription factors do not operate in dorsal spinal progenitors	147
4.1.1.3	<i>Gsh1/2</i> function in regulating the expression of bHLH factors, which are the primary determinants of dorsal interneuron fate	150
4.1.2	<i>Gsh1/2</i> and <i>Mash1</i> play a role in the specification of late-born neurons	153

4.2	Mash1 acts cell-autonomously as well as non-cell-autonomously in the specification of late-born neurons	154
4.3	Changes between early and late neurogenesis in the spinal cord	158
4.4	Relationship between early-born versus late-born sensory neurons.....	160
4.5	Comparison of Gsh1 and Gsh2 function in the spinal cord and telencephalon.....	161
4.6	Concluding remarks.....	163
5	Summary.....	165
6	References.....	166
7	Appendix.....	184
7.1	Primer sequences	184
7.1.1	Primers used for genotyping of KO mice.....	184
7.1.2	Vector-specific primers.....	185
7.1.3	Primers for cloning	185
7.2	Sequences of cloned cDNAs.....	186
7.2.1	Ngn1 sequence	186
7.2.2	Ptf1a sequence	187
8	Acknowledgements.....	188
	Lebenslauf	189

Abbreviations

A	adenine
Amp	ampicillin
A-P	anterior-posterior
ATP	adenosine triphosphate
bHLH	basic helix-loop-helix
BMP	bone-morphogenetic-proteins
C	cytosine
ch	chick
CNS	central nervous system
cpm	counts per minute
CTP	cytosine triphosphate
°C	degrees Celsius
Da	Dalton
DEPC-H ₂ O	diethylpyrocarbonate-H ₂ O
dI	dorsal interneuron
DIG-RNA	digoxygenin-labeled RNA
dIL	late-born dorsal interneuron
DNA	deoxyribonucleid acid
dNTP	deoxyribonucleotide triphosphate
DRG	dorsal root ganglion
DV	dorso-ventral
E	embryonic day
EtOH	ethanol
FGF	fibroblast growth factor
Fig	figure
G	guanine
GABA	gamma-aminobutyric acid
GTP	guanosine triphosphate
GOF	gain-of-function
h	hour(s)
HD	homeodomain
IN	interneuron
kb	kilo base
KO	knock-out
l	liter
LB	Luria Broth
LGE	lateral ganglionic eminence
LOF	loss-of-function
max.	maximal
MGE	medial ganglionic eminence
MCS	multiple cloning site
MN	motor neurons
ms	mouse
μ	micro
NICD	intracellular domain of Notch
OD	optical density
PBS	phosphate-buffered saline
PBT	phosphate-buffered saline with Triton
PCR	polymerase chain reaction

PFA	paraformaldehyde
PNS	peripheral nervous system
RA	retinoic acid
rab	rabbit
RNA	ribonucleic acid
rpm	rounds per minute
RT	room temperature
Shh	Sonic hedgehog
T	thymine
TAE	Tris-acetate-EDTA
T _{ann}	annealing temperature
TGFβ	transforming growth factorβ
T _m	melting temperature
Tris	Tris(hydroxymethyl)-aminoacetate
U	units
UTP	uridine triphosphate
VIAAT	vesicular inhibitory amino acid transporter
vol	volume
vz	ventricular zone
wt	wild type
x g	times gravity

1 Introduction

1.1 Basic anatomy and function of the spinal cord

The spinal cord constitutes the most caudal component of the central nervous system (CNS). In addition to receiving and processing sensory information from the skin, joints and muscles of the limbs and trunk of the body, it also regulates limb and trunk movements. The spinal cord contains many neurons, including preganglionic motor neurons that activate the sympathetic nervous system.

The adult spinal cord is composed of a core region of gray matter surrounded by white matter tracts. In mammals, the adult gray matter has a butterfly-shaped form, which is anatomically subdivided into two bilaterally symmetrical halves comprising of dorsal and ventral horns (see Fig.1). The gray matter, which is derived from the embryonic mantle zone, is mainly composed of neuronal cell bodies and associated glia. These neurons are organized into ten anatomical distinct laminae (Rexed, 1952). The neurons in the dorsal and ventral horns have functionally different roles. The ventral horn contains locomotor interneurons and motor neurons, whose axons exit the spinal cord through the ventral roots and innervate skeletal muscles. Neurons in the ventral horn are primarily dedicated to controlling efferent motor outputs. Dorsal horn interneurons process and gate somatosensory information that is carried by afferent sensory axons that terminate on them. These neurons integrate sensory information from the periphery and then relay it to other regions of the CNS, including the brainstem and thalamus (Gillespie and Walker, 2001; Julius and Basbaum, 2001). Dorsal sensory interneurons that respond to cutaneous stimulation also modulate spinal cord reflexes (Schmidt and Thews, 1983).

The white matter is composed of both ascending and descending tracts of myelinated nerve fibers. Many of the axons in these tracts are from neurons that project over multiple spinal cord segments, or are ascending/descending tracts that connect the spinal cord to other regions of the CNS. These axon tracts are localized within three funiculi: the dorsal funiculus, which is positioned between the dorsal horn gray matter; the left and right lateral funiculi that lie between the dorsal and ventral root entrances, and the ventral funiculus, which is found between the sulcus at the ventral midline and the ventral root.

1.2 The dorsal horn of the spinal cord

The dorsal horn of the spinal cord is the primary receptive field for somatosensory information that is transduced by sensory neurons in the peripheral nervous system (PNS). In higher mammals, five distinct laminae (I-V) can be distinguished within the dorsal horn by differences in their cytoarchitecture. These laminae differ from each other in size, shape and relative numbers of the neurons contained within them (Rexed, 1952; Brichta and Grant, 1985). Lamina I is very thin and is localized along the dorsal edge of the dorsal horn. It can be discriminated from the ventrally adjacent lamina II by the presence of a few large marginal cells (Waldeyer cells), however most of the cells in this layer are much smaller. Lamina II, which is also referred to as substantia gelatinosa, is localized just ventral of lamina I and can be subdivided into two parts, lamina II_{outer} and lamina II_{inner}. The outer part is densely packed with neurons, whereas the inner subdivision is more cell sparse. The primary identifying characteristic of the substantia gelatinosa is its relatively low number of myelinated fibers. Lamina III also contains small diameter cells that are tightly packed. It lies between lamina II_{inner} and lamina IV, which is broader and contains larger neurons than the laminae described above. Even larger cells are found in lamina V. Laminae IV and V are often referred to as the deep layers of the dorsal horn, whereas laminae I, II and III constitute the superficial layers of the dorsal horn (Willis and Coggeshall, 1991).

Each of the dorsal laminae receives differing types of input from afferent sensory fibers. Three types of sensory fibers innervate the dorsal horn: 1) Nociceptive fibers that transmit pain. These afferent fibers can be separated into two main groups, A δ and C fibers. A δ fibers have small diameter axons and a thin myelin sheath, whereas C fibers are not myelinated. These nociceptive fibers terminate predominantly in lamina I and lamina II_{outer}. 2) Medium diameter mechanoreceptive fibers (A β fibers), which are myelinated, transmit stimuli, such as touch and sound. These axons terminate on interneurons in laminae II_{inner}, III and IV. The third type of primary afferent fibers consists of large diameter proprioceptive fibers. They transmit information that relates to the position of body parts relative to each other. These fibers terminate in the deeper dorsal horn in lamina V on Clarke's column neurons. They also project to motor neurons and other interneurons in the ventral horn.

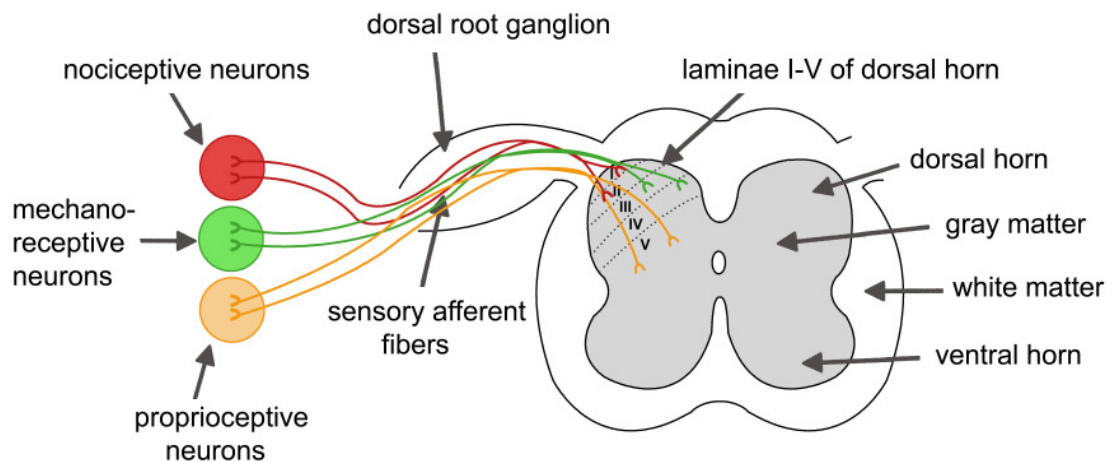


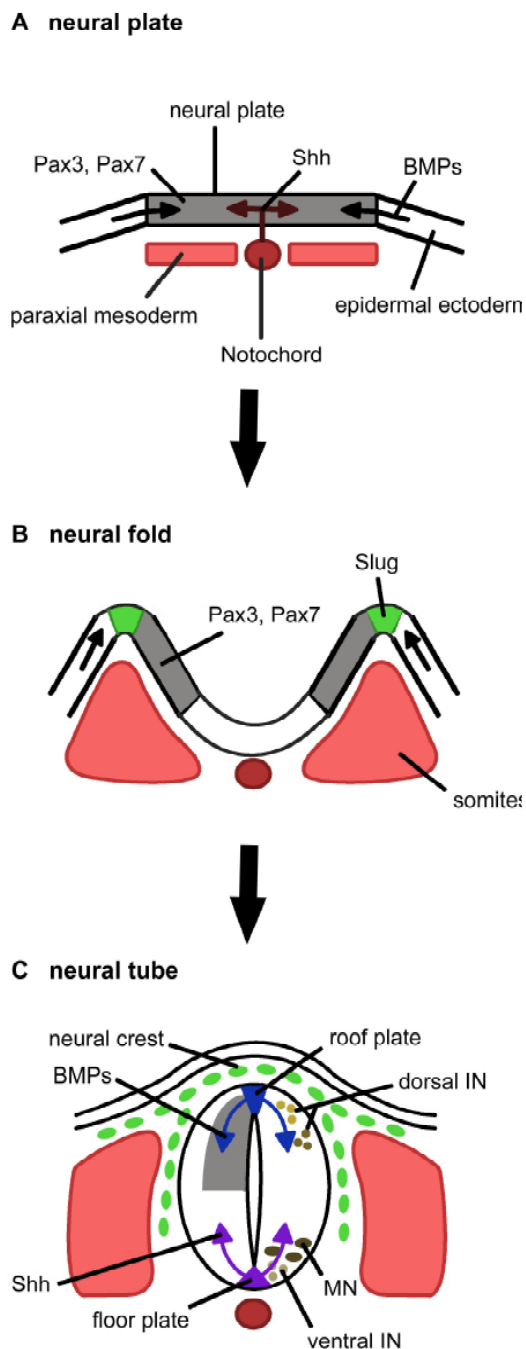
Figure 1: Schematic of the basic anatomy of the adult mouse spinal cord. The spinal cord consists of an internal gray matter surrounded by white matter. The butterfly shape of the gray matter can be anatomically subdivided into two dorsal and two ventral horns. Neurons in the dorsal horn differ by size and shape and can be divided into five distinct laminae according to their cytoarchitecture. Each lamina receives different input from sensory afferent fibers. Three types of primary afferent fibers enter the dorsal horn of the spinal cord through the dorsal root ganglion: nociceptive fibers (red) make connections with neurons in laminae I and II; mechanoreceptive fibers (green) connect to laminae III and IV neurons and proprioceptive fibers (yellow) terminate in lamina V.

1.3 Early development of the spinal cord

The formation of the nervous system begins with neural induction, the process by which dorsal ectodermal cells of the gastrula-stage embryo are directed towards a neural identity. The induction of neural tissue in response to signals from the underlying mesoderm was first defined by experiments undertaken by Spemann and Mangold (1924) in which they described the presence of an organizer region in the early embryo that functions instructively to generate a new neural axis. However, it was not until the mid-90's that the factors responsible for the neural-inducing activity of Spemann's "organizer" were identified. It is now known that the bone morphogenetic proteins (BMPs) and the transforming growth factor β (TGF β) inhibitors Noggin, Chordin and Follistatin,

which are secreted by the organizer, act on the overlying dorsal ectoderm to block this BMP signaling, leading to the formation of the neural plate (Smith and Harland, 1992; Sasai et al., 1994; Hemmati-Brivanlou et al., 1994). Conversely, BMP-mediated signaling in the dorsal ectoderm promotes a non-neural fate (Wilson and Hemmati-Brivanlou, 1995). Initially, the neural plate is thought to have an anterior character, as the inhibition of BMP signaling by BMP inhibitors induces the expression of anterior marker proteins, but not of posterior markers and is therefore referred to as the anterior groundstate of the CNS. To develop a more posterior character, such as the spinal cord, this anterior groundstate is modified by posteriorizing signals (Nieuwkoop, 1952; Muhr et al., 1997). Retinoic acid (RA), members of the fibroblast growth factor (FGF) and Wnt families, as well as GDF11, all contribute to this posteriorizing activity (Cox and Hemmati-Brivanlou, 1995; Doniach et al., 1995; McGrew et al., 1995; Blumberg et al., 1997; Bang et al., 1997; 1999; Liu et al., 2001).

Subsequently, the neural plate undergoes convergence-extension to form an elongated structure that then folds along the ventral midline (Keller, 2002). In a process known as neurulation in amphibians, birds and mammals, the progressive folding and fusion of the dorsal edges of the neural plate leads to the formation of a hollow tube called the neural tube (Fig. 2). For a more detailed explanation of the figure see also 1.5.2. In contrast, the neural tube in zebrafish is formed by cavitation.



adapted from Lee and Jessell, 1999

Figure 2: Schematic of inductive signals during neurulation and generation of neural cell types during spinal cord development.

(A) Neural plate stage: the spinal cord develops from the neural plate, which is overlying the notochord and paraxial mesoderm. The neural plate is flanked by epidermal ectoderm. The generation of different spinal cell types is controlled by the combination of ventralizing and dorsalizing signals. Sonic hedgehog (Shh, brown arrows) functions as a ventralizing signal and is secreted by the notochord. The epidermal ectoderm is a source of dorsalizing BMP signals (black arrows). Pax3 and Pax7 are initially expressed throughout the neural plate (Bang et al., 1997). (B) Neural fold stage: Pax3/Pax7 expressions are maintained dorsally by BMP signaling but repressed ventrally by Shh. BMPs also induce the expression of Slug in premigratory neural crest cells. (C) Neural tube stage: once the neural tube folds (B), its lateral edges fuse to generate the neural tube. As the neural tube closes, neural crest cells (green) leave the dorsal neural tube and migrate either above the somites or between the somites and neural tube. Roof plate cells (blue triangle) are generated at the dorsal midline and are a source of BMP signals (blue arrows), which regulate the differentiation of dorsal interneurons (IN). Distinct populations of ventral INs and motor neurons (MN) are induced by Shh (purple arrows), which is secreted by the floor plate (purple triangle).

The generation of neurons in the developing caudal neural tube exhibits a rostral-caudal gradient of maturation. In the mouse spinal cord, the first neurons to be born are found at hindbrain/cervical levels around E9.0. At this time, the neural tube comprises a simple neuroepithelium of neural progenitor cells that have the potential to generate both neurons and glia. Previous studies have shown that the differentiation of neural progenitors into neurons is controlled by the so-called “proneural” genes, many of which encode basic Helix-Loop-Helix transcription factors (bHLH). Members of these proneural bHLH proteins include neuroD, Ngn1, Ngn2, and Mash1, which also induce the expression of different neuronal genes, thus assigning a specific fate to each cell (Bertrand et al., 2002). As these progenitor cells differentiate, they exit the cell cycle, leave the ventricular zone and migrate laterally, settling in their final positions within the neural tube according to their cell fate. This migration and settling underlies the laminar organization of the mantle zone/gray matter in the mature spinal cord.

Evidence that the proneural bHLH genes play a critical role in neurogenesis has come from overexpression studies in frogs (Kintner, 2002) and from loss of function studies in mice (Bertrand et al., 2002). Mouse mutants for the proneural bHLH factors exhibit defects in neurogenesis due to the loss of specific progenitor populations (Ma et al., 1999; Parras et al., 2002; Bermingham et al., 2001). Some of these mutants also display a premature generation of glial cells, indicating that proneural bHLH factors not only promote neurogenesis but also inhibit gliogenesis (Tomita et al., 2000; Nieto et al., 2001; Sun et al., 2001). The premature initiation of gliogenesis may be in part due to altered signaling via the transmembrane protein Notch, which functions not only to inhibit neural cell differentiation by repressing proneural bHLH gene expression, but also to promote gliogenesis (Gaiano et al., 2000; Morrison et al., 2000).

1.4 The Notch signaling pathway of lateral inhibition in neural development

The Notch signaling pathway plays an important role in the process of maintaining dividing progenitor populations and the subsequent generation of different types of neurons and non-neuronal cells. The Notch pathway was first described in *Drosophila* and is highly conserved throughout the animal kingdom (Knust, 1994; Campos-Ortega, 1994). Notch (including Notch 1, 2 and 3 in

vertebrates) encodes a transmembrane protein consisting of an extracellular domain that binds Delta-like ligands, a transmembrane domain, and an intracellular domain. The extracellular domain binds to the Notch ligands Delta (Dll1, Dll3) and Serrate/Jagged that are expressed on the surface of adjacent cells. Binding of the ligands Delta/Jagged to the Notch extracellular domain leads to the subsequent cleavage and release of the Notch intracellular domain (NICD), which then translocates into the nucleus. The Presenilin family of intramembrane proteases regulates the cleavage of Notch and thus Notch signaling (Kopan, 2002). After NICD is released, it translocates into the nucleus, where it binds to the DNA-binding protein RBPJ- κ , the mammalian homolog of Suppressor-of-Hairless (Su(H)) in *Drosophila*. The complex NICD/RBPJ- κ then activates the transcription of downstream targets such as Hes1 and Hes5 that are homologs of the *Drosophila* Enhancer-of-split [E(spl)] proteins. Hes1 and Hes5, which are the primary targets of Notch signaling, normally function as inhibitors of neuronal fate by repressing the expression of the proneural genes, e.g. Mash1, NeuroD and Ngn1/2 (Lai, 2004; Louvi and Artavanis-Tsakonas, 2006). This process of lateral inhibition results in these proneural genes being expressed in a salt-and-pepper fashion in the neuroepithelium.

The proneural bHLH genes, in addition to promoting neuronal differentiation, are also required for the expression of Delta. As such, cells expressing high levels of Delta are committed to a neuronal cell fate. This high level of Delta expression in turn leads to a high level of Notch signaling in the adjacent cells, which results in the repression of the proneural gene expression in these cells, causing them to remain in an undifferentiated proliferative state. In this way, the Notch signaling pathway of lateral inhibition provides an elegant and powerful way to amplify small differences in the level of Delta and NICD expression between neighboring cells and thereby ensuring that these cells adopt different developmental fates.

1.5 Dorso-ventral patterning

In the developing spinal cord, the position that a progenitor cell occupies along the dorso-ventral axis is the primary determinant of its eventual fate. Several neuronal cell types with distinct fates, such as neural crest cells, motor neurons and multiple types of interneurons are generated in appropriate numbers and at precise positions along the dorso-ventral axis. Each of these cell types expresses a unique combination of cell type determinants, many of which are transcription factors. Based on the expression patterns of these proteins, eight distinct interneuron populations have been described in the dorsal half of the spinal cord (Gross et al., 2002; Muller et al., 2002; Goulding et al., 2002; Caspary and Anderson, 2003), whereas five distinct neuronal cell types can be distinguished in the ventral half (Jessell, 2000; Goulding and Lamar, 2000).

1.5.1 Ventral patterning

Much of what we know about dorso-ventral patterning comes from studies in the ventral neural tube. Early studies show that signals from the ventral midline and the notochord in particular are able to induce ventral cell types in a distance-dependent manner, suggesting that the notochord acts as a source of a morphogen (van Straaten et al., 1989; Yamada et al., 1991). The notochord-derived morphogen is the secreted protein Sonic hedgehog (Shh), a member of the Hedgehog family (Roelink et al., 1995). This protein plays a preeminent determinative role in generating the different neuronal cell types that are present in the ventral spinal cord. At high concentrations, Shh induces the differentiation of the floor plate (Ericson et al., 1996), a small non-neural region in the ventral most part of the spinal cord that also acts as the hinge region for the neural plate during neurulation (Schoenwolf and Smith, 1990). The floor plate, in turn, secretes Shh, which acts over long-ranges to induce ventral interneurons and motor neurons (Placzek et al., 1991; Ericson et al., 1996; Jessell, 2000) at distinct positions in the ventral spinal cord. The addition of Shh to “naive” neural plate explants is also able to induce various ventral cell types in a concentration-dependent manner, indicating that Shh acts as an instructive signal (Ericson et al., 1997a). When Shh is absent, ventral cell types fail to develop, and there is an expansion of the dorsal progenitor domain, which is marked by the expression of Pax3 and Pax7 (Chiang

et al., 1996). These findings indicate that Shh is both essential and sufficient for the induction of neuronal cell types in the ventral half of the developing spinal cord.

The primary mediators of Shh signaling are the Gli zinc-finger proteins. In the mouse, Gli1, Gli2 and Gli3 are all expressed in the neural tube (Hui et al., 1994). Evidence that Gli proteins are the direct targets of Shh signaling comes from studies in *Drosophila* (Chen et al. 1999) and from the observation that Gli1 is able to induce ventral cell types in the spinal cord similar to the effects seen by Shh (Hynes et al., 1997; Ruiz I Altaba et al., 1998). The *Gli1*^{-/-} mice show no defects in neural development; therefore, it is unlikely that Gli1 is the primary downstream effector of Shh (Park et al., 2000). Gli2 is however needed for Shh signaling in the ventral neural tube (Bai et al., 2002). *Gli2*^{-/-} mice lack the floor plate, as well as V3 interneurons, with a concomitant ventral expansion of the adjacent motor neuron (MN) domain, suggesting progenitors that normally experience high level Shh signaling require Gli2. Gli3, the third member of this family is expressed in dorsal and intermediate regions of the neural tube, in contrast to Gli2 expression, which is uniform. Mice lacking *Gli3* show no defects in the ventral spinal cord; however, intermediate regions expand dorsally, resulting in a switch in cell fate in this region (Persson et al., 2002).

Shh/Gli signaling plays a key role in the spatial organization of neurons that arise in the ventral neural tube. This partitioning of the ventral ventricular zone into five progenitor domains is mediated by Class II factors that are induced by Shh and Class I factors that are repressed by Shh. These factors are either homeodomain-containing proteins or bHLH proteins that are members of the Pax, Nkx, Dbx, Irx and Olig families (Briscoe et al., 2000; Goulding and Lamar, 2000; Novitsch et al., 2001), and they are expressed in discrete subsets of progenitors. The concentration-dependent induction/repression of different sets of homeodomain proteins therefore results in broadly restricted progenitor domains in the ventricular zone. For instance, high concentration of Shh near the floor plate induces the expression of the transcription factor Nkx2.2 in progenitors of V3 interneurons (Briscoe et al., 1999). Pax6 is repressed in this domain of the neural tube by high concentration of Shh.

The establishment of sharp boundaries between discrete progenitor domains is accomplished by a cross-inhibitory mechanism in which homeodomain proteins expressed in adjacent progenitor domains repress each other's

expression. These cross-repressive interactions are mediated in part by the recruitment of Groucho-like co-repressors (Muhr et al., 2001). Nkx2.2 and Pax6 mutually repress each other in the ventral neural tube, and this is thought to establish the boundary between the MN progenitor domain and the p3 domain (see Fig. 3). Nkx6.1 is induced at lower concentrations of Shh, and its expression domain extends more dorsally than that of Nkx2.2. Nkx6.1 represses Dbx2 expression in the p2 domain, thus establishing a ventral limit to the p1 domain (Fig. 3). In addition to restricting the expression of each other, these transcription factors also act as transcriptional determinants to direct progenitors to differentiate along particular pathways (Briscoe et al., 1999; Ericson et al., 1997b; Goulding and Lamar et al., 2000). For instance, Dbx1 is required for the initiation of the V0 differentiation program. In mice lacking *Dbx1*, prospective V0 interneurons differentiate as either V1 interneurons or dl6 neurons (Lanuza et al., 2004). Likewise, Nkx2.2 is required for establishing a ventral p3 domain that will give rise to V3 interneurons (Briscoe et al., 1999).

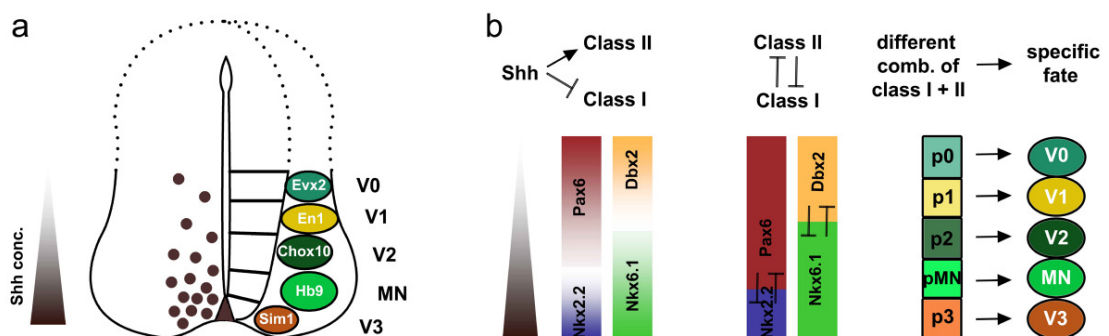


Figure 3: Ventral patterning. (Fig. 2a) A gradient of Sonic hedgehog (Shh) secreted by the floor plate induces five distinct types of neurons (four types of interneurons (IN) (V0, V1, V2, V3) and motor neurons (MN)) in the ventral half of the spinal cord. (Fig. 2b) Different concentrations of Shh induce/repress Class II/Class I proteins, respectively, at different dorso-ventral positions in the ventral half of the spinal cord. These Class I and Class II proteins repress each other, thereby establishing sharp boundaries of expression. Distinct progenitor populations marked by the expression of different combinations of Class I and Class II proteins give rise to five different types of neurons in the ventral spinal cord, each with a specific fate.

1.5.2 Dorsal patterning

1.5.2.1 Early patterning of the dorsal neural tube

Signals from the ectoderm and underlying mesoderm play a prominent role in patterning the neural plate along its prospective dorso-ventral (DV) and anterior-posterior (AP) axes; however, AP patterning will not be discussed in detail here.

The ectoderm and dorsal midline cells play essential instructive roles in patterning cells within the dorsal neural tube. These cells secrete signals, which induce Pax3 and Pax7 expression. This Pax3/7 expression defines a dorsal territory that will give rise to six distinct populations of early-born dorsal interneurons. Msx1/2 and Olig3 are also induced by signals from the dorsal midline in the dorsal-most regions of the ventricular zone.

Early signals that arise from the surface ectoderm and underlying mesoderm specify roof plate cells and the neural crest (Chizhikov and Millen, 2004b). At later times they also act on neural progenitors to generate a number of dorsal cell types that are known as Class A neurons (Lee and Jessell, 1999; Lee et al. 2000; Goulding et al., 2002; Muller et al., 2002, 2005). The roof plate, which develops at the dorsal midline of the neural tube, is composed of specialized glial cells (Altman and Bayer, 1984) and acts as a secondary source of dorsalizing signals to induce the development of Class A neurons. In mouse embryos that lack roof plate cells as a result of their selective ablation with diphtheria toxin under the control of the GDF7 promoter, Class A (i.e. dl1-dl3) neurons are no longer formed (Lee et al., 2000; Muller et al., 2002).

Neural crest cells are the most prominent cell type that arises from the dorsal neural tube (Le Douarin, 1990; Knecht and Bronner-Fraser, 2002). As the neural plate folds and fuses along the dorsal midline, neural crest cells detach from the dorsal rim of the neuroepithelium and migrate either dorsally above the somites to form melanocytes or ventrally between somites and neural tube to form primary sensory and autonomic neurons, a variety of non-neural cells and the glial cells of the peripheral nervous system (see Fig. 2).

1.5.2.2 The molecular basis of dorsal cell type specification

Three different classes of signaling molecules have been implicated in the specification of dorsal cell types in the neural tube. These secreted molecules are members of the FGF-, Wnt- and TGF β families. Studies in *Xenopus* have shown that FGFs are able to induce the differentiation of neural crest cells in neuralized ectodermal cells (LaBonne and Bronner-Fraser, 1998). Further evidence for the ability of FGFs to specify dorsal cell fate comes from overexpression experiments in which a truncated form (dominant negative) of an FGF receptor was ectopically expressed in neural plate cells, which then leads to a failure in generating neural crest cells (Mayor et al., 1997). Both loss-of-function and gain-of-function experiments have outlined a role for Wnt-signaling in specifying dorsal cell types, including the neural crest (Mayor et al., 1995; LaBonne and Bronner-Fraser, 1998). For example, Wnt1 and Wnt3a are expressed by dorsal midline cells, including the roof plate. *Wnt1/3A*^{-/-} mice embryos exhibit a reduction in the number of melanocytes, as well as cranial and sensory neurons (Muroyama et al., 2002). Conversely, co-electroporation of *Wnt1* and *Wnt3a* in *Xenopus* leads to an increase in expression of several neural crest markers, such as Slug and Krox-20 (Saint-Jeannet et al., 1997). Two other members of the Wnt-family, Wnt7B and Wnt8 induce expression of the crest marker Slug when overexpressed in neuralized ectodermal explants (Chang et al., 1998; LaBonne and Bronner-Fraser, 1998). Moreover, Wnt signals from the underlying mesoderm are known to induce Msx1 and Pax3 (Bang et al., 1999), both of which are required for neural crest development (Goulding et al., 1991; Dottori et al., 2001; Monsoro-Burq et al., 2005; Sato et al., 2005). There is also evidence that non-canonical signaling in response to Wnt11 regulates the migration of neural crest cells away from the neural tube (De Calisto et al., 2005).

BMP4, BMP5, BMP7, GDF6/7 and activin-B are all expressed in or adjacent to the roof plate (Liem et al., 1997; 1999; Lee et al., 1998; Lee and Jessell, 1999), where they function to induce the development of dorsal spinal interneurons. Treatment of naive chick neural plate tissue with these TGF β -like molecules leads to the induction of dl1 and dl3 neurons (Liem et al., 1997). In contrast, inhibition of BMP signaling by BMP inhibitors, such as Noggin, or by a conditional inactivation of the BMP receptors 1A and 1B (BMPR1A/1B), blocks dorsal interneuron development, as demonstrated by the loss of the two most

dorsal interneuron populations (Chesnutt et al., 2004; Chizhikov and Millen, 2004; Wine-Lee et al., 2004). Further evidence for the involvement of TGF β molecules comes from the analysis of mice lacking *Gdf7*, which is expressed in roof plate cells (Lee et al., 1998). These animals show a selective loss of the most dorsal population of interneurons (dl1 neurons). Signaling via the activin pathway appears to selectively specify dl3 neurons (Timmer et al., 2005), with overexpression of the activin receptor 1B in the chick neural tube generating excess dl3 neurons without affecting other dorsal cell types (Timmer et al., 2005). This suggests that dorsal progenitors are differentially responsive to the TGF β -like proteins that are secreted by the roof plate and dorsal neuroepithelium. It therefore appears that the combinatorial activity of multiple BMP/TGF β -like molecules is responsible for the patterning of dorsal cell types in the developing spinal cord.

Wnt signaling is also involved in the specification of dorsal cell types in the spinal cord. Two members of the Wnt-family of signaling molecules, Wnt1 and Wnt3a are expressed in the roof plate as soon as the neural tube closes. Each single mutant shows a normal patterning of the dorsal spinal cord. However, *Wnt1/Wnt3a*^{-/-} embryos develop fewer dorsal interneurons with a concomitant increase in more medially located neuron populations (Muroyama et al., 2002).

1.5.2.3 Interneuron development in the dorsal spinal cord (early phase)

The DV patterning signals described activate the expression of cell type specific determinants within the dorsal neuroepithelium. This results in the generation of six populations of dorsal interneurons at specific dorso-ventral positions within the dorsal half of the neural tube. Each of these cell populations expresses a characteristic set of transcription factors (Goulding et al., 2002; Muller et al., 2002; 2005; Caspary and Anderson, 2003). Fig. 4 shows a schematic summary of some of the key transcription factors that define these six early-born interneuron populations (right) and their dividing progenitors (left).

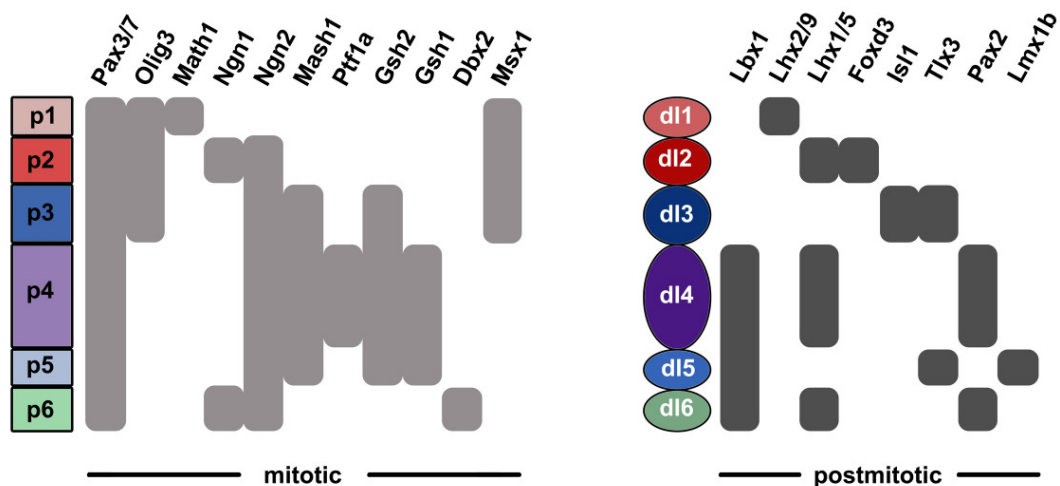


Figure 4: Schematic summary of transcription factors expressed in dorsal interneuron progenitors (p1-p6), as well as in the six types of dorsal postmitotic interneurons (dl1-dl6).

The six early-born cell types that are generated in the spinal cord (E10.0-E11.5 in mouse and E3-E5 in chick) can be subdivided into two major classes of neurons: 1) dorsal relay neurons (dl1-3) and 2) association interneurons (dl4-5). The fate and identity of the dl6 population remains to be determined. Class A dl1-3 relay neurons are dependent upon BMP/TGF β signaling for their generation, while the more ventrally positioned Class B dl4-dl6

neurons are not (Fig. 5). These two major neuronal classes are also delineated by the complementary expression of *Olig3*, a bHLH factor that is expressed in the progenitors of Class A neurons (Muller et al., 2005) and the homeodomain transcription factor *Lbx1*, which is expressed in postmitotic dl4-dl6 neurons. *Lbx1* is also required for the correct specification of Class B neurons, and in mice lacking *Lbx1* these cells adopt the fate of the more dorsally positioned dl2 and dl3 neuronal cell types (Gross et al., 2002; Muller et al., 2002). The molecular pathways that pattern the progenitors of dl4 -dl6 interneurons remain to be discovered. Nonetheless, their downstream effectors are likely to include homeodomain factors such as *Gsh1/2* (Kriks, 2003), *Gbx1* (Waters et al., 2003; John et al., 2005) and the *Ptf1a* bHLH factor (Glasgow et al., 2005).

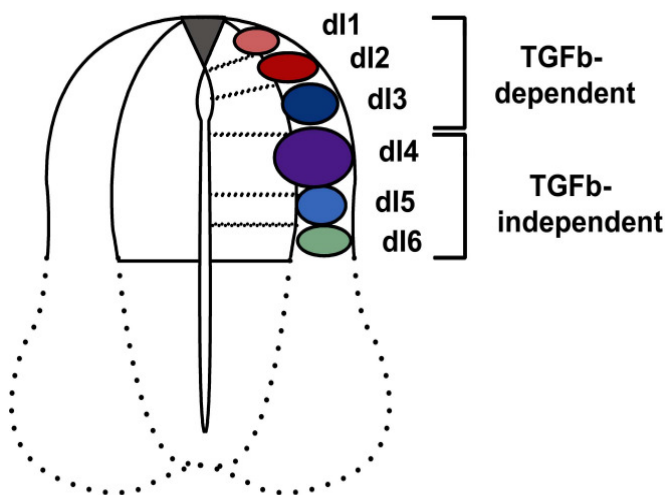


Figure 5: The first wave of neurogenesis in the dorsal half of the spinal cord between E10.0 and E11.5. Six different types of interneurons develop in the dorsal half of the spinal cord (dl1-dl6) between E10.0 and E11.5. The three most dorsal populations (dl1-dl3) develop as relay neurons and are dependent on TGF β -signaling, whereas dl4-6 neurons are association neurons and develop independently of TGF β signals.

1.5.2.4 Interneuron development in the dorsal spinal cord (late phase)

The majority of interneurons that are present in the dorsal horn are generated during a later second wave of dorsal neurogenesis. In the mouse, this phase takes place between embryonic day E12.0 and E13.5, and it is characterized by the co-generation of two neuronal cell types, dIL_A and dIL_B neurons, from a single dorsal progenitor domain, the dIL domain. The cell types found in the superficial laminae of the dorsal horn (laminae I, II III) are almost exclusively derived from dIL_A and dIL_B neurons. These late-born neurons also make a significant contribution to lamina IV and to a lesser extent to lamina V, which constitute the deep dorsal horn. These neurons in the substantia gelatinosa (lamina II) and nucleus propius (lamina III/IV) are association interneurons that project locally within the dorsal horn. As with their early-born dI4 /dI5 counterparts, dIL_A and dIL_B neurons express the transcription factor Lbx1 (Gross et al., 2002; Muller et al., 2002). In addition to Lbx1, dIL_A neurons express the homeodomain transcription factors Pax2 and Lhx1/5, whereas dIL_B neurons are marked by the expression of Lmx1b and Tlx1/3.

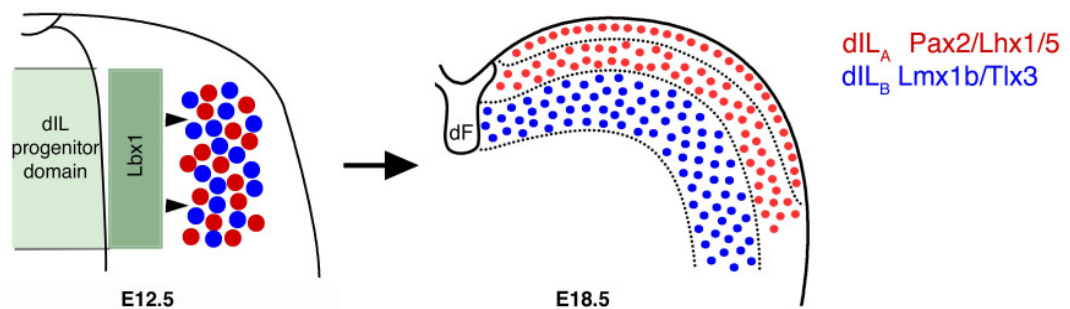


Figure 6: The second wave of neurogenesis in the dorsal half of the spinal cord between E12.0 and E13.5. Two types of late-born neurons (dIL) develop from a single progenitor domain (dIL progenitor domain) in the dorsal half of the spinal cord. Both of these dIL subtypes express the transcription factor Lbx1. However, the dIL_A subtype of late-born neurons expresses also the transcription factors Pax2 and Lhx1/5 (red), whereas the dIL_B subtype expresses Lmx1b and Tlx3 (blue). The dIL neurons are generated in the svz between E12.0 and E13.5, from where they migrate to the dorsal horn. At E18.5 the dIL_B neurons have settled predominantly in the two most superficial laminae, whereas dIL_A neurons have preferentially settled in deeper laminae of the dorsal horn. dF = dorsal funiculus

The two populations of late-born neurons also differ in their function, with dIL_A neurons being inhibitory and utilizing the inhibitory neurotransmitters GABA and glycine, while dIL_B neurons are excitatory and use the neurotransmitter glutamate. Inhibitory GABAergic cells specifically express two genes that encode for the two mammalian forms of glutamic acid decarboxylase, GAD1 and GAD2 (Erlander et al., 1991). Both of these enzymes are required for GABA synthesis from glutamate. Inhibitory neurons also selectively express the vesicular inhibitory amino acid transporter (VIAAT) that loads GABA and glycine into synaptic vesicles (McIntyre et al., 1997). Excitatory glutamatergic neurons in the CNS are marked by the expression of three vesicular glutamate transporters VGluT1-3 (Fremeau et al., 2001; Kaneko et al., 2002). Interneurons in the embryonic spinal cord almost exclusively express VGluT2 (Fremeau et al., 2001; Kaneko et al., 2002), although there are a few neurons in the cord that express VGluT3.

Recent work has deciphered the molecular mechanisms that control the choice between excitatory and inhibitory cell fates in neurons populating the dorsal horn of the spinal cord. These studies reveal that *Tlx1* and *Tlx3* are postmitotic determinants of glutamatergic fate (Cheng et al., 2004). The dorsal horn of *Tlx1/3*^{-/-} embryos shows a complete loss of VGluT2 expression with a concomitant increase in the number of inhibitory neurons. Not only are the *Tlx1/3* genes necessary for excitatory cell fate specification, but they are also sufficient to induce an excitatory over an inhibitory cell fate in the dorsal neural tube (Cheng et al., 2004). *Tlx3*, when misexpressed in the chick spinal cord, actively induces VGluT2 at the expense of GAD1 and VIAAT expression.

While *Tlx1/3* mark excitatory neurons, the paired transcription factor *Pax2* is expressed in postmitotic neurons that are inhibitory. In late-born dorsal interneurons, *Pax2* is required for neurons to acquire an inhibitory cell fate. *Pax2*^{-/-} mice exhibit a loss/reduction in inhibitory neurotransmitter expression in the dorsal horn (Cheng et al., 2004). *Pax2* is, however, unable to induce inhibitory markers when it is misexpressed in the chick spinal cord. Consequently, while *Pax2* is necessary for inhibitory neuron differentiation, it is not sufficient. This finding suggests that additional factors control the specification of inhibitory neurons in the dorsal horn. One such factor is *Lbx1*. Although *Lbx1* is expressed in inhibitory *Pax2*⁺ dIL_A neurons, as well as in excitatory *Tlx3*⁺ dIL_B neurons, the dorsal horn of *Lbx1*^{-/-} embryos exhibits a strong reduction in GABAergic cells with a concomitant increase in glutamatergic neurons, indicating that *Lbx1* promotes

GABAergic differentiation over glutamatergic differentiation. This has led to a model in which Tlx3 functions to promote excitatory neuron development by antagonizing the activity of Lbx1 (Cheng et al., 2005).

1.6 The role of transcription factors expressed in neuronal progenitors in the dorsal spinal cord

A number of transcription factors are expressed in the dorsal neural tube, with some of them being restricted to subsets of dorsal interneuron progenitors. Two prominent classes of transcription factors that are known to pattern spinal cord progenitors are bHLH transcription factors and homeodomain proteins (Jessell, 2000; Goulding et al., 2002; Gowan et al., 2001).

1.6.1 basic Helix-Loop-Helix (bHLH) proteins

The bHLH proteins are identified by the presence of two structural motifs, a Helix-Loop-Helix domain and a basic region that mediates DNA binding. The HLH domain is characterized by two α -helices separated by a loop of variable size. The α -helices mediate protein-protein dimerization, whereas the basic domain is required for DNA binding. Recent studies have outlined important roles for the bHLH proteins in the specification of dorsal interneurons (Helms and Johnson, 2003). Four bHLH proteins, named Math1, Ngn1, Ngn2 and Mash1 are expressed in subsets of dorsal progenitors, where they specify distinct interneuronal differentiation programs. Math1 is expressed by progenitor cells that are adjacent to the roof plate. These cells give rise to the dl1 population of dorsal interneurons, which express the LIM homeodomain transcription factors Lhx2 and Lhx9 (Lee and Jessell, 1999). Mice lacking *Math1* do not generate Lhx2/9-expressing neurons, demonstrating that Math1 is required for the development of dl1 neurons in the dorsal spinal cord (Bermingham et al., 2001).

Ngn1 is expressed in the progenitors that lie immediately ventral to the Math1-expressing progenitor domain. These cells give rise to dl2 neurons and transgenic mice expressing the Green Fluorescent Protein (EGFP) under the control of the *Ngn1* promoter exhibit expression in postmitotic dl2 neurons (Gowan et al., 2001). Although, *Ngn1* null mice do develop dl2 neurons, most

likely as a result of functional compensation by *Ngn2*, *Ngn1/Ngn2*^{-/-} embryos show a complete lack of dl2 neurons. This is seen as a loss of the most dorsal *Lhx1/5*-expressing neurons coupled with a ventral expansion of the *Lhx2/9*⁺ dl1 population (Gowan et al., 2001). *Math1* expression expands ventrally in the *Ngn1/2*^{-/-} cord into the domain, which normally expresses *Ngn1*. It therefore appears that the specification of dl1 and dl2 neurons is controlled by the region-specific expression of the aforementioned proneural bHLH proteins, and the boundary between these two distinct dorsal interneuron progenitor domains is established through cross-inhibitory regulations between *Ngn1/Ngn2* and *Math1* (Gowan et al., 2001).

Mash1 is expressed immediately ventral to *Ngn1* in a progenitor domain that gives rise to dl3, dl4 and dl5 neurons. *Mash1* plays a critical role in specifying neuronal identity in the CNS and in the PNS (Guillemot et al., 1993; Bertrand et al., 2002). A role of *Mash1* in cell type specification was first described in the sympathetic nervous system (Guillemot et al., 1993). Subsequently, *Mash1* has been shown to be important for the development of adrenergic neurons in the locus coeruleus, GABAergic neurons in the basal forebrain (Casarosa et al., 1999; Hirsch et al., 1998) and for the development of a subset of V2 interneurons in the ventral spinal cord (Mizuguchi et al., 2001; Parras et al., 2002). *Mash1* is expressed in a narrow stripe in the ventral VZ, which gives rise to V2 interneurons (Mizuguchi et al., 2001). Loss-of-function analysis demonstrated that *Mash1* expression is necessary for the proper development of V2a neurons, as the number of *Chx10*⁻ (marker for V2a INs) expressing neurons is drastically reduced in *Mash1*^{-/-} mice embryos. Further evidence for this instructive role of *Mash1* in specifying V2 INs in the ventral spinal cord comes from misexpression analysis in which ectopically expressed *Mash1* induces *Chx10* expression in MN precursors (Parras et al., 2002). *Mash1* cooperates with *Foxn4*, a forkhead domain transcription factor to specify V2a interneurons (Li et al., 2005).

Roles for two other members of the bHLH protein family, *Olig3* and *Ptf1a*, have been described in the specification of interneurons in the dorsal spinal cord. *Olig3*, a member of the *Olig* subgroup of bHLH proteins, is expressed in dorsal progenitors that give rise to class A neurons and is an important determinant for specifying these neurons (Muller et al., 2005). *Olig3*^{-/-} mice show a reduction in the number of dl1 neurons, as well as a loss of dl2 and dl3 neurons. The reduction/loss of class A neurons is accompanied by an increase in the

number of neurons that express homeodomain factors typical of class B neurons, such as *Lbx1*. This suggests that *Olig3* functions as a suppressor of class B neurons through repression of *Lbx1* expression. *Olig3* also provides instructive information essential for specification of one particular class A neuronal subtype, the dl3 neurons, as overexpression of *Olig3* in the chick neural tube leads to an induction of *Isl1*-expressing cells, a marker of dl3 neurons.

A role of the bHLH transcription factor *Ptf1a* in the specification of two types of dorsal interneurons has recently been described (Glasgow et al., 2005). Stainings with an antibody specific against mouse *Ptf1a*, as well as cell lineage tracing experiments, have shown that *Ptf1a* is expressed in the spinal ventricular zone in a domain that gives rise to dl4 neurons. Between E11.5-E13 *Ptf1a* expression is seen throughout the entire *Mash1*⁺ domain, arguing that *Ptf1a* is expressed in progenitors of late-born dIL neurons. *Ptf1a* is necessary for the development of early-born dl4 and late-born dIL_A neurons. In embryos lacking *Ptf1a*, *Pax2*-expressing dl4 neurons do not develop. Instead, *Lmx1b*-positive dl5 neurons are generated in the domain, where dl4 neurons are normally found in wild type embryos. *Pax2*-expressing dIL_A neurons also fail to develop. There is a concomitant increase in the number of *Lmx1b*⁺ dIL_B neurons in the *Ptf1a*^{-/-} cord, demonstrating a switch from a dIL_A to a dIL_B fate. This cell fate switch was also observed on the neurotransmitter level, with a loss of GABAergic marker expression (e.g. GAD67 and VIAAT) and an increase in the number of VGLuT2⁺ neurons (Glasgow et al., 2005). *Ptf1a* appears to be a critical determinant of inhibitory interneuron development in the dorsal CNS, with the cerebellum and hindbrain of *Ptf1a*^{-/-} mice also lacking inhibitory cell types (Hoshino et al., 2005).

1.6.2 Homeodomain proteins

The homeobox genes are a conserved family of genes that often occupy high-level positions in the genetic hierarchy of development (Kessel et al., 1990; Lufkin et al., 1991; McGinnis and Krumlauf, 1992; Small and Potter, 1993). The proteins encoded by these genes, the homeodomain transcription factors, share a common 60-amino acid helix-turn-helix motif. This domain mediates site-specific DNA binding. In addition to the so-called *Hox* genes, which comprise of a colinear complex and are organized in four main clusters in vertebrates, there are numerous orphan homeobox genes that are scattered throughout the genome. In many instances, these genes have been named after their *Drosophila* homologs. The *Gsh1* and *Gsh2* (genomic screened homeobox) homeobox genes share a high degree of similarity to the clustered *Hox* genes (Singh et al., 1991), but are most homologous to the *Drosophila* intermediate neuroblast defective gene, *Ind* (Weiss et al., 1998; von Ohlen et al., 2000).

1.6.2.1 The role of Gsh1/2 in neuronal development

1.6.2.1.1 The role of the Ind, the *Drosophila* homolog of Gsh1/2, in neuronal development

The Ind homeodomain protein is essential for establishing a dorso-ventral cell fate in the ventral cord of *Drosophila* larvae (Weiss et al., 1998). Neuroblasts in the *Drosophila* neuroectoderm develop from three columns of cells along the dorso-ventral axis: ventral, intermediate and dorsal. These columns selectively express the homeodomain proteins ventral nervous system defective (*Vnd*) (ventral), *Ind* (intermediate) and muscle segment homeobox (*Msh*) (dorsal). *Ind* controls the establishment of intermediate cell fate in the ventral neuroectoderm. In the absence of *Ind*, a majority of intermediate neuroblasts are respecified and adopt either a ventral or dorsal fate. The intermediate domain and the boundaries between the three columns of neuroblasts in the ventral neuroectoderm are established via the repression of *Ind* by *Vnd* ventrally and dorsally via *Ind*-dependent repression of *Msh* expression (Weiss et al., 1998). The mammalian orthologs of *Vnd* (*Nkx2.1* and *Nkx2.2*) and *Msh* (*Msx1*, *Msx2* and *Msx3*) are expressed in equivalent domains of the vertebrate neural tube. The *Nkx*

proteins are found in the ventral half, while *Msx1/2* expression is restricted to dorsal progenitors (Weiss et al., 1998). This has led to the concept of dorso-ventral patterning as a conserved process during evolution (Cornell et al., 2000), and it raises the possibility that the mammalian *Ind* homologs *Gsh1/2* function similarly in vertebrate development.

1.6.2.1.2 *Gsh1/2* function in the brain

When I began this thesis research project, there was no information on the function of *Gsh1* and *Gsh2* in the development of the spinal cord. Functional studies on these two homeodomain transcription factors have focused exclusively on the developing brain. First described in 1991 (Singh et al., 1991), both genes are localized on chromosome five and belong to the group of orphan *Hox* genes. They are closely related with their homeodomains being approximately 96% identical. Expression of both genes displays partial overlap in the developing ganglionic eminences, diencephalon and parts of the developing mid- and hindbrain (Hsieh-Li et al., 1995; Valerius et al., 1995). In 1997, Szucsik and co-workers generated *Gsh2*-deficient mice and first reported the occurrence of *Gsh2* in the spinal cord. *Gsh2*^{-/-} mice perish due to cardiorespiratory problems within the first 24 hours following birth.

Subsequent analyses revealed that *Gsh2* plays an important role in the development of the ventral telencephalon (Szucsik et al., 1997; Toresson et al., 2000; Corbin et al., 2000; Yun et al., 2001). *Gsh2* is essential for the early expression of a number of genes that mark the developing lateral ganglionic eminence (LGE). The development of this domain is most profoundly affected by the lack of *Gsh2* in mutant mice (Szucsik et al., 1997). Patterning analyses showed a marked reduction of the transcription factors *Dlx1/2*, *Mash1* and *Ebf1*, as well as *GAD67*. An expansion of the cortical progenitor markers *Pax6* and *Ngn2* into the GE (ganglionic eminence) was evident in the telencephalon of *Gsh2*^{-/-} mice, indicating an expansion of the dorsal telencephalon in these mice. In *Pax6*-deficient mice these alterations are mirrored, leading to the assumption that *Pax6* and *Gsh2* play opposing roles in telencephalic development (Toresson et al., 2000). *Gsh2* therefore contributes to the development of distinct telencephalic domains and the establishment of the cortico-striatal boundary, the border between the developing cortex and the LGE.

Gsh1 is expressed together with Gsh2 in the developing brain. However, expression in the LGE is only partially overlapping. In *Gsh2*^{-/-} mice, a dramatic expansion of the Gsh1 expression domain in the LGE was observed, and this results in less pronounced developmental alterations at later stages. Additionally, some regions, such as the diencephalon, appear unaffected, albeit that they lack Gsh2. These observations led to the assumption that Gsh1 might compensate for the loss of Gsh2 (Toresson and Campbell, 2001). This is supported by the ability of Gsh1 to compensate in part for the loss of Gsh2 in striatal and olfactory bulb development. *Gsh1*^{-/-} mice have shown that this gene is important for the development of the pituitary and hypothalamus. To date, only the growth hormone-releasing hormone (GHRH) gene has been identified as a target of Gsh1 (Li et al., 1996).

1.6.2.1.3 The role of Gsh1/2 in the embryonic spinal cord

In contrast to the developing forebrain, Gsh2 expression in the spinal cord is restricted to the dorsal half. Gsh2 is expressed in the ventricular zone and marks the dl3-5 progenitor domains. Loss-of-function analysis revealed that *Gsh2* is necessary for the development of the dl3 subtype of dorsal interneurons (Kriks, 2003). Mice lacking *Gsh2* exhibit an almost complete loss of Isl1⁺/Tlx3⁺ dl3 neurons. My previous studies suggest that the boundary to the adjacent dl2 progenitor domain is established in part through repression of Ngn1. In wt embryos, this bHLH transcription factor is expressed in the dl2 progenitor domain adjacent to the Gsh2⁺ domain. In *Gsh2*^{-/-} mice embryos Ngn1 expands ventrally and encompasses the presumptive dl3 progenitors. This ventral expansion of Ngn1 results in a reduction in Mash1 expression in dl3 progenitors; however, Mash1 continues to be expressed in dl4 and dl5 progenitors. Consistent with this, *Gsh2*^{-/-} mice show an increase in the number of Foxd3-expressing dl2 neurons. When *Gsh2* is overexpressed in the neural tube of E3 chick embryos, few ectopic Isl⁺ cells are found in the electroporated half of the spinal cord. This induction is not observed in every embryo and seems to be in a non-cell autonomous manner, suggesting that Gsh2 is not the primary inducing factor for dl3 neurons.

The related homeodomain protein Gsh1 is also expressed in the dorsal spinal ventricular zone, overlapping with Gsh2 in progenitors of dl4 and dl5 neurons (Kriks, 2003). Its expression is not dependent on Gsh2, as Gsh1

expression is unchanged in the *Gsh2*^{-/-} spinal cord. So far, no studies have investigated the role of Gsh1 in patterning the dorsal spinal cord.

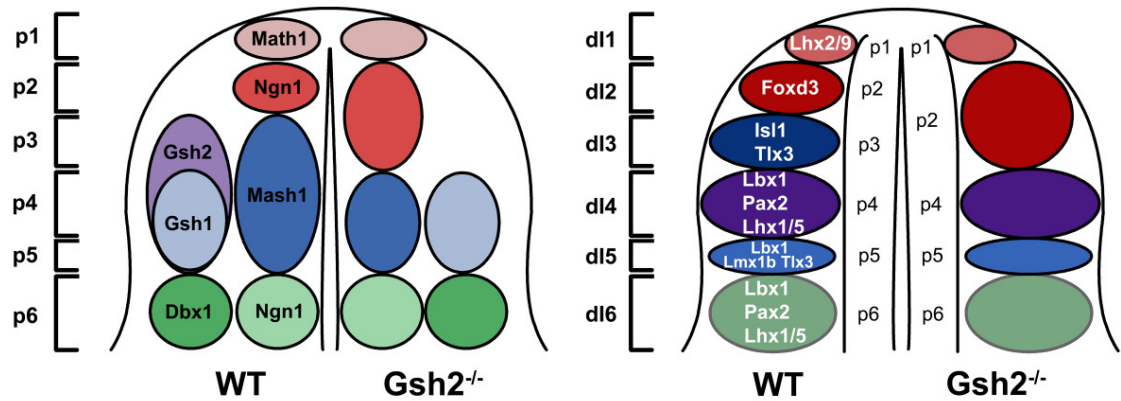


Figure 7: Schematic summary of the phenotypes seen in E11.5 *Gsh2*^{-/-} spinal cords. *Gsh2*^{-/-} mice do not develop dl3 neurons, as evidenced by the loss of Isl1/Tlx3-expressing cells. The presumptive dl3 neurons develop as dl2 neurons, which are marked by the expression of Foxd3. This switch in cell fate, with dl3 neurons develop as dl2 neurons, is due to an expansion of Ngn1 encompassing presumptive dl3 progenitors. This ventral expansion of Ngn1 represses Mash1 in dl3 progenitors. However, Mash1 remains to be expressed in dl4 and dl5 progenitors, most likely due to the unchanged expression of Gsh1 in the *Gsh2*^{-/-} spinal cord.

1.7 Aim

With the exception of my preliminary analysis (Kriks, 2003), no studies have been undertaken to elucidate the functions of the homeodomain proteins Gsh1 and Gsh2 in the developing spinal cord. The experiments undertaken for this PhD project set out to establish the function of Gsh1 and Gsh2 in the spinal cord and examine the molecular mechanism that regulates their expression and function in the dorsal spinal cord. In undertaking this thesis research, I set out to answer the following questions.

1) What are the roles of Gsh1 and Gsh2 in early dorsal interneuron specification?

In the spinal cord of *Gsh2*-deficient mice, there is a specific loss of dl3 neurons, although Gsh2 is also expressed in dl4 and dl5 progenitors. Does Gsh1 play a role in the specification of these interneuron populations? One possibility is that Gsh1 alone is necessary for their development. Alternatively, Gsh1 and Gsh2 are functionally redundant in specifying dl4 and dl5 neurons of these interneuron populations.

2) How is the expression boundary of Gsh1/2 achieved?

Are cross-inhibitory interactions between Gsh1/2 and other classes of homeodomain proteins, such as the Msx- and Dbx family of transcription factors involved in establishing the dorsal and ventral boundaries of Gsh1/2?

3) Do Gsh1/2 and Mash1 interact genetically?

The bHLH transcription factor Mash1 is expressed together with Gsh1/2 in dl3 - 5 progenitor cells and Mash1 is reduced in the dl3 progenitor domain in the absence of Gsh2. It is not known whether Mash1 is also playing a role in the specification of dorsal interneurons, e.g. dl3 neurons.

4) Does Mash1 regulate Ngn1/2 and do Ngn1/2 in turn regulate dl4/dl5 neuron development?

The characterization of the repressive function with respect to Ngn1 and Ngn2 in dl2/dl3 boundary formation also needs to be addressed. Is Mash1 responsible for the establishment of this boundary by repressing Ngn expansion into dl3 progenitors? To what extent is Gsh2 involved in this process? During my diploma thesis I showed that Gsh2 represses Ngn1/2, but it is not clear whether this is a direct effect on Ngn1/2, or whether it is accomplished indirectly through the action

of Mash1. These two hypotheses need to be analyzed.

5) What is the role of Gsh1 and Gsh2 in late dorsal interneuron specification?

Another question that needs to be investigated is the role of Gsh1 and Gsh2 in the specification of late-born $dIL_{A/B}$ neurons, which arise also from Gsh1/2 positive progenitors. Is their development perhaps due to an integrated effect of both genes or is the role of Gsh1 and 2 in defining these progenitors only secondary?

2 Material and methods

2.1 Material

2.1.1 Equipment

Electroporator T820	BTX
Fluorescence microscope Stemi SV11	Zeiss
Fluorescence microscope Eclipse E400	Nikon
Fluorescence microscope EFD-3	Nikon
Cryostate CM 3050S	Leica
Incubator BSS1200-110	Kuhl
Confocal microscope LSM 510	Zeiss
Needle puller P80/PC	Sutter Instruments
Photometer DU 530	Beckman
Thermocycler PTC-200	MJ Research

Centrifuges:

Microfuge 18	Beckmann
Refridgerated centrifuge Sorvall RC-5B	DuPont Instruments
Megafuge 1.0	Baxter
Ultracentrifuge L-80	Beckmann
Table centrifuge TL-100	Beckmann

2.1.2 Chemicals

The suppliers of chemicals, unless otherwise mentioned, are BioRad (Hercules, USA), Difco Laboratories (Sparks, USA), Sigma-Aldrich (St. Louis, USA), EM Science (Gibbstown, USA), Calbiochem (San Diego, USA). All chemicals were of molecular biology reagent quality.

2.1.3 Supplies

Culture dishes and test tubes were supplied by Becton Dickenson, Corning, Eppendorf, Falcon, Fisher, Greiner and USA Scientific.

2.1.4 Detergents

Triton X-100	Sigma
Tween 20	Sigma

2.1.5 Enzymes, antibiotics

Ampicillin	Calbiochem
Amplitaq-DNA-polymerase	Roche
Alkaline phosphatase	Roche
Kanamycin sulfate	Calbiochem
Proteinase K	Roche
Restriction endonucleases	New England BioLabs
Reverse transcriptase	Gibco BRL
SP6-, T3-, T7-RNA polymerase	Promega
T4-DNA ligase	New England BioLabs

2.1.6 Commercial kits

The following kits from the company Qiagen were used:

- Plasmid Midi kit
- QIAquick gel extraction kit

2.1.7 Antibodies

2.1.7.1 Primary antibodies

name	dilution	source
gp anti msLmx1b	1:1000	T. Jessell (Columbia University, NY, USA)
ms anti BrdU	1:50	Calbiochem
ms anti Isl1	1:10	DSHB
ms anti Lhx1/5	1:20	DSHB
ms anti chLmx1b	1:10	DSHB
ms anti Mash1	1:20	J. Johnson (UTSMC, Dallas, USA)
ms anti NeuN	1:200	Chemicon
ms anti Pax7	1:15	DSHB
rab anti calbindin	1:10000	Swant
rab anti Foxd3	1:200	M. Goulding
rab anti Gsh2	1:2000	K. Campbell (Children's Hospital, Cincinnati, USA)
rab anti Gsh1/2	1:2000	S. Kriks
rab anti Lbx1	1:100	M. Goulding
rab anti Mash1	1:1000	Babco
rab anti NICD (cleaved Notch1;Val1744)	1:100	Cell Signalling
rab anti Pax2	1:200	Zymed
rab anti Ptf1a	1:1000	H. Edlund (University of Umea, Sweden)
rab antiTrkA	1:5000	L.Reichardt (UCSF, San Francisco, USA)
rat anti Lbx1	1:80	M. Goulding

2.1.7.2 Secondary antibodies

Cy2-, cy3-, cy5-conjugated anti guinea pig

Cy2-, cy3-, cy5-conjugated anti mouse

Cy2-, cy3-, cy5-conjugated anti rabbit

Cy2-, cy3-, cy5-conjugated anti rat

Fluorochrome-conjugated secondary antibodies were obtained from Jackson Research and used at a working dilution of 1:200.

2.1.8 Vectors

The pBluescript II SK+ plasmid vector (Stratagene) was used for standard clonings. For chick electroporations, a modified version of the pIRES-EGFP2 expression plasmid (Clontech) was used. The modifications included the exchange of the CMV (cytomegalovirus) promoter with a chicken β -actin promoter and an insertion of a CMV enhancer element. These modifications were performed by Mirella Dottori (Monash University, Melbourne, Australia).

2.1.9 DNA molecular weight markers

The size of DNA fragments was determined using the 1kb ladder from Invitrogen.

2.1.10 Buffers and stock solutions

Distilled water for solutions was purified through a Millipore filtration system and autoclaved prior to use.

<u>10x PBS:</u>	137 mM NaCl
	2.7 mM KCL
	10 mM Na ₂ HPO ₄
	2 mM KH ₂ PO ₄
	adjust to 1l with dH ₂ O, final pH 7.4

<u>1x PBT:</u>	0.1% Triton in 1x PBS
----------------	-----------------------

<u>50x TAE:</u>	2 M Tris-HCl 50 mM EDTA pH 8.0
<u>20 % SDS:</u>	20g SDS (sodiumdodecyl sulfate) per 100 ml dH ₂ O
<u>10x Tris EDTA (TE) (pH 8,0)</u>	100 mM Tris-HCl (pH 8.0) 10 mM EDTA (pH 8.0)
<u>DEPC-H₂O:</u>	dH ₂ O was mixed with 0.1% diethylpyrocarbonate (DEPC) and incubated at room temperature (RT) overnight to inactivate RNAses before autoclaving to inactivate DEPC.

All solutions used were made after the protocol in the laboratory manual Sambrook et al. (1998).

2.1.11 Cultures to grow bacteria

<u>Luria-Broth-(LB) media:</u>	10 g Bacto-trypton 5 g Bacto-yeast-extract 5 g NaCl adjust to 1l dH ₂ O, pH 7.5
--------------------------------	---

Bacterial colonies were grown on LB plates containing a proper antibiotics. 15 g of agar was added to 1l LB media, autoclaved and cooled to 50°C, at which time antibiotics were added to a final concentration of 100 µg/ml. The liquid was then poured into petridishes, allowed to solidify overnight and stored at 4°C.

2.1.12 Organisms

2.1.12.1 Bacteria

The *E. coli* strain XL1 Blue was used for standard clonings.

2.1.12.2 Chicken embryos

Fertilized White Leghorn chicken eggs were obtained from McIntyre Farms, Lakewood, USA. Eggs were typically incubated at 38°C in a force-draft humidified incubator for either three days (early analysis) or six days (late analysis), before being used.

2.1.12.3 Mice

A variety of genetically modified mouse strains were used in this study.

strain	source
ICR (wt)	Harlan (Indiana, USA)
Gsh2 ^{+/-}	K. Campbell (Children's Hospital, Cincinnati, USA)
Gsh1 ^{+/-}	Steve Potter (Children's Hospital, Cincinnati, USA)
Gsh1 ^{+/-} /Gsh2 ^{+/-}	Sonja Kriks
Mash1 ^{+/-}	Quifu Ma (Dana-Farber Cancer Institute, Harvard Medical School, Boston, USA)
Ngn1 ^{-/-} /Ngn2 ^{-/-} embryos	Francois Guillemot (National Institute for Medical Research, London, UK)
Presenilin ^{+/-}	Jackson Laboratory
Delta1 ^{hypo/-} embryos	Ralf Cordes (Institute for Molecular Biology, Hannover, Germany)

2.2 Molecular biology methods

2.2.1 General methods for working with DNA

The methods that were used in this study are listed below, and unless otherwise stated, were taken from the laboratory manual "Molecular Cloning" by Sambrook et al. (2001).

2.2.2 Concentration measurement of nucleic acids

The concentration of nucleic acids was quantified by spectrophotometry at 260 nm, where an OD_{260} of 1 equals a concentration of 50 $\mu\text{g/ml}$ double stranded DNA or 40 $\mu\text{g/ml}$ RNA. The purity of the nucleic acids was determined by the absorbance ratio $A_{260/280}$. Ratios below 1.8 for DNA indicate contamination with proteins. The ratio for RNA should be ~ 1.9 -2.0.

2.2.3 Restriction digestion of DNA

Restriction endonucleases catalyze sequence-specific hydrolysis and thus formation of double-stranded breaks. The sequences recognized by the enzymes are characteristic for the bacteria from which the enzyme was isolated. Type II endonucleases, which are used in this study, recognize 6 bp palindromic target sequences to either produce 3' or 5' overhangs, so called sticky ends, or blunt ends. The activity of restriction endonucleases is defined in Units (U), with one unit corresponding to the amount of enzyme required to fully digest 1 μg Lamda DNA in one hour.

DNAs to be used for ligation were subjected to preparative restriction digestion. Analytical restriction digests were used to identify cloned fragment inserts as well as to check their orientation.

2.2.6 Isolation of DNA fragments from agarose gels

(Qiagen gel extractions kit manual, april 2000)

DNA isolated from agarose gels was purified using a Qiagen gel extraction kit. To isolate DNA fragments for cloning, the DNA band of choice was cut out under UV light and weighed. After addition of 3 vol. of QG buffer the agarose was melted at 50 °C for 10 min. 1 vol. of isopropanol was then added, and the solution was pipeted onto a QIAquick centrifugation column and centrifuged for 1 min. at 13000 rpm. The bound DNA was washed with 750 µl PE buffer and the remaining EtOH removed through a second centrifugation step. The DNA was then eluted from the column in 30 µl dH₂O.

2.2.7 Ligation of DNA fragments into plasmids

The covalent joining of DNA fragments with compatible ends is called DNA ligation. This method was used to clone various DNA fragments into plasmid vectors that had previously been linerized with restriction enzymes. T4 DNA ligase from the T4 bacteriophage was used to catalyze the joining of a 5' phosphate group with a 3' hydroxy group. In addition to ligating complementary overlapping DNA ends, it also catalyses the ligation of blunt DNA ends, albeit less efficiently.

Ligation reaction:

1 µl	plasmid DNA (0.2 µg/µl)
x µl	DNA fragment (3-5 molar excess)
1 µl	10x T4-ligase-buffer (New England BioLabs)
1 µl	T4-DNA-ligase
	adjust to 10 µl with dH ₂ O

The ligation reaction was incubated at 16 °C overnight.

2.2.8 Amplification of plasmid DNA in bacteria

2.2.8.1 Production of competent *E.coli* cells

Competent bacteria suitable for transformation were obtained as follows: 3 ml of LB media were inoculated with *E.coli* (XL1-Blue) and incubated overnight at 37°C. 100 ml of media A was inoculated with this pre-culture and further incubated at 37°C until an OD₆₀₀ of 0.4-0.6 was reached. The bacteria suspension was cooled for 10 min. on ice and centrifuged at 5000 rpm at 4°C for 15 min. The supernatant was removed and the bacteria pellet resuspended in 1 ml of cold media A. 2.5 ml of solution B was then added to the cells and carefully mixed before the bacteria were aliquoted into 100 µl and 200 µl lots and frozen in liquid nitrogen. The aliquots were stored at -80°C until used.

100 ml media A: LB media with 10 mM MgSO₄ x 7H₂O + 0.2 % glucose

10 ml solution B: 36 % glycerol, 12 % PEG, 12 mM MgSO₄ in LB media, pH 7.0

2.2.8.2 Transformation of competent XL1-Blue *E.coli* bacteria with plasmid DNA

Transformation was performed using a heat shock method: 100 µl of competent cells were thawed on ice and mixed with the ligation reaction. After a 30 min. incubation period, the bacteria were heat shocked at 42°C for 90 sec. and subsequently cooled on ice for 2-3 min. 1 ml of LB media was added, followed by a 1h incubation at 37°C with shaking. After incubation, 20% and 80% of the transformed bacteria were plated onto separate LB-plates containing antibiotics (50 µg/ml ampicillin or kanamycin) and incubated overnight at 37°C. On the following day, several colonies were picked and used to inoculate 2 ml of LB media containing the appropriate antibiotic. Each colony was then grown up overnight in a larger liquid culture (200 ml LB) at 37°C.

<u>QC-Puffer:</u>	1.0 M	NaCl
	50 mM	MOPS, pH 7.0
	15 %	EtOH

<u>QF-Puffer:</u>	1.25 M	NaCl
	50 mM	Tris/HCL, pH 8.5
	15 %	EtOH

2.2.9 Preparation of genomic DNA

Genomic DNA was prepared in order to genotype the various mouse strains used in this study (see 2.1.12.3). Tail tissue of mice was digested overnight in 0.5 ml lysis buffer containing 10 µl proteinase K (20mg/ml) in a shaker at 55 °C. The next day, the samples were centrifuged for 10 min. at 13000 rpm and the supernatant, which contains the genomic DNA, was transferred to a new tube. DNA was precipitated by adding an equal volume of isopropanol and mixing. Following a centrifugation step at 10000 rpm, the DNA pellet was washed with 70% EtOH to remove salt and airdried before resuspension in 500 µl dH₂O. To fully dissolve the DNA, the solution was incubated for an additional 15 min. in a shaker at 50 °C. All DNAs were stored at -20 °C.

<u>Lysis buffer:</u>	50 mM	Tris/HCl, pH 8.0
	100 mM	EDTA
	100 mM	NaCl
	1 %	SDS

2.2.10 Preparation of total RNA from spinal cord tissue

Five to six spinal cords dissected from embryonic day 11.5 (E11.5) mouse embryos were homogenized in TRIzol reagent (Gibco BRL) (0.75 ml/100 mg tissue). The homogenate was pipetted up and down several times to lyse the cells and incubated for 5 min. at RT. 200 μ l chloroform per 0.75ml TRIzol reagent were then added, shaken and incubated at RT for an additional 15 min. The solution was separated into a lower phenol/chloroform phase, an interphase and an upper aqueous phase, which contains the RNA, by centrifugation at 13000x g for 15 min. at 4°C. After transferring the upper phase to a new tube, the RNA was precipitated by adding 0.5 ml isopropanol per 0.75 ml. TRIzol. After incubating for 10 min., the RNA was then pelleted by centrifuging at 7500x g for 5 min. After air drying, the RNA pellet was resuspended in 20 μ l RNase-free H₂O.

2.2.11 Ethanol precipitation of DNA and RNA

DNA and RNA samples were routinely concentrated by ethanol precipitation. The salt concentration was adjusted to 0.3 M by adding 1/10 vol. of 3 M sodium acetate (pH 5.2) to the DNA. To precipitate the DNA, 2.5 vol. of 100% EtOH was added to the DNA, mixed and then incubated for 10 min. at -20°C. The DNA was pelleted by centrifuging for 10 min. at 13000 rpm. Each DNA pellet was washed with 70% EtOH to remove any remaining salt. The DNA was then air-dried and resuspended in 20-100 μ l of dH₂O, depending on the size of the pellet, to achieve a concentration of 1-2 μ g/ μ l.

2.2.12 Phenol/chloroform extraction of DNA

Phenol/chloroform extraction was used to remove proteins from nucleic acid preparations. The volume of the DNA solution was increased to 200 μ l with sterile dH₂O and an equal amount of saturated phenol (pH 8.0) was added. After vigorous shaking, the solution was centrifuged for 1 min. at maximum speed. This centrifugation step leads to a separation of a lower phenol phase, an interphase and an upper aqueous phase, which contains the DNA. This upper phase was transferred to a new tube and the same procedure repeated. After the second transfer, residual phenol was removed by adding one volume of

chloroform, mixing and centrifuging. The upper phase was once again transferred to a new tube and the DNA was precipitated by EtOH precipitation.

2.2.13 Making cDNA using reverse transcriptase

Total RNA containing rRNA, tRNA and mRNA (see 2.2.10) was used as a template. To amplify transcripts specifically from mRNA, an oligo-dT primer, which anneals to the polyA-tail of mRNA, was used for 1st strand synthesis.

<u>Reaction:</u>	total RNA	1-2 µg
	oligo-dT primer (Invitrogen, 0.1 nmol/µl)	1 µl
	dNTP (0.2 mM)	1 µl
	adjust to 12 µl with dH ₂ O	

The reaction was heated for 10 min. at 70°C to denature secondary structures in the RNA and then snap-cooled by placing it on ice for a few minutes. 4 µl 5x transcription buffer, 2 µl 0.1 M DTT (dithiothreitol) and 1 µl RNase inhibitor were then added, and the reverse transcription reaction was initiated by adding 1 µl reverse transcriptase (Superscript, Invitrogen). The reaction was incubated at 42°C for 1h, followed by a denaturing step at 70°C for 15 min., which was used to separate the RNA from the complementary cDNA. The RNA template was then digested by adding 1µl RNaseH and incubating the reaction at 37°C for 15-20 min. cDNAs were stored in RNase-free dH₂O at -20°C.

2.2.14 Polymerase chain reaction (PCR)

The polymerase chain reaction is a method used to amplify a specific region/sequence of DNA. This method is based on three steps:

1. Denaturing of the double-stranded DNA into single strands.
2. Annealing of a complementary oligonucleotide primer pair onto both single strands.
3. Elongation of the DNA fragment between the sense and the antisense primer by a thermophilic DNA polymerase.

Either genomic DNA from tail tissue (see 2.2.9) or cDNA from a reverse transcription reaction (see 2.2.13) was used as a template in PCR reactions.

Please refer to 7.1.1 for all the sequences of oligonucleotide primers used in this study.

2.2.14.1 Designing of primers

Following points are important for designing primers:

1. The annealing temperature of two primers from a pair have to be similar.
2. The base pair length of each primer should be in the range between 20 and 30 bp and should contain ~ 50% G/Cs.
3. To prevent primer dimerization the primer sequences should not contain complementary sequences, especially at the 3' end.

2.2.14.2 PCR to amplify from cDNA

100 ng cDNA template was used to amplify DNA fragments.

<u>Reaction:</u>	cDNA template (0.5µg/µl)	1.0 µl
	sense primer (100 µM)	0.3 µl
	antisense primer (100 µM)	0.3 µl
	dNTP-mix (10 mM each)	1.0 µl
	10x buffer (Invitrogen)	5.0 µl
	Taq-polymerase (5 U/µl)	0.4 µl
	adjust to 25 µl with dH ₂ O	

10x PCR-Puffer: 500 mM KCl, 100 mM Tris/HCl, pH 9.0

<u>PCR-Program:</u>	94 °C	2 min	
	94 °C	1 min] <u>30 cycles</u>
	X °C	1 min	
	72 °C	1 min	
	72 °C	5 min	
	4 °C	∞	

The temperature (X) for annealing of the primers was calculated using the following formula:

$$T_m = 4 \times (G + C) + 2 \times (A + T)$$

G,C,A,T are the numbers of each base in the primer sequence. T_{ann} is generally 5-10°C below T_m .

2.2.14.3 Genotyping of knock-out (KO) mice

Homozygous Knock-out mice were typically generated by breeding heterozygous males with heterozygous females. To acquire the specific genotype of each embryo, PCR was performed to amplify a fragment of the wt locus and a fragment of the targeted knock-out allele. The sequence of the primer pairs used for each KO mouse strain is listed in the appendix (7.1.1). DNA from either tail or head tissue was used as template DNA. The PCR reaction is equivalent to the one listed under 2.2.14.2. The general PCR program used was similar to the one used to amplify specific cDNAs (see 2.2.14.2).

The annealing temperatures for the different primer pairs used to genotype KO embryos were established by running gradient PCR reactions between 55°C and 65°C using template DNA from heterozygous founder animals, which have both the wt and the KO allele. The temperature which gave the cleanest band for the predicted size was used in all following PCR reactions. The annealing temperatures for each primer pair used for genotyping mice embryos are listed below.

allele to amplify	temperature (°C)
Gsh1 WT	65
Gsh1 KO	65
Gsh2 WT	65
Gsh2 KO	66
Mash1 WT	65
Mash1 KO	66
Psen1 WT	66
Psen1 KO	66

2.2.15 Sequencing of DNA

All DNA sequencing was performed by the Sequencing Core Facility at the Salk Institute. The sequences were analyzed by comparing them with known sequences published online at the National Center for Biotechnology Information (NCBI) (www.ncbi.nih.org).

2.3 Developmental and analytical methods

2.3.1 In vivo electroporation of chick embryos

2.3.1.1 Electroporation of chick embryos at embryonic day 3 (E3)

Fertilized chicken eggs were incubated at 38°C for three days. The electroporation was performed at stage Hamburger/Hamilton 11-13 (HH11-13) (Hamburger und Hamilton, 1951). Approx. 5-7 ml of egg albumin was removed through a small hole at the side of the egg to lower the embryo inside the egg. The egg shell over the embryo was taped and windowed to allow access to the embryo. Ink (India Black (Pelican) diluted 1:10 in 1x PBS) was injected underneath the now visible chick embryo to make the neural tube more visible and to facilitate DNA injection/electroporation. Afterwards, the plasmid DNA, which was mixed with dye (1% Fast Green in 1x PBS) to see if the DNA enters the neural tube, was injected into the lumen of the neural tube by air pressure (25 psi) from a Pico spritzer. Platinum wired electrodes (5 mm) from the electroporator were then placed on either side of the neural tube and current was applied (25mV, 50 msec, 6 pulses). The negatively charged DNA enters the side of the neural tube on which the cathode was placed. Following electroporation, eggs were sealed with tape and incubated for an additional 24-28h to allow the embryos to further develop. After dissecting out the chick embryos, membranes were removed and the embryos were washed in 1x PBS before fixing them 1h in 4% PFA (paraformaldehyde). Following fixation, the embryos were washed thoroughly in 1x PBS to remove any residual PFA and then cryoprotected overnight in 25% sucrose-PBS.

2.3.1.2 Electroporation of chick embryos at E6

For electroporation at later timepoints, egg white was removed on day three of the incubation as previously described (see 2.3.1.1), and the incubation was continued until E6. The procedure is similar to the one performed at E3. The only difference is that at this later stage the embryo is much larger and is now lying on its side rather than with its dorsal side up. To be able to inject the DNA and place the electrodes along both sides of the neural tube, the chick embryo must first be rotated inside the egg without causing major injuries to the membrane or blood vessels. This was accomplished by applying some pressure on the embryos head using a cottoned tip, which was moistened in 1x PBS. This pressure rotates the embryo slightly so that its dorsal side is now facing upward, making it possible to inject the DNA into the neural tube. Upon removal of the cottoned tip the embryo falls back into its previous pose. The same pressure is then applied once again, so the two electrodes can be placed on either side of the embryo in order to electroporate the DNA. The conditions for electroporation are the same as described for the procedure at E3.

2.3.2 Anterograde labeling of primary afferent fibers using Dil

Carbocyanines are fluorescent lipophilic dyes, which are incorporated by cell bodies and moved by anterograde transport to axon terminals. One of the most commonly used is Dil (1,1-dilinoleyl-3,3,3',3'-tetramethylindocarbocyanine perchlorate). In this study, liquid Dil was injected into the dorsal root ganglia (DRGs) of E18.5 mice embryos in order to label the afferent sensory fibers that project from the DRGs into the dorsal horn. Removing overlying tissue, as well as the vertebral column, exposed the spinal cord including the dorsal roots of E18.5 embryos. The tissue was fixed with 4% PFA overnight (fixing does not block the transport of Dil). On the following day, fixed spinal cords were washed with 1x PBS, and the DRGs were filled with Dil. For this purpose, thinly pulled glass capillaries were filled with liquid Dil, which was subsequently injected into the DRGs. Four DRGs were filled per spinal cord, with each being separated by 4-5 mm. Anterograde transport was allowed to proceed for seven days at RT, after which the spinal cords were completely dissected out and

processed for vibratome sectioning (see 2.3.8).

Liquid Dil: One Dil crystal (Molecular Probes) was dissolved in 15 μ l DMF (Dimethylformamide).

2.3.3 Injection of 5-bromo-2'-deoxy-uridine (BrdU) into pregnant females

To label dividing cells, BrdU (0.1 ml (stock: 10 mg/ml) /10 g mouse) was injected into the peritoneum of pregnant females. BrdU is an analog of deoxyuridine and is incorporated into DNA in place of thymidine. Dividing cells that have incorporated BrdU into their DNA can be visualized by staining tissues with an antibody against BrdU.

2.3.4 Preparation of mice embryos

Heterozygous mice were bred together and a daily vaginal check was performed to observe the vaginal plug, which is an external marker for successful copulation. The plug day was considered embryonic day 0.5 (E0.5). Pregnant females were euthanized on the wanted day by cervical dislocation. The embryos were dissected out of the uterus and pinned down straight before fixing in 4% PFA (in 1x PBS) for 1-1.5 h. After extensive washing with 1x PBS to remove residual PFA, the embryos were cryoprotected overnight in 25% sucrose.

2.3.5 Embedding of embryos

After cryoprotecting overnight in sucrose, the embryos were rinsed in OCT (TissueTek, Sakura), transferred to a plastic mold containing OCT and then quickly frozen with dry ice. The blocks were stored at -80 °C.

2.3.6 Dissecting out spinal cords

From E16.5 onwards, whole mouse embryos are too big to ensure proper fixing of tissue. Therefore, the spinal cords were dissected out from the embryos. First, the embryos were dissected from the female's uterus and then sacrificed by decapitation. After evisceration, the cords were pinned down with the ventral side up in a dish containing 1x PBS. The ventral side of the vertebral column was removed to expose the spinal cords. Next, spinal cords were removed from the embryos by cutting the dorsal and ventral spinal roots. After removal, the spinal cords were pinned down in a dish to straighten them and fixed with 4% PFA for 1h at RT.

2.3.7 Sectioning of tissue using a cryostat

Cutting of the frozen tissue was performed utilizing a cryostat (Leica). After adapting to -20°C, the blocks were attached to the chuck with OCT. The tissue was then cut in 20 µm thick sections starting at lumbar levels until reaching forelimb levels. Sections were melted onto slides, which were then dried at 30°C for 1h before either being immediately used or instead stored at -20°C.

2.3.8 Sectioning of tissue using a vibratome

Freezing tissue which contains Dil is not recommended, as freezing quenches the fluorescence of Dil. Therefore, vibratome sectioning was performed on spinal cords of E18.5 embryos in which Dil was injected into the DRGs. The isolated spinal cords were embedded in 3% agarose and allowed to harden. These blocks were then trimmed and glued onto the chuck. The tissue was cut into 50 µm thick sections, which were collected in a series in 1x PBS. Later, each section was transferred to a dish containing 10 ml 1x PBS and 10 µl DAPI (4'-6-Diamidino-2-phenylindole) (1 mg/ml) to stain all cell nuclei before mounting each section onto a slide. The slides were coverslipped with 50% glycerol/PBS prior to analysis.

2.3.9 Preparation of hybridoma supernatant

2.3.9.1 Initiation and maintenance of cell culture

An aliquot of frozen hybridoma cells was thawed by rapid agitation in a 37°C water bath (thawing should be quick - within 40-60 sec.). The cell suspension was transferred to 5 ml of fresh media in a centrifuge tube and centrifuged at 125x g for 5-10 min. Media was drawn off, and the cells were resuspended in 1 ml of fresh cell culture media and subsequently transferred to a T-75 flask containing 20 ml of the media. Hybridoma cells grow as a suspension culture doubling in cell number approx. every 20-24h. The cells were split in half 1-2 days later to maintain the recommended cell density between 2×10^5 and 10^6 cells/ml in T-75 flasks, and 10 ml of fresh media was added for a total volume of 20 ml.

Complete media: 400 ml Iscove's DMEM
 100 ml fetal bovine serum
 5 ml L-glutamine
 5 ml Pen-Strep (10000 units penicillin and 10 mg streptomycin/ml)

2.3.9.2 Getting the supernatant

After splitting the cells they were allowed to grow for a further 24-36h until they reached the recommended density and were still in log phase growth. They were then centrifuged and the supernatant collected and aliquoted in 1 ml aliquots, which were stored at -80°C .

2.3.9.3 Making cell stocks

New stocks of each hybridoma cell line were made from 20 ml cell cultures in which cells were in growth phase. Cell suspensions were centrifuged at 1000 rpm for 5 min. After removing the supernatant, cells were resuspended in 5 ml ice-cold complete media containing 10% DMSO (to cryoprotect cells). Cells

were divided into 1 ml aliquots, placed in 1.8 ml cryotubes and kept on ice for several minutes before being frozen at -80°C . Frozen aliquots were then transferred to liquid nitrogen for long-term storage.

2.3.10 Immunohistochemical staining of tissue sections

In most instances, freshly cut sections were used for immunohistochemistry. If frozen sections were used, the slides were first thawed and dried prior to use. After drying, they were washed 3x for 10 min. each with 1x PBT. Non-specific binding sites were blocked by incubating the sections with 10% heat inactivated goat serum (HIGS) for 1h (if primary antibodies which were raised in goat were used, heat inactivated horse serum (HIHS) was utilized for the blocking step). After blocking, the primary antibody/antibodies were diluted in 10% HIGS (HIHS) to a proper concentration (see 2.1.7.1) and were applied to each slide. Antibody incubation took place overnight at 4°C in a humidified dark box to prevent drying out. On the following day, slides were washed 3x with 1x PBT for 10 min. each to remove unbound antibody. Fluorochrome-conjugated secondary antibodies (see 2.1.7.2) diluted in 10% HIGS (or HIHS) were then applied, and the slides were incubated for either 5h at RT or overnight at 4°C . Slides were then washed 3x with 1x PBT, dehydrated and coverslipped. The dehydration series included 25 %, 50%, 75%, 95%, 2x 100% EtOH followed by 2x xylene. Slides were then coverslipped in DPX mounting media and allowed to harden overnight before being imaged with a confocal microscope.

1x PBT: 1x PBS containing 0.1% Triton

2.3.11 Alternative staining procedures for some antibodies

For some antibodies a special protocol was required for optimal staining. Two of these antigen retrieval procedures were performed for antibodies against BrdU and the Notch intracellular domain (NICD).

2.3.11.1 Immunohistochemistry using an antibody against BrdU

When anti-BrdU antibody was used in combination with other primary antibodies, the stainings against the latter were performed first as described under 2.3.10. The slide was then fixed with 4% PFA to cross-link the antibodies and to ensure that they remain bound during the following procedure. After fixation, the slide was washed 3x 5 min. with 1x PBT. The sections were then treated with 2N HCl in PBT for 20 min., followed by a treatment with 0.1M borate (pH 8.5) for 20 min. Afterwards, the slide was washed 3x with 1x PBT and blocked with 10% HIGS for 1h. Following the blocking step, the anti-BrdU antibody diluted in 10% HIGS was added and incubated overnight at 4°C. Incubation with a secondary antibody and visualization was the same as described in 2.3.10.

2.3.11.2 Immunohistochemistry using an antibody against NICD

Antigen retrieval for the antibody against NICD requires heating the tissue in 50 mM citric acid. For this purpose, the slide was placed in a glass cuvette containing 50 mM citric acid (in 1x PBS), which had been preheated for 2 min. The solution containing the slide was then heated again until almost boiling (stopped when small bubbles were visible on the inside of the glass dish). The solution containing the heat-treated slide was allowed to cool down to RT for 30 min. prior to addition of the NICD antibody diluted in 10% HIGS. The remainder of the protocol is the same as described in 2.3.10.

2.3.12 *In situ* hybridization

In many instances, including those where specific antibodies were not available, gene expression was determined by *in situ* hybridization. Two *in situ* hybridization methodologies were used:

- a) Non-radioactive *in situ* hybridization with digoxigenin- (DIG) labeled probes
- b) *In situ* hybridization using radioactive labeled antisense probes to hybridize and visualize specific mRNAs

In this study, radioactive *in situ* hybridization was performed for only *VIAAT* and *VGluT2*, as this method of *in situ* hybridization is more sensitive and DIG-labeled probes against these two genes did not result in a proper staining.

2.3.12.1 *In situ* hybridization using digoxigenin-labeled antisense probes

2.3.12.1.1 Labeling of antisense probes with digoxigenin

The following reagents were mixed together in the order indicated:

dH ₂ O (sterile)	13 µl
10x transcription buffer (Promega)	2 µl
0.2 M DTT (Promega)	1 µl
nucleotid mix (10 mM each)	2 µl
linearised plasmid (1 µg/µl)	1 µl
ribonuclease inhibitor (1000 U/µl)	0.5 µl
SP6, T7 oder T3 RNA-Polymerase (10 U/µl)	1 µl

The reaction mix was incubated at 37°C for 2h, after which 2 µl DNase I (RNase-free) were added to digest the template DNA. The digestion took place for 20 min at 37°C. Afterwards, the RNA was precipitated by adding 100 µl TE, 10 µl 4 M LiCl and 300 µl EtOH (100%) and incubated for 30 min. at -20 °C. After centrifuging at 13000 rpm for 10 min., the RNA pellet was washed with 70% EtOH. The antisense probes were resuspended in 50 µl DEPC-H₂O and stored at -20°C.

<u>Nucleotide mix :</u>	10 mM GTP
	10 mM ATP
	10 mM CTP
	6.5 mM UTP
	3.5 mM digoxigenin-UTP

2.3.12.1.2 Pretreatment and hybridization

Freshly cut or frozen sections were dried for 1h at 30°C before processing. Slides were washed once with 1x PBS for 5 min. and fixed in 4% PFA (in 1x DEPC-PBS) for 10 min. After 3x washes with 1x DEPC-PBS for 5 min. each, the tissue was treated with proteinase K (3 µl/ml in 1x DEPC-PBS) for 5 min., followed by a second fixation step with 4% PFA for 5 min. The slides were then washed 3x with 1x DEPC-PBS for 5 min. each and acetylated to prevent non-specific binding of the antisense RNA probe. Acetylation was performed by placing the slides for 10 min. in a glass cuvette containing 200 ml DEPC-dH₂O with 3 ml triethanolamine (TEA), 0.4 ml HCL (conc.) and 500 µl 100% acetic anhydride. Tissue sections were then permeabilized for 30 min. with 1% Triton/DEPC-PBS followed by 3 washes with 1x DEPC-PBS. The slides were then prehybridized for at least 1h with hybridization solution. For the hybridization, 1 µg/ml DIG-labeled antisense probe was added to 150 µl hybridization solution, mixed and heated at 80°C for 5 min. After cooling down on ice for several minutes the probe was added to the slide and then coverslipped to prevent drying out. Hybridization took place overnight at 68°C in a humidified box containing 50% formamide.

<u>Hybridization solution:</u>	50% formamide, deionized
	5x SSC, RNase free
	5x Denhardt solution
	250 µg/ml yeast t-RNA
	adjust to 40 ml with DEPC-H ₂ O

deionized formamide: Formamide was stirred with Amberlite MB resin (10 g per 100 ml) for 1h to deionize before filtering through Whatman paper (3mm). 50 ml aliquots were stored at -20°C.

Denhardt solution: 2% BSA
2% Polyvinylpyrrolidone (PVP-40)
2% Ficoll 400
adjust to 40 ml with DEPC-H₂O

2.3.12.1.3 Incubation of anti-DIG antibody

After RNA hybridization, the coverslips were removed and the slides were washed 3x 45 min. with preheated 50% formamide/2x SSC at 68°C to remove unbound probe. Subsequently, the slides were rinsed in B1 solution for 5 min. and blocked for 1h at RT with 10% heat inactivated lamb serum (HILS) (in B1) to prevent non-specific binding of the antibody. The incubation with the anti-DIG antibody (Roche) (diluted 1:2000 in 10% HILS) was done overnight at 4°C.

B1: 1 M Tris-Cl (pH 7.5) 4.0 ml
4 M NaCl 1.5 ml
20% Tween-20 50 µl
adjust to 40 ml with dH₂O

2.3.12.1.4 Color reaction

After incubation with the antibody the slides were washed 3x 10 min. with B1. The slides were then adjusted to a more basic pH with B3 for 5-10 min. Afterwards, staining solution (B4) containing the substrates for AP was added onto the slides. The incubation occurred at RT until the desired color intensity was reached. The reaction was stopped by extensive washing with 1x PBT. The slides were then coverslipped using 50% glycerol in PBS.

<u>B3:</u>	1 M Tris-Cl (pH 9.5)	2 ml
	5 M NaCl	0.4 ml
	1 M MgCl ₂	1 ml
	20% Tween-20	0.1 ml

B4: 10 ml B3 with 35 µl BCIP and 15 µl NBT

2.3.12.2 *In situ* hybridization using radioactive-labeled antisense probes

2.3.12.2.1 Labeling of antisense probes with S-35

The following reaction was assembled:

0.7 µl	dH ₂ O
2 µl	5x transcription buffer
1 µl	0.1 M DTT
1.5 µl	1:1:1 rATP, rCTP, rGTP (10 mM each)
0.5 µl	RNAsin
2.0 µl	linearized plasmid (0.5 µg/µl)
1.3 µl	S-35 UTP, 40 mCi/ml (50 µCi)
1.0 µl	RNA polymerase

The transcription reaction was incubated at 37°C for 2h, followed by digestion of the DNA template by addition of DNase:

59 µl	dH ₂ O
10 µl	yeast tRNA (20mg/ml)
1 µl	1 M DTT
9 µl	DNase 10x buffer
1 µl	RNase-free DNase

This reaction was incubated for 15 min. at 37°C and the RNA precipitated by adding:

100 µl	dH ₂ O
70 µl	NH ₄ OAc (7.5M)
700 µl	100% EtOH

After placing the reaction on dry ice for 15 min., the RNA was pelleted by centrifuging 13000 rpm for 20 min. and the supernatant was removed. The pellet was washed by adding 900 µl of ice cold 70% EtOH and centrifuging for another 10 min. The EtOH was then aspirated from the pellet, which was allowed to air dry for several minutes and then resuspended in 70 µl deionized formamide, 70 µl dH₂O and 10 µl DTT (1M). The radioactivity of 1 µl probe was determined using a scintillation counter. Probes with a radioactivity between 400000-600000 cpm/µl were used for hybridization.

2.3.12.2.2 Pretreatment and hybridization

Slides holding either freshly cut or frozen sections were dried at 50°C for 30 min. before fixing the tissue with 4% PFA for 20 min. and washed twice with 1x DEPC-PBS for three min. The slides were then treated with 2x DEPC-SSC at 65°C for 30 min. and then rinsed in 1x DEPC-PBS for 3 min. The samples were then acetylated by adding the following reagents:

2.2 ml triethanolamine
0.5 ml acetic anhydrid
0.265 ml HCl (conc.)
adjust to 200 ml with DEPC-H₂O

The reaction was incubated for 10 min. at RT. Slides were then transferred to a chamber containing 1% TritonX-100 in 1x DEPC-PBS, where they were allowed to permeabilize for 30 min. The slides were then washed twice with 1x DEPC-PBS for three min. and then dehydrated using the following series of ethanol washes for three minutes each: 30% EtOH in 1x PBS, 60% EtOH in 0.5x PBS, 80% EtOH, 95% EtOH, and finally 100% EtOH. The slides were then air dried in a fume hood for at least 30 min. prior to proceeding to hybridization.

Hybridization buffer: 50% deionized formamide
10% dextran sulfate
1x Denhardt solution
0.3 M NaCl
10 mM Tris, pH 7.5
10 mM sodium phosphate, pH 6.8
5 mM EDTA
25 mM DTT (added on day used)
50 mM mercaptoethanol (added on day used)

For each slide a total volume of 150 µl containing probe (final concentration of 50000 cpm/µl) and hybridization buffer was assembled, heated to 80°C for 5 min. and then cooled on ice before adding onto the slide. A glass coverslip was placed on top. Slides were then placed in a humidified box (containing 5x SSC and 50% formamide) and incubated at 61 °C overnight.

2.3.12.2.3 Post-hybridization washes

All buffers used in the washing steps were pre-heated prior to use. Coverslips were removed by dipping slides into a beaker containing 5x SSC (61 °C). Forceps were used to remove the coverslip. Slides were then transferred to a tray and washed in 5x SSC and 50% formamide (61 °C) for 30 min. Samples were subsequently transferred to a solution containing 2x SSC, 50 % formamide, 20 mM β -mercaptoethanol (65 °C) for 60 min. The slides were then cooled by placing them in room temperature buffer with the same composition for 10 min. Slides were then placed in 37 °C TE containing 0.5 M NaCl for 10 min., after which time 400 μ l of 10mg/ml RNase A was added and allowed to incubate for an additional 15 min. The samples were then incubated twice in buffers containing 2x SSC, 50% formamide, 1 mM EDTA, 20 mM β -mercaptoethanol at 61 °C with mild shaking. This was followed by two additional 30 min. (61 °C) washes in first 0.3x SSC, 500 μ M EDTA, 10 mM β -mercaptoethanol and then 0.1x SSC and 5 mM β -mercaptoethanol, both with mild shaking. The slides were dehydrated using the following ethanol washes for three minutes each at RT:

30% EtOH, 125 mM NH_4OAc

60% EtOH, 63 mM NH_4OAc

80% EtOH, 3 mM NH_4OAc

95% EtOH

100% EtOH

The slides were then laid flat in a hood and allowed to dry for at least 15 min.

2.3.12.2.3 Exposure and development

After drying, slides were placed in a film cassette with a sheet of Kodak Biomax MR film. After exposing overnight, the film was developed using an automatic developing machine. The strength of the signal on this film was used to determine the length of time (generally 7-10 days) that samples would be exposed to the emulsion film. To coat the slides with a photographic emulsion, a water bath in the dark room was pre-heated to 45 °C and was used to warm the

film emulsion, which was composed of 11 ml dH₂O and 11 ml NTB-2 (Kodak) for 45 min. The emulsion was mixed by gentle inversion just before being placed in the water bath and again approximately 20 min. later. The warmed emulsion was then poured into a dipping dish that was placed in the water bath. Large bubbles were removed from the emulsion by dipping several blank slides into the emulsion. Sample slides were dipped into the dish and immediately pulled back out (approximately 3 sec. total time in emulsion). Excess emulsion was allowed to run off the slides. The slides were then placed upright and allowed to air dry in the dark for 2h. Emulsion-covered slides were then placed in a light-safe slide box, which was then wrapped in aluminum foil and stored at 4°C until development.

Slides were developed with D-19 developer solution (Kodak) diluted 1:1 with dH₂O for four min. and rinsed for 30 sec. in dH₂O. Slides were then transferred to fixer solution for 5 min., followed by two 5 min. washes in dH₂O. Samples were then counterstained with 1 µg/ml DAPI in dH₂O for five min. and again washed twice for five min in dH₂O. The slides were then allowed to air dry in the hood for approximately 30 min. and coverslipped using DPX mounting medium.

2.3.12.2.4 Photography

The radioactive *in situ* signal was photographed using dark field microscopy and the white silver grain signal was converted to a red signal. DAPI counterstain was photographed on the same microscope using UV fluorescence and was converted into a blue signal. The two images were then overlaid using Adobe Photoshop.

3 Results

3.1 Functional analysis of Gsh1

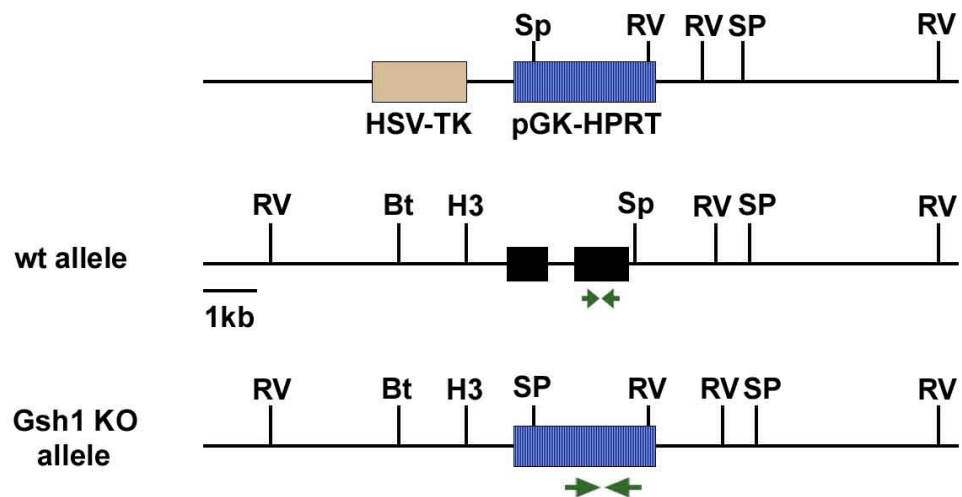
The expression domain of the homeodomain protein Gsh1 overlaps with Gsh2 in progenitors of dl4 and dl5 neurons. Gsh1 is still expressed in mice lacking *Gsh2* (Kriks, 2003). The unchanged expression pattern of Gsh1 in the *Gsh2*^{-/-} spinal cord, in addition to the relocation of the *Ngn1* boundary and the proper development of dl4 and dl5 neurons in *Gsh2*^{-/-} embryos, suggest that Gsh1 and Gsh2 may be functionally redundant. To analyze this hypothesis I examined the development of dorsal interneuron populations by antibody stainings of cross-sections of E11.5 *Gsh1*^{-/-} and *Gsh1/2*^{-/-} mice embryos using specific markers for each of the dorsal interneuron populations. Foxd3 was used as a marker of dl2 neurons and Isl1 for the dl3 subtype. dl4-dl6 neurons express the homeodomain factor Lbx1, while Lhx1/5 labels dl2, dl4 and dl6 dorsal interneurons. Pax2 is expressed in both dl4 and dl6 neuron subtypes and Lmx1b labels early-born dl5 neurons.

3.1.1 Generation of *Gsh1*^{-/-} mice embryos

Male mice heterozygous for *Gsh1* were provided by Steve Potter (University of Cincinnati). To expand the colony and to obtain heterozygous females, the founder males were bred with wt ICR females. Litters were genotyped by PCR using primers that amplify a 1.4 kb sequence from the HPRT cassette, which was used to inactivate the *Gsh1* locus. Mice positive for HPRT were collected for further breedings. Fig. 8 shows a schematic of the gene targeting strategy, with arrows indicating the primers used for genotyping.

30% of the *Gsh1*^{-/-} mice die within 48h after birth, and another 45% of the mutants die after four weeks. Surviving *Gsh1*^{-/-} adults rarely live beyond 18 weeks (Li et al., 1996); therefore, homozygous embryos were obtained by breeding *Gsh1*^{+/-} females with *Gsh1*^{+/-} males. Vaginal plug checks were performed daily to observe the day of conception. The plug day is considered embryonic day 0.5 (E0.5). Pregnant females were allowed to continue their pregnancies for an additional eleven days before the female was sacrificed and the E11.5 old

embryos were dissected out. DNA samples for genotyping were extracted from the embryos' head tissue. Genotyping was performed by PCR using two primer pairs to detect both wt and mutant alleles. To detect the wt allele one primer pair was used, which amplifies a 650 bp long fragment of the *Gsh1* wt locus (Fig. 9) that is replaced by the HPRT cassette in the *Gsh1*^{-/-} mice. The primer pair mentioned above, which amplifies a 1.4 kb fragment of the HPRT cassette was used to detect the mutated allele (Fig. 9). Wild type, *Gsh1*^{+/-} and *Gsh1*^{-/-} embryos from one litter were processed for the following experiments.



adapted from Li et al., 1996

Figure 8: Schematic of the gene targeting strategy of *Gsh1*. Genomic structure and restriction map of the mouse *Gsh1* gene and targeting vector are shown. The two black boxes represent the exons in the *Gsh1* gene. Green arrows mark the regions in the wt and KO allele, which get amplified by the two primer pairs. H3=HindIII, RV=EcoRV, Bt=BstEII, Sp=SpeI

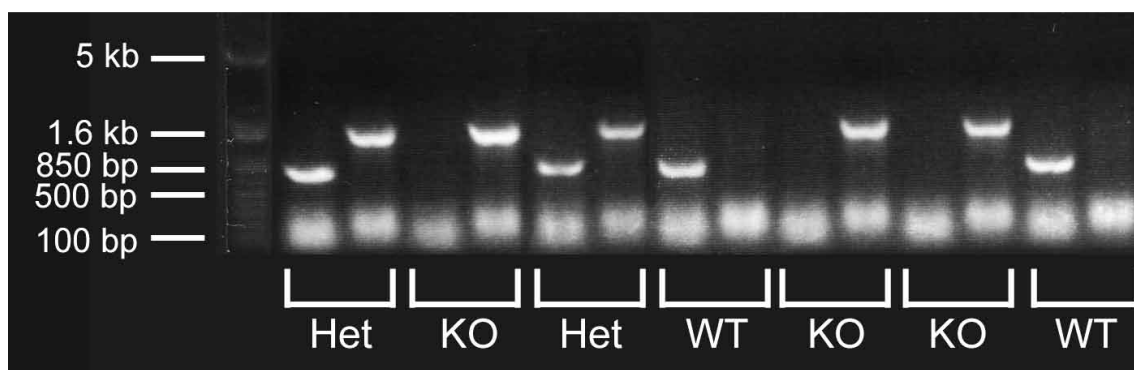


Figure 9: Example of genotyping for *Gsh1*^{-/-} and wt alleles. PCR reactions using a primer pair, which amplifies a fragment of the wt locus results in a 650 bp band, whereas PCR reactions using a primer pair that amplifies part of the KO allele gives a 1.4 kb band. Embryos heterozygous for both the wt, as well as KO alleles, give PCR products with each set of primers, while wt embryos only have the band for the wt allele and *Gsh1*^{-/-} embryos only have the 1.4 kb band for the KO allele.

3.1.2 Analysis of *Gsh1*^{-/-} spinal cords

Cross-sections of E11.5 *Gsh1*^{-/-} embryos and wt littermates were stained with antibodies against Foxd3 (dl2), Isl1 (dl3), Lbx1 (dl4-6), Pax2 (dl4, dl6), Lhx1/5 (dl2, dl4, dl6) and Lmx1b (dl5), thereby allowing me to determine whether the dl2-dl6 dorsal interneuron populations are being generated properly in the absence of *Gsh1*. The expression patterns of these specific interneuron markers are unchanged in mice lacking *Gsh1* compared to wt littermates. Neurons expressing Foxd3, Isl1, Lbx1, Pax2, Lhx1/5 and Lmx1b are expressed at the appropriate position in the spinal cord and in normal numbers (Fig. 10). These unchanged expression patterns of marker proteins demonstrate that all early-born interneuron populations in the dorsal spinal cord of *Gsh1*^{-/-} embryos are specified correctly.

The proper specification of dorsal interneurons suggests that the early transcriptional programs that control dorsal interneuron development are still operating in the *Gsh1*^{-/-} spinal cord. To further test this hypothesis I

examined the expression of transcription factors in dividing progenitors in the ventricular zone (vz) that are known to be necessary for the specification of dorsal interneurons. Gsh2 expression is still present in the *Gsh1*^{-/-} spinal cord, and its expression pattern is unchanged compared to wt embryos (Fig. 10m, n). This indicates that Gsh2 expression is not dependent on Gsh1 function, arguing that both homeodomain proteins are regulated independent of each other. Mash1 expression also overlaps with Gsh1 in the progenitors of dl4 and dl5 in wt spinal cords (Kriks, 2003). Not surprisingly, Mash1 expression is also unchanged in the ventricular zone of *Gsh1*^{-/-} embryos (Fig. 10o, p). This is most likely due to the maintained expression of Gsh2.

In summary, I propose that the lack of changes in transcription factor expression in the vz of *Gsh1*^{-/-} embryos accounts for the proper specification of early-born interneurons in the dorsal half of the spinal cord.

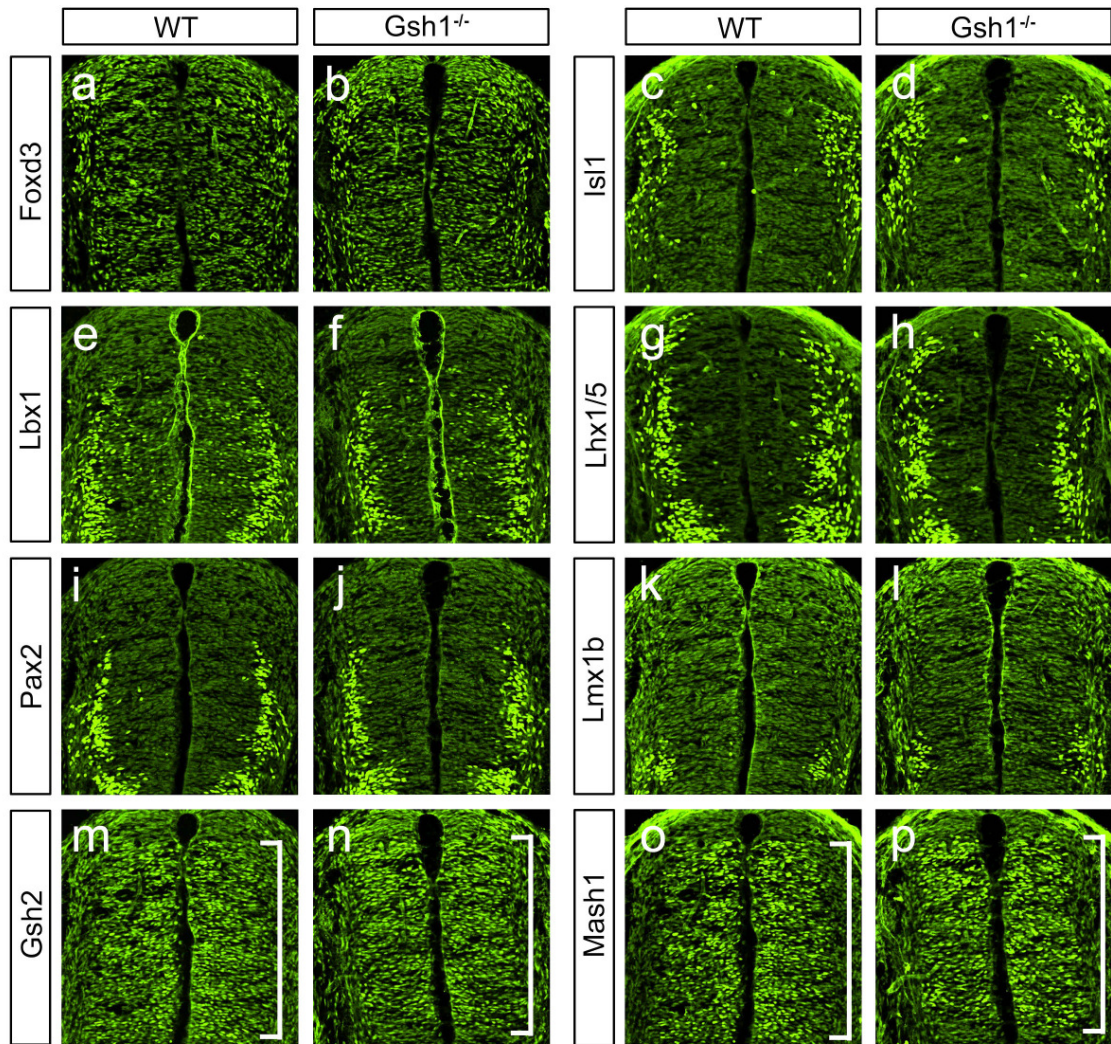


Figure 10: Analysis of *Gsh1*^{-/-} spinal cords at E11.5. Frozen wt and *Gsh1*^{-/-} embryos were cut into 20µm thick sections using a cryostat. Slides containing these tissue sections were stained by immunohistochemistry using antibodies against marker proteins of distinct interneuron populations. (Fig. 10a, b) dl2 neurons expressing Foxd3 develop normally in mice lacking *Gsh1*. (Fig. 10c, d) Isl1 marks dl3 neurons, which are unchanged in the *Gsh1*^{-/-} spinal cord. (Fig. 10e, f) Lbx1 expression is unchanged in *Gsh1*^{-/-} mice compared to wt littermates indicating a proper development of dl4, dl5 and dl6 neurons. (Fig. 10g, h) The unchanged expression of Lhx1/5 in mice lacking *Gsh1* confirms the correct specification of dl2, dl4 and dl6 neurons. (Fig. 10i, j) Pax2 expression is also unchanged in the *Gsh1*^{-/-} (Fig. 10k, l) At E11.5 Lmx1b is expressed in dl5 neurons, which develop normally in the *Gsh1*^{-/-} spinal cord. (Fig. 10m, n) Gsh2 is unchanged in dl3-5 progenitors in *Gsh1* null mutants (brackets) as well as Mash1 expression (brackets) (Fig. 10o, p).

3.1.3 Analysis of postmitotic IN populations in the spinal cord of *Gsh1/2^{-/-}* embryos

To further investigate the hypothesis that *Gsh1* and *Gsh2* are functionally redundant, *Gsh1/2^{-/-}* mice were generated and analyzed. Both *Gsh1* and *Gsh2* are located on the same chromosome (chromosome five) and because of this, genetic crosses were necessary to obtain mice that lack both alleles of *Gsh1* and *Gsh2*. First, *Gsh1* heterozygous mice were mated with mice heterozygous for *Gsh2*. The resulting litters were screened for heterozygous animals for both alleles. These animals were further bred with wt ICR mice to obtain progeny, which have the *Gsh1* and the *Gsh2* KO alleles on the same chromosome through homologous recombination. Double heterozygous mice in which both mutant alleles are located on the same chromosome were used as founder animals to generate a colony of *Gsh1/2* heterozygous mice. To obtain homozygous mutants for both *Gsh1* and *Gsh2*, these double-heterozygous animals were crossed. Although, I expected to obtain double mutant embryos at a 1/4 Mendelian ratio, the actual ratio turned out to be much lower, with an average of one double-mutant embryo per litter. The genotyping of embryos was performed as previously described for each single mutant (see Fig. 8; Kriks, 2003).

Spinal cords of E11.5 *Gsh1/2^{-/-}* embryos were analyzed for changes in dorsal interneuron differentiation by immunohistochemistry using a battery of antibodies specific to distinct subtypes of interneuron populations including *Isl1*, *Tlx3*, *Lbx1*, *Lhx1/5*, *Pax2* and *Lmx1b*. Not surprisingly, these embryos exhibit a similar phenotype seen in the *Gsh2^{-/-}* embryos (Kriks, 2003) with a loss of *Isl1*-expressing dl3 neurons (Fig. 11a, b). *Tlx3*, which is normally expressed in dl3 and dl5 neurons in wt embryos, is all but absent in the *Gsh1/2^{-/-}* spinal cord (Fig. 11c, d), confirming not only the loss of dl3 neurons, but also indicating a loss of dl5 neurons. Further evidence for the missing dl5 subtype is the complete loss of *Lmx1b* expression, which exclusively marks differentiated dl5 neurons at E11.5 (Fig. 11e, f). Instead, the interneurons present in the dl5 domain in the *Gsh1/2^{-/-}* embryos express the transcription factors *Pax2* (Fig. 11g, h) and *Lhx1/5* (Fig. 11i, j), suggesting either a switch in cell fate from a dl5 to a dl4 or dl6 identity or the loss of dl5 neurons with the dl4 neuron population, which is still present in the *Gsh1/2^{-/-}* spinal cord, as evidenced by the

unchanged pattern of Lbx1/Pax2/Lh1/5⁺ neurons (Fig. 11g-l), shifting down. To distinguish between these two possibilities, I performed cell counts of Lbx1⁺ dl4-dl6 neurons, as well as Pax2⁺ dl4 neurons on cross sections of E11.5 wt and *Gsh1/2*^{-/-} spinal cords at lumbar levels. If prospective dl5 neurons adopt a dl4 or a dl6 identity in *Gsh1/2*^{-/-} embryos, the number of Lbx1-expressing cells would be unchanged compared to wt littermates and the number of Pax2-expressing neurons would be increased. In the second possibility, Lbx1⁺ cells would be decreased in numbers due to the loss of dl5 neurons, but Pax2-expressing dl4 neurons would be unchanged. The cell counts prove the second hypothesis to be right. Lbx1⁺ cells are reduced by ~17%, while dl4 neurons expressing Pax2 are unchanged in numbers (Fig. 11m). This indicates that, in the absence of *Gsh1* and *Gsh2*, dl5 neurons are lost and do not get respecified.

In summary, these findings indicate that *Gsh1* and *Gsh2* are partially functional redundant. In each single mutant dl4 and dl5 neurons are specified correctly, but *Gsh2* is required for dl3 neurons independently of *Gsh1*, which is due to the fact that *Gsh1* is not expressed in dl3 progenitors. However, in the absence of both *Gsh1* and *Gsh2*, dl5 neurons are lost. The development of dl4 neurons seemed to be independent of *Gsh1/2*, as these interneurons develop normal in the *Gsh1/2*^{-/-} spinal cord.

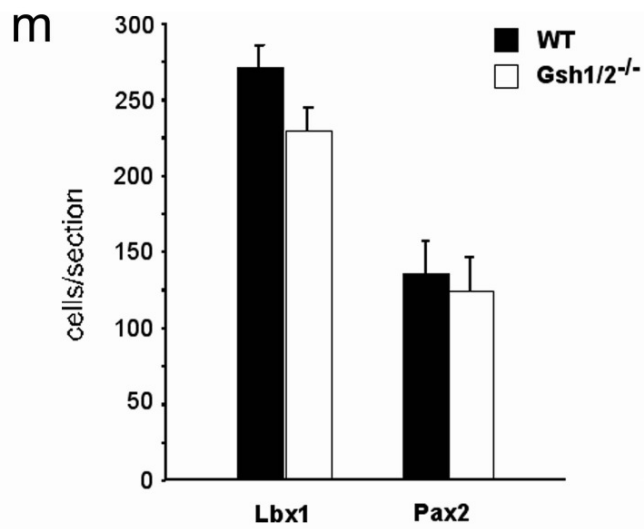
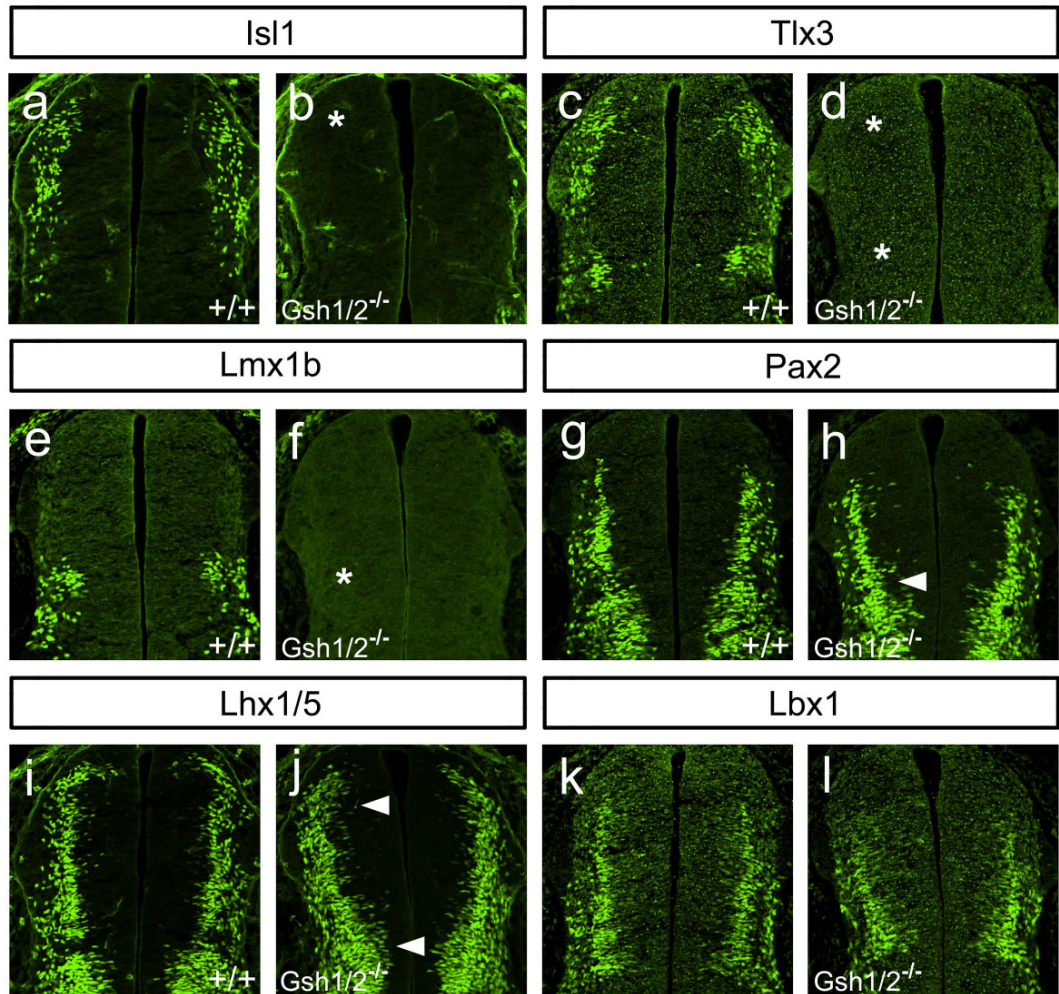


Figure 11: Analysis of *Gsh1/2*^{-/-} spinal cords at E11.5. (Fig. 11a, b) Isl1-expressing dl3 neurons are completely missing (asterisk in b) in *Gsh1/2*^{-/-} mice. (Fig. 11c, d) Tlx3 expression is all but absent in mice lacking *Gsh1* and *Gsh2*, indicating a loss of dl3 as well as dl5 neurons (asterisks in d). (Fig. 11e, f) Lmx1b is absent in the *Gsh1/2*^{-/-} spinal cord, confirming the loss of dl5 neurons (asterisks in f). (Fig. 11g, h) Presumptive dl5 neurons express Pax2 (arrowhead in h), suggesting that these cells adopt a dl4 or dl6 fate in the *Gsh1/2*^{-/-} spinal cord. (Fig. 11i, j) dl3 and dl5 neurons, which are Lhx1/5 negative in wt embryos, express Lhx1/5 when both *Gsh1* and *Gsh2* are absent (arrowheads in j), indicating a switch in cell fates of dl3 and dl5 neurons. (Fig. 11k, l) Lbx1 expression is unchanged in the *Gsh1/2*^{-/-} spinal cord. (Fig. 11m) Cell counts of Lbx1-expressing dl4-dl6 neurons in wt and *Gsh1/2*^{-/-} spinal cords at lumbar level revealed a reduction in Lbx1⁺ neurons in the absence of *Gsh1* and *Gsh2*. The number of Pax2⁺ dl4 neurons, however, was unchanged compared to wt littermates. These data indicate that dl5 neurons do not get respecified as dl4 neurons in *Gsh1/2*^{-/-} embryos. Instead, the dl5 population is lost.

3.1.4 Analysis of dorsal IN progenitors in *Gsh1/2*^{-/-} embryos

The loss of dl3 and dl5 neurons in the *Gsh1/2*^{-/-} spinal cord led me to question whether the patterning of the neuronal precursors that give rise to these interneuron populations is altered in these mice. To investigate this, I analyzed the expression pattern of several transcription factors including *Msx1*, *Dbx2*, *Olig3*, *Ngn1* and *Mash1* in the dorsal vz of wt and *Gsh1/2*^{-/-} spinal cords. All of these transcription factors are expressed in subsets of dorsal progenitors.

At E10.5 the homeodomain protein *Msx1* is expressed in dl1-3 Class A precursors in wt embryos, where it overlaps with *Gsh2* in the progenitors of dl3 interneurons. In contrast, *Msx1* and *Gsh1* share a boundary between dl3 and dl4 progenitors. In *Drosophila*, *Msh* and *Ind*, which are the homologs of *Msx1/2* and *Gsh1/2*, respectively, repress each other, thereby establishing two non-overlapping domains. I reasoned that *Gsh1* might repress *Msx1* expression and that *Msx1* would expand ventrally into the dl4 and dl5 progenitors in *Gsh1/2*^{-/-} embryos. However, *Msx1* expression remains restricted to dl1-dl3 progenitors in the absence of *Gsh1/2* (Fig. 12a, b), indicating that cross-inhibitory regulations between *Msx1* and *Gsh1/2* do not play a prominent role in establishing the boundary between TGFβ-dependent Class A neurons and TGFβ-independent Class B neurons in the dorsal spinal cord.

The homeodomain protein *Dbx2* is expressed ventrally to *Gsh1/2* in progenitors of dl6, V0 and V1 interneurons. *In situ* hybridization analysis indicates that the expression pattern of *Dbx2* is unchanged in the *Gsh2*^{-/-} spinal cord (Kriks, 2003). Nevertheless, it is possible that *Gsh1* and *Gsh2* together are required for the establishment of the dl5/dl6 boundary and that in their absence *Dbx2* would expand dorsally. I investigated this, by analyzing the expression of *Dbx2* by *in situ* hybridization in mice lacking both *Gsh1* and *Gsh2*. No change in *Dbx2* expression is observed in the *Gsh1/2*^{-/-} spinal cord compared to wt littermates, demonstrating that *Gsh1/2* do not establish the boundary between dl5 and dl6 progenitors by repressing *Dbx2* expression (Fig. 12c, d).

Recently, Muller et al. (2005) outlined a role for the bHLH transcription factor *Olig3* in specifying Class A (dl1-dl3) neurons. *Olig3* is expressed in dl1-dl3 progenitors in spinal cords at E10.5 and mice lacking *Olig3* do not develop dl3 neurons, which I also observe in *Gsh2*^{-/-} and *Gsh1/2*^{-/-} animals. To test whether *Olig3*-expressing Class A progenitors expand ventrally when *Gsh1* and *Gsh2* are inactivated, I examined the expression of *Olig3* by *in situ* hybridization in E10.5 wt and *Gsh1/2*^{-/-} embryos. *Olig3* expression is unaltered, indicating that cross-repressive interactions between *Gsh1/2* and *Olig3* do not position the boundary between Class A and Class B neurons (Fig. 12e, f). This lack of *Olig3* expansion might explain, why dl4 neurons are still present in the *Gsh2*^{-/-} and *Gsh1/2*^{-/-} spinal cords.

Another bHLH transcription factor, *Ngn1*, is expressed in the progenitors of dl2 and dl6 interneurons, which abut the *Gsh1/2* expression domain dorsally and ventrally. This pattern of *Ngn1* expression, together with my previous demonstration that *Ngn1* expression expands ventrally into the dl3 progenitor domain in *Gsh2*^{-/-} embryos (Kriks, 2003), suggested that *Gsh1/2* might repress *Ngn1* expression in presumptive dl3-dl5 progenitors. This, in turn, led me to ask whether *Ngn1* would expand into the dl4/dl5 progenitor domain in the *Gsh1/2*^{-/-} spinal cord. *In situ* hybridization analysis of the *Ngn1* expression pattern prove this hypothesis to be right: In *Gsh1/2*^{-/-} spinal cords, *Ngn1* expression encompasses dl3, dl4 and dl5 neurons, in addition to their endogenous dl2 and dl6 expression domains (Fig. 12g, h).

In the *Gsh2*^{-/-} spinal cord, *Mash1* expression is reduced in putative dl3 progenitors due to the ventral expansion of *Ngn1* expression (Kriks, 2003). The ectopic *Ngn1* expression in dl3, dl4 and dl5 precursors in *Gsh1/2*^{-/-} embryos

therefore predict a downregulation of Mash1 protein. Indeed, immunohistochemical analysis using an antibody specific against Mash1 show a strong decrease in the level of Mash1 expression throughout its entire dorsal expression domain (Fig. 12i, j). However, low levels of Mash1 protein are still detectable in the *Gsh1/2*^{-/-} cord.

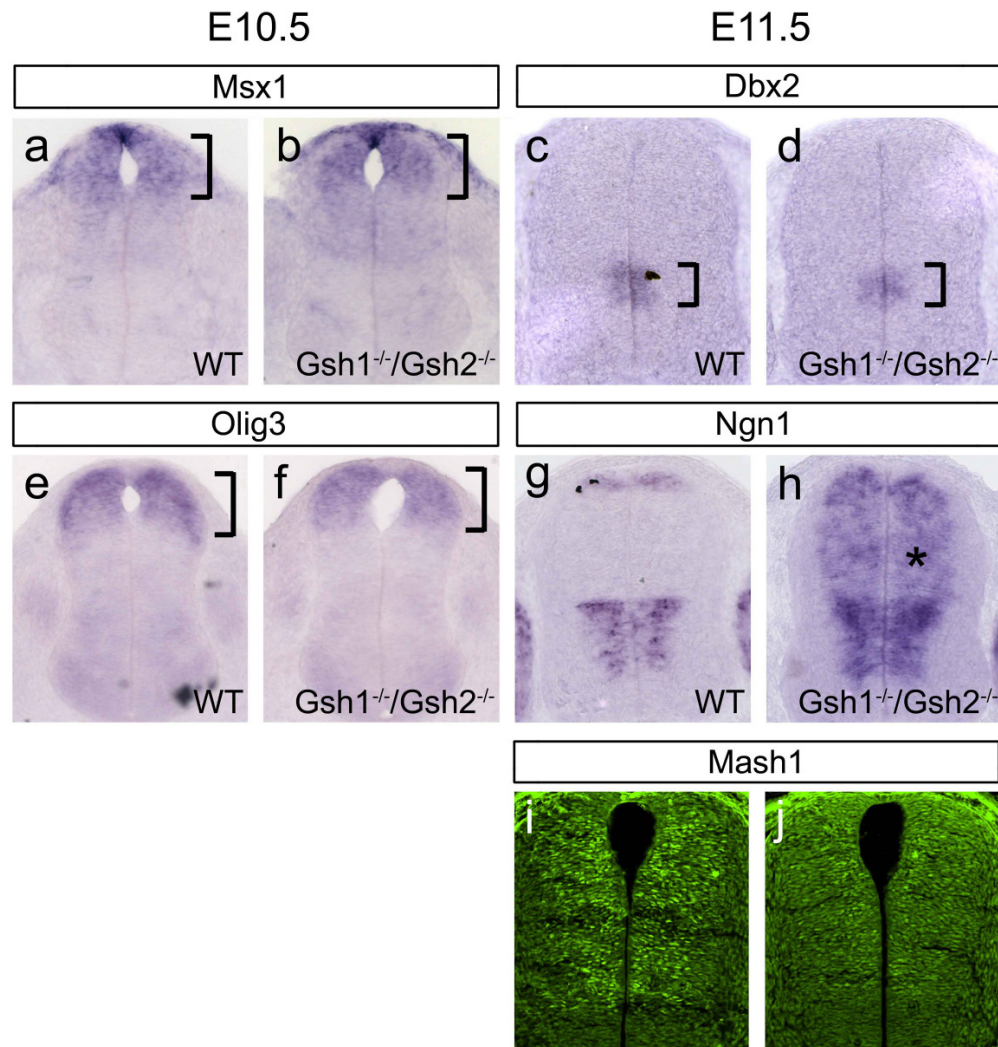


Figure 12: Expression of transcription factors in the ventricular zone of E10.5 and E11.5 *Gsh1/2*^{-/-} embryos. (Fig. 12a, b) At E10.5 *Msx1* is expressed in progenitors of dl1-3 neurons and does not expand ventrally in the absence of *Gsh1* and *Gsh2* (brackets). (Fig. 12c, d) *Dbx2* expression is unchanged in E11.5 *Gsh1/2*^{-/-} cords (brackets). (Fig. 12e, f) The bHLH transcription factor *Olig3* is expressed in dl1-3 progenitors at E10.5 and its expression is unaltered in *Gsh1/2*^{-/-} embryos indicating that *Gsh1/2* do not function by restricting *Olig3* expression. (Fig. 12g, h) *Ngn1* is expressed in dl2 and dl6 progenitors in the dorsal spinal cord. In the absence of *Gsh1/2*, *Ngn1* expands to encompass also dl3, dl4 and dl5 precursors. (Fig. 12i, j) *Mash1* is significantly reduced in E11.5 *Gsh1/2*^{-/-} spinal cords, most likely due to the repression by *Ngn1*.

3.2 Functional analysis of bHLH factors expressed in dorsal interneuron progenitors

My expression analyses of proteins/genes in the dorsal vz indicate that cross-inhibitory interactions between homeodomain proteins, as it is also seen in the ventral spinal cord of vertebrates and in *Drosophila*, might not play a prominent role in establishing discrete progenitor populations in the dorsal half of the spinal cord. In particular, no change in the expression of *Msx1* and *Dbx2* occurs in the spinal cord of *Gsh1/2*^{-/-} embryos. Instead, my data suggests a model in which the homeodomain proteins *Gsh1* and *Gsh2* regulate the expression of the bHLH transcription factors *Mash1* and *Ngn1* and that this regulation might be the critical step for the activation of differentiation programs for distinct dorsal interneuron populations.

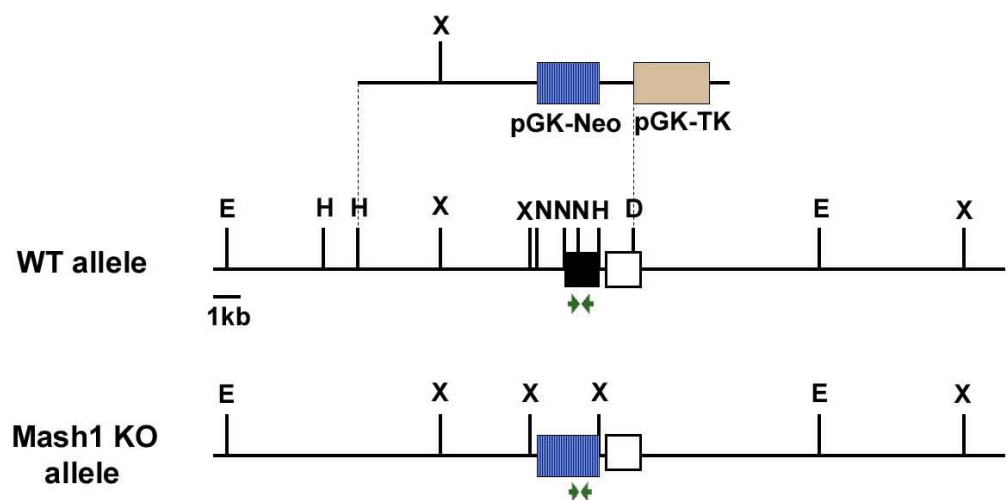
3.2.1 Functional analysis of *Mash1*

The bHLH transcription factor *Mash1* is co-expressed in the same domain as *Gsh2* in progenitors of dl3, dl4 and dl5 neurons (Kriks, 2003). In the *Gsh2*^{-/-} cord, *Mash1* expression is reduced in dl3 precursors but is maintained in progenitors of dl4 and dl5 neurons, suggesting that *Mash1* may also play a role in the development of dorsal interneurons. Further evidence for this hypothesis comes from the analysis of mice lacking *Gsh1* and *Gsh2*. These animals exhibit a strong reduction in the level of *Mash1* expression that is concomitant with the loss of two dorsal types of interneurons. To address whether *Mash1* functions as an

important determinant of dorsal interneuron cell fate, I analyzed *Mash1*^{-/-} embryos at E11.5 for expression of *Foxd3* (dl2), *Isl1* (dl3), *Lbx1* (dl4-dl6), *Lhx1/5* (dl2, dl4, dl6), *Pax2* (dl4, dl6) and *Lmx1b* (dl5).

3.2.1.1 Genotyping of *Mash1*^{-/-} embryos

Mice in which the gene encoding the bHLH transcription factor Mash1 has been inactivated, were obtained from Francois Guillemot (National Institute for Medical Research, London, UK). A colony of *Mash1*^{+/-} mice was established by breeding these heterozygous founder animals with wt ICR females. Litters were screened for heterozygous animals by PCR against the neomycin-resistance cassette. Homozygous *Mash1*^{-/-} animals are not viable; therefore homozygous embryos were generated by mating females heterozygous for the *Mash1* allele with heterozygous *Mash1*^{+/-} males. PCR was used to genotype the offspring of these crosses. For this purpose two primer pairs were utilized (Fig. 13). The wt allele was detected using one set of primers that amplifies a 680 bp fragment of the *Mash1* coding region, which is located within the sequence deleted by the insertion of the neomycin-resistance gene in *Mash1*^{-/-} mice. The second primer pair amplified a 380 bp sequence from the neomycin resistance gene to detect the mutant allele (Fig. 14). Mutant embryos were obtained in a 1:4 Mendelian ratio.



adapted from Guillemot et al., 1993

Figure 13: Schematic of the gene targeting strategy to delete *Mash1*. The black box represents the protein-coding sequence of the gene; the white box represents the 3' untranslated region (Guillemot et al., 1993). Green arrows mark the regions in the wt and KO allele, which get amplified by the two primer pairs. D=DraI, E=EcoRI, H=HpaI, N=NotI, X=XbaI

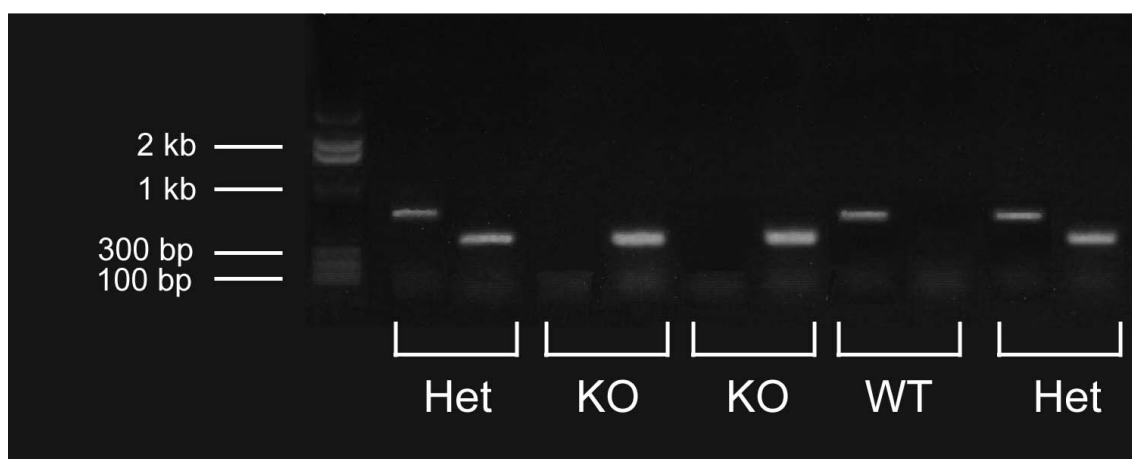


Figure 14: Example of genotyping for *Mash1* mutant and wt alleles. Two sets of primers were used to amplify fragments from the wt and the *Mash1* KO alleles. The PCR reaction for the wt locus resulted in a 680bp band, whereas the reaction for the KO allele gives a 380 bp PCR product. Embryos heterozygous for both alleles, wt as well as KO, show PCR products with both sets of primers, while wt embryos only have the band for the wt allele. *Mash1*^{-/-} embryos only have the band for the KO allele.

3.2.1.2 Analysis of *Mash1*^{-/-} spinal cords

Cross-sections of E11.5 *Mash1*^{-/-} embryos were analyzed for the proper specification of early-born dorsal interneurons by immunohistochemistry, using antibodies against marker proteins specific for each of the interneuron populations. In *Mash1*^{-/-} cords, the number of Isl1-expressing dl3 neurons is significantly reduced compared to wt littermates (Fig. 15a, b). To test whether

most of the presumptive dl3 cells in the *Mash1*^{-/-} cord develop as dl2 neurons, as seen in the *Gsh2*^{-/-} cord, antibody stainings are performed against Foxd3. The number of Foxd3-positive dl2 neurons is slightly increased in mice lacking *Mash1* compared to age-matched wt littermate embryos (Fig. 15c, d). Moreover, these cells are expressing Lhx1/5 (Fig. 15e, f), supplying further evidence that these neurons develop a dl2 instead of a dl3 cell fate. Cell counts on Foxd3-positive dl2 neurons and Isl1-expressing dl3 neurons are performed to examine this switch in cell fate in more detail. Cells labeled with either of these two markers were counted in forelimb level sections of E11.5 *Mash1*^{-/-} cords and wt littermates. These cell counts reveal that *Mash1*^{-/-} embryos exhibit a ~75% loss of dl3 neurons with a concomitant ~30% increase in dl2 neurons (Fig. 15m). The reduction of dl3 neurons in the *Mash1*^{-/-} spinal cord is less pronounced than in the *Gsh1/2*^{-/-} spinal cord, where almost all Isl1-expressing dl3 neurons are absent (Fig. 15m). It therefore appears that while *Mash1* is necessary for the specification of dl3 neurons, *Gsh2* and possibly *Olig3*, which are positioned upstream in the genetic hierarchy specifying dl3 interneurons, play a more marked role.

Antibody stainings in *Mash1*^{-/-} embryos against Lhx1/5 reveal another striking phenotype. Lhx1/5 is expressed in dl2, dl4 and dl6 interneurons in wt spinal cords, leaving a gap of expression in dl3 and dl5 neurons. These gaps in the expression pattern of Lhx1/5 are not visible in the *Mash1*^{-/-} cord (Fig. 15e, f), implying that either dl5 neurons express ectopic Lhx1/5, or that dl5 neurons are no longer generated in the absence of *Mash1*. To distinguish between these two possibilities, I used an antibody against Lmx1b, which specifically labels the dl5 subtype of interneurons at E10.5-E11.5. Not surprisingly, Lmx1b-positive cells are missing in the *Mash1*^{-/-} spinal cord, indicating that dl5 neurons are absent in the *Mash1*^{-/-} spinal cord (Fig. 15g, h). Further evidence for the loss of this interneuron population comes from antibody stainings against Pax2. Pax2, which is normally expressed in the dl4 and the dl6 neurons, but not in dl5 neurons, is expanded (Fig. 15k, l). Pax2 is therefore expressed in neurons populating the presumptive dl5 domain in addition to its normal expression in dl4 and dl6 neurons, which is consistent with the loss of dl5 neurons.

In contrast to the reduction/loss of the dl3 and dl5 interneuron populations that occurs in the *Mash1*^{-/-} spinal cord, dl4 neurons appear to be properly specified as indicated by the unchanged expression pattern of Lhx1/5 and Pax2 in this domain (Fig. 15e, f, k, l). Further evidence for the correct

development of dl4 neurons comes from an unchanged expression pattern of *Lbx1*. This transcription factor marks dl4-dl6 interneurons in wt cords, and no change in its expression is detected in the *Mash1*^{-/-} spinal cord (Fig. 15i, j).

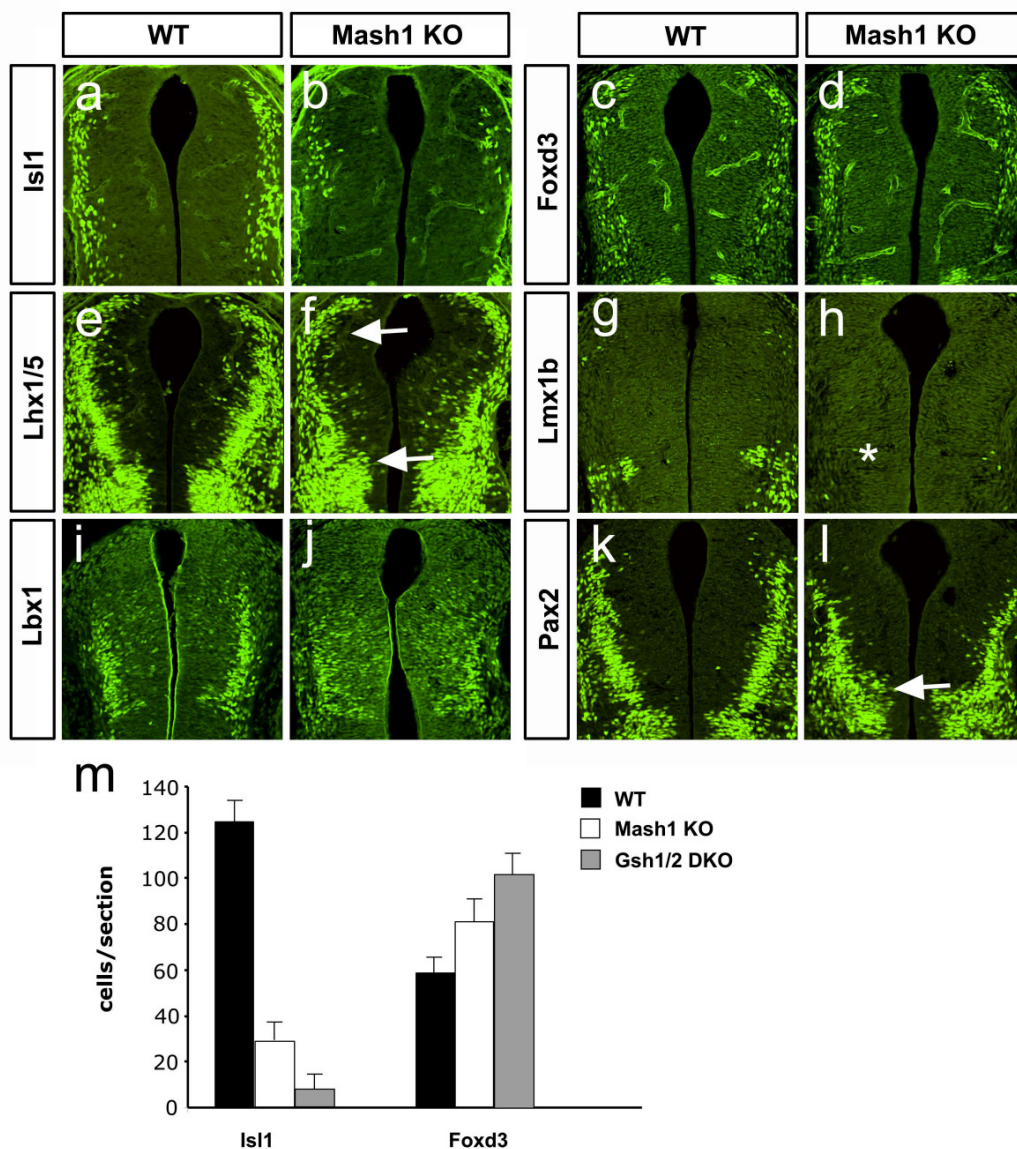


Figure 15: Analysis of *Mash1*^{-/-} spinal cords at E11.5. (Fig. 15a, b) dl3 neurons are strongly reduced in *Mash1*^{-/-} embryos, as evidenced by the reduced number of *Isl1*-expressing cells. (Fig. 15c, d) The number of *Foxd3* neurons is increased in mice lacking *Mash1*, suggesting that prospective dl3 neurons develop as dl2 cells. (Fig. 15e, f) Further evidence for the switch in cell fate from a dl3 to a dl2 fate comes from antibody staining against *Lhx1/5*. dl2 neurons, which normally do not express *Lhx1/5*, are *Lhx1/5*⁺ in the *Mash1*^{-/-} embryo. Prospective dl5 neurons also express *Lhx1/5*, suggesting that dl5 neurons are incorrectly specified. (Fig. 15g, h) Further support for the

loss of dl5 neurons in the *Mash1*^{-/-} spinal cord comes from Lmx1b staining. Lmx1b-expressing cells are missing in the absence of *Mash1*. (Fig. 15i, j) Lbx1 expression does not change in the *Mash1*^{-/-} spinal cord, suggesting that dl4 neurons develop normally. (Fig. 15k, l) Pax2 continues to be expressed in dl4 and dl6 neurons, which indicates a proper specification of these interneuron subtypes. However, prospective dl5 neurons are also Pax2⁺, which is consistent with the loss of Lmx1b. These neurons adopt either a dl4 or a dl6 fate. (Fig. 15m) Cell counts of Isl1-expressing dl3 and Foxd3-expressing dl2 neurons in both E11.5 *Mash1*^{-/-} and *Gsh1/2*^{-/-} spinal cords at forelimb levels. *Gsh1/2*^{-/-} embryos exhibit a more dramatic loss of dl3 neurons than *Mash1*^{-/-} embryos, with more neurons adopting a dl2 identity.

Taken together, these findings demonstrate that Mash1 is an obligate determinant of two populations of dorsal interneurons, the dl3 and the dl5 subtypes. However, a third population of interneurons in the dorsal half of the spinal cord, dl4 neurons, that develop from Mash1-positive progenitors, develop independently from Mash1 function. The changes in the early-born interneuron populations in the *Mash1*^{-/-} cord mirror the changes in spinal interneuron development that are seen in mice lacking *Gsh1* and *Gsh2* and imply that *Mash1* acts downstream of *Gsh1/2* in the genetic hierarchy necessary for the generation of dl3 and dl5 interneurons in the dorsal half of the spinal cord.

3.2.1.3 Changes in transcription factor expression in dorsal IN progenitors of *Mash1*^{-/-} spinal cords

The cell fate switches observed in the *Mash1*^{-/-} spinal cord most likely result from the respecification of their progenitor domains. To test this hypothesis, the expression pattern of several transcription factors that are expressed in dividing progenitors in the ventricular zone were examined by either *in situ* hybridization or immunohistochemistry. The expression of the bHLH protein Ngn1 is unchanged in E11.5 *Mash1*^{-/-} embryos, with its dorsal domain being restricted to the dl2 progenitors, as seen in wt littermates. The ventral Ngn1 expression domain, including dl6, V0 and V1 precursors, is also unchanged (Fig. 16 a, b). However, in E10.5 mice embryos lacking *Mash1*, a transient ventral expansion of the dorsal Ngn1-positive domain, similar to that seen in the *Gsh2*^{-/-} cord, comprising the adjacent ventral dl3 progenitor domain is observed (Fig. 16e, f). It

therefore appears that at early times there is a transient expansion of dl2 progenitors into the dl3 progenitor domain. This observation is consistent with the increase in postmitotic dl2 neurons, concomitant with a reduction in dl3 neurons in the *Mash1*^{-/-} spinal cord (see Fig. 15a-d, m), as *Ngn1* is known to induce dl2 neurons (Gowan et al., 2002).

To test whether *Mash1* function is necessary for the expression of *Gsh1* and *Gsh2*, cross-sections of E11.5 *Mash1*^{-/-} embryos were stained with an antibody recognizing both *Gsh1* and *Gsh2*. In the absence of *Mash1*, *Gsh1/2* expression is still present in dl3-dl5 progenitors, consistent with the unchanged expression pattern of *Ngn1* at E11.5 (Fig. 16c, d). However, at E10.5 *Gsh1/2* expression is down regulated in the progenitors of the dl3 neurons in the *Mash1*^{-/-} cord. No change in *Gsh1/2* expression is seen in the adjacent dl4 and dl5 precursor domains (Fig. 16 g, h).

Taken together, these findings provide evidence that *Mash1* participates in the early formation of the dl2/dl3 boundary, either by directly blocking *Ngn1* expression in dl3 progenitors, or by activating *Gsh2* expression, which may in turn repress *Ngn1*. However, in the absence of *Mash1* the ventral *Ngn1* domain does not expand dorsally. This is most likely due to the unchanged expression of *Gsh1/2* in dl4 and dl5 progenitors, which may function to repress early dl6 determinants.

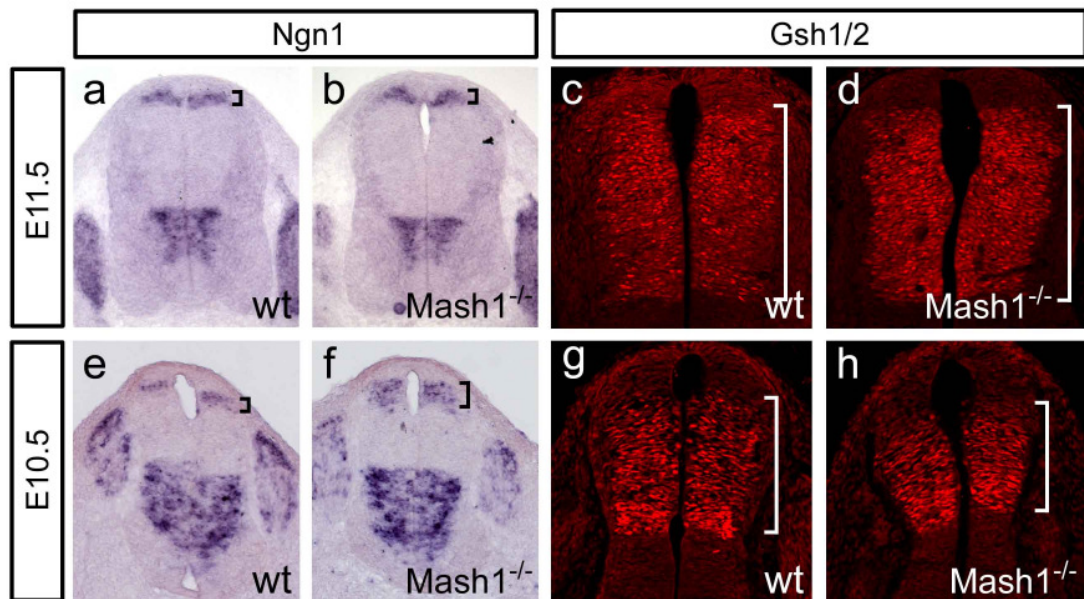


Figure 16: Expression analysis of *Ngn1* and *Gsh1/2* in E11.5 and E10.5 *Mash1*^{-/-} embryos. (Fig. 16a, b) *Ngn1* expression is unchanged in E11.5 *Mash1*^{-/-} cords (brackets). (Fig. 16c, d) *Gsh1/2* expression is also unchanged in mice lacking *Mash1* at E11.5. (Fig. 16e, f) However, at E10.5 the most dorsal *Ngn1* expression domain expands ventrally encompassing prospective dl3 neurons (brackets). This *Ngn1* expansion is consistent with dl3 neurons developing as dl2 cells in the *Mash1*^{-/-} spinal cord. (Fig. 16g, h) *Gsh1/2* is also reduced in dl3 progenitors in E10.5 *Mash1*^{-/-} embryos (brackets).

3.2.1.4 Gain-of-function analysis of *Mash1*

In my preliminary examination of the function of *Gsh2*, I showed that misexpression of *Gsh2* in the chick neural tube induces ectopic *Isl1*⁺ dl3 neurons (Kriks, 2003). However, this induction is not very robust, as ectopic *Isl1*-expressing cells are not found in every electroporated chick embryo. Besides, only a subset of cells expressing ectopic *Gsh2*, which are marked by the expression of GFP, expresses *Isl1*. Rather, the sporadic induction of *Isl1* seems to occur in a non-cell autonomous manner, as few GFP/*Isl1* double-labeled cells are found. These observations suggest that *Gsh2* alone is not the main activator of a dl3 cell fate. One possible candidate as the primary determinant of dl3 cell fate is *Mash1*. This transcription factor is expressed in progenitors of dl3 neurons and its expression is

reduced in *Gsh2*^{-/-} embryos that lack the dl3 population. Moreover, *Mash1*^{-/-} mice show a strong reduction in dl3 neurons (see Fig. 15a, b, m), suggesting Mash1 is necessary for dl3 neuron development.

To test whether Mash1 might function as a key inducing factor for promoting dl3 cell fate, an expression construct containing the full-length coding region of rat *Mash1* was injected into the lumen of HH12 staged chick embryos and then electroporated into one side of the neural tube by applying a current across the spinal cord. Because the expression vector used for this experiment does not contain an IRES sequence followed by GFP, electroporation efficiency was detected by staining with an antibody, which specifically recognizes Mash1 protein. Electroporated chick embryos were allowed to develop for 24-48h before analyzing them. Analysis of chick embryos electroporated with the Mash1 construct reveals a dramatic upregulation of Isl1-expressing cells, showing that Mash1 alone is sufficient to activate the dl3 differentiation program (Fig. 17a, b).

To test if *Mash1* also upregulates Tlx3 expression, adjacent sections were stained with an antibody against Tlx3. The expression of this transcription factor is also strongly upregulated on the electroporated side of the spinal cord (Fig. 17e, f). As Tlx3 is expressed in both, dl3 and dl5 interneurons, these ectopic Tlx3-expressing cells may have either a dl3 or a dl5 cell fate. To examine if *Mash1* also induces dl5 neurons, I stained with an antibody against Lmx1b, which specifically marks dl5 neurons at this stage. An increase in the number of Lmx1b-expressing dl5 neurons is also seen following *Mash1* overexpression. Ectopic Lmx1b⁺ neurons are found close to their endogenous domain and not throughout the whole spinal cord, as it is seen with Isl1 (Fig. 17g, h). In addition, a concomitant reduction in Lhx1/5 in presumptive dl2, dl4 and dl6 neurons is observed, arguing that *Mash1* induces dl3 and dl5 neurons at the expense of dl2, dl4 and dl6 neurons (Fig. 17c, d).

To test whether Mash1 is an active inducer of dl3 and dl5 cell fate or whether this upregulation is indirect and due to an upregulation of *Gsh2*, I analyzed the expression of *Gsh2* after *Mash1* misexpression. Chick embryos harvested 48h after electroporation do not show any evidence of *Gsh2* upregulation (Fig. 17i, j). However, embryos harvested 24h after electroporation show an induction of *Gsh2* in cells expressing ectopic Mash1. Moreover, these ectopic *Gsh2* positive cells are typically located close to the endogenous expression domain and not throughout the whole spinal cord, even though Mash1

is expressed throughout the entire neural tube (Fig. 17k, l). The induction of *Gsh2* in presumptive dl2 progenitors suggests that both *Mash1* and *Gsh2* function to repress the dl2 differentiation program. To further support this hypothesis, I investigated the expression of *Ngn1* in chick embryos following *Mash1* misexpression. Other studies have shown that *Ngn1* is an obligate determinant of dl2 cell fate, and thus the repression of *Ngn1* appears to be at the center of the mechanism by which *Mash1* and *Gsh2* regulate dl2/dl3 identity in the developing spinal cord. Electroporation of *Mash1* results in a significant decrease in *Ngn1* expression (Fig. 17m, n), showing that *Mash1* is able to down regulate *Ngn1* in dl2 progenitors and thus is able to repress a dl2 cell fate.

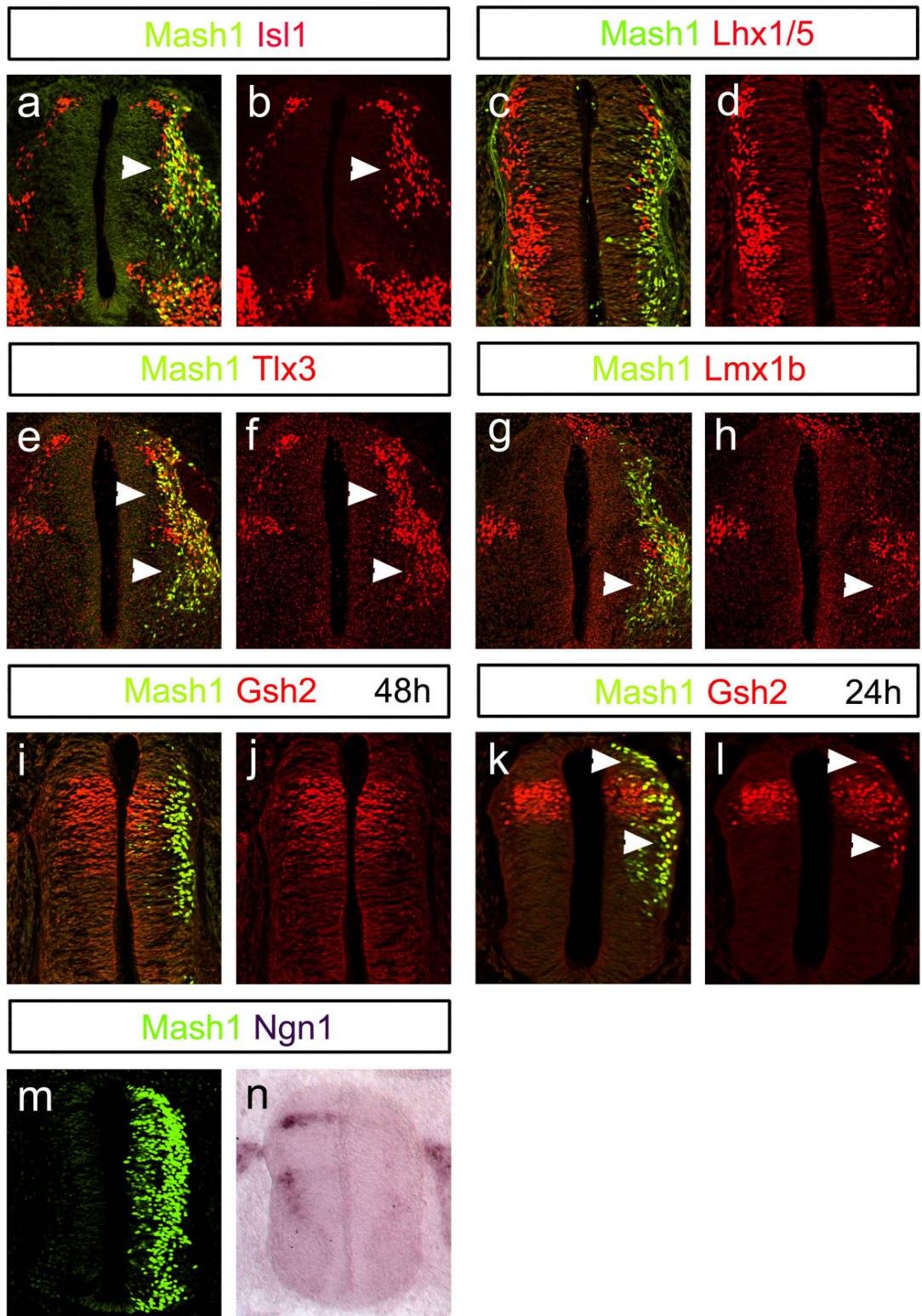


Figure 17: Overexpression analysis of *Mash1* in E3 chick neural tubes. (Fig. 17a, b) *Mash1* is able to induce a dl3 cell fate, as many ectopic *Isl*-expressing cells are seen on the electroporated side of the spinal cord (arrow). (Fig. 17c, d) dl2 and dl4 neurons expressing *Lhx1/5* are reduced following *Mash1* misexpression. (Fig. 17e, f) *Tlx3*-expressing cells are induced by *Mash1*, further supporting an induction of dl3 neurons by *Mash1* (upper arrow). Ectopic *Tlx3*⁺ cells are also found in the dl5 domain suggesting that *Mash1* can also induce dl5 neurons (Lower arrow). (Fig. 17g, h) More evidence for the induction of dl5 neurons by *Mash1* comes from antibody staining against *Lmx1b*. The number of *Lmx1b*⁺ cells is increased on the electroporated side of the spinal cord. Ectopic *Lmx1b*-expressing cells are expressing *Mash1*, indicating that *Mash1* induces dl5 neurons in a cell autonomous manner (arrow). (Fig. 17i, j) 48 hours after *Mash1* overexpression no change in *Gsh2* expression is noted. (Fig. 17k, l) However, 24 hours after electroporation of *Mash1* ectopic *Gsh2* cells are found (arrows), indicating that *Mash1* is able to transiently induce *Gsh2*. (Fig. 17m, n) *Ngn1* expression is strongly reduced following *Mash1* misexpression. The reduction of *Ngn1* is not only seen in dl2 progenitors, also the ventral *Ngn1* expression domain is almost completely missing.

3.3 Misexpression of *Gsh2*

The downregulation of *Ngn1* in the chick spinal cord following *Mash1* misexpression can be explained by either active repression of *Ngn1* by *Mash1* or by an indirect effect in which *Mash1* induces *Gsh2*, which in turn represses *Ngn1* expression. To test this hypothesis, I misexpressed a *Gsh2-EGFP* expression vector in the chick neural tube (Fig. 18a) and then analyzed the expression pattern of *Ngn1* and *Ngn2* mRNAs. The genes encoding both bHLH transcription factors are strongly repressed on the electroporated half of the neural tube compared to the control half. This repression is not only restricted to the dorsal *Ngn1* domain, but also occurs throughout the entire spinal cord, with dorsal and ventral *Ngn1* expression being almost completely abolished (Fig. 18b). *Ngn2* expression is also downregulated following *Gsh2* overexpression, although to a lesser extent than *Ngn1* (Fig. 18c).

The downregulation of *Mash1* in the dorsal spinal cord of *Gsh2*^{-/-} embryos suggests the possibility that *Gsh2* is also necessary for *Mash1* expression. To determine whether *Gsh2* actively induces *Mash1* expression, I analyzed the expression of *Mash1* protein in the chick neural tube after *Gsh2*

misexpression. No ectopic Mash1 protein is found following *Gsh2* overexpression, indicating *Gsh2* alone is not sufficient for Mash1 upregulation in dorsal progenitors (Fig. 18d, e).

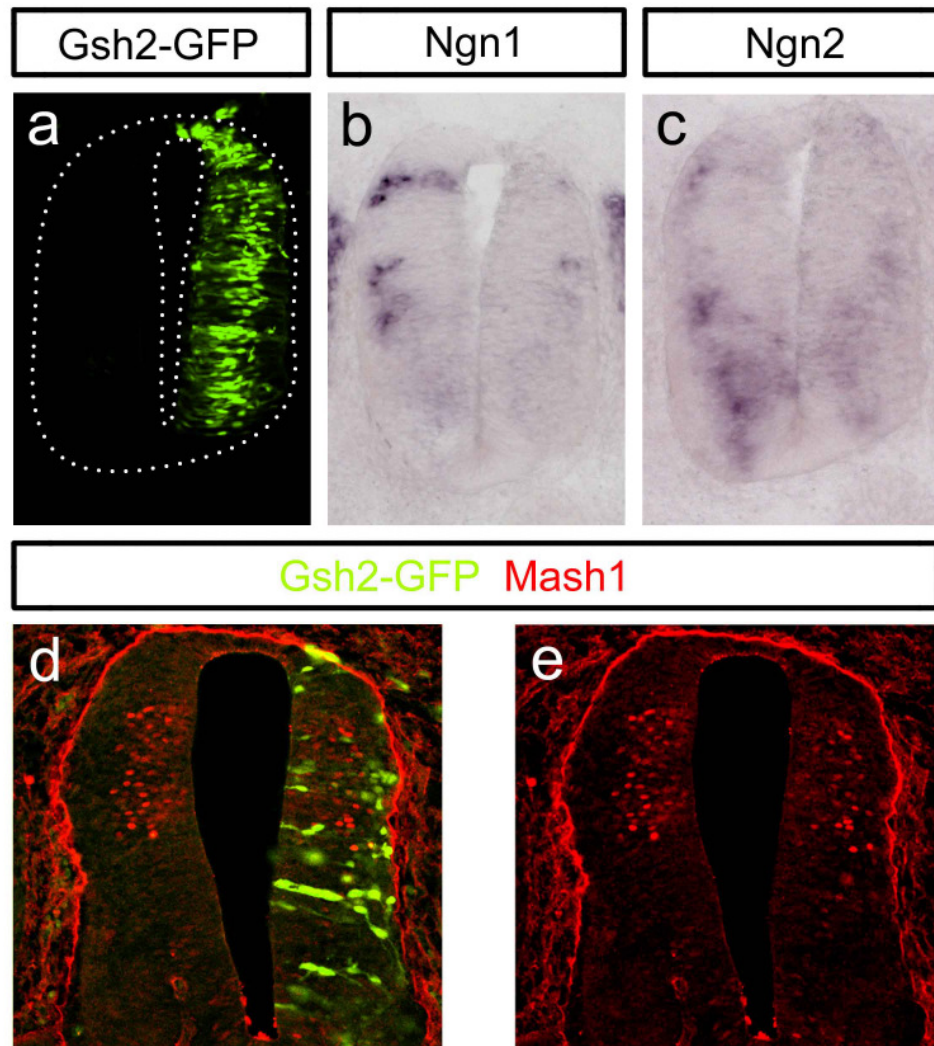


Figure 18: Overexpression analysis of *Gsh2* in E3 chick neural tubes. (Fig. 18a-c) *Ngn1* expression (Fig. 18b) and *Ngn2* expression (Fig. 18c) are strongly reduced on the electroporated side of the neural tube following *Gsh2* misexpression. (Fig. 18d, e) *Gsh2* does not induce Mash1, indicating that *Gsh2* alone is able to repress *Ngn1* and *Ngn2*.

Taken together, my results suggest a model in which *Gsh2* directly represses *Ngn1* and *Ngn2* in dl3 progenitors. This repression of *Ngn1/2* acts as a permissive signal for *Mash1*. Other factors may interact with *Gsh2* to specify dl3 neurons, one candidate being *Olig3*.

3.4 Functional analysis of *Ngn1*

The observed expansion of *Ngn1* expression in both the *Gsh2*^{-/-} and the *Mash1*^{-/-} spinal cord, together with the concomitant increase in dl2 neurons led me to ask whether *Ngn1* promotes a dl2 cell fate by repressing the transcriptional machinery necessary for the differentiation of dl3 neurons. To address this question I performed gain-of-function (GOF) as well as loss-of-function (LOF) analysis.

3.4.1 Gain-of-function analysis of *Ngn1*

3.4.1.1 Cloning of a full-length *Ngn1* cDNA

A construct for overexpressing the *Ngn1* gene in the chick spinal cord was generated by amplifying the *Ngn1* open-reading frame from E4 chick cDNA. A primer pair was designed, with the sense primer annealing 70 bp before the start codon and the antisense primer annealing at the stop codon. The sense primer also contained an *EcoRI* restriction site, and a *BamHI*-site is included in the antisense primer (see 7.1.3 for sequence). The amplified *Ngn1* cDNA was subsequently cloned into the pIRES-EGFP expression vector (Clontech) using the *EcoRI* and *BamHI* restriction sites in the multiple cloning site (MCS) of the vector. Sequencing from the 5' end was utilized to determine that the insert was in the proper orientation and did not contain point mutations from the PCR amplification reaction. This sequence was compared to the published *Ngn1* mRNA sequence (accession number: NM_010896) in the NCBI nucleotide database (<http://www.ncbi.nlm.nih.gov>) (see 7.2.1).

3.4.1.2 Electroporation of *Ngn1* into the chick spinal cord

E3 (HH11-13) chick embryos were electroporated with the *Ngn1*-IRES-*EGFP* expression construct and harvested 24-48h after electroporation. Cross-sections from these chick embryos were analyzed for the expression pattern of factors involved in the dl3 differentiation program, such as *Isl1*, *Gsh1/2* and *Mash1*. Differentiated dl3 neurons, marked by the expression of *Isl1* are all but absent following *Ngn1* misexpression (Fig. 19a, b). However, the generation of motor neurons (mn), which also express *Isl1*, is not repressed by *Ngn1*, as evidenced by the large number of cells expressing both GFP (*Ngn1*) and *Isl1* in the mn domain (Fig. 19a, b). *Pax2*-positive dl4, dl6, V0 and V1 neurons are also not reduced by ectopic *Ngn1*, suggesting that *Ngn1* specifically represses a dl3 cell fate (Fig. 19c, d). *Gsh2* (Fig. 19e, f) and *Mash1* expression (Fig. 19g, h) are almost completely abolished in dl3 precursors, suggesting that *Ngn1* alters the identity and specification of dl3 progenitors, which in turn results in the loss of dl3 neurons.

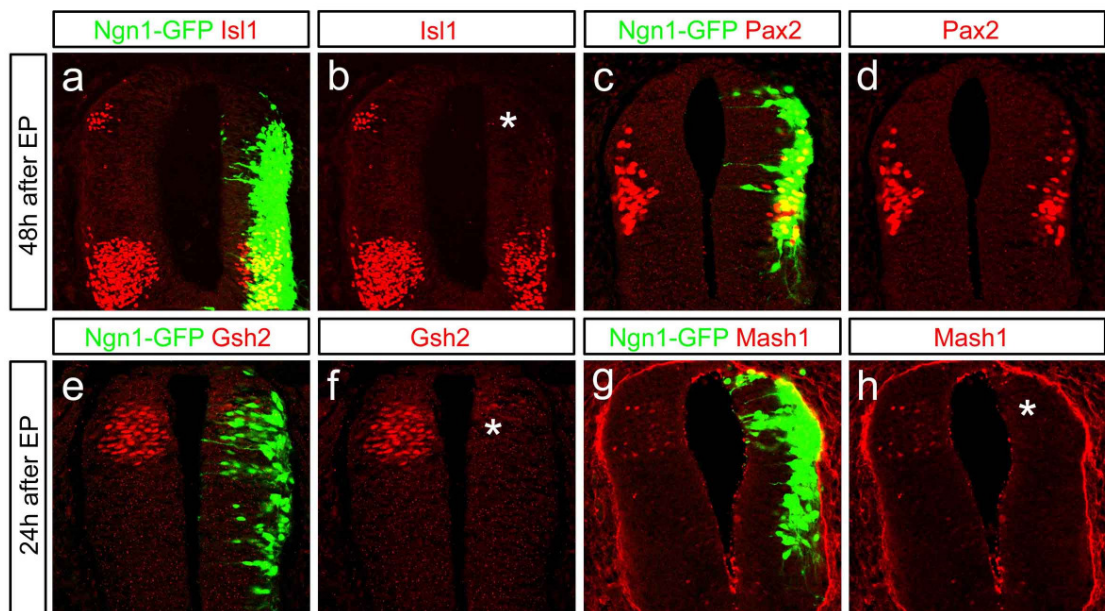


Figure 19: Misexpression of *Ngn1* in E3 chick spinal cords. (Fig. 19a-d) Embryos were allowed to develop for 48 hours after electroporation. (Fig. 19e-h) Embryos were allowed to develop for 24 hours after electroporation. (Fig. 19a, b) *Ngn1* represses a dl3 cell fate when overexpressed in the chick neural tube, as evidenced by the loss of *Isl1*-expressing dl3 neurons (asterisk in b). Motor neurons, however, are still present on the electroporated side. (Fig. 19c, d) *Pax2* was still expressed following misexpression of *Ngn1*, indicating that *Ngn1* does not effect dl4 and dl6 neuron development. (Fig. 19e, f) *Ngn1* strongly represses *Gsh2* (asterisk in f); therefore, *Ngn1* is able to repress a dl3 cell fate. (Fig. 19g, h) *Mash1* expression is also strongly down-regulated by *Ngn1* (asterisk in h).

3.4.2 Loss-of-function analysis of *Ngn1/2*

The ventral expansion of *Ngn1* in the *Gsh2*^{-/-} and *Mash1*^{-/-} spinal cords suggests that the dl3 progenitor domain may expand dorsally when *Ngn1* is lost. To examine this hypothesis, I analyzed the expression of *Gsh2* and *Mash1* in E11.5 *Ngn1/2*^{-/-} embryos. Interestingly, the dorsal expression of *Gsh2* and *Mash1* remains restricted to the dl2/dl3 progenitor boundary (Fig. 20a-d), although in some instances a few ectopic *Mash1*-positive cells are found more dorsal in dl2 precursors (Fig. 20d, arrow heads). The limited dorsal expansion of both transcription factors in the absence of *Ngn1/2* can be explained by a ventral expansion of the bHLH protein *Math1*, whose expression is restricted to dl1 progenitors in wt embryos but expands ventrally, also encompassing dl2 progenitors in the absence of both *Ngn1* and *Ngn2* (Gowan et al., 2001). Interestingly, ectopic cells expressing *Gsh2* and *Mash1* are located ventral to the dl5/dl6 border compared with wt littermates (Fig. 20a-d, arrows in b and d), indicating that *Ngn1* functions to repress both *Gsh2* and *Mash1*. I also analyzed the expression of the dl3 marker *Tlx3* to further investigate whether dl3 interneurons develop in the appropriate position. The number and position of *Tlx3*-expressing cells was unchanged compared to wt cords (Fig. 20e, f), consistent with the unaltered expression domain of *Gsh1/2* and *Mash1* in dl3 precursors.

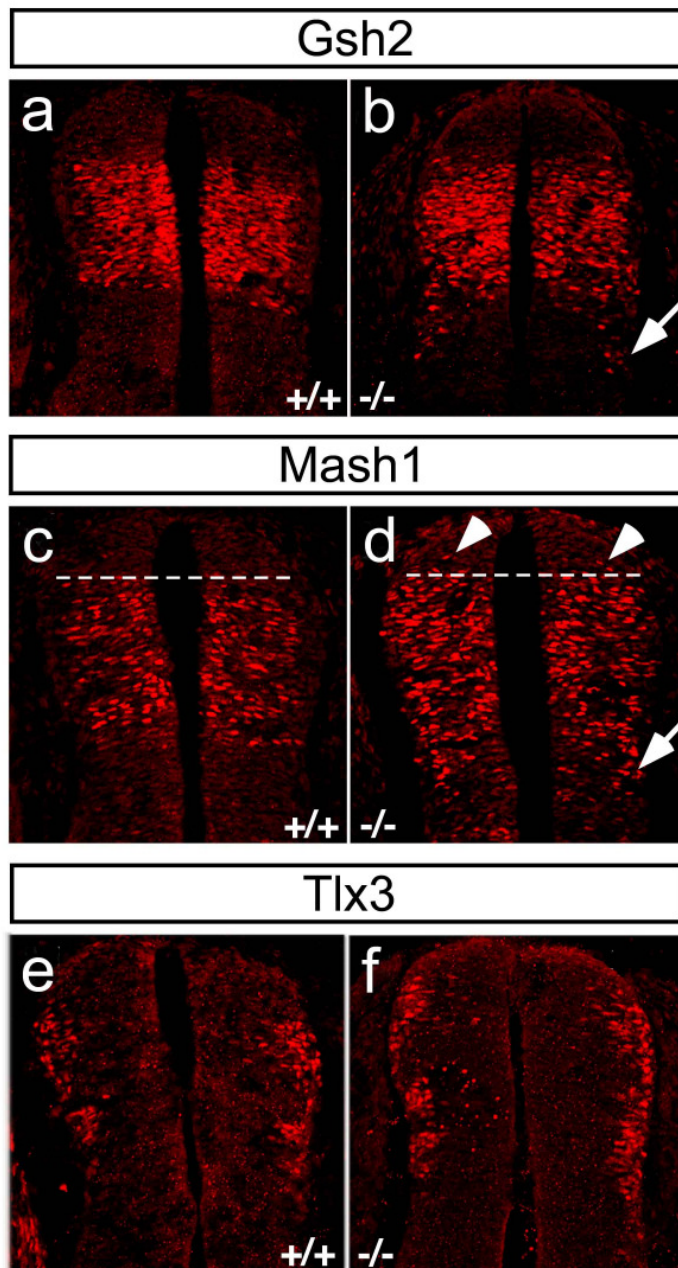


Figure 20: Analysis of E11.5 *Ngn1/2*^{-/-} spinal cords. (Fig. 20a, b) *Gsh2* does not expand dorsally in the absence of *Ngn1/2*. However, ectopic *Gsh2*⁺ cells are found ventral to the dl5/dl6 boundary in the *Ngn1/2*^{-/-} cord (arrow in b), indicating that *Ngn1/2* repress *Gsh2* expression. (Fig. 20c, d) A few ectopic *Mash1*-expressing cells are found dorsal to the dl2/dl3 boundary in the absence of *Ngn1/2* (arrowheads in d). *Mash1* expression expands ventrally compared to wt littermates in mice lacking *Ngn1/2* (arrow in d), showing that *Ngn1/2* repress *Mash1* expression in dl6 progenitors. (Fig. 20e, f) *Tlx3*⁺ dl3 neurons are unchanged in the *Ngn1/2*^{-/-} spinal cord, consistent with the lack of change in the dorsal boundary of *Gsh2* and *Mash1* expression.

3.5 The two late-born interneuron populations arise from Gsh1/2 positive progenitors

Early-born dl1-dl6 neurons are generated between E10.5-E11.5. A second phase of neurogenesis occurs between E12.0-E13.5. Neurons born during this time migrate to the dorsal horn, where they populate the most superficial layers of the dorsal horn (laminae I-III). These late-born neurons (dIL) express the transcription factor Lbx1 (Fig. 21a-c) and can be divided into two subtypes: dIL_A neurons that express the transcription factors Pax2 and Lhx1/5 (Fig. 21a, b) and differentiate as inhibitory GABAergic interneurons, and dIL_B neurons that are excitatory glutamatergic interneurons. dIL_B neurons can be distinguished from dIL_A cells by the expression of the transcription factors Lmx1b and Tlx1/3 (Fig. 21a, c).

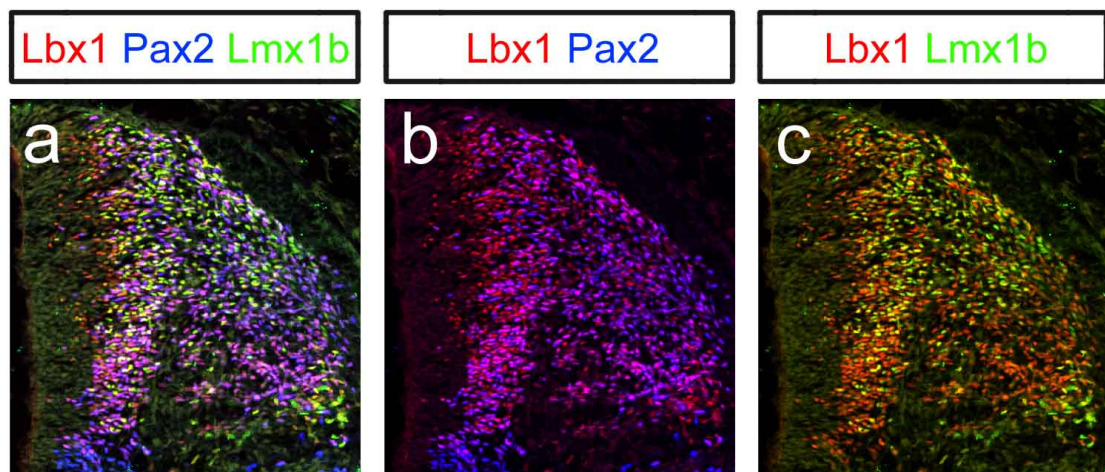


Figure 21: Distinction between two types of late-born (dIL) neurons in E12.5 wt spinal cords. (Fig. 21a-c) Two types of late-born neurons, which are generated between E12.0-E13.5, express the transcription factor Lbx1 (red). The dIL_A subtype can be distinguished from dIL_B neurons by the expression of Pax2 (blue) (Fig. 21a, b), whereas the dIL_B subtype express Lmx1b (green) (Fig. 21a, c).

Both of these two populations of late-born interneurons arise from a single dorsal progenitor domain, called the dIL progenitor domain, and are initially

intermingled within the subventricular zone (svz) (Gross et al., 2002; Muller et al., 2002). Once generated, these neurons leave the svz and migrate to the superficial dorsal horn, where each of the two subtypes preferentially populate different laminae. dIL_B neurons settle predominantly in the superficial laminae I and II, whereas dIL_A neurons preferentially populate laminae III and IV.

The neural precursors within the dIL progenitor domain express the homeodomain transcription factors Gsh1 and Gsh2 and the bHLH transcription factor Mash1 (Fig. 22a-g). As seen in E11.5 spinal cords, the Gsh1/2 and Mash1 expression overlaps completely in the dorsal spinal cord (Fig. 22c), and all three transcription factors appear to be co-expressed in the same cells (Fig. 22d). However, several cells express Gsh1/2, but are Mash1-negative (Fig. 22d, arrows), and vice versa (Fig. 22d, asterisks). These expression profiles, as well as their function in specifying subtypes of early-born dorsal interneurons, suggest that these transcription factors might act instructively to specify the identity of late-born dIL_A and dIL_B interneurons.

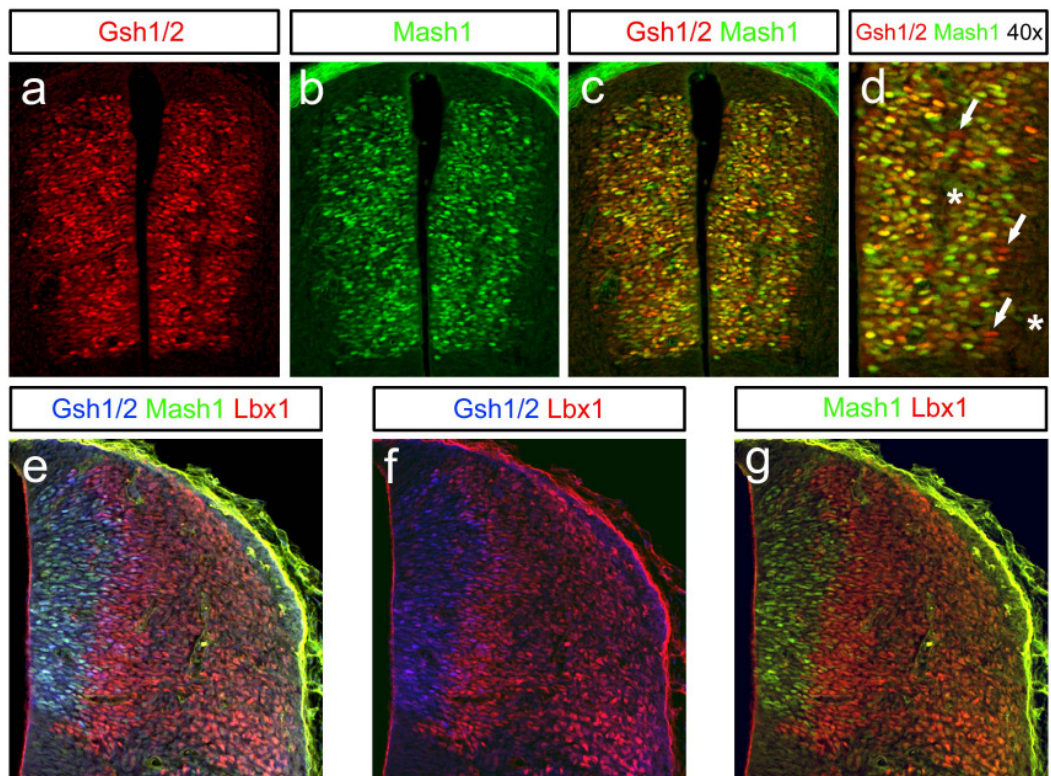


Figure 22: Expression pattern of markers of dIL progenitors in E12.5 wt spinal cords. (Fig. 22a-d) *Gsh1/2* and *Mash1* continue to be expressed during the second wave of neurogenesis (E12.0-E13.5). (Fig. 22c, d) *Gsh1/2* are expressed in the same domain as *Mash1* with most cells co-expressing both *Gsh1/2* and *Mash1*. However, a few cells are only *Gsh1/2*⁺ (arrows in d), whereas others only express *Mash1* (asterisks in d). (Fig. 22e-g) *Lbx1*⁺ late-born dIL neurons develop from *Gsh1/2*⁺ and *Mash1*⁺ progenitors.

3.6 Analysis of *Gsh1/2*^{-/-} spinal cord at E12.5, when late-born INs are being born

To investigate whether *Gsh1/2* play a critical role in specifying late-born interneurons (dIL), I analyzed the expression of *Lbx1*, which marks both subtypes of late-born interneurons in mice lacking either *Gsh1* or *Gsh2*, or *Gsh1* and *Gsh2*. The number of *Lbx1*-positive cells in the *Gsh1*^{-/-}, *Gsh2*^{-/-} and *Gsh1/2*^{-/-} embryos at E12.5 is similar to wt littermates (Fig. 23a-i).

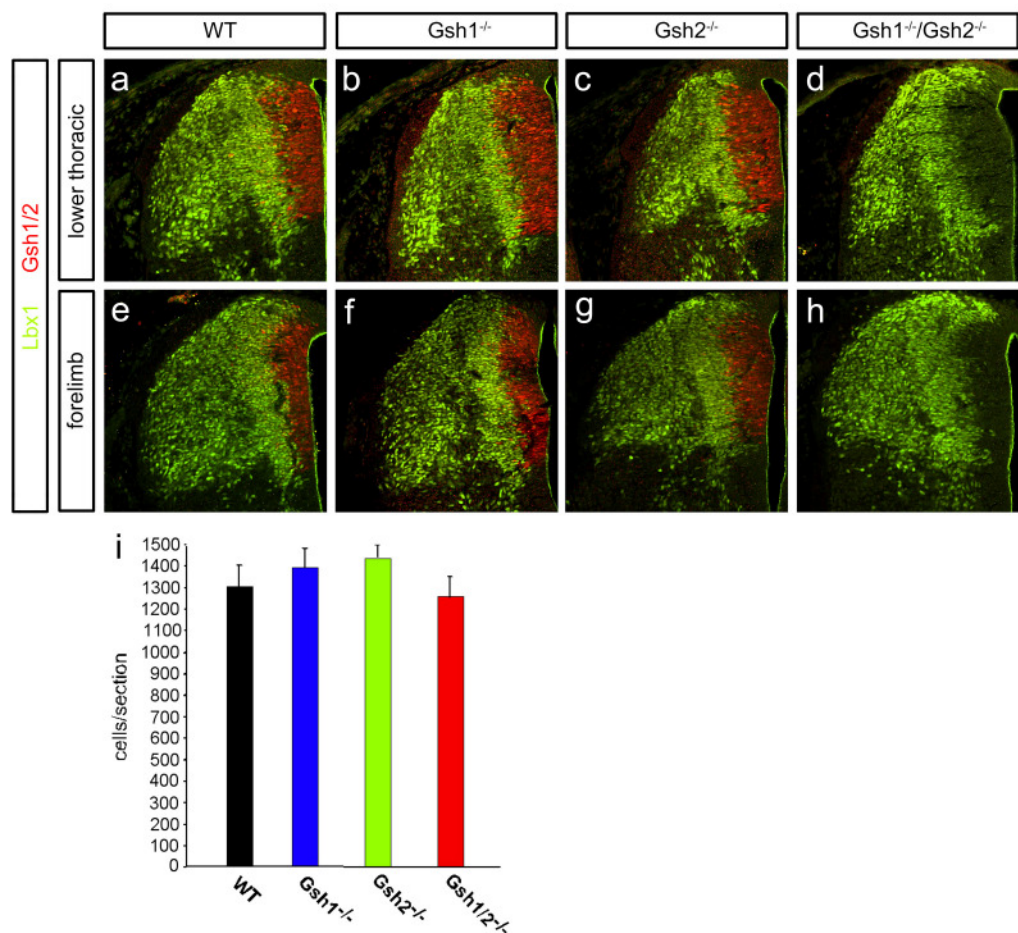


Figure 23: Analysis of Lbx1⁺ dIL neurons in E12.5 wt, *Gsh1*^{-/-}, *Gsh2*^{-/-} and *Gsh1/2*^{-/-} spinal cords at lower thoracic- and forelimb-levels. (Fig. 23a-c, e-g) Lbx1 (in green) is unchanged in mice lacking either *Gsh1* or *Gsh2* compared to age-matched wt littermates at both lower thoracic and forelimb levels. (Fig. 23d, h) The number of Lbx1⁺ dIL cells appears unchanged in the *Gsh1/2*^{-/-}, suggesting that late-born interneurons develop in the absence of *Gsh1* and *Gsh2*. (Fig. 23i) Cell counts of Lbx1-expressing cells at forelimb levels in wt, *Gsh1*^{-/-}, *Gsh2*^{-/-} and *Gsh1/2*^{-/-} spinal cord sections confirm that the number of dIL neurons is hardly changed in the *Gsh1*^{-/-} and *Gsh2*^{-/-} as well as the *Gsh1/2*^{-/-} spinal cord.

Considering that Lbx1 labels both of the late-born subtypes of interneurons, I analyzed the expression of Pax2 (dIL_A) and Lmx1b (dIL_B) in wild type, *Gsh1*^{-/-} and *Gsh2*^{-/-}, as well as in the *Gsh1/2*^{-/-} spinal cord, to distinguish between the dIL_A and dIL_B interneuron subtypes. In both, the *Gsh1*^{-/-} and *Gsh2*^{-/-} single mutants, Pax2 and Lmx1b expression are unchanged compared to wt embryos (Fig. 24a-c, e-g, i-k, m-o), indicating that late-born neurons develop correctly when only one of the *Gsh* genes is deleted. However, an increase in the number of Pax2-expressing dIL_A interneurons is noted in the svz and the mantle zone of *Gsh1/2*^{-/-} embryos (Fig. 24d, h). A concomitant loss of Lmx1b is observed in the spinal cord of *Gsh1/2*^{-/-} embryos (Fig. 24l, p), indicating a switch from dIL_B to dIL_A fate.

Neurons expressing Lhx1/5, another marker for dIL_A interneurons, are also increased in number in the *Gsh1/2*^{-/-} cord (Fig. 25d, h), whereas Tlx3, a postmitotic determinant for dorsal glutamatergic interneurons, is also completely missing in *Gsh1/2*^{-/-} mice (Fig. 25l, p). No change in Tlx3 and Lhx1/5 expression is detected in the *Gsh1*^{-/-} and *Gsh2*^{-/-} embryos, confirming the normal specification of dIL cells in these animals (Fig. 25a-c, e-g, i-k, m-o).

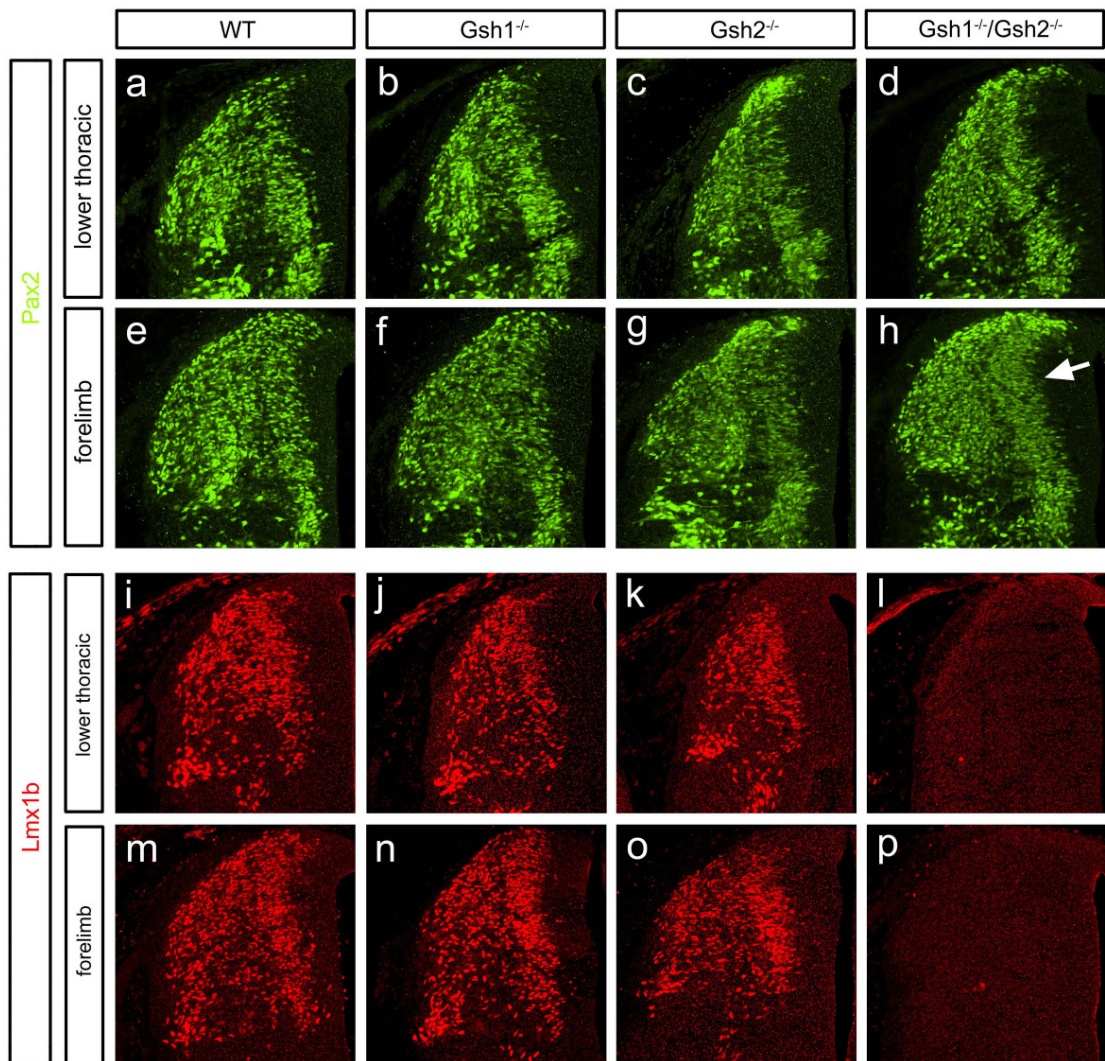


Figure 24: Examination of Pax2⁺ dIL_A and Lmx1b⁺ dIL_B neurons in E12.5 wt, *Gsh1*^{-/-}, *Gsh2*^{-/-} and *Gsh1*^{-/-}*Gsh2*^{-/-} spinal cords at lower thoracic- and forelimb-levels. (Fig. 24a-c, e-g) *Gsh1*^{-/-} and *Gsh2*^{-/-} cords show no difference in Pax2 expression compared to wt at both anterior-posterior levels, indicating a normal development of dIL_A neurons, when only one of the *Gsh* genes is missing. (Fig. 24d, h) The number of Pax2-expressing dIL_A neurons is increased in *Gsh1*^{-/-}*Gsh2*^{-/-} spinal cords. This increase is especially obvious in the svz at forelimb levels (arrow in h). (Fig. 24i-k, m-o) Lmx1b⁺ dIL_B neurons are properly specified in the *Gsh1*^{-/-} and *Gsh2*^{-/-} spinal cord compared to wt littermates at both early thoracic as well as forelimb levels. (Fig. 24l, p) However, in mice lacking *Gsh1* and *Gsh2*, Lmx1b-expressing neurons are completely missing, indicating a loss of late-born dIL_B neurons and confirming the loss of early-born dI5 neurons. These data indicate that both *Gsh1* and *Gsh2* together are required for the proper development of the dIL_B subtype of late-born neurons, whereas dIL_A neurons develop independently of *Gsh1/2*.

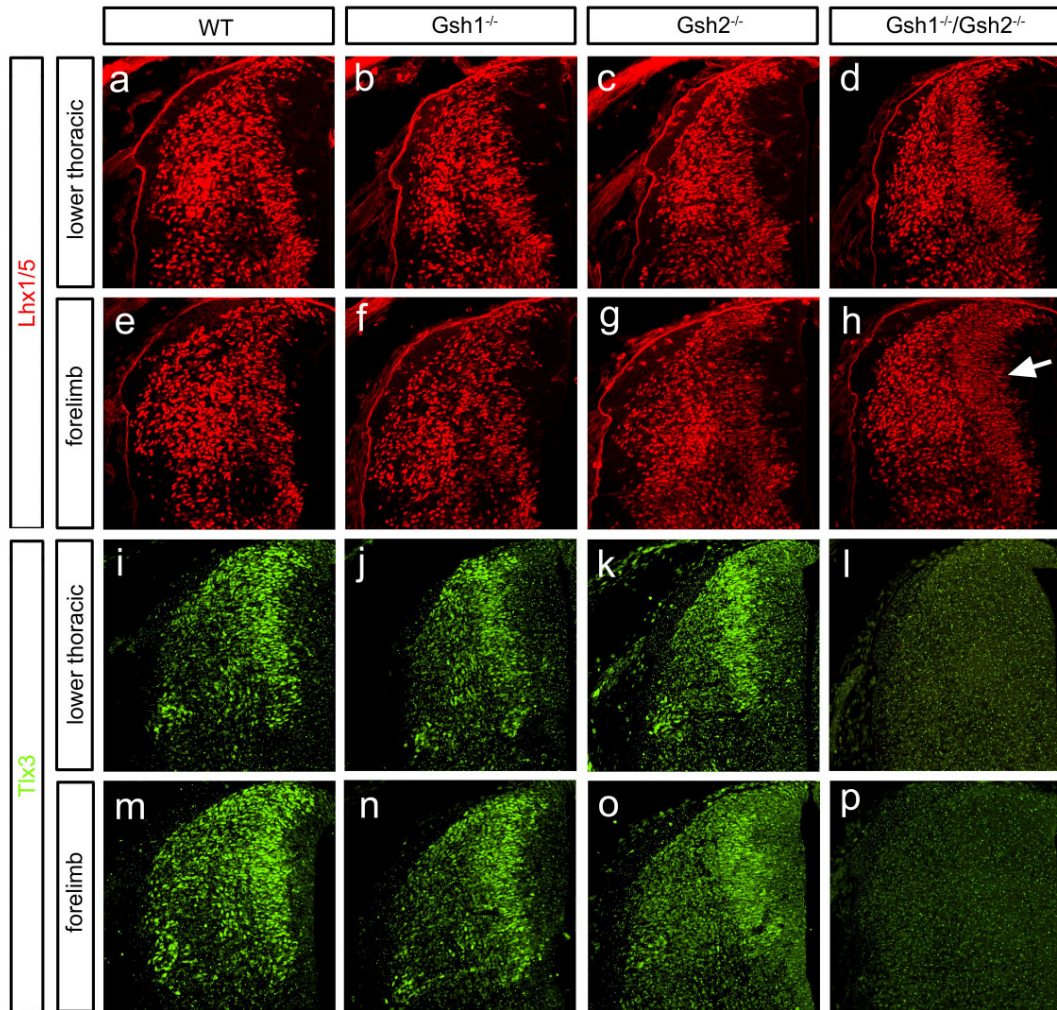


Figure 25: Analysis of dIL_A and dIL_B neurons marked by the expression of Lhx1/5 and Tlx3, respectively, in E12.5 *Gsh1/2*^{-/-} spinal cords at lower thoracic and forelimb levels. (Fig. 25a-c, e-g) Lhx1/5 expression is unchanged in *Gsh1*^{-/-} and *Gsh2*^{-/-} embryos compared to wt littermates at both A-P levels, indicating a proper development of dIL_A neurons in these mice. (Fig. 25d, h) *Gsh1/2*^{-/-} embryos show an increase in Lhx1/5⁺ dIL_A neurons. This increase is most obvious in the svz (arrow in h). (Fig. 25i-k, m-o) No change in Tlx3 expression is observed in mice lacking *Gsh1* and *Gsh2*, indicating a proper specification of dIL_B neurons when either *Gsh1* or *Gsh2* is missing. (Fig. 25l, p) The loss of TLx3 in the *Gsh1/2*^{-/-} cord confirms the loss of dIL_B neurons in the absence of *Gsh1* and *Gsh2*.

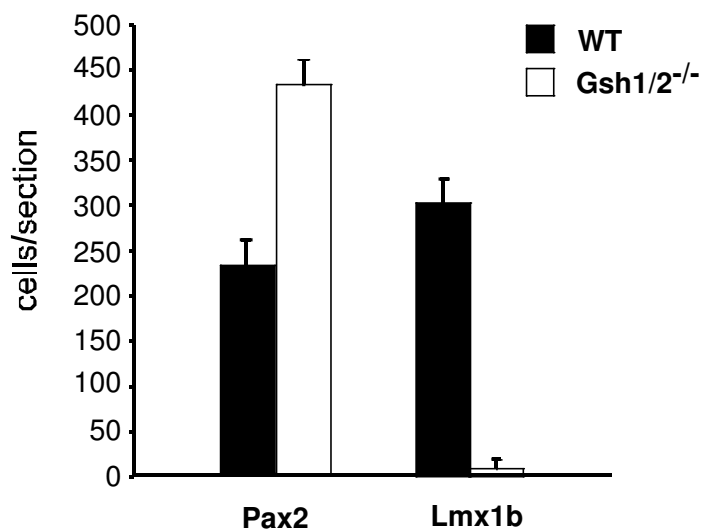


Figure 26: Cell counts of Pax2⁺ dIL_A and Lmx1b⁺ dIL_B neurons in forelimb sections of E12.5 wt and *Gsh1/2*^{-/-} spinal cords. Pax2-expressing dIL_A neurons are almost doubled in number in the *Gsh1/2*^{-/-} spinal cord. Concomitant with the loss in dIL_A neurons, Lmx1b⁺ dIL_B neurons are almost completely missing in the absence of *Gsh1* and *Gsh2*, indicating a switch in cell fate from a dIL_B to a dIL_A cell fate.

The loss of Lmx1b/Tlx3-positive dIL_B neurons and the increase in Pax2/Lhx1/5-positive dIL_A interneurons is increasingly more obvious at later developmental time points (E14.5 and E16.5). In E14.5 wild type embryos most Lmx1b-positive cells are localized within the most superficial laminae of the dorsal horn and fewer neurons expressing Lmx1b in the deeper dorsal horn. Antibody staining against Pax2 protein shows the opposite expression pattern with fewer Pax2-expressing neurons in the superficial laminae and more Pax2⁺ neurons in the deeper dorsal horn below the Lmx1b-expressing cells (Fig. 27a, c). However, in the *Gsh1/2*^{-/-} cord Lmx1b-expressing dIL_B neurons are all but absent (Fig. 27a-d, i-l). Conversely to wt embryos, the most superficial laminae in the dorsal horn of *Gsh1/2*^{-/-} embryos contain large numbers of Pax2⁺ neurons, which are much more densely packed compared with the wt dorsal horn (Fig. 27a-h). Cell counts of Pax2- and Lmx1b-expressing neurons in the same section reveal an ~80% increase of dIL_A neurons in the *Gsh1/2*^{-/-} dorsal horn with a > 99% loss of dIL_B neurons (Fig. 27m).

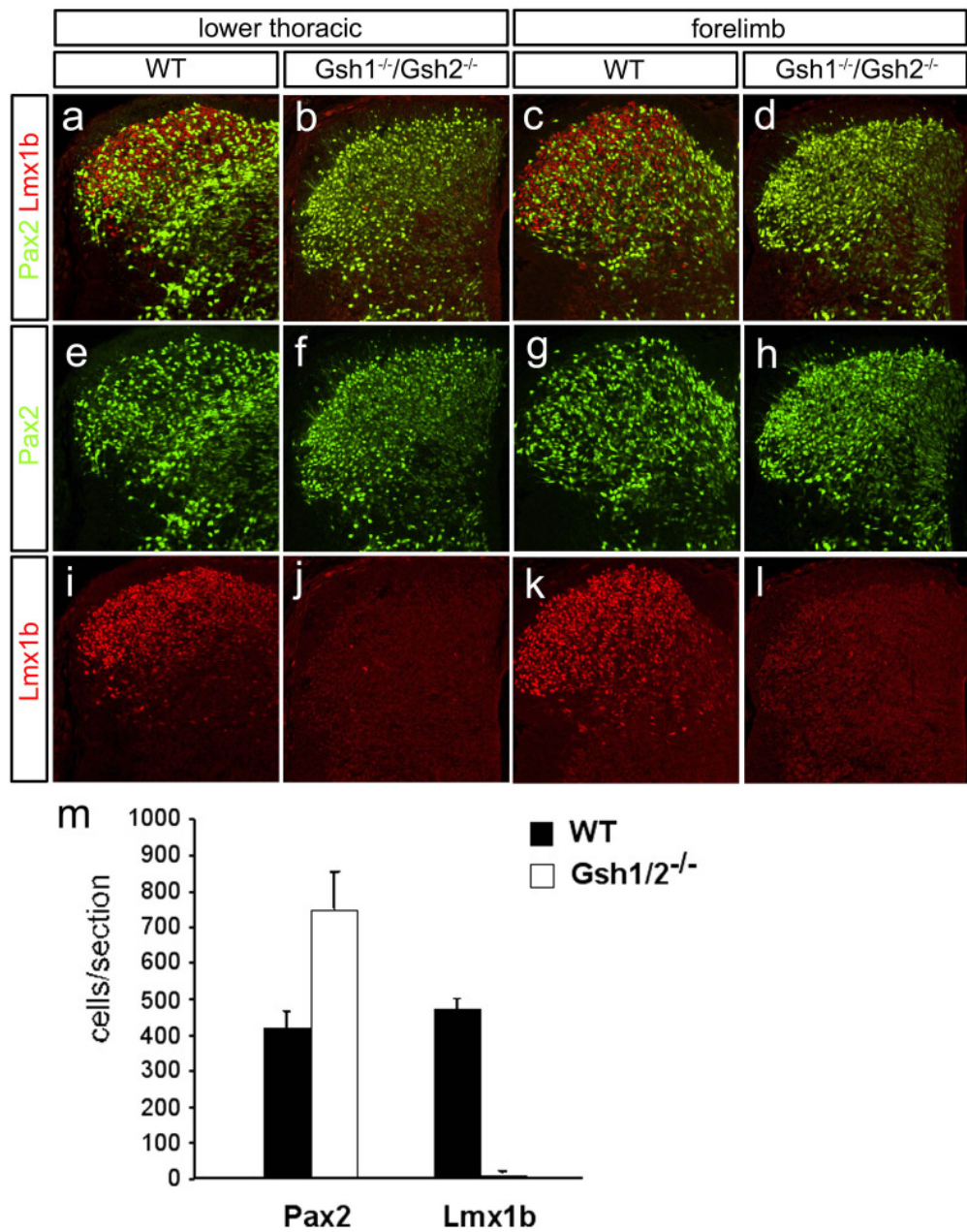


Figure 27: Analysis of the dorsal horn of E14.5 *Gsh1/2^{-/-}* spinal cords at lower thoracic and forelimb levels. (Fig. 27a-h) Pax2-expressing dIL_A neurons (green) are much more densely packed in the dorsal horn of *Gsh1/2^{-/-}* embryos, indicating that dIL_A neurons are increased in number in the absence of *Gsh1* and *Gsh2*. (Fig. 27a-d, i-l) Lmx1b-expressing cells are completely absent in the dorsal horn of *Gsh1/2^{-/-}* embryos, indicating a loss of dIL_B neurons. (Fig. 27m) Cell counts of Pax2⁺ dIL_A neurons and Lmx1b⁺ dIL_B neurons in the dorsal horn of E14.5 wt and *Gsh1/2^{-/-}* embryos at forelimb levels. These cell counts reveal an 80% increase in Pax2-expressing neurons with a concomitant 99% loss of Lmx1b-expressing cells in the *Gsh1/2^{-/-}* spinal cord. This confirms a switch in cell fate with dIL_B neurons adopting a dIL_A fate in *Gsh1/2^{-/-}* embryos.

At E16.5, Pax2⁺ dIL_A neurons and Lmx1b⁺ dIL_B neurons mainly occupy distinct laminae, with Lmx1b-expressing neurons populating the superficial laminae I and II, whereas Pax2-expressing neurons are localized mainly in deeper laminae. In the absence of *Gsh1* and *Gsh2*, large numbers of Pax2⁺ dIL_A neurons are present in the superficial laminae (Fig. 28a-h) and Lmx1b⁺ dIL_B neurons are completely absent (Fig. 28a-d, i-l). Further evidence for the absence of dIL_B interneurons comes from the expression analysis of DRG11, a paired homeodomain transcription factor that is expressed in the dorsal root as well as in dIL_B interneurons (Chen et al., 2001). DRG11 expression is completely absent in the dorsal horn of *Gsh1/2*^{-/-} mutants, even though its expression is unchanged in the dorsal roots (Fig. 28m-p). This suggests that there is a specific loss of DRG11⁺ dIL_B neurons in the *Gsh1/2*^{-/-} cord.

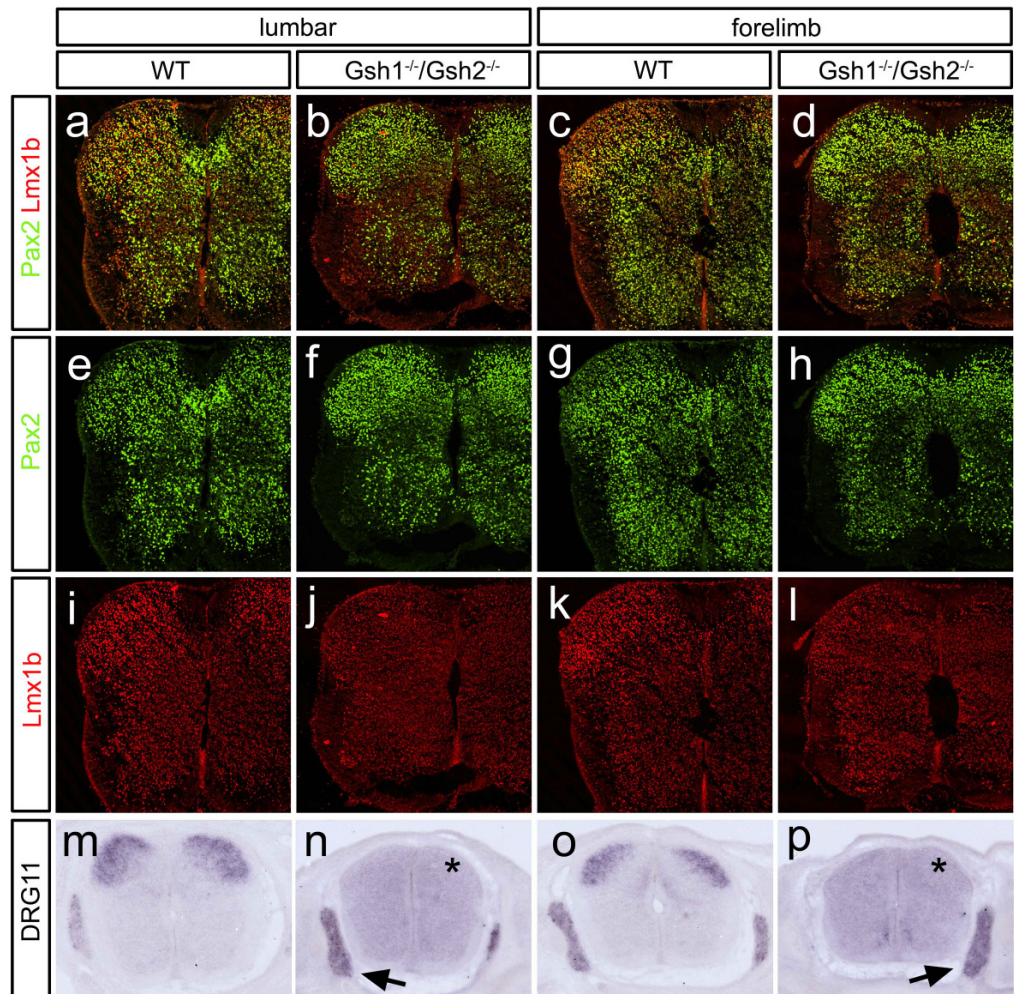


Figure 28: Analysis of markers of late-born neurons in E16.5 wt and *Gsh1/2*^{-/-} spinal cords at lower thoracic and forelimb levels. (Fig. 28a-h) dLL_A neurons, marked by the expression of Pax2, are increased in mice lacking *Gsh1* and *Gsh2*, whereas dLL_B neurons, which express Lmx1b, are completely absent in the dorsal horn of *Gsh1/2*^{-/-} embryos (Fig. 28 a-d, i-l). (Fig. m-p) *DRG11*, another marker of dLL_B neurons, is missing in the dorsal horn of *Gsh1/2*^{-/-} embryos (asterisks in n, p), but continues to be expressed in the dorsal roots (arrows in n, p), indicating a specific loss of dLL_B neurons.

Higher magnification of the dorsal horn of E16.5 wt and *Gsh1/2*^{-/-} spinal cords (Fig. 29) more clearly shows the switch in cell fate with dLL_B neurons adopting a dLL_A cell fate in *Gsh1/2*^{-/-} embryos.

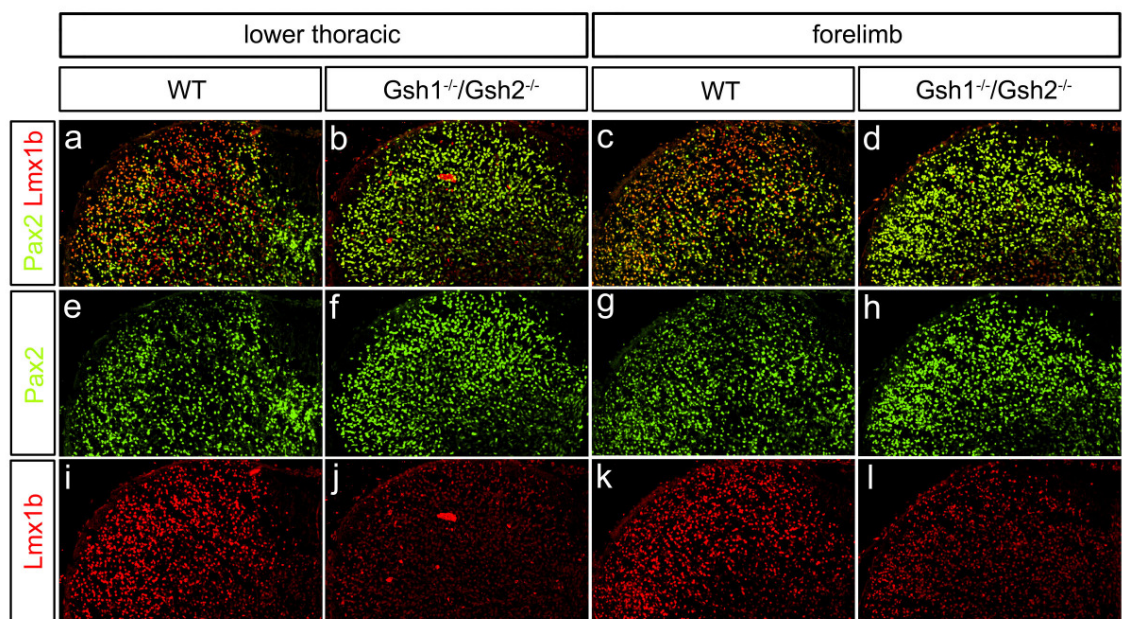


Figure 29: 25x magnification of the dorsal horn of E16.5 wt and *Gsh1/2*^{-/-} spinal cords at forelimb level. (Fig. 28a-d) Pax2⁺ dLL_A neurons are increased in number and occupy the most superficial laminae in the dorsal horn of *Gsh1/2*^{-/-} embryos. (Fig. 29a, b, e, f) Lmx1b⁺ dLL_B neurons, which are localized in the most superficial laminae in E16.5 wt embryos, are essentially absent in the *Gsh1/2*^{-/-} dorsal horn.

3.7 ***Gsh1/2*^{-/-} embryos show a respecification from excitatory to inhibitory interneurons in the dorsal horn.**

The increase in Pax2-positive dIL_A interneurons, coupled with a concomitant loss of Lmx1b/Tlx3-positive dIL_B interneurons, suggests that a switch in fate of late-born interneurons occurs in the dorsal horn of *Gsh1/2*^{-/-} embryos. It has been shown recently that the postmitotic transcription factors Tlx1/3 and Pax2 are important factors for determining glutamatergic and GABAergic phenotypes, respectively. Mice lacking both *Tlx1* and *Tlx3* exhibit a complete loss of glutamatergic excitatory neurons in the dorsal horn, concomitant with a strong increase in GABAergic neurons (Cheng et al., 2004). This switch in neurotransmitter identity in the dorsal horn of *Tlx1/3*^{-/-} spinal cords may be due to a lifting of the inhibition of Lbx1 function, which biases cells toward a GABAergic identity. *Pax2* deficient mice exhibit the opposite phenotype, with a loss of inhibitory GABAergic neurons (Cheng et al., 2004). However, numbers of excitatory glutamatergic neurons do not increase in the absence of *Pax2*, suggesting that *Pax2* is not part of the early switch that determines dIL_A versus dIL_B fate. Thus, Tlx3, Pax2 and Lbx1 are important postmitotic determinants for the specification of inhibitory and excitatory neurons of the dorsal horn.

To test whether the switch in transcription factor expression in the *Gsh1/2*^{-/-} cord also leads to a switch in the neurotransmitter identity of these neurons, the expression of several neurotransmitter specific markers such as *VIAAT* and *VGluT2* was analyzed in E14.5 spinal cords, a time point when late-born sensory neurons are settling in the dorsal horn. All inhibitory GABAergic and glycinergic neurons express *VIAAT*, the gene that encodes the vesicular transporter for both inhibitory amino acids. *VGluT2* encodes the main glutamate vesicular transporter in the nervous system that marks excitatory glutamatergic neurons.

Radioactive *in situ* hybridization analysis of *VIAAT* expression in E14.5 embryos lacking both *Gsh1* and *Gsh2* show a substantial increase in *VIAAT*-expressing cells in the superficial layers of the dorsal horn (Fig. 30a, b). In contrast, *VGluT2* expression is strongly decreased in the dorsal horn, particularly in the substantia gelatinosa (Fig. 30c, d). *VGluT2* expression is largely unchanged in the medial and ventral regions of the spinal cord, suggesting that only late-born dIL_A cells undergo a switch in their neurotransmitter phenotype. These data are

also consistent with the changes in transcription factor expression that occur in the *Gsh1/2*^{-/-} spinal cord and demonstrates a switch in cell fate from an excitatory dIL_B to inhibitory dIL_A cell fate in the superficial dorsal horn of *Gsh1/2*^{-/-} spinal cords.

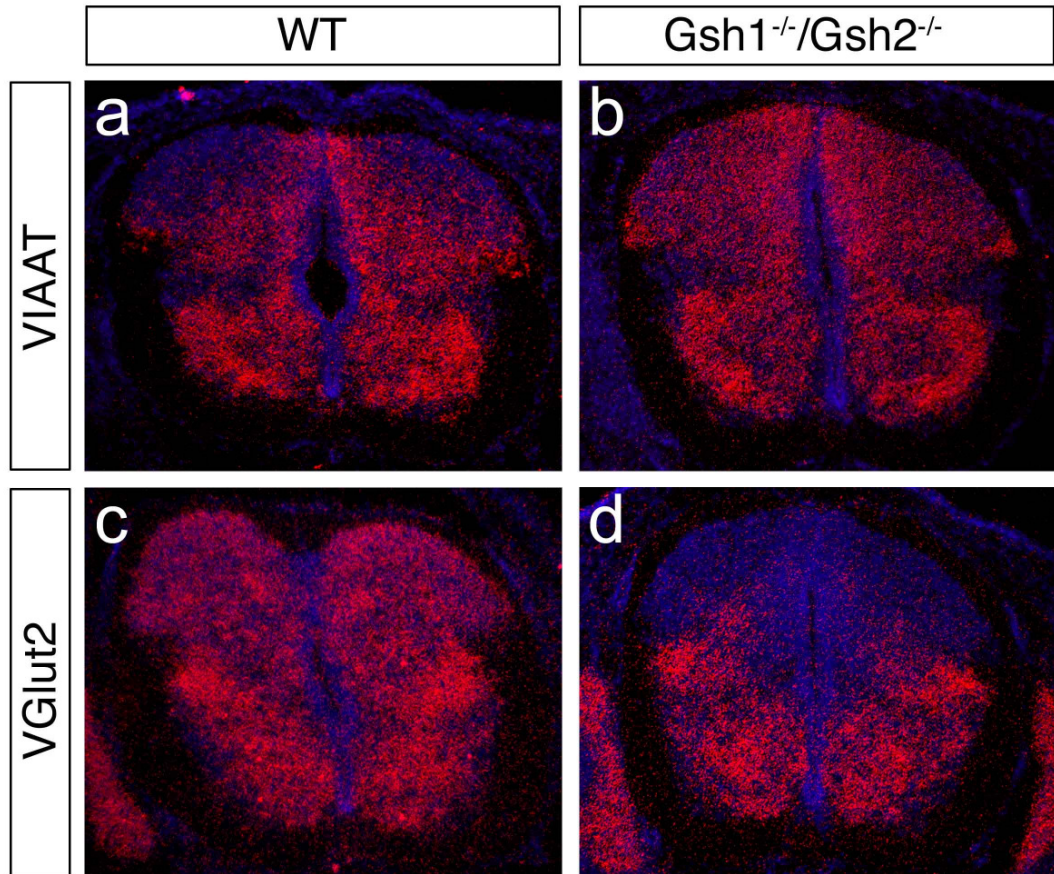


Figure 30: VIAAT and VGlut2 expression in E14.5 wt and *Gsh1/2*^{-/-} spinal cords. (Fig. 30a, b) *VIAAT* marks inhibitory neurons and is strongly upregulated in the dorsal horn, but unchanged in the ventral half of the spinal cord of *Gsh1/2*^{-/-} embryos. (Fig. 30c, d) *VGlut2* marks excitatory neurons and is almost completely missing in the dorsal horn of mice lacking *Gsh1/2* (Fig. 30c, d). However, the intermediate and ventral *VGlut2* expression is unchanged in the dorsal horn of *Gsh1/2*^{-/-} embryos. These data show that *Gsh1/2* are necessary for the specification of excitatory neurons in the dorsal horn of the spinal cord. In the absence of *Gsh1* and *Gsh2* excitatory neurons develop as inhibitory neurons, confirming the switch in cell fate seen with the change in transcription factor expression.

3.8 Expression of Mash1, Ngn1 and Ngn2 in the vz of *Gsh1/2*^{-/-} spinal cords

The switch in cell fate of late-born neurons in mice lacking *Gsh1/2* led me to ask whether the progenitors of these interneuron populations are also re-specified. My previous analysis of the early phenotype in E11.5 *Gsh1/2*^{-/-} have shown a strong reduction in the level of Mash1 expression with a concomitant expansion of *Ngn1*, such that *Ngn1* expression also encompasses the progenitors of dl3-5 neurons. To analyze whether the ventral expansion of *Ngn1* and the resulting reduction of Mash1 persists in the vz of *Gsh1/2*^{-/-} spinal cords until E12.5 when the late-born dIL neurons are being generated, I examined the expression of *Ngn1* in E12.5 *Gsh1/2*^{-/-} embryos by *in situ* hybridization. In sections from wt embryos, *Ngn1* is restricted to the progenitor domains that abut the *Gsh1/2*⁺ domain dorsally and ventrally. However, *Ngn1* mRNA expression expands ventrally in the vz of *Gsh1/2*^{-/-} spinal cords, such that it encompasses the whole dorsal vz except the most dorsal domain (Fig. 31a, b).

The expression of *Ngn2* in wt and *Gsh1/2*^{-/-} spinal cord cross-sections was also examined. In E12.5 wt spinal cord sections, *Ngn2* is expressed throughout the lateral edges of the dorsal vz and svz, except the most dorsal progenitor domain. This demonstrates that *Ngn2* is expressed in the progenitor domain of late-born dIL neurons, and it is therefore possible that this bHLH transcription factor plays a role in specifying a subset of dIL neurons. To analyze whether *Ngn2* acts downstream of *Gsh1/2*, I examined the expression pattern of *Ngn2* in *Gsh1/2*^{-/-} cords by *in situ* hybridization using a specific probe against *Ngn2* mRNA. *Ngn2* mRNA is still present in the *Gsh1/2*^{-/-} cord. However, its expression domain is wider compared to the one seen in wt sections (Fig. 31c, d). Therefore, more cells are expressing *Ngn2* in the absence of both *Gsh1* and *Gsh2* suggesting that *Gsh1/2* limits the expression of *Ngn2* in the wt spinal cord.

To test once again whether the expansion of *Ngn1* expression leads to a reduction in the level of Mash1 protein expression, I analyzed adjacent sections for the expression of Mash1 by immunohistochemistry. In these sections the level of Mash1 expression is strongly reduced, but not completely absent. While Mash1 protein is still expressed in the same dorsal domain, the level of Mash1 in dIL progenitors is strongly reduced (Fig. 31e, f). This reduction is similar to that seen at E11.5.

The changes in expression pattern of *Ngn1*, *Ngn2* and *Mash1* in the progenitors of late-born neurons argue that the precursors for dIL neurons are not correctly specified in the absence of *Gsh1/2*. These findings also suggest that the altered expression of *Ngn1*, *Ngn2* and *Mash1* may account for the switch in dIL cell fate that occurs in the *Gsh1/2*^{-/-} dorsal horn.

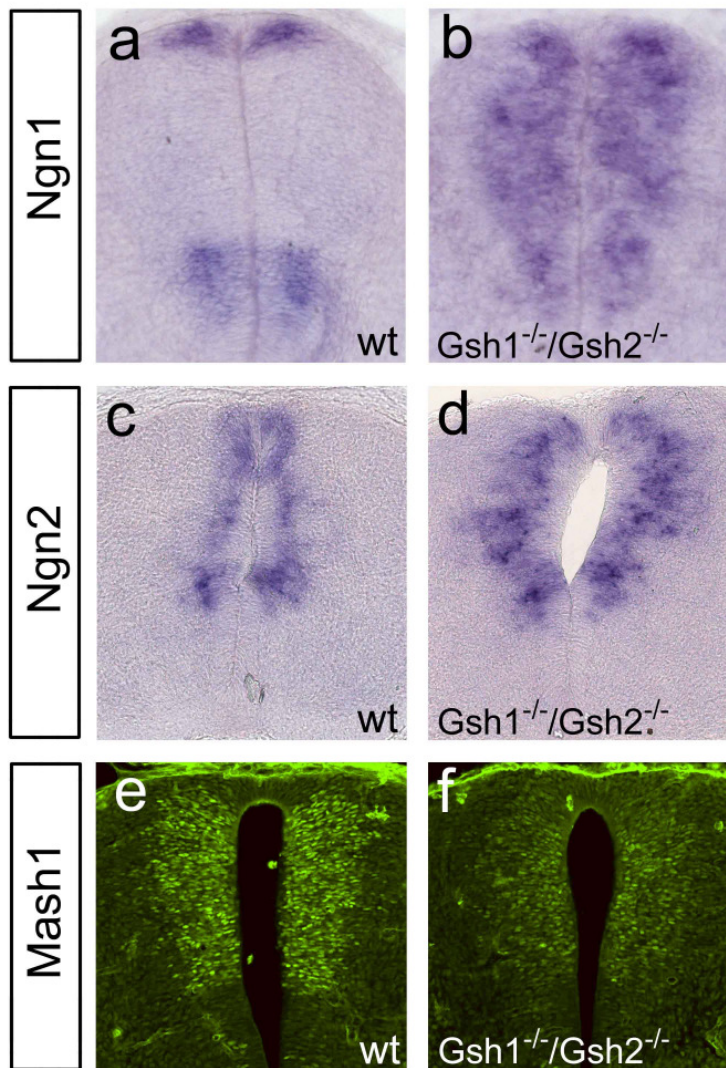


Figure 31: Expression of transcription factors in the dorsal ventricular zone of E12.5 wt and *Gsh1/2*^{-/-} embryos. (Fig. 31a, b) *Ngn1* expands into the dl3-, dl4- and dl5 progenitors in the absence of *Gsh1/2*. (Fig. 31c, d) *Ngn2* expression is normally expressed in the lateral edges of the dorsal vz and svz, but is wider in the *Gsh1/2*^{-/-} embryos. These data indicate that *Gsh1/2* repress the expression of *Ngn1* and *Ngn2*. (Fig. 31e, f) *Mash1* is co-expressed with *Gsh1/2* in dIL progenitors, but its expression is strongly reduced in the vz of *Gsh1/2*^{-/-} cords. This reduction is most likely due to the ventral expansion of *Ngn1* into the dIL progenitor domain.

3.9 Functional analysis of *Ngn1* and *Ngn2*

dIL progenitors in E12.5 wt embryos express *Ngn2*. This expression of *Ngn2*, coupled with the ventral expansion of *Ngn1* in the vz of E12.5 *Gsh1/2^{-/-}* embryos, suggests that *Ngn1* and *Ngn2* might play important roles in the specification of late-born neurons. With this in mind, a series of experiments was undertaken to elucidate whether *Ngn1* and/or *Ngn2* are involved in the generation of dIL neurons and/or whether they are responsible for the specific loss of dIL_B neurons in the *Gsh1/2^{-/-}* cord.

3.9.1 Overexpression analysis of *Ngn1* in the chick spinal cord

Ngn1 expands in the spinal cord of *Gsh1/2^{-/-}* embryos encompassing the dIL progenitor domain. Therefore, it is possible that the expansion of *Ngn1* in the *Gsh1/2^{-/-}* spinal cord accounts for the specific loss of dIL_B interneurons in the dorsal horn. To test this hypothesis, misexpression analysis of *Ngn1* in the chick spinal cord was performed using an expression vector, which contains the full-length *Ngn1* coding sequence. Electroporations were performed at E6, a time point when the late-born neurons begin to be generated. After two days, the spinal cords of these electroporated chick embryos were isolated and analyzed for the expression of *Lbx1*, *Pax2*, *Lhx1/5*, *Lmx1b* and *Tlx3*. All five proteins show a dramatic reduction in their expression on the electroporated half compared to the control half, with the decrease in *Lhx1/5* expression being the least obvious (Fig. 32a-j). Only *Lhx1/5*-positive cells are double labeled with GFP (*Ngn1*) (Fig. 32e, f). While these electroporation experiments suggest that *Ngn1* may be able to repress the generation of late-born neurons, this repression is not cell type specific. Both, dIL_A and dIL_B neurons are strongly repressed. The less obvious reduction in *Lhx1/5* expression can be explained by an induction of early-born dI2 interneurons, as *Ngn1* is known to be able to induce dI2 cells (Gowan et al., 2001). The strong repression of all markers by *Ngn1* may reflect the proneural activity of this protein. In this instance, the precocious induction of neural differentiation might have depleted the dIL progenitor pool, thereby leading to a reduced number of late-born neurons that express different combinations of all five markers.

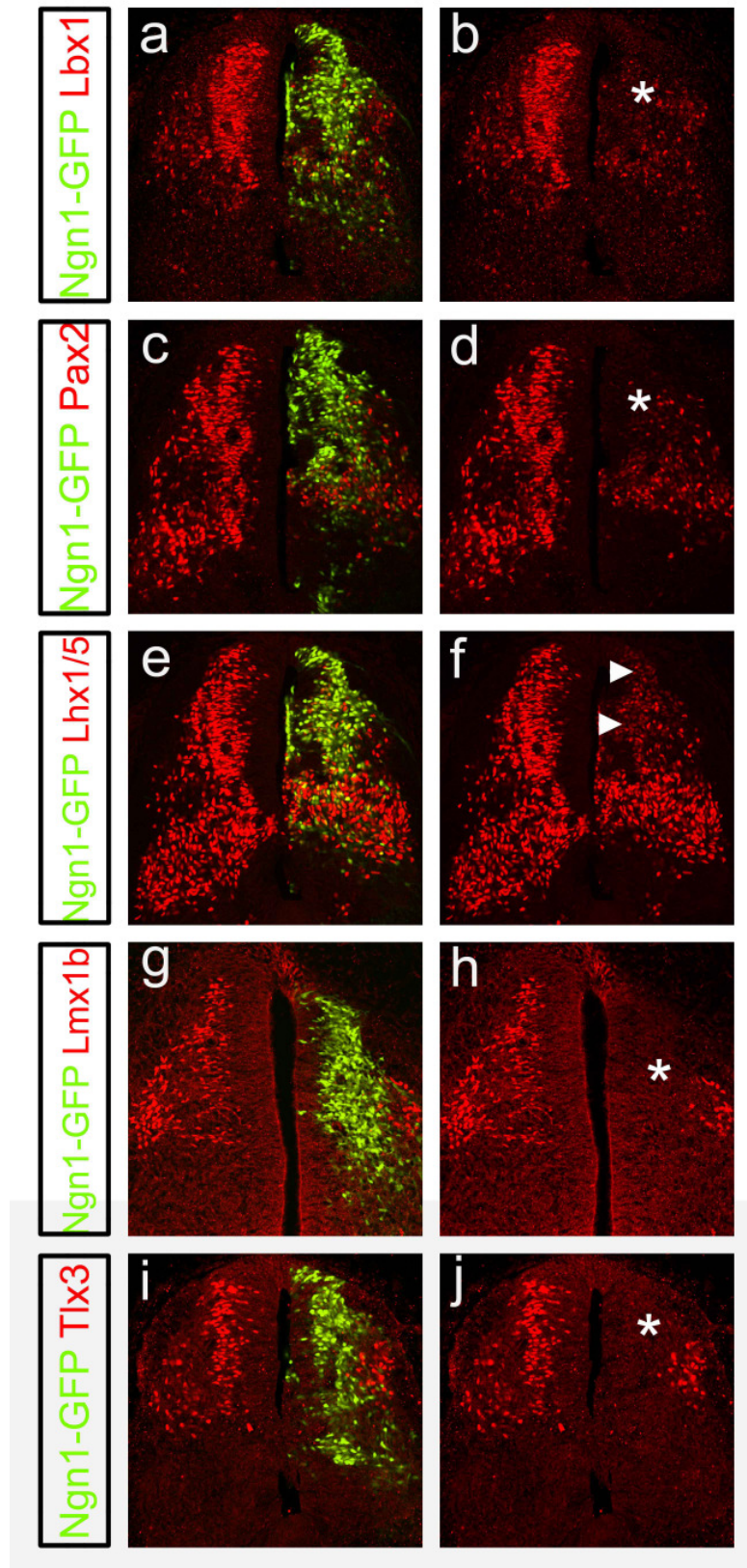


Figure 32: Misexpression of *Ngn1* into E6 chick spinal cords. After *Ngn1* electroporation, chick embryos were allowed to develop for 24h before analyzing the expression of late-born neurons markers. (Fig. 32a, b) *Lbx1* is completely absent in the svz of the electroporated side of the spinal cord (asterix in b), indicating that *Ngn1* represses the development of dIL neurons. (Fig. 32c, d) dIL_A neurons expressing *Pax2* are almost completely absent following *Ngn1* overexpression (asterix in d). (Fig. 32e, f) *Lhx1/5*⁺ dIL_A neurons are also reduced by *Ngn1* misexpression; however, many cells expressing low levels of *Lhx1/5* are present on the electroporated side in the dorsal spinal cord (arrow heads in f). Most likely, these cells are dI2 neurons induced by *Ngn1*. (Fig. 32g, h) *Lmx1b*-expressing dIL_B neurons are also repressed following *Ngn1* misexpression (asterix in h). (Fig. 32i, j) *Tlx3* is completely absent in the svz on the electroporated side of the spinal cord (asterix in j), confirming the loss of dIL_B neurons following misexpression of *Ngn1*.

3.9.2 Gain-of-function analysis of *Ngn2*

Ngn2 was also tested to see if it is capable of promoting a particular dIL cell fate. Once again, overexpression studies were performed in E6 chick spinal cords using an expression vector, which contains the full-length sequence of rat *Ngn2*. Electroporated embryos were allowed to develop for 24h before harvesting. In this instance, the ectopic *Ngn2*⁺ cells are still present in the svz, where the late-born interneurons begin to differentiate. To analyze the expression of dIL neurons following *Ngn2* overexpression, I first used an antibody against *Lbx1* to ask what happens to the dIL population as a whole. *Lbx1*-expressing dIL neurons are reduced in number in the svz of the electroporated side, indicating an overall reduction of late-born neurons (Fig. 33a-c). However, when I analyzed the number of *Pax2*⁺ neurons, no marked change is noted (Fig. 33d-f). This suggests that *Ngn2* does not affect the specification of dIL_A neurons. Instead, the reduction in *Lbx1* expression appears to be due to a reduction in dIL_B neurons, as there are fewer *Tlx3*-expressing cells in the svz of the electroporated half of the spinal cord compared to the endogenous control side (Fig. 33g-i). These data suggest that *Ngn2* can repress the development of dIL_B, but not dIL_A neurons.

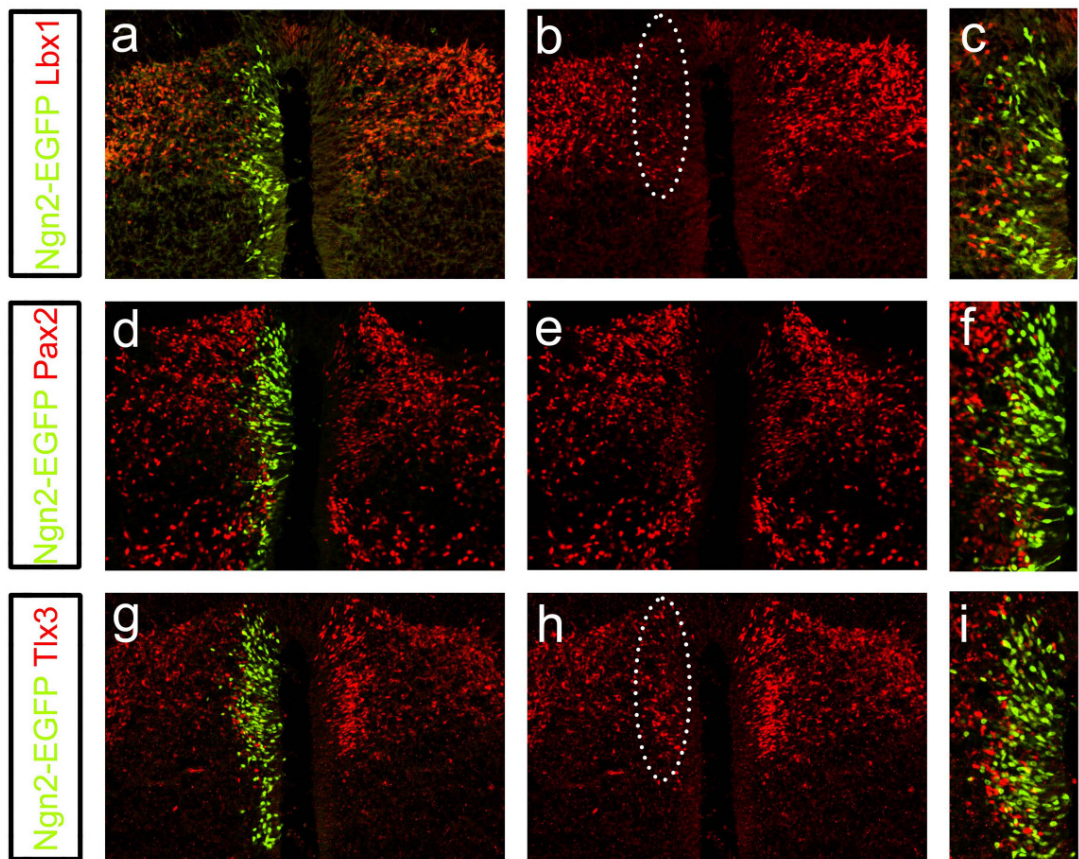


Figure 33: Expression analysis of markers of dIL neurons 24h after overexpression of *Ngn2* into the spinal cords of E6 chick embryos. (Fig. 33a-c) *Lbx1* is strongly reduced on the electroporated side following *Ngn2* misexpression (circle in b). Only a few *Lbx1*⁺ cells remain after *Ngn2* overexpression, with no *Lbx1*/*Ngn2*-GFP double-labeled cells left, indicating that *Ngn2* is repressing dIL neuron development. (Fig. 33c) Magnification of the electroporated side in a. (Fig. 33d-f) dIL_A neurons expressing *Pax2* are not affected by *Ngn2* misexpression. (Fig. 33f) Magnification of the electroporated side in d. (Fig. 33g-i) *Tlx3*, which is expressed in dIL_B neurons, is strongly reduced following *Ngn2* overexpression (circle in h), indicating that *Ngn2* represses a dIL_B fate, but not a dIL_A fate. (Fig. 33i) Magnification of the electroporated side in g.

3.9.3 Gain-of-function analysis of *Ngn1/2*

In the *Gsh1/2^{-/-}* spinal cord both *Ngn1* and *Ngn2* are co-expressed in dLL progenitors. Therefore, it is possible that both together have a different effect on late-born neurons than *Ngn1* or *Ngn2* by themselves, when misexpressed in E6 chick spinal cords. To test this hypothesis, I electroporated expression constructs of *Ngn1* and *Ngn2* together into the lumen of E6 old chick spinal cords. The analysis of this experiment does not show any marked changes compared to the overexpression of *Ngn2* alone. Again, *Lbx1* staining is reduced in the svz on the electroporated side of the spinal cord (Fig. 34a-c), which is consistent with a reduction in dLL neurons. Once again, this reduction is due to a decrease in *Tlx3*-expressing dLL_B cells in the svz (Fig. 34g-i). *Pax2*-expressing dLL_A neurons are only minimally affected, showing only a small reduction, if any, after the overexpression of both *Ngn1* and *Ngn2* (Fig. 34d-f).

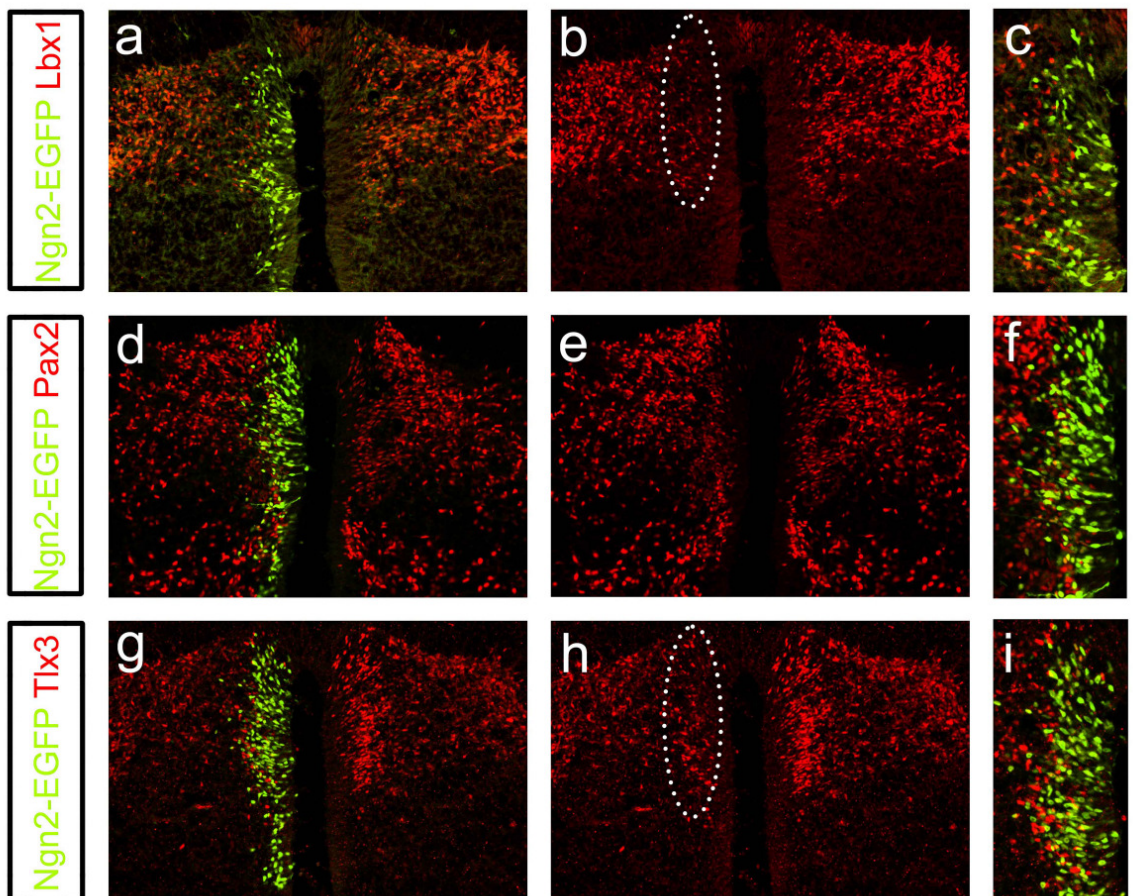


Figure 34: Expression analysis of markers of dIL neurons 24h after overexpression of *Ngn1/2* into the spinal cords of E6 chick embryos. (Fig. 34a-c) Lbx1 expressing dIL neurons are reduced in the svz of the electroporated side of the spinal cord (circled in b). (Fig. 34c) Magnification of the electroporated side in a. (Fig. 34d-f) Pax2⁺ dIL_A neurons are largely unchanged following *Ngn1/2* overexpression. However, hardly any double-labeled cells for Pax2 and Ngn1/2-GFP are seen in the svz (Fig. 34f). (Fig. 34f) Magnification of the electroporated side in d. (Fig. 34g-i) Tlx3-expressing cells are strongly reduced by *Ngn1/2* indicating a reduction of dIL_B neurons. The misexpression of *Ngn1* and *Ngn2* together leads to the same phenotype seen with *Ngn1* and *Ngn2* misexpression alone. (Fig. 34i) Magnification of the electroporated side in g.

3.10 Loss-of-function analysis of *Mash1*

The expression of *Mash1* in the progenitors of late-born neurons, together with the reduction in *Mash1* expression in mice lacking *Gsh1/2* at E12.5, suggests that *Mash1* may play a significant role in specifying dIL neurons. Rumiko Mizuguchi, a postdoc in the lab tested this hypothesis by analyzing the spinal cord of *Mash1*^{-/-} embryos at E12.5 and E14.5 for the expression of markers for late-born neurons, such as Lbx1, Pax2, Lmx1b, Tlx3 and Lhx1/5. Interestingly, when Rumiko analyzed the expression of several markers of dIL_A and dIL_B neurons, she observed the opposite phenotype seen in the *Gsh1/2*^{-/-} embryos. Namely, she observed marked reduction in the number of Pax2⁺ (Fig. 35a, b) and Lhx1/5⁺ (Fig. 35e, f) dIL_A neurons in the subventricular zone of the dorsal spinal cord, coupled with an increase in the number of Lmx1b⁻ (Fig. 35c, d) and Tlx3-expressing (Fig. 35g, h) dIL_B cells. In wt spinal cords of E12.5 embryos ~50% of Lbx1-expressing cells in the svz co-label with Pax2 (Fig. 35i), while the other 50% co-express Lmx1b (Fig. 35k). However, in the *Mash1*^{-/-} very few Lbx1-positive cells are seen to express Pax2 (Fig. 35j). Instead, most Lbx1⁺ cells co-express Lmx1b (Fig. 35l), indicating a switch in cell fate with dIL_A neurons developing as dIL_B neurons.

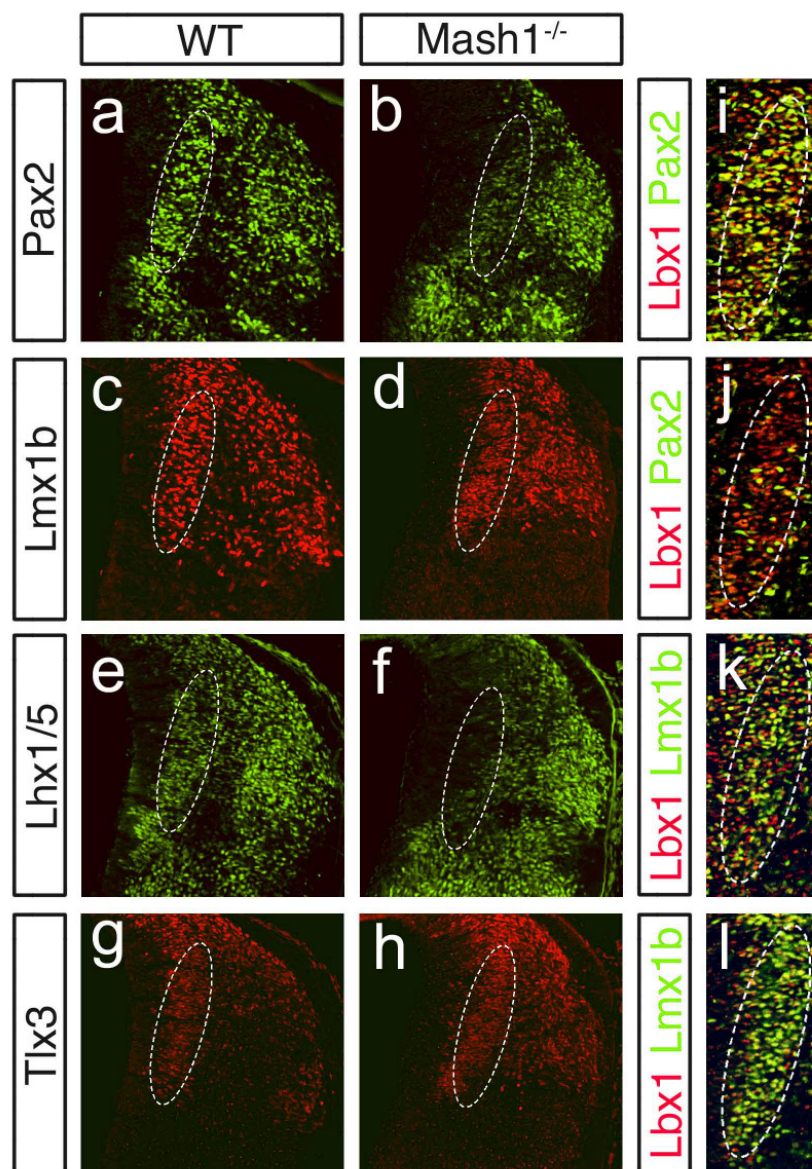


Figure 35: Immunostainings for late-born neuron markers in the dorsal horn of E12.5 *Mash1*^{-/-} embryos. (Fig. 35a, b) *Mash1*^{-/-} embryos exhibit a marked decrease in Pax2⁺ cells in the subventricular zone (svz) (circled). Pax2-expressing neurons are still present in the more lateral region of the dorsal horn. These cells represent dl4 neurons and the dlL_A neurons born at E11.5 that have migrated laterally. (Fig. 35c, d) Lmx1b is upregulated in the *Mash1*^{-/-} cord in areas where Pax2 is decreased (circled). (Fig. 35e, f) Lhx1/2 is, similar to Pax2 expression, decreased in the svz (circled), indicating a reduction in dlL_A neurons in *Mash1*^{-/-} embryos. (Fig. 34g, h) In contrast, Tlx3 is upregulated in the svz (circled) of the *Mash1*^{-/-} spinal cord. (Fig. 35i, k) In wild type embryos, approximately half of the Lbx1⁺ cells (red) in the svz express Pax2 (green in i) and the other half express Lmx1b (green in k). (Fig. 35j) In contrast, *Mash1*^{-/-} embryos have very few Lbx1/Pax2 double-labeled neurons in the svz of the dorsal horn. (Fig. 35k) Rather, most cells in the svz co-express Lbx1 (red) and Lmx1b (green). This figure was kindly provided by Rumiko Mizuguchi.

At E14.5, this reduction in Pax2-expressing neurons, coupled with an increase in the number of Lmx1b-expressing dLL_A neurons, is even more obvious. The dorsal horn of *Mash1*^{-/-} embryos is more densely packed with cells positive for Lmx1b compared to their wt littermates (Fig. 36c, d). On the other hand, the number of Pax2-expressing neurons in the superficial dorsal horn is strongly reduced (Fig. 36a, b). *Mash1* is therefore required for the proper development of late-born Pax2⁺ dLL_A neurons, but is dispensable for Lmx1b⁺ dLL_B neuron development.

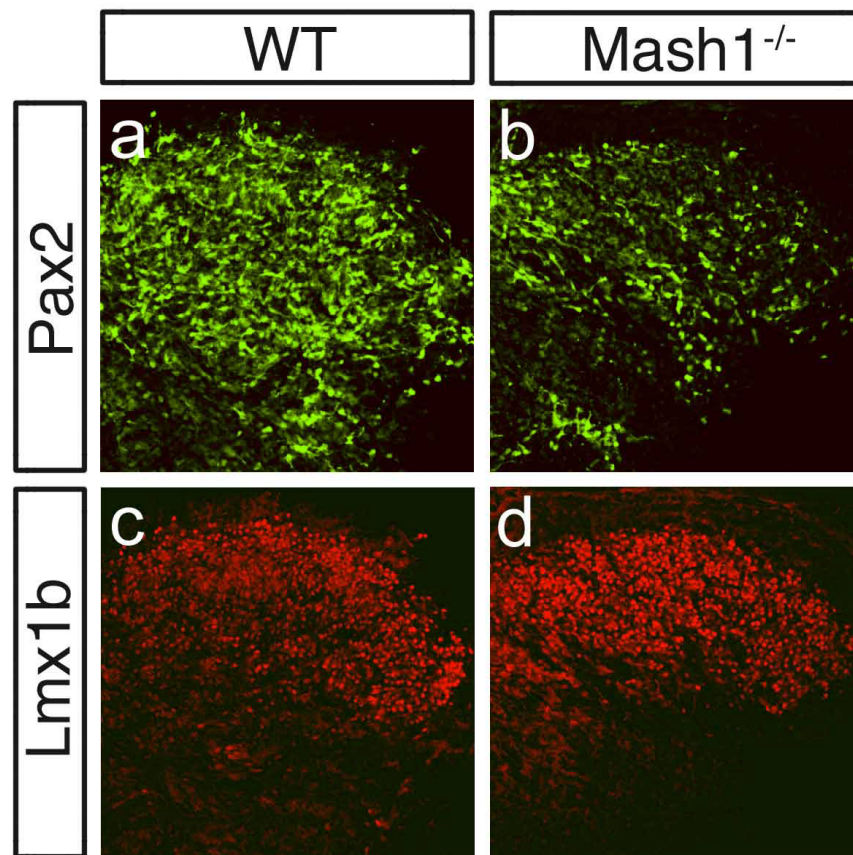


Figure 36: Expression analysis of the late-born neuron markers Pax2 and Lmx1b in the dorsal horn of E14.5 wt and *Mash1*^{-/-} embryos. (Fig. 36 a, b) Pax2-expressing dLL_A neurons are strongly reduced in number in the *Mash1*^{-/-} dorsal horn compared to wt littermates. (Fig. 36c, d) Lmx1b-expressing dLL_B neurons are increased in *Mash1*^{-/-} cords. These data suggest that *Mash1*^{-/-} embryos exhibit a switch in cell fate, with dLL_A neurons adopting a dLL_B cell fate. This figure was kindly provided by Rumiko Mizuguchi.

To further demonstrate the switch from an excitatory dIL_A to an inhibitory dIL_B fate in the *Mash1*^{-/-} spinal cords, Rumiko examined the expression of various neurotransmitter markers in E14.5 *Mash1*^{-/-} spinal cords. The reduction in Pax2 expression, with a concomitant increase in Lmx1b/Tlx3⁺ neurons, suggested that neurons expressing inhibitory neurotransmitter markers would be reduced in the *Mash1*^{-/-} spinal cord. We also expected that the number of neurons with an excitatory neurotransmitter phenotype would be increased. To confirm this hypothesis, *in situ* hybridization experiments were performed, using a DIG-labeled antisense probe against *VIAAT*, as a marker for inhibitory neurotransmitters, as well as *VGluT2*, as a marker for excitatory neurons. The expression of GAD67, which marks inhibitory GABAergic neurons, was also analyzed using an antibody against GAD67 protein. These analyses reveal a strong reduction in *VIAAT* and GAD67 expression in the dorsal horn of E14.5 *Mash1*^{-/-} embryos (Fig. 37a- f). Excitatory neurons expressing *VGluT2* are drastically upregulated in the superficial layers of the dorsal horn (Fig. 37c, d). These data show that Mash1 is an important determinant for the specification of late-born inhibitory neurons in the dorsal horn, but is dispensable for late-born excitatory neuron development. Interestingly, this late function of Mash1 is opposite to its function in specifying early-born dorsal interneurons. At early times (E10.0-E11.5), Mash1 is necessary for the generation of excitatory Tlx3/Lmx1b-expressing dl5 neurons, but is dispensable for inhibitory Pax2-expressing dl4 neurons (see Fig. 15).

The opposite phenotypes seen in the *Gsh1/2*^{-/-} and in the *Mash1*^{-/-} cord show that *Gsh1/2* and Mash1 have differing roles in determining the neurotransmitter phenotype of late-born sensory neurons in the dorsal horn of the spinal cord.

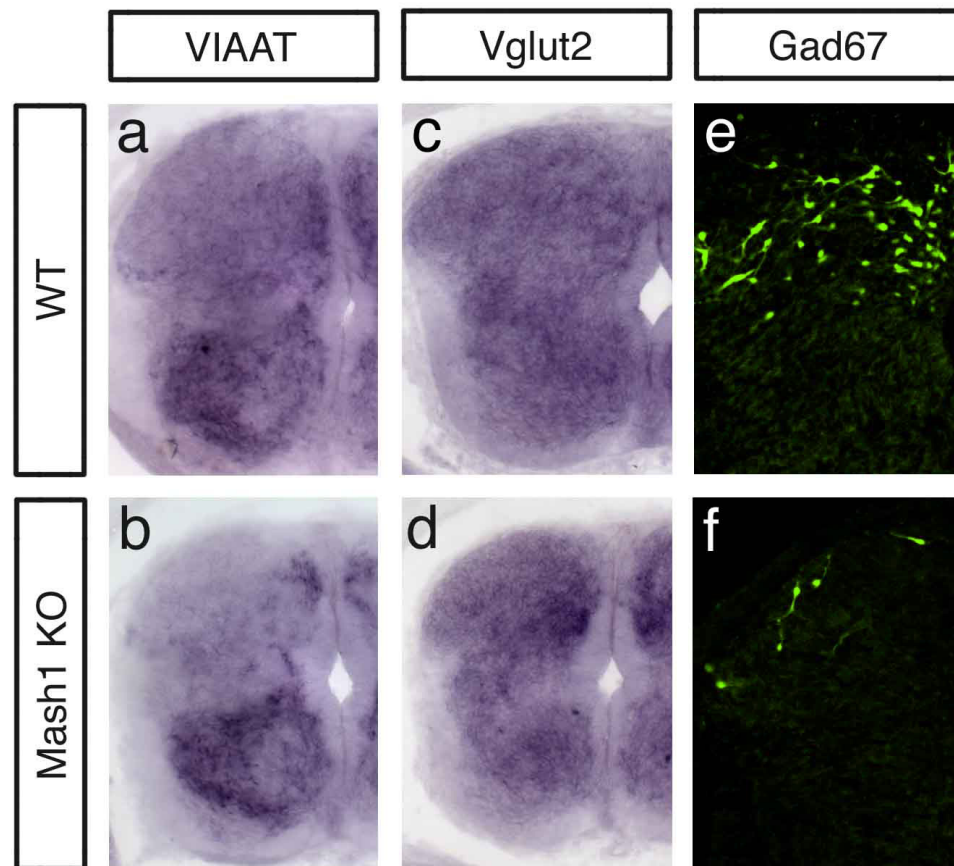


Figure 37: Expression analysis of neurotransmitter markers at E14.5. The dorsal horn of *Mash1*^{-/-} mice was analyzed by *in situ* hybridization using *VIAAT* and *VGluT2*, as markers of inhibitory and excitatory neurons, respectively, as well as by immunohistochemistry against the inhibitory marker *Gad67*. (Fig. 37a, b) Mice lacking *Mash1* show a reduction in the expression of inhibitory *VIAAT* in the substantia gelatinosa with a concomitant increase in the excitatory marker *VGluT2* (Fig. 37 c, d). (Fig. 37e, f) The inhibitory marker *Gad67* is also strongly decreased in the dorsal horn of *Mash1*^{-/-} embryos. This figure was kindly provided by Rumiko Mizuguchi.

3.11 Misexpression analysis of *Mash1* in E6 chick spinal cords

To test whether *Mash1* is able to actively induce a dLL_A cell fate, a *Mash1* expression construct was electroporated into E6 chick neural tubes and analyzed 24h later for the expression of Pax2 and Lhx1/5, to examine dLL_A neuron development, as well as Lmx1b and Tlx3 expression for dLL_B neurons. However, no change in the numbers of Pax2- (Fig. 38b) and Lhx1/5-expressing cells (Fig. 38c) is observed on the electroporated half of the spinal cord compared to the endogenous control side, indicating that *Mash1* alone does not efficiently induce dLL_A neurons. The expression of Lmx1b and Tlx3 was also analyzed on adjacent sections. Interestingly, the expression of Lmx1b is dramatically reduced following *Mash1* overexpression, indicating that *Mash1* represses a dLL_B fate (Fig. 38e). The expected downregulation of Tlx3 is not detectable and many Tlx3-expressing cells were found in the svz of the electroporated side where late-born neurons are located (Fig. 38f). One explanation for the presence of these Tlx3-positive cells is that they are dl3 cells, as Tlx3⁺ dl3 neurons are known to be upregulated following *Mash1* overexpression at E3 (see Fig. 17). Nonetheless, these data show that *Mash1* alone is not sufficient to promote a dLL_A cell fate, although high levels of *Mash1* appear to repress dLL_B neurons.

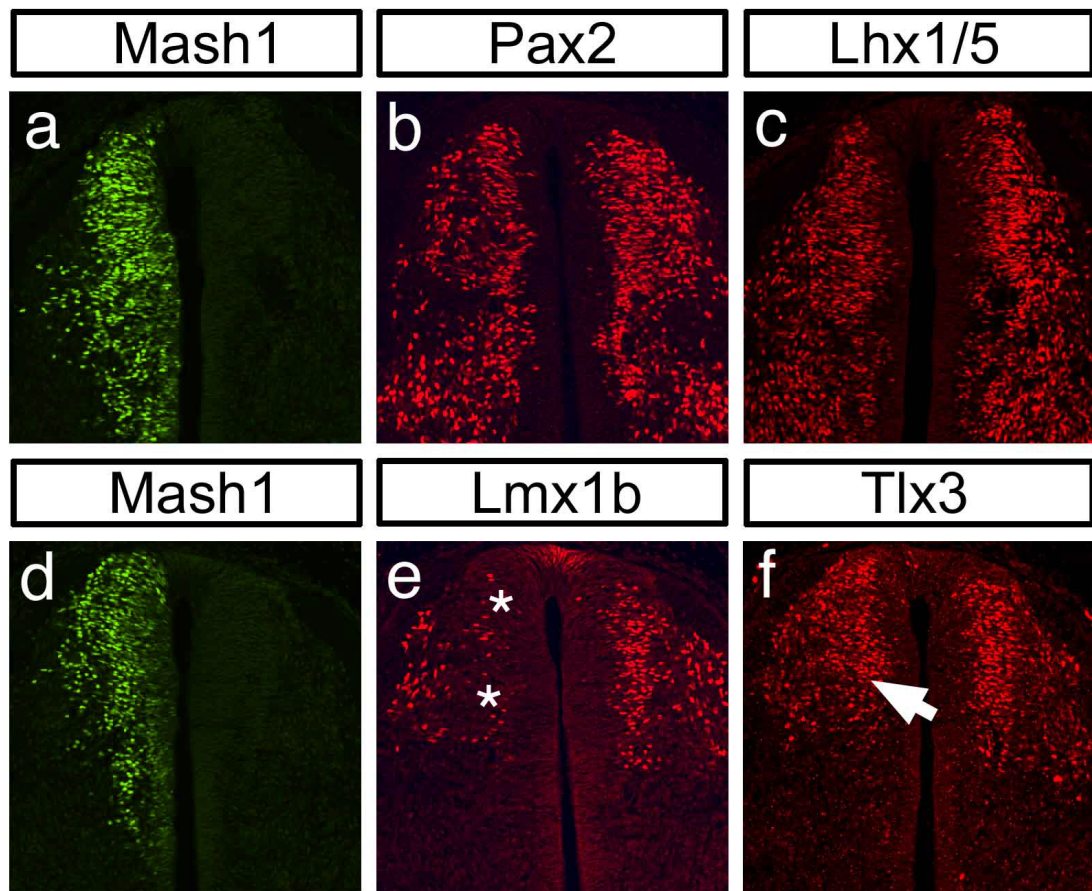


Figure 38: Overexpression analysis of *Mash1* in E6 old chick spinal cords. E6 chick spinal cords were co-electroporated with *Mash1*- and *GFP*-expression vectors and analyzed 24h later. At this time, *Mash1*-expressing cells (green) are still located in the vz/svz (Fig. 38a, d). (Fig. 38b, c) Pax2- and Lhx1/5-expressing dIL_A neurons do not change following *Mash1* misexpression. This suggests that *Mash1* does not induce dIL_A neurons. (Fig. 38d, e) *Mash1* represses the generation of Lmx1b⁺ dIL_B neurons (asterisks). (Fig. 38f) Tlx3⁺ neurons are not reduced after *Mash1* overexpression (arrow). Most likely, these cells represent early-born dl3 and dl5 neurons and not dIL_B neurons.

3.12 Overexpression of a transcriptional activator form and a transcriptional repressor form of *Mash1*

As shown previously, *Mash1* is a necessary factor for the development of two excitatory interneuron populations in the dorsal spinal cord at early developmental stages. However, during the second wave of neurogenesis in the spinal cord, *Mash1* function is dispensable for excitatory neuron specification. Instead, *Mash1* is necessary for inhibitory neuron development. What triggers this change in *Mash1* function? To begin to investigate this interesting observation in more detail, I misexpressed a transcriptional activator form (*Mash1bHLH-VP16*) (Triezenberg et al., 1988) and a transcriptional repressor form (*Mash1bHLH-EnR*) (Smith and Jaynes, 1996) of *Mash1*, together with an empty EGFP expression vector, in the neural tube of E3 and E6 chick embryos. GFP expression was used to identify neurons expressing ectopic *Mash1-VP16/Mash1-EnR*. Embryos electroporated at E3 were allowed to develop for 48h before being harvested, ensuring that ectopic gene expression is located at the lateral edges of the neural tube, where early-born INs are located. To analyze the effect of the overexpression on late-born interneurons, chick embryos were electroporated at E6 and analyzed 24h later, thus ensuring that ectopic *Mash1* expression was located in the svz, where dIL neurons arise. The effects of the electroporation on early-born and late-born inhibitory and excitatory interneurons were investigated by analyzing the expression of *Lbx1*, *Pax2* and *Tlx3*. *Lbx1* expression in chick embryos electroporated with the transcriptional activator form of *Mash1* at E3 is unchanged when compared to the control half, indicating proper development of dI4, dI5 and dI6 interneurons (Fig. 39a, b). Some reduction in *Pax2*-expressing dI4 neurons is seen, suggesting a reduction in dI4 cells (Fig. 39c, d). Moreover, no double-labeled GFP⁺ and Pax2⁺ cells are detected in the dI4 domain, which is consistent with a block in dI4 specification. *Tlx3*-expressing dI3 neurons are increased in number (Fig. 39e, f), and the dI5 domain is slightly more densely packed on the electroporated half compared to the control side.

In summary, electroporation of the *Mash1bHLH-VP16* construct, which functions as a transcriptional activator, leads to the same phenotype seen with a “normal” *Mash1* expression vector, namely resulting in an increase in dI3 and dI5 neurons, with a concomitant decrease in the adjacent dI4 population.

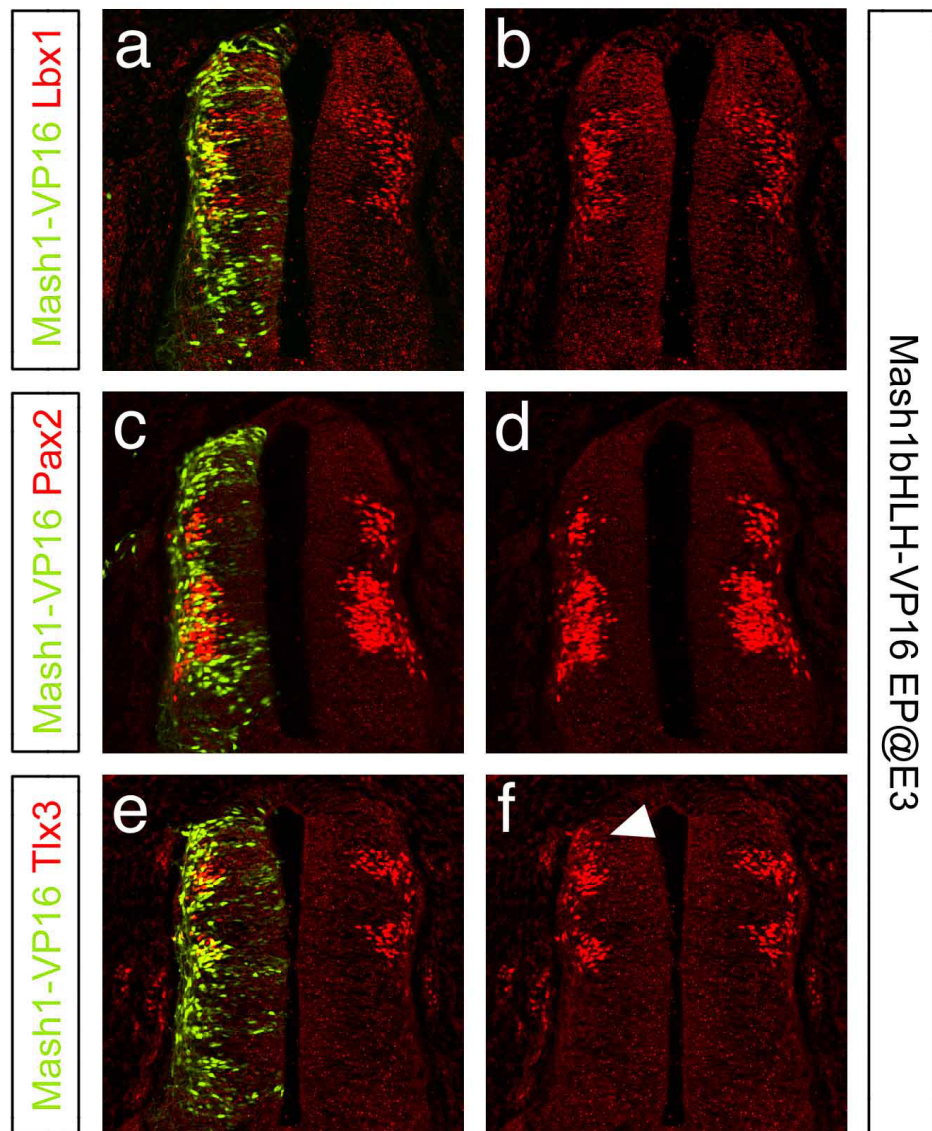


Figure 39: Overexpression of a transcriptional activator form of *Mash1* (*Mash1bHLH-VP16*) into E3 chick neural tubes. An expression construct containing an activated form of *Mash1* was electroporated together with an empty GFP expression construct into E3 chick neural tubes, which were harvested 48h later and analyzed for the expression of *Lbx1*, *Pax2* and *Tlx3*, which mark subpopulations of early-born neurons. (Fig. 39a, b) *Lbx1* expression is unchanged following activated *Mash1* misexpression. (Fig. 39c, d) *Pax2* is slightly reduced, indicating that *Mash1* represses dl4 neuron development. (Fig. 39e, f) Activated *Mash1* induces ectopic *Tlx3* expression (arrow heads in f), thereby mimicking the induction of dl3 and dl5 *Tlx3*⁺ neurons by “normal” *Mash1*.

Electroporation with the Mash1bHLH-VP16 construct at E6, however, has very little or no effect on late-born excitatory Tlx3-expressing neurons. Overall, the number of dIL neurons on the electroporated side is unchanged compared to the control half. Lbx1, which is expressed by both dIL_A and dIL_B neurons is unaffected (Fig. 40a, b), as are expression of Pax2 (Fig. 40c, d) and Tlx3 (Fig. 40e, f), indicating that an activated Mash1 transcription factor is not able to induce inhibitory dIL_A neuron differentiation or to suppress the development of excitatory dIL_B neurons.

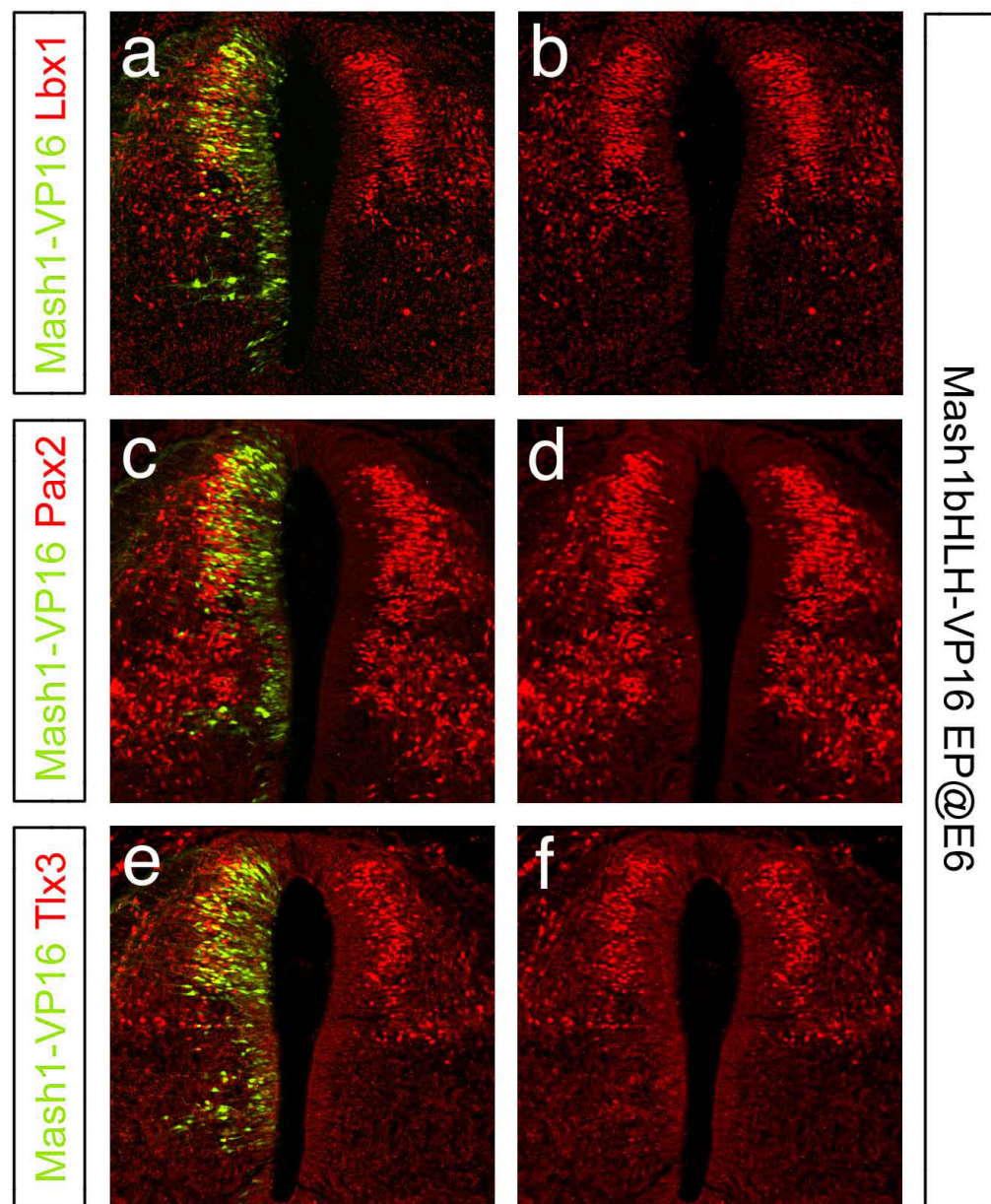


Figure 40: Overexpression of an activated form of Mash1 (Mash1bHLH-VP16) into E6 chick neural tubes. Chick embryos were harvested 24h after electroporation and then analyzed for the development of late-born neurons by the expression of Lbx1, Pax2 and Tlx3. (Fig. 40a, b) Lbx1 expression is unchanged on the electroporated side of the spinal cord compared to the endogenous control side, indicating that a transcriptional activator form of *Mash1* has no effect on late-born neurons. (Fig. 40c, d) The number of Pax2-expressing dL_A neurons, as well as Tlx3-expressing dL_B neurons, does not change following Mash1bHLH-VP16 overexpression. This is consistent with the lack of change in Lbx1 expression and confirms that a transcriptional activator form of *Mash1* has no effect on late-born neuron development.

The expression pattern of Lbx1, Pax2 and Tlx3 were also analyzed after electroporating a form of Mash1 that functions as a transcriptional repressor i.e. Mash1bHLH-EnR. In these experiments, I expected to see a downregulation of Tlx3 in presumptive dl3 and dl5 neurons, which would be consistent with the LOF and GOF analyses described above. This hypothesis turns out to be correct; dl5 neurons are completely missing on the electroporated half of the spinal cord, and dl3 neurons are strongly reduced in numbers with no Tlx3/GFP double-labeled cells remaining (Fig. 41e, f). Consistent with the reduction of dl5 neurons, Lbx1 expression is slightly decreased after electroporation of the repressor form of *Mash1*. However, a few precocious Lbx1⁺ cells are found in the vz of the spinal cord (Fig. 41a, b). These ectopic Lbx1-expressing cells are most likely dl4 neurons, as numerous Pax2-expressing dl4 neurons are also found in the vz of the electroporated side of the spinal cord (Fig. 41c, d).

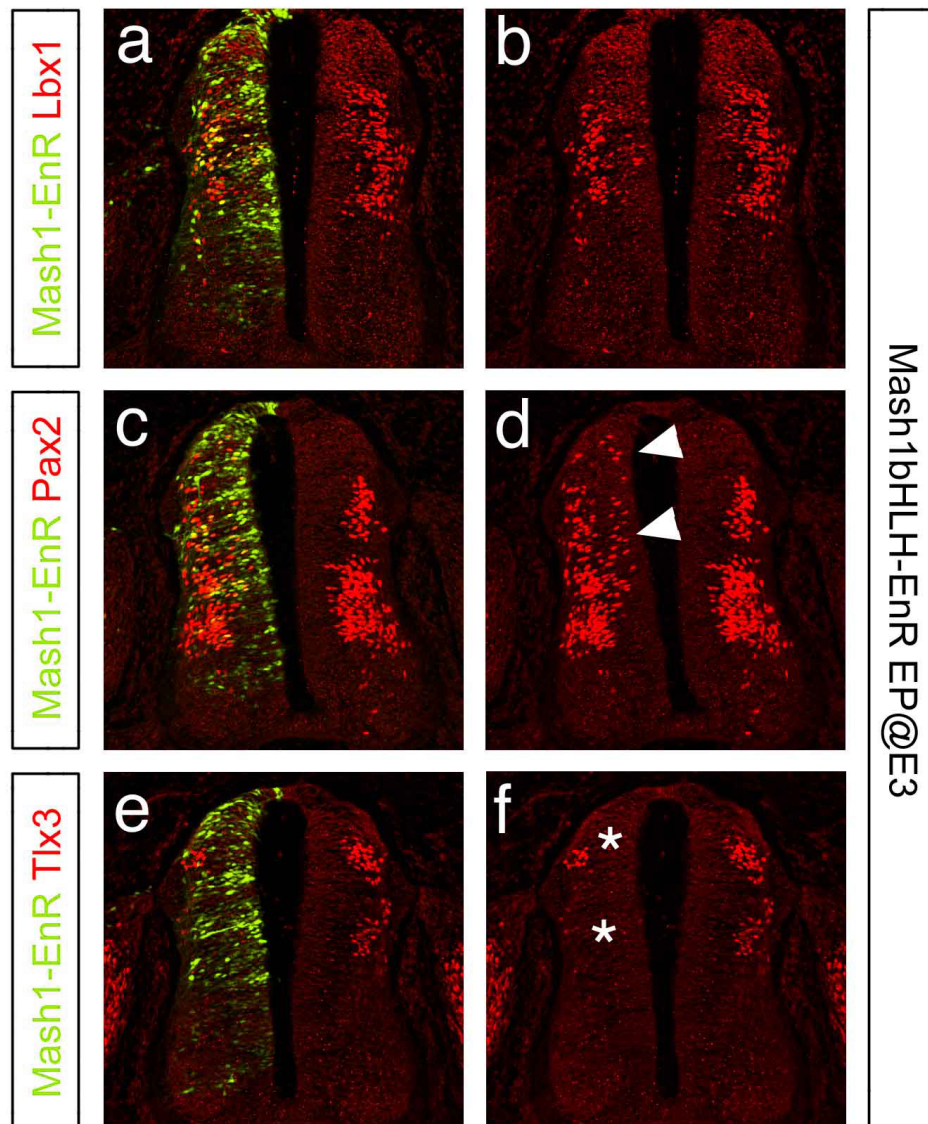


Figure 41: Overexpression of a transcriptional repressor form of *Mash1* (*Mash1bHLH-EnR*) into E3 chick neural tubes. After electroporation, chick embryos were allowed to develop for 24h before analyzing the development of early-born neurons by immunohistochemistry. (Fig. 41a, b) The number of Lbx1-expressing neurons is slightly decreased; however, several ectopic Lbx1⁺ neurons are found in the vz of the electroporated side of the spinal cord (arrow head in b). (Fig. 41c, d) Several ectopic Pax2⁺ cells are seen in the vz following the electroporation with the repressor form of *Mash1* (arrow heads in d). (Fig. 41e, f) Tlx3-expressing dl3 and dl5 neurons were strongly reduced on the electroporated side of the spinal cord (asterisks in f), consistent with the results from previous LOF and GOF analyses showing that *Mash1* acts as an activator to induce early-born dl3 and dl5 neurons. This reduction in dl5 neurons also explains the overall lower numbers of Lbx1-expressing neurons.

To determine the effect of the repressor form of the transcription factor Mash1 on dLL neurons, I electroporated the Mash1bHLH-EnR construct into the neural tube of E6 old chick embryos and analyzed the expression of Lbx1, Pax2 and Tlx3 24h later. Lbx1 expression is largely unchanged in the svz on the electroporated side. However, several cells expressing Lbx1 are found within the vz of the electroporated half of the spinal cord (Fig. 42a, b). A similar precocious expression is observed with Pax2 (Fig. 42c, d), suggesting that a transcriptional repressor form of Mash1 can induce a dLL_A cell fate. Tlx3 expression is unchanged following Mash1bHLH-EnR overexpression, suggesting that a repressor form of *Mash1* has no effect on excitatory neuron development (Fig. 42e, f).

In summary, these data further support the earlier observation that *Mash1* has different roles at early versus late phases of dorsal interneuron development.

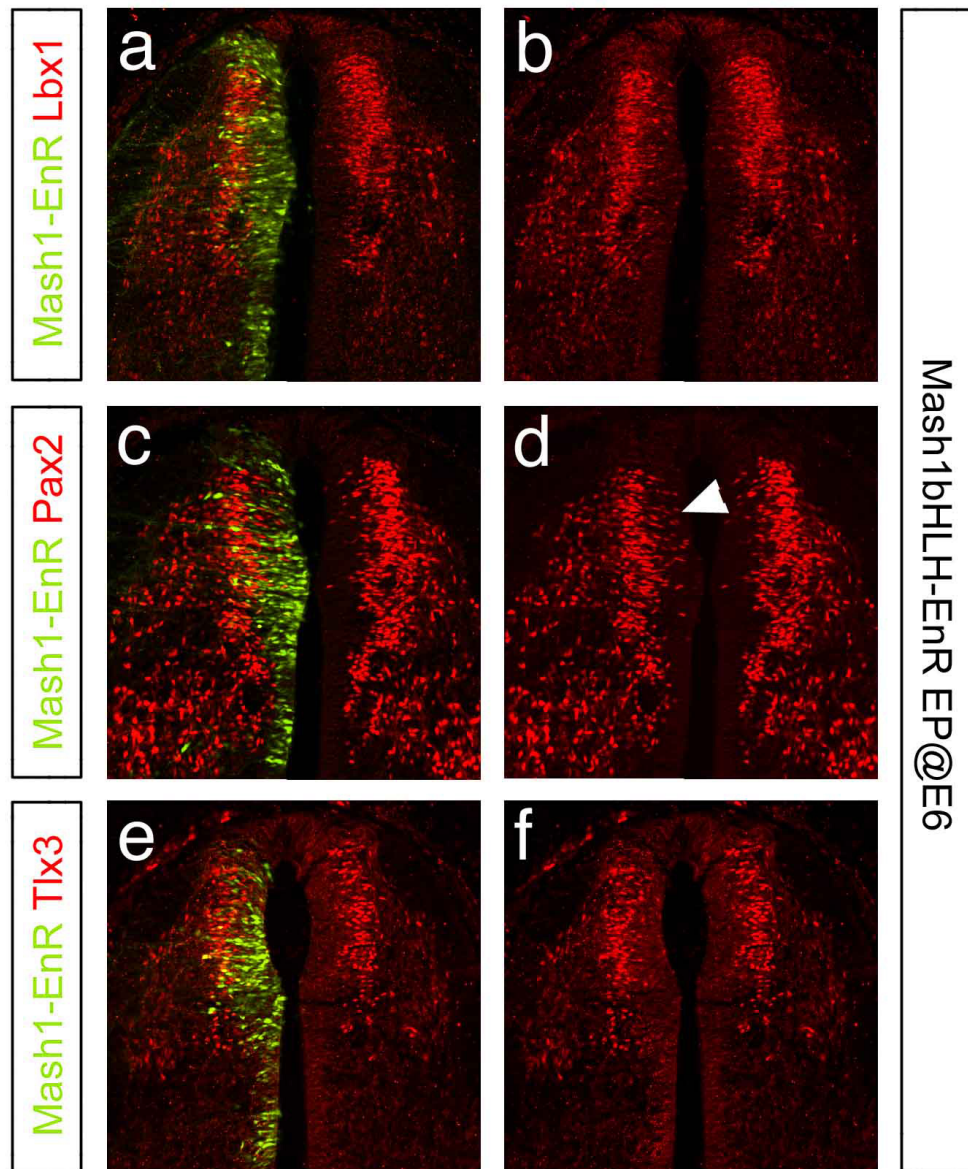


Figure 42: Overexpression of a transcriptional repressor form of *Mash1* (*Mash1bHLH-EnR*) into E6 chick neural tubes. Chick embryos were harvested 24h after electroporation and analyzed by immunohistochemistry to analyze the effects on late-born neurons. (Fig. 42a, b) The expression of *Lbx1* appears mostly unchanged, except for some ectopic *Lbx1*⁺ cells in the vz of the electroporated side (arrow head in b). (Fig. 42c, d) A precocious *Pax2* expression in the vz is also noted following overexpression with a transcriptional repressor form of *Mash1* (arrow head in d). These data suggest that a transcriptional repressor form of *Mash1* induces *Pax2*-expressing dIL_A neurons. (Fig. 42e, f) *Tlx3* expression is unchanged, showing that the repressor form of *Mash1* has no effects on dIL_B neuron development.

3.13 Progenitor gene expression during early and late phases of dorsal interneuron development.

Gsh1, Gsh2 and Mash1 are co-expressed in progenitors of both inhibitory dI4 and dIL_A and excitatory dI5 and dIL_B neurons. Whereas early-born dI4 and dI5 neuron subtypes are generated from distinct progenitor domains, late-born dIL_A and dIL_B neurons arise from a common progenitor pool. Our earlier analyses of Mash1 function suggested that the molecular mechanism that generates these cells differs between the early and late phases of dorsal neurogenesis.

A recent study has outlined a role for the bHLH transcription factor Ptf1a in the generation of inhibitory Pax2⁺ neurons in the dorsal spinal cord. Ptf1a is expressed in progenitors of dI4 and dIL neurons, and mice lacking *Ptf1a* show a dramatic loss of early-born Pax2⁺ dI4 and late-born Pax2⁺ dIL_A neurons with a concomitant increase in excitatory Lmx1b/Tlx3⁺ dI5 and dIL_B neurons (Glasgow et al., 2005).

This lead me to investigate whether Ptf1a plays a role in this change of genetic interactions between the transcription factors involved in generating early-born versus late-born interneurons. I compared the expression pattern of Gsh1, Gsh2, Mash1 and Ptf1a in early and late dorsal interneuron progenitors in wt embryos at times ranging from E10.5-E12.5. Spinal cords were stained with antibodies against these four transcription factors. At E10.5 Gsh1/2 and Mash1 are each expressed in progenitors of dI3-dI5 neurons (Fig. 43a-c), as described previously (Kriks, 2003). Ptf1a expression is more restricted and overlaps with Gsh1/2 and Mash1 only in the progenitors of dI4 neurons (Fig. 43c, d). At later time points, the expression of Ptf1a undergoes a change from this broad expression in the dI4 progenitors to a more mosaic pattern of expression at E11.5 (Fig. e, f). This change coincides with the switch from early to late patterns of dorsal interneuron generation. At E12.5 this “salt-and-pepper” expression continues with PTF1a⁺ cells positioned predominantly at the lateral edge of the ventricular zone and in the subventricular zone (Fig. 43i, k), which suggests that cells positive for Ptf1a are withdrawing from the cell cycle. Most of these cells expressing Ptf1a are also Gsh1/2 positive (Fig. 43k) and express at least low levels of Mash1 (Fig. 43i, j). However, several Ptf1a⁺ cells are not double-labeled with either Gsh1/2 or Mash1.

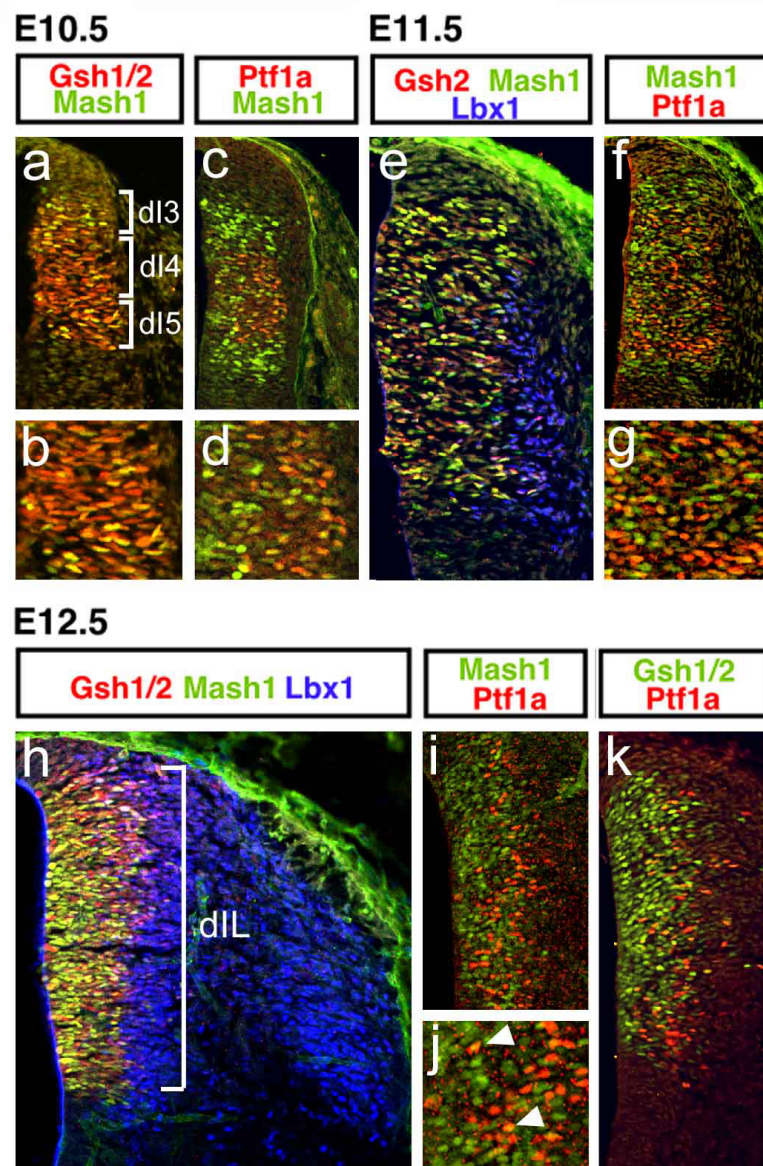


Figure 43: Expression patterns of Gsh1/2, Mash1 and Ptf1a between E10.5 and E12.5 in the dorsal spinal cord. (Fig. 43a-d) At E10.5, Gsh1, Gsh2 and Mash1 are expressed in dividing dl3-dl5 precursors. (Fig. 43b, c) Ptf1a (red) is expressed in dl4 progenitors, while Mash1 (green) is expressed in dl3, dl4, and dl5 progenitors, although at a reduced intensity in Ptf1a⁺ dl4 progenitors. (Fig. 34e) At E11.5, Mash1 (green) is co-expressed with Gsh2 (red) in dl3-dl5 progenitors, with the dl4 and dl5 progenitor domains giving rise to Lbx1⁺ (blue) interneurons. (Fig. 34f g) At this stage, the Ptf1a expression domain begins to expand with most Ptf1a⁺ cells expressing some levels of Mash1. (Fig. 34h) At E12.5, late-born Lbx1⁺ neurons arise from a single progenitor domain where Gsh1/2 and Mash1 are co-expressed. (Fig. 34i-k) At this stage, Ptf1a⁺ cells are located primarily at the lateral edge of the ventricular zone (vz) and express little or no Gsh1/2 (Fig. 34k). Mash1 and Ptf1a are co-expressed in some dIL progenitors (Fig. 34i, j, arrowheads).

To assess whether Ptf1a is expressed at different times during the cell cycle, I performed co-labeling experiments of Ptf1a and Mash1 with the cell cycle markers phospho-histone H3 (PH3) and Ki67. PH3 only labels cells that are in M-phase (Hendzel et al., 1997). Ki67 labels all proliferating cells, but has a higher expression level in M-phase cells (Gerdes et al., 1984). Both, Ptf1a and Mash1 double-label with Ki67, a marker for all dividing cells. These Ptf1a- and Mash1-expressing cells are not in M-Phase, as they do not co-label with cells expressing PH3 (Fig. 44a, b) or high levels of Ki67 (Fig. 44c-f). To test if any of the Ptf1a⁺ neurons are in S-Phase, I analyzed E12.5 wt embryos pulsed with BrdU for 1h. Cells labeled with BrdU express Ptf1a in a few cells, and most of the Ptf1a-expressing cells are BrdU negative (Fig. 44g, h). Mash1 is expressed in many more BrdU⁺ cells in the same pulse experiment (Fig. 44i, j), indicating that Mash1 is expressed in dividing progenitors, whereas Ptf1a may be restricted to late dLL progenitors, which are about to withdraw from the cell cycle.

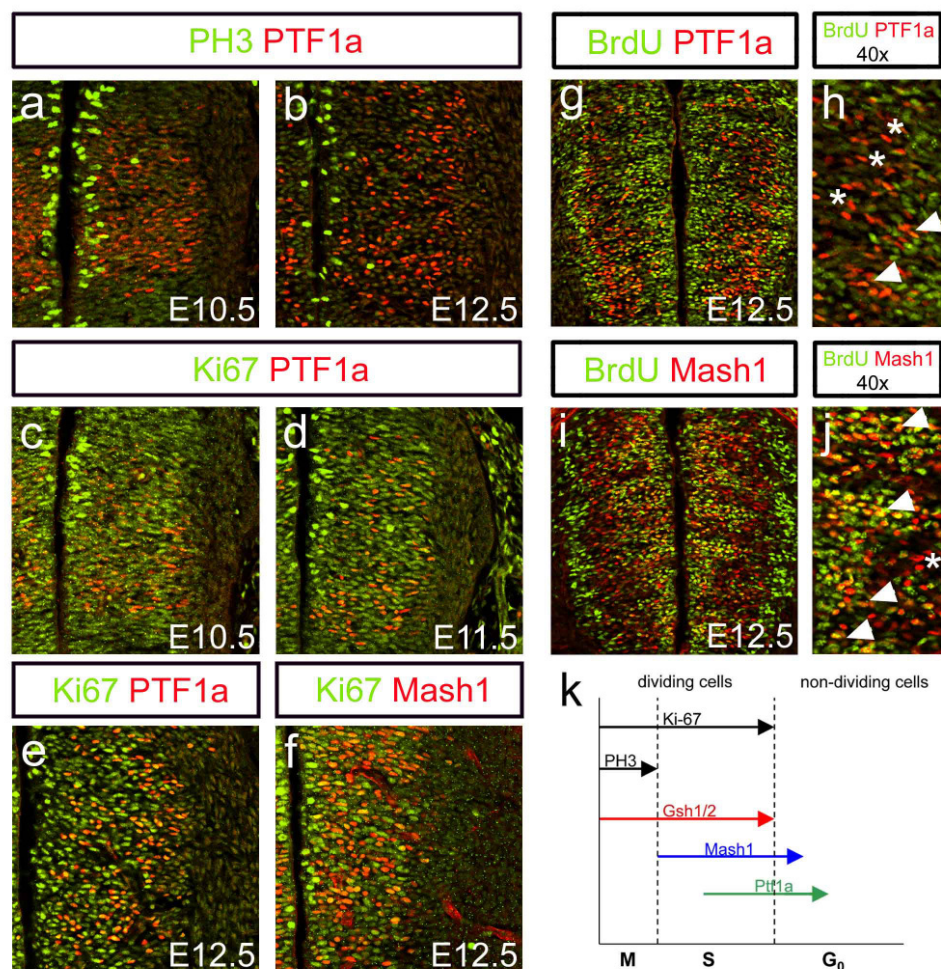


Figure 44: Ptf1a is expressed in dorsal progenitors, which have not exited the cell cycle. Double-immunostaining was performed with antibodies against Ptf1a as well as Mash1 and cell cycle markers at E10.5 - E12.5. (Fig. 44a, b) Cells in M-phase that express PH3 (green) do not express Ptf1a (red) at either E10.5 or E12.5. (Fig. 44c, d) However, most of the Ptf1a⁺ cells (red) at E10.5 and E11.5 and many Ptf1a⁺ cells at E12.5 (Fig. 44e) are co-labeled with Ki67 (green), a marker for all dividing cells though not M-phase, indicating that Ptf1a⁺ cells have not exited the cell cycle. (Fig. 44f) At E12.5, most of the Mash1⁺ cells are double labeled with Ki67, showing that Mash1⁺ cells are dividing. (Fig.44g-j) 1h BrdU pulse was performed at E12.5 to examine whether Ptf1a and Mash1 are expressed during S-phase. (Fig.44g, h) h is a magnification of g. Most of Ptf1a-expressing cells do not express BrdU (asterisks in h), and only a few cells co-express Ptf1a and BrdU (arrow head in h), indicating that Ptf1a-expressing cells are withdrawing from the cell cycle. (Fig. 44i, j) j is a magnification of i. Most Mash1⁺ cells express also BrdU (arrow heads in j). Only few Mash1-expressing cells are BrdU-negative (asterix in j). This shows that Mash1 is predominantly expressed in cells in S-phase. (Fig. 44k) Schematic summary of Gsh1/2, Mash1 and Ptf1a expression during the cell cycle.

Recent studies have shown that Ptf1a is necessary for the development of inhibitory dl4 and dl_A neurons in the spinal cord (Glasgow et al., 2005) as well as inhibitory neurons in the cerebellum (Hoshino et al., 2005). To test if Mash1 is necessary for Ptf1a expression in dl4 progenitors and if Mash1 controls the differentiation of late-born inhibitory neurons by regulating Ptf1a expression in presumptive dl_A progenitors, Rumiko Mizuguchi analyzed Ptf1a expression in *Mash1*^{-/-} embryos between E10.5 and E12.5 (Fig. 45a-f). At E10.5 Ptf1a expression is unchanged in dl4 progenitors (Fig. 45a, b), suggesting that Ptf1a is not dependent upon Mash1 expression at this time. However, at E12.5 Ptf1a expression is drastically reduced (Fig. 45e, f). These data explain the development of Pax2⁺ dl4 neurons in E10.5 and E11.5 *Mash1*^{-/-} spinal cords and the reduction of Pax2⁺ dl_A neurons during the later phase of dorsal interneuron development. Early on, Ptf1a is not dependent on Mash1 function and continues to be expressed in the absence of *Mash1*, thus accounting for the proper specification of dl4 neurons in the E10.5 and E11.5 *Mash1*^{-/-} spinal cord. However, from E11.5 onwards Mash1 is required for Ptf1a expression in dlL progenitors. In E12.5 *Mash1*^{-/-} spinal cords, Ptf1a is reduced and this decrease accounts for the reduction of Pax2⁺ dl_A neurons. I also analyzed the expression of Gsh1/2 on adjacent sections. Gsh1/2 is unchanged in the E12.5 *Mash1*^{-/-} cord (Fig. 45g, h),

demonstrating that the loss of Ptf1a expression is not due to the downregulation of Gsh1/2.

Due to the loss of inhibitory neurons, along with the concomitant increase in numbers of excitatory neurons in the *Ptf1a*^{-/-} spinal cord, I expected an upregulation of Ptf1a in *Gsh1/2*^{-/-} embryos. Surprisingly, antibody staining against Ptf1a in E10.5 *Gsh1/2*^{-/-} reveals no change in Ptf1a expression (Fig. 45i, j), arguing that Ptf1a does not depend on Gsh1/2 function at this time point. This may explain, why the development of dl4 neurons precedes in the absence of *Gsh1/2*. Strikingly, at E11.5 and E12.5 Ptf1a expression is markedly reduced (Fig. 45 k-n), which is most likely due to the decrease in Mash1 expression in the *Gsh1/2*^{-/-} spinal cord (Fig. 45o, p).

The analysis of dorsal interneuron development in the *Gsh1/2*^{-/-} cord suggests that Mash1 and Ptf1a are both dispensable for inhibitory neuron specification in the dorsal spinal cord when *Gsh1/2* are absent. Moreover, the concomitant loss of Mash1 and Ptf1a in mice lacking *Gsh1/2* provides further evidence that Mash1 regulates Ptf1a expression in dIL progenitors.

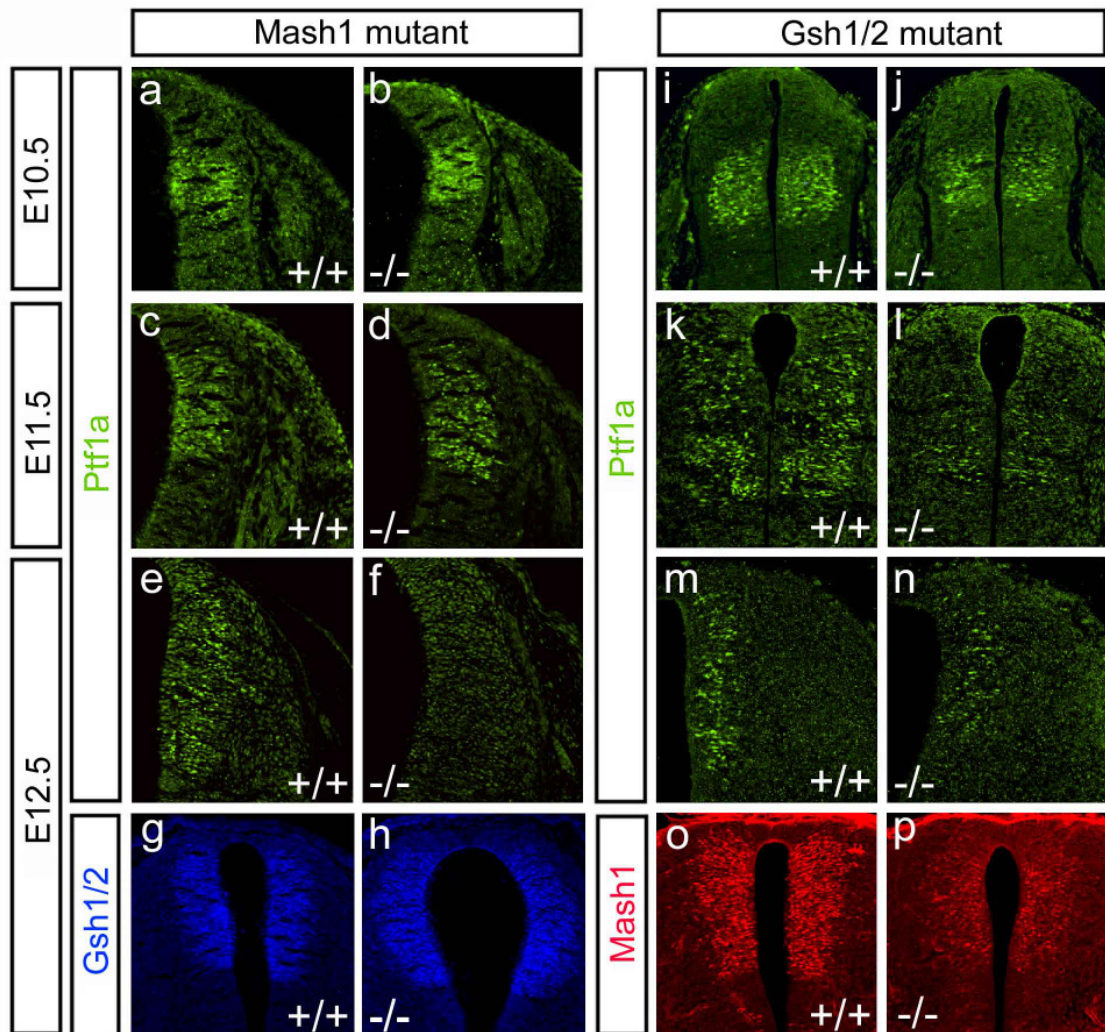


Figure 45: Analysis of Ptf1a expression in *Gsh1/2*^{-/-} and *Mash1*^{-/-} mice between E10.5 and E12.5. Expression of Ptf1a in *Mash1*^{-/-} (Fig. 45a-f) and *Gsh1/2*^{-/-} (Fig. 45i-n) spinal cords. (Fig. 45 a, b) Ptf1a expression is unchanged at E10.5 and E11.5, however, it is strongly reduced at E12.5 in the vz of *Mash1*^{-/-} cords relative to age matched wild type (wt) cords (Fig. 45e, f). (Fig. 45g,h) This decrease is not due to a change in *Gsh1/2* expression, as *Gsh1/2* exhibits a normal expression pattern at E12.5 in *Mash1*^{-/-} embryos. (Fig. 45i, j) Expression of Ptf1a is unchanged in E10.5 *Gsh1/2*^{-/-} cords, but markedly decreased at E11.5 and E12.5 (Fig. 45k-n). *Mash1* is strongly reduced in the *Gsh1/2*^{-/-} cord at E12.5 (Fig. 45o, p). Fig. 45a-f was kindly provided by Rumiko Mizuguchi.

To test whether Mash1 actively induces Ptf1a expression, I misexpressed *Mash1* in the chick spinal cord and analyzed Ptf1 expression by *in situ* hybridization. Ectopic *Ptf1*⁺ cells are found throughout the entire spinal cord, indicating that Mash1 induces *Ptf1a* expression (Fig. 46a, b).

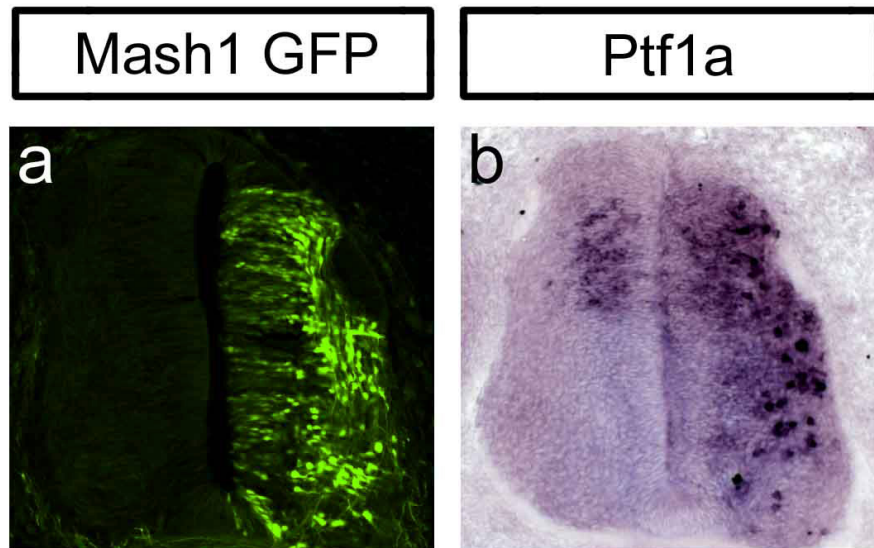


Figure 46: Effect of *Mash1* overexpression on *Ptf1a*. An expression construct containing full-length *Mash1* was electroporated, together with an empty GFP expression vector into E5 chick spinal cords. The embryos developed for an additional 48h, before being analyzed for the expression of *Ptf1a* by *in situ* hybridization. (Fig. 46a, b) *Ptf1a* mRNA is strongly upregulated following *Mash1* overexpression, showing that Mash1 induces *Ptf1a* expression.

Together these findings support a model in which Gsh1/2 regulate Mash1 expression, which in turn activates Ptf1a in prospective GABAergic precursors. Ptf1a then acts to antagonize Gsh1/2, thereby allowing a subset of Gsh1/2⁺ progenitors to differentiate as inhibitory neurons.

3.14 *Ptf1a* misexpression analysis

The loss of inhibitory Pax2⁺ neurons in the *Ptf1a*^{-/-} spinal cord together with the reduction in Ptf1a expression in the *Mash1*^{-/-} cord, led me to ask whether Ptf1a might be directly upstream of Pax2. To test whether Ptf1a is sufficient to induce a dIL_A fate I cloned the full-length coding region of *Ptf1a* into the expression vector pIRES-EGFP and performed misexpression analysis in the chick spinal cord.

3.14.1 Cloning of the *Ptf1a* full-length coding sequence

Total RNA, which was isolated from spinal cords of E11.5 wt embryos, was used as a template to prepare cDNA. The full-length region of *Ptf1* was amplified from this cDNA by using two primer pairs (see 7.1.3 for sequences). The first set contained a sense primer, which annealed 100 bp upstream of the start codon and included a SacII site. The antisense primer annealed in the middle of the Ptf1a sequence and had a BamH1 restriction site. The second primer set contained a sense primer, which had the reversed sequence of the antisense primer of the first pair. The antisense primer annealed just past the stop codon and also contained a BamH1 site. The first fragment of the Ptf1a coding sequence was cloned into the pIRES-EGFP expression vector using the SacII and BamH1 site of the MCS. In the second cloning step, this vector was cut with BamHI, into which the second half of the Ptf1a sequence was ligated. Since the second half could ligate in either direction, restriction digests were used to confirm the proper orientation. Finally, the construct was sequenced and compared to the published *Ptf1a* mRNA sequence (accession number: NM_018809) in the NCBI nucleotide database (<http://www.ncbi.nlm.nih.gov>) to ensure that it does not contain mutations (see 7.2.2).

3.14.2 Misexpression analysis of *Ptf1a* in the chick spinal cord

To test whether *Ptf1a* induces Pax2⁺ dIL_A neurons, I electroporated the *Ptf1a*-IRES-EGFP expression construct into the spinal cord of E6 chick embryos and harvested the embryos 24h after electroporation. The spinal cords of these embryos were then analyzed for the expression of Pax2, Lhx1/5, Tlx3 and Lmx1b by immunohistochemistry. Ectopic Pax2- (Fig. 47a-d) and Lhx1/5-expressing neurons (Fig. 47e-h) are found in the dorsal vz following overexpression of *Ptf1a*, indicating that *Ptf1a* actively induces a dIL_A cell fate in a cell autonomous manner, as shown by the co-expression of GFP (*Ptf1a*) with Pax2/Lhx1/5 (Fig. 47c, g). The generation of dIL_B neurons is strongly downregulated by *Ptf1a*, insofar, as the expression of Tlx3 (Fig. 47i-l) and Lmx1b (Fig. 47m-p) are reduced following *Ptf1a* misexpression. These findings suggest that *Ptf1a* blocks dIL_B cell differentiation and promotes the development of dIL_A neurons from late-born dIL progenitors.

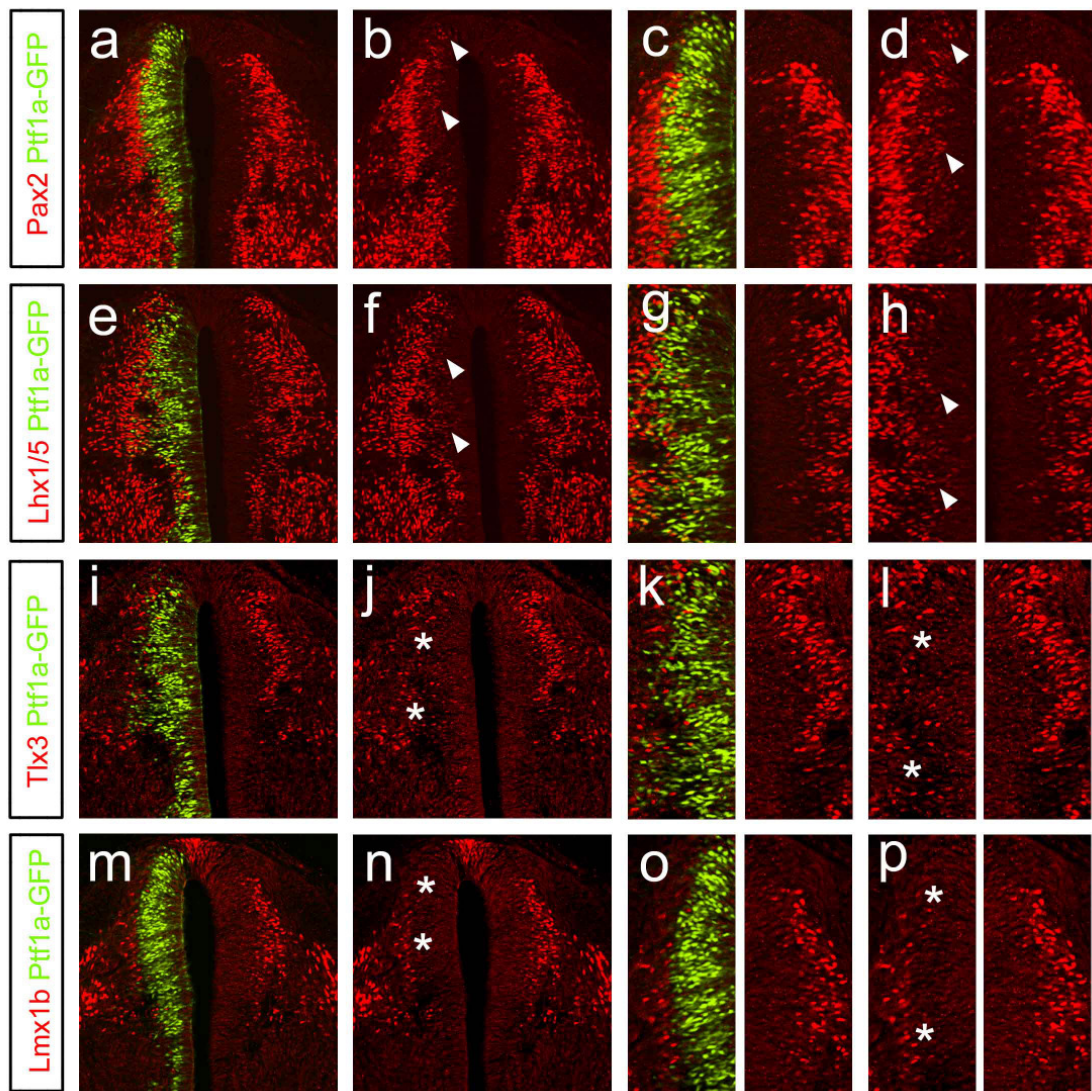


Figure 47: Misexpression analysis of *Ptf1a*. A *Ptf1a* expression construct was electroporated into E6 chick spinal cords, which were harvested 2h later to analyze the effect of *Ptf1a* on the development of late-born neurons. (Fig. 47a-d) c and d are magnifications of a and b. Ectopic Pax2⁺ cells are found in the svz of the electroporated side of the spinal cord following *Ptf1a* misexpression (arrow heads in b, d). This indicates that *Ptf1a* induces dLL_A neurons. (Fig. 47e-h) g and h are magnifications of e and f. Lhx1/5 are also induced following *Ptf1a* misexpression, confirming the induction of dLL_A neurons by *Ptf1a*. (Fig. 47i-l) k and l are magnifications of i and j. The number of Tlx3⁺ neurons is strongly reduced on the electroporated side (asterisks in j, l), indicating that *Ptf1a* represses dLL_B neuron differentiation. (Fig. 47m-p) o and p are magnifications of m and n. Lmx1b is also strongly repressed by *Ptf1a* (asterisks in n, p).

3.15 Analysis of Notch signaling in spinal cords of *Gsh1/2*^{-/-} and *Mash1*^{-/-} embryos.

At E12.5, dIL_A and the dIL_B subtypes of late-born neurons both arise from a single progenitor domain in an intermingled fashion. How is it that these two cell types can be generated in appropriate numbers? One potential mechanism includes the Notch signaling pathway and the process of lateral inhibition, which this signaling pathway controls. This pathway is used throughout development to regulate binary cell fate choices. For example, Notch signaling is involved in the neuron/glia decision, which arise from the same precursors. *Mash1*, which is necessary for late-born neurons to acquire a dIL_A fate in the presence of *Gsh1/2*, is both a downstream target of Notch signaling and also regulates *Delta1*, a ligand for the Notch receptor. The transmembrane protein *Delta1* binds to and activates the receptor Notch on the neighboring cells. This binding leads to the cleavage of the intracellular domain of Notch (NICD), which is then able to enter the nucleus, where it activates Notch target genes, e.g. *Hes1* and *Hes5*. In many instances, these Notch targets regulate bHLH proteins such as *Ngn1* and *Mash1* (Kageyama et al., 2005).

To begin testing whether Notch signaling is involved in the specification of dIL neurons, Rumiko Mizuguchi analyzed the expression of NICD and Notch ligand *Delta-like1* (*Dll1*) in E10.5 and E12.5 spinal cords of *Mash1*^{-/-} embryos and wt littermates. NICD (Fig. 48a, b) and *Dll1* expression (Fig. 48e, f) are significantly reduced in the E12.5 *Mash1*^{-/-} spinal cord. However, NICD expression is unchanged in dorsally and ventrally adjacent domains (Fig. 48a, b). The downregulation of NICD and *Dll1* at this time point shows that NICD signaling is impaired in mice lacking *Mash1* and suggests that the lateral inhibition pathway is involved in the development of late-born neurons.

Surprisingly, at E10.5 the level of NICD expression in wt embryos is very weak in dorsal progenitors and this low expression of NICD is also observed in the *Mash1*^{-/-} cord (Fig. 48c, d). *Dll1*, however, is expressed in the dorsal vz, but its expression is unchanged in E10.5 *Mash1*^{-/-} embryos compared to wt littermates (Fig. 48g, h).

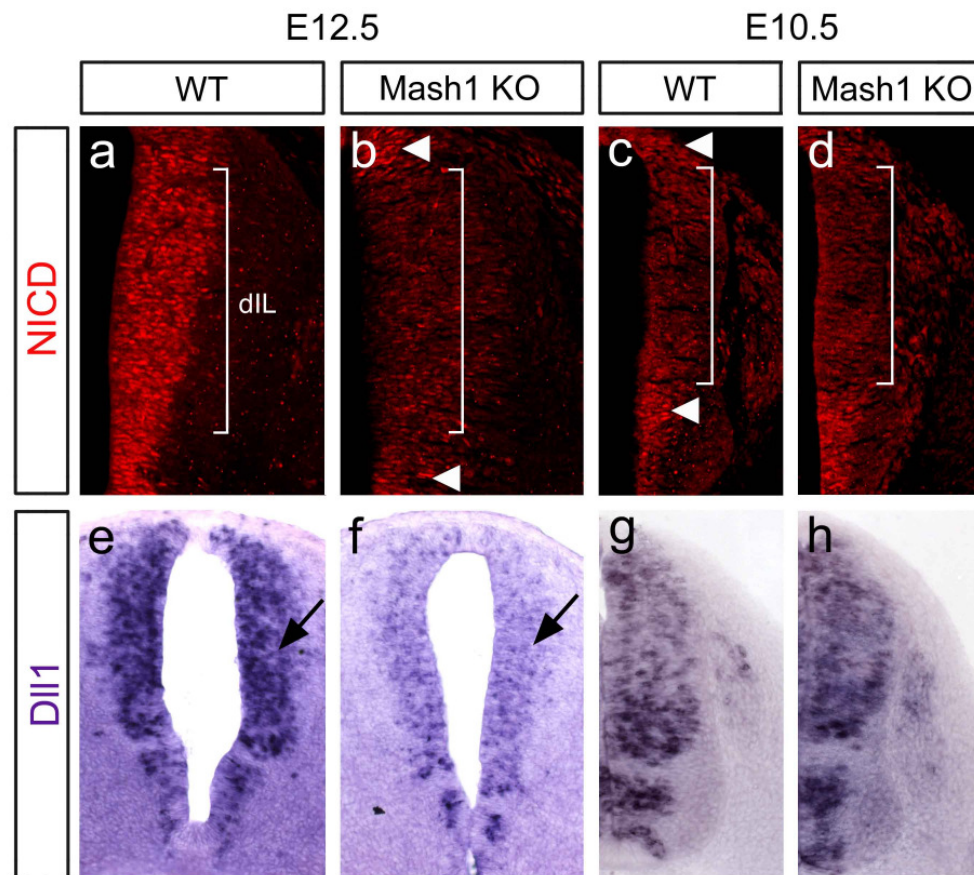


Figure 48: NICD and *Dll1* expression in *Mash1*^{-/-} spinal cords. Expression pattern of NICD (Fig. 48a-d) and *Dll1* (Fig. 48e-h) were analyzed in wt and *Mash1*^{-/-} cord at E12.5 and E10.5. (Fig. 48a, b) The level of NICD expression is strongly reduced in E12.5 *Mash1*^{-/-} embryos compared to wt littermates. (Fig. 48c, d) The dorsal progenitor domain (brackets) expresses only low levels of NICD in both wt and *Mash1*^{-/-} cord at E10.5. Note that NICD is expressed in elevated levels in ventral progenitors and near the dorsal midline (asterisks in c). (Fig. 48e, f) *Dll1* expression is also markedly decreased in *Mash1*^{-/-} dorsal progenitors (arrows) at E12.5. (Fig. 48g, h) *Dll1* is expressed at high levels in the dorsal progenitors at E10.5. There is no difference in either *Dll1* or NICD expression in E10.5 wt and *Mash1*^{-/-} spinal cords. This figure was kindly provided by Rumiko Mizuguchi.

The reduction in Mash1 levels in dIL progenitors in the *Gsh1/2*^{-/-} led me to ask whether Notch signaling is involved in the late phenotype seen in the

Gsh1/2^{-/-} spinal cord. Surprisingly, no changes are observed in various components of the Notch signaling pathway. The expression of Notch ligands, Delta1 and Delta3 (Fig. 49a-d), the Notch intracellular domain (NICD) (Fig. 49i, j), and Notch target genes Hes1 and Hes5 (Fig. 49e-h) are all unchanged in E11.5 *Gsh1/2*^{-/-} embryos compared to wt littermates.

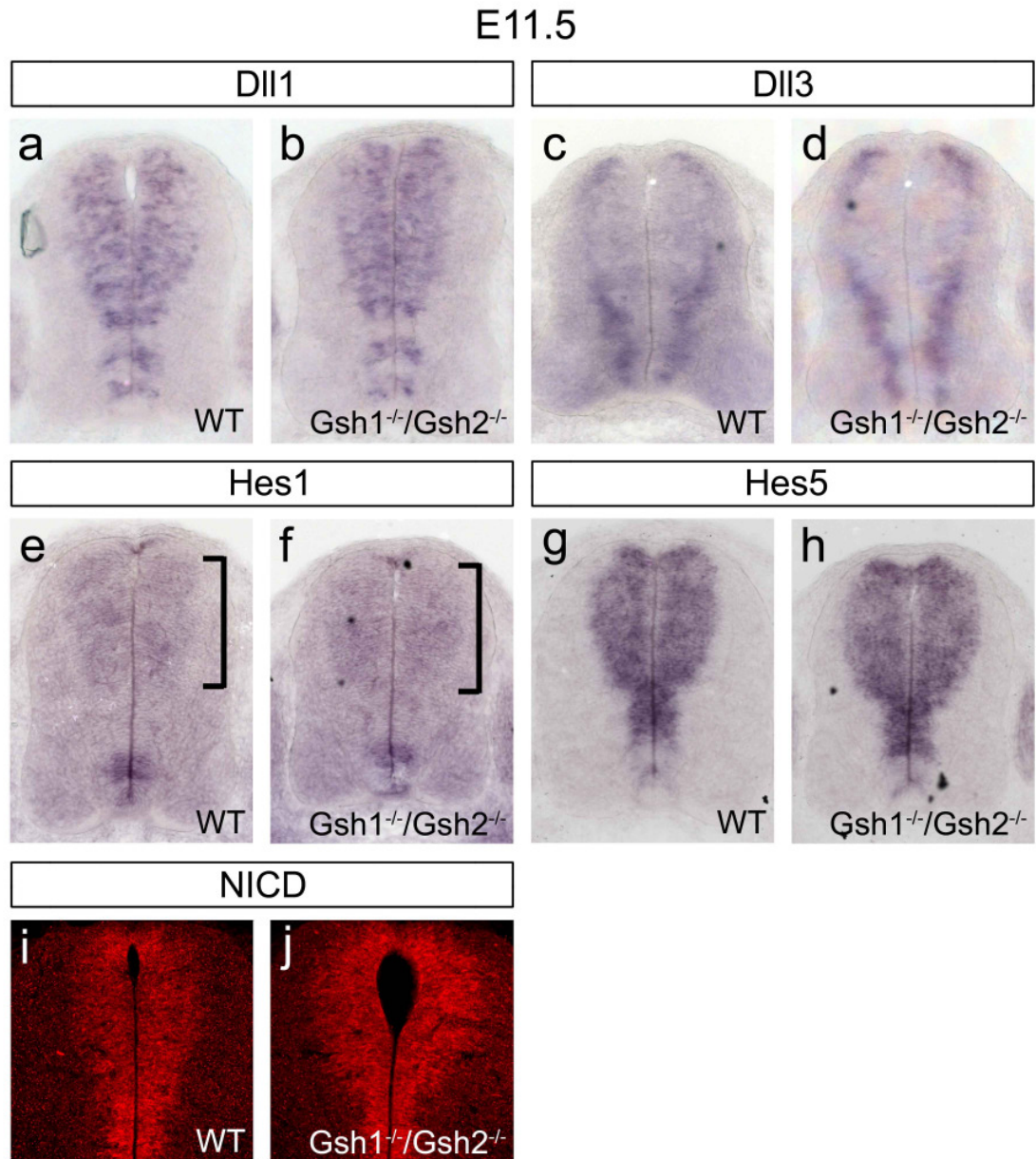


Figure 49: Notch signaling in the *Gsh1/2*^{-/-} spinal cords at E11.5. The expression of Notch ligands *Dll1* and *Dll3* and Notch targets *Hes1* and *Hes5* were analyzed by *in situ* hybridization, as well as NICD expression by immunohistochemistry. (Fig. 49a, b) *Dll1* expression, as well as *Dll3* expression (Fig. 49c, d), is unchanged in the spinal cord of *Gsh1/2*^{-/-} embryos. (Fig. 49e, f) No change is noted in *Hes1* expression in mice lacking *Gsh1* and *Gsh2*. (Fig. 49g, h) *Hes5* expression is also unchanged in the *Gsh1/2*^{-/-} embryos compared to wt littermates. (Fig. 49i, j) NICD expression is also similar in both wt and *Gsh1/2*^{-/-} embryos.

No changes in *Dll1*, *Dll3*, *Hes5* or NICD expression are noted in E12.5 *Gsh1/2*^{-/-} spinal cords compared to wt littermates (Fig. 50a-h).

These data indicate that Notch signaling is normal in the absence of *Gsh1* and *Gsh2* during both the early and the later waves of neurogenesis in the dorsal spinal cord.

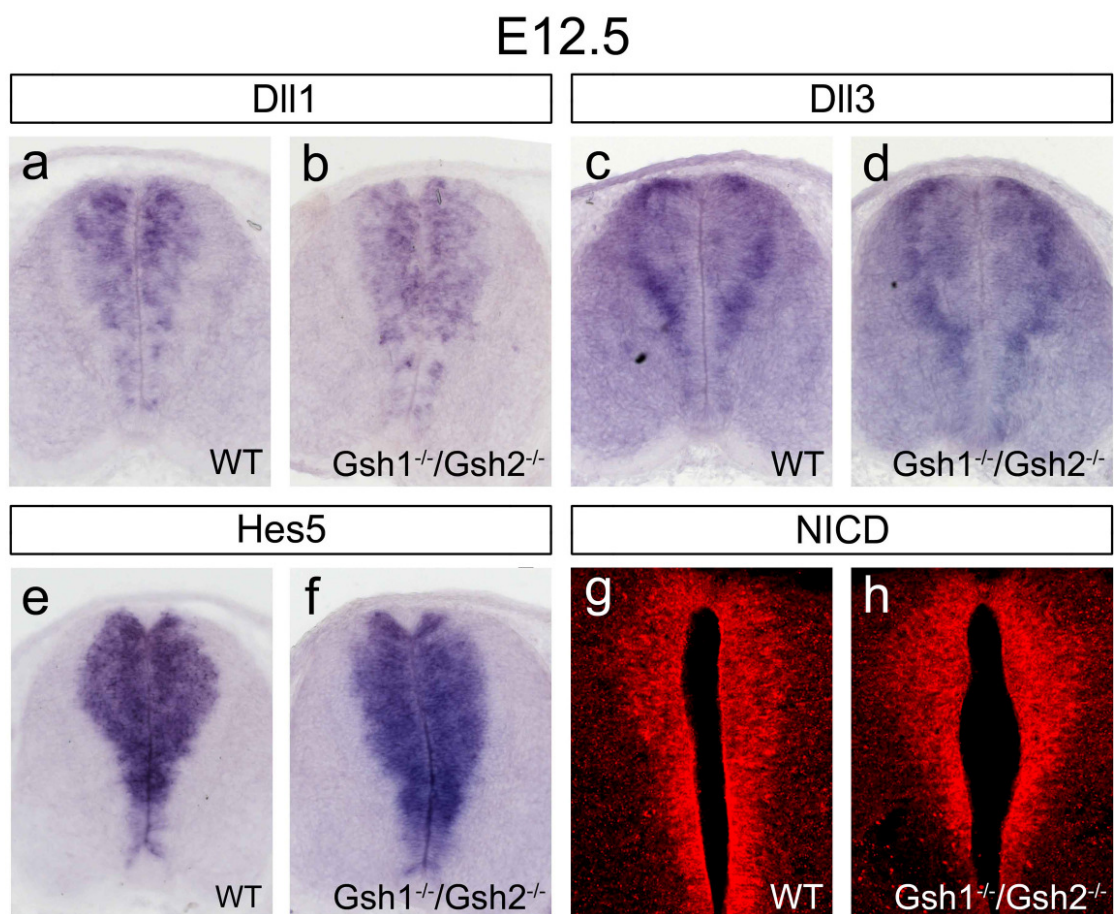


Figure 50: Notch signaling in the *Gsh1/2*^{-/-} spinal cords at E12.5. *Dll1* (Fig. 50a, b), *Dll3* (Fig. 50c, d), as well as *Hes5* (Fig. 50e, f) and NICD expression (Fig. 50g, h) are unchanged in the *Gsh1/2*^{-/-} spinal cords compared to wt littermates, indicating that Notch signaling is unchanged in mice lacking *Gsh1* and *Gsh2* during the second wave of neurogenesis.

3.16 Analysis of *Presenilin1*^{-/-} and *Delta1*^{hypo/-} embryos

To further investigate if/how Notch signaling is important for the specification of a subtype of dLL neurons, Rumiko analyzed *Presenilin1*^{-/-} (*Psen1*) embryos, which have reduced Notch signaling due to the lack of cleavage of the intracellular domain of the Notch receptor. She performed immunohistochemical analyses using specific antibodies against NICD, Mash1, Lmx1b and Pax2 on cross-sections of embryos lacking *Presenilin1*. Staining against NICD confirms that activated Notch is reduced in the *Psen1*^{-/-} spinal cord (Fig. 51a, b). These embryos have a spinal cord with a much smaller dorsal half and therefore have a shorter dorsal vz. However, Mash1-expressing cells are more densely packed in comparison with age-matched wt embryos (Fig. 51c, d). The dorsal horn of *Psen1*^{-/-} also exhibits a strong decrease in Lmx1b⁺ neurons indicating a reduced number of dLL_B cells (Fig. 51e, f). The number of Pax2-expressing dLL_A neurons is unchanged in mice lacking *Presenilin1* (Fig. 51g, h), suggesting that Notch signaling is necessary for the correct specification of dLL_B interneurons, but is dispensable for the generation of dLL_A neurons.

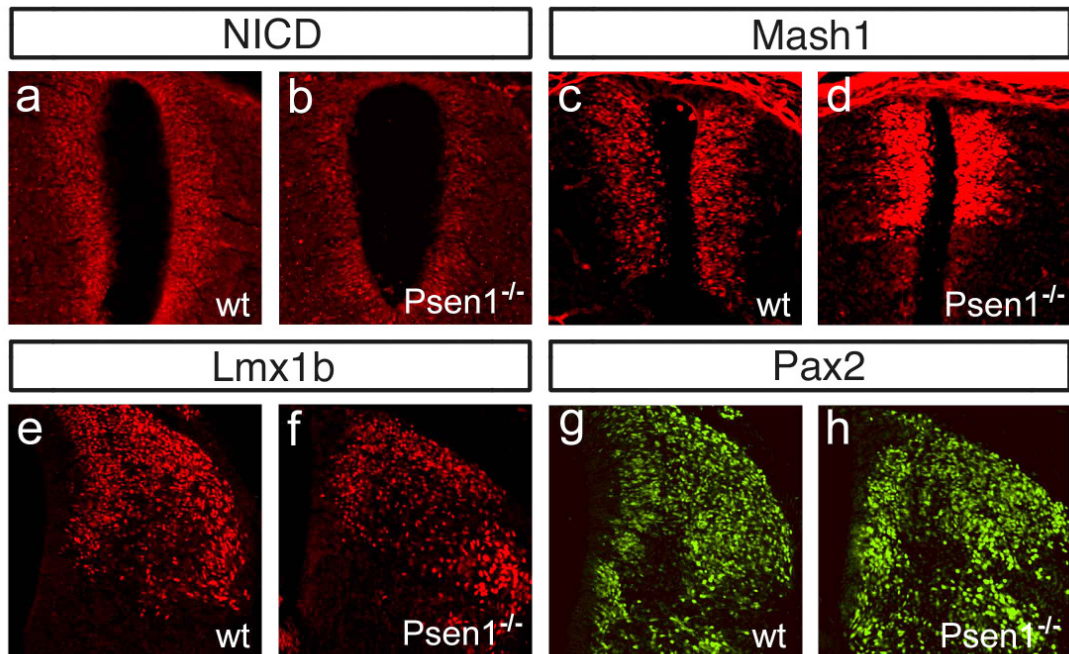


Figure 51: Analysis of *Presenilin1*^{-/-} (*Psen1*^{-/-}) embryos at E12.5. Cross sections of E12.5 wt and *Psen1*^{-/-} were analyzed by immunohistochemistry to examine the specification of late-born neurons. (Fig. 51a, b) Expression of activated Notch (NICD) is strongly down-regulated in the vz of *Psen1*^{-/-} embryos. (Fig. 51c, d) At E12.5, the density of Mash1⁺ cells in the dIL progenitors is increased in the *Psen1*^{-/-} spinal cord compared to wild type embryos. (Fig. 51e, f) In E12.5 dorsal horns of *Psen1*^{-/-} embryos, the number of Tlx3⁺ dIL_B neurons is significantly reduced, while the number of Pax2⁺ dIL_A neurons are unchanged (Fig. 51g, h). This figure was kindly provided by Rumiko Mizuguchi.

To further investigate the role that Notch signaling plays in the specification of late-born neurons, Rumiko analyzed mouse embryos with reduced Delta1 activity. Ralph Cordes and Achim Gossler (Medizinische Hochschule Hannover, Germany) generated mice with a hypomorphic allele for *Dll1*. These animals were crossed with mice heterozygous for *Dll1*, which resulted in litters with hypomorphic mutant embryos (*Dll1*^{hypo/-}). The expression of Pax2 (dIL_A) and Lmx1b (dIL_B) was examined by immunohistochemistry in these mutants. The number of Pax2-expressing dIL_A cells in the dorsal horn of *Dll1*^{hypo/-} embryos is unchanged compared to wt littermates (Fig. 52a, b); however, Lmx1b⁺ dIL_B neurons are significantly reduced in numbers (Fig. 52c, d). The analysis of *Dll1*^{hypo/-} shows that reduced Dll1/Notch signaling leads to a reduction of dIL_B

neurons in the dorsal horn of the spinal cord, whereas dIL_A neurons remain properly specified.

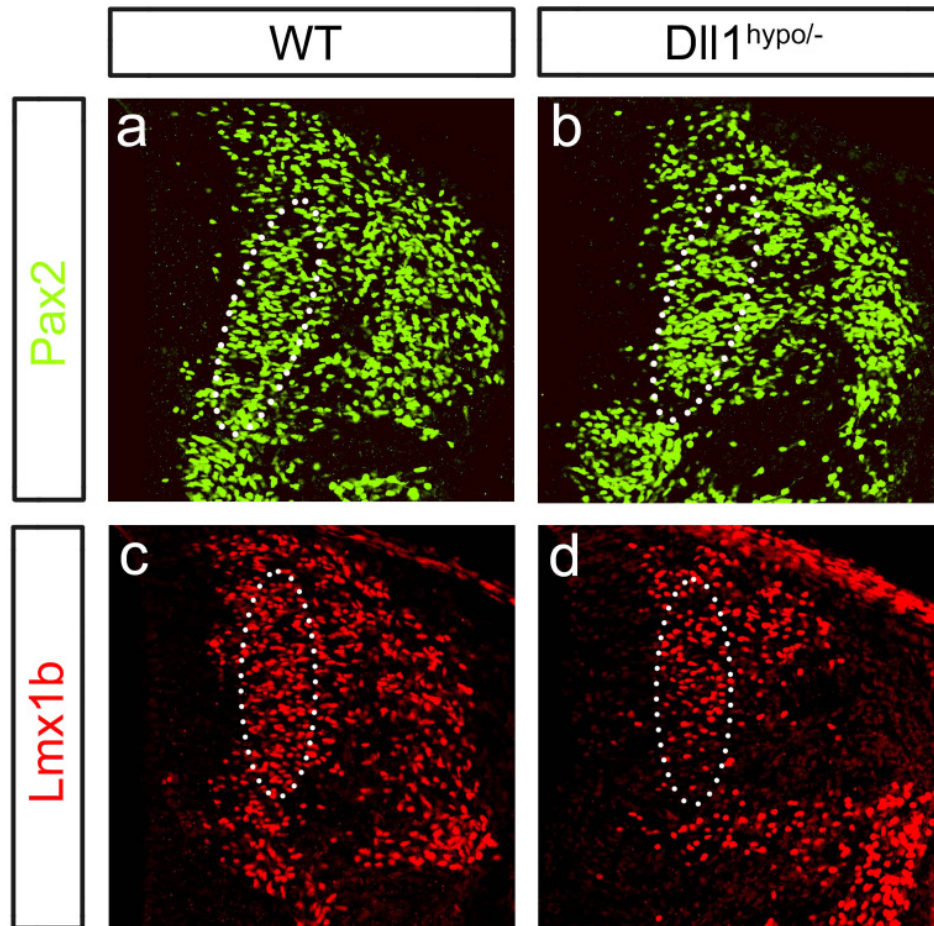


Figure 52: Analysis of the specification of late-born neurons in E12.5 *Dll1*^{hypo/-} embryos. In the svz of dorsal horn of E12.5 *Dll1*^{hypo/-} embryos, the number of Pax2⁺ dIL_A neurons (green) is unchanged compared to the wt control (Fig. 52a, b, circles), while fewer Lmx1b⁺ (red) dIL_B neurons are present in the svz (Fig. 52c, d, circles). These results confirm that Notch signaling is involved in dIL_B neurons generation, but is dispensable for dIL_A neuron specification. This figure was kindly provided by Rumiko Mizuguchi.

3.17 Overexpression analysis of *Dll1*

The reduction of dIL_B neurons in the dorsal horn of *Dll1*^{hypo/-} embryos led me to ask whether *Dll1* actively biases dIL neurons to adopt a dIL_B fate. To address this question, I performed misexpression analysis of *Dll1* in E6 chick spinal cords. The expression construct used for these overexpression experiments contained the full-length coding sequence of the rat *Delta1* gene followed by an IRES sequence and an *EGFP* cassette. This construct allows me to identify cells that express *Dll1* by the expression of GFP. After electroporation, chick embryos were incubated for 24h before harvesting. The immunohistochemical analysis of chick embryos electroporated with the *Dll1*-expression construct reveals two very interesting phenotypes. Since electroporation efficiency varies from embryo to embryo, some chick embryos exhibit widespread *Dll1* expression, whereas *Dll1* is expressed in a scattered mosaic pattern in other embryos. E7 chick embryos, which display mosaic *Dll1* expression, are characterized by a strong upregulation of Tlx3-expressing cells throughout the dorsal svz (Fig. 53a-d). Strikingly, these ectopic Tlx3⁺ neurons do not co-label with GFP (*Dll1*) indicating that *Dll1* induces Tlx3-expressing dIL_B neurons in a non-cell autonomous manner (Fig. 53d). In contrast, when high amounts of *Dll1* are ectopically induced in a broad manner, Tlx3/Lmx1b⁺ neurons are almost completely abolished on the electroporated half of the spinal cord (Fig. 53e-h). However, the numbers of Pax2-expressing dIL_A neurons are unchanged following either low (Fig. 53i-l) or high levels of ectopic *Dll1* (Fig. 53m-p). Previous studies in *Drosophila* and *Xenopus* embryos have shown that broadly expressed *Delta1* blocks Notch signaling in a cell autonomous manner (Chitnis et al., 1996; Chris Kintner, Salk Institute, MNL-K, pers. comm.), whereas mosaic *Delta1* expression activates Notch signaling in adjacent cells. The results of the *Dll1*-misexpression experiments are therefore consistent with a model in which *Dll1* induces the differentiation of dIL_B neurons in a non-cell autonomous manner by activating Notch signaling in the surrounding dIL progenitor cells.

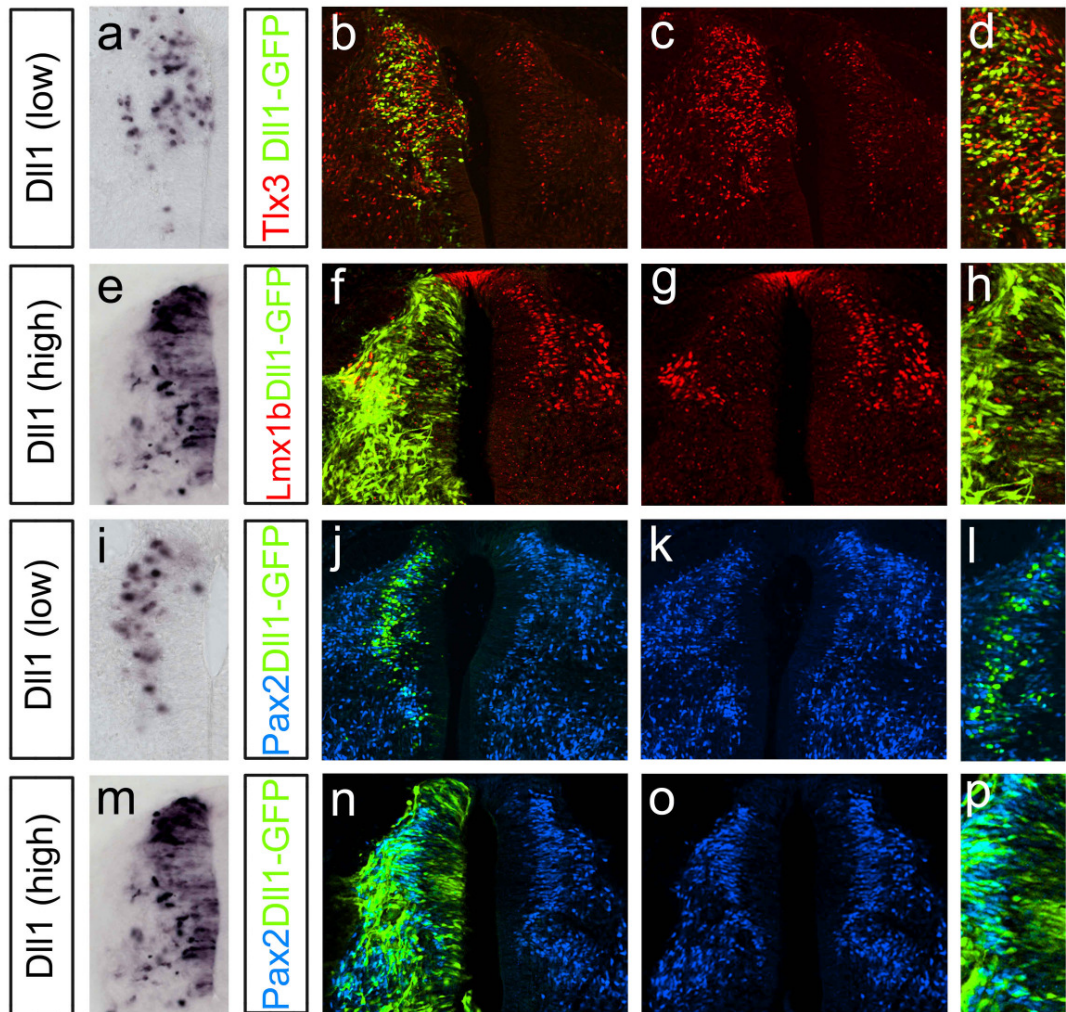


Figure 53: Overexpression of *Dll1* into E6 chick spinal cords. E6 chick spinal cords were electroporated with a *Dll1-IRES-EGFP* expression vector and analyzed 24h later. d, h, l and p are magnifications of the electroporated side in b, f, j and n, respectively. (Fig. 53a-d) When *Dll1* is misexpressed at low levels, expression of *Tlx3* is induced in a non-cell autonomous manner. Note that very few ectopic *Tlx3*⁺ cells co-express GFP (Fig. 53d). (Fig. 53e-h) When *Dll1* is misexpressed at high levels, which is known to reduce Notch activity, expression of *Lmx1b* is strongly suppressed in a cell autonomous manner. The few *Lmx1b*⁺ cells that remain do not express GFP (Fig. 53h). Expression of *Pax2* on the electroporated side does not significantly change after low (Fig. 53i-l) and high amounts of *Dll1* (Fig. 53m-p).

In summary, my results, together with those of Rumiko's, argue that Mash1 has two roles in the specification of dLL_A and dLL_B subtypes of late-born neurons: Mash1 is required for the induction of Ptf1a, which then activates the dLL_A differentiation pathway; Mash1 also biases adjacent cells to adopt a dLL_B fate by upregulating *Delta1* expression, which in turn activates Notch in the surrounding cells that become dLL_B neurons.

3.18 ***Gsh1/2*^{-/-} embryos show a defect in the anatomy of the dorsal horn**

The respecification of dLL_B into dLL_A neurons in mice lacking both *Gsh1* and *Gsh2* revealed a defect in lamination in the deep layers of the dorsal horn. To examine the effect of the loss of Lmx1b⁺ dLL_B cells on the lamination, I performed immunohistochemical staining with antibodies against the pan-neuronal marker NeuN and calbindin, which is expressed in lamina II_{inner} and in a cluster of cells lateral to the dorsal funiculus in lamina IV at lumbar levels. Lamina III in the wt is recognizable as the layer with big bright NeuN⁺ cells below the stripe of calbindin⁺ cells (Fig. 54a, c, e, g). In mice lacking *Gsh1* and *Gsh2*, lamina II_{inner} is missing, as evidenced by the loss of the stripe of calbindin⁺ cells. The cells of lamina III are now located in the outer most layers indicating the loss of lamina I and II (Fig. 54b, f, d, h).

In addition, the anatomy of the dorsal funiculus is changed. In wt embryos it has a U-shape form (Fig. 54i, k), whereas in *Gsh1/2*^{-/-} cords it is truncated ventrally, and instead exhibits a wide V-shape character (Fig. 54j, l).

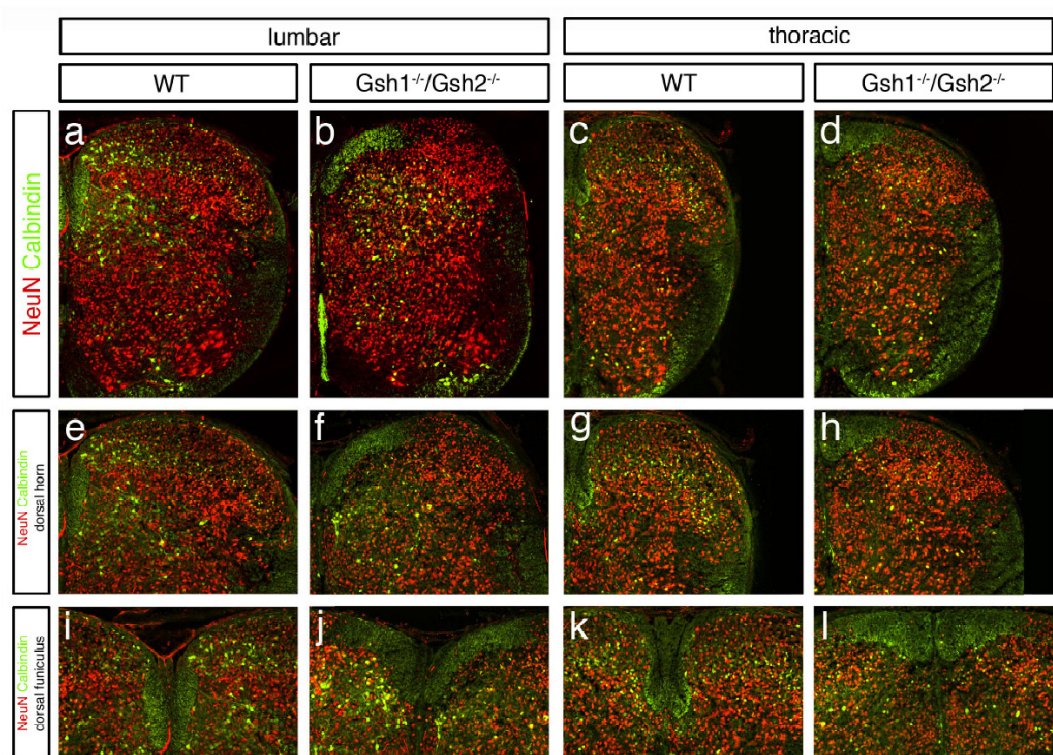


Figure 54: Changes in the anatomy of E18.5 *Gsh1/2^{-/-}* spinal cords. (Fig. 54a, b, e, f, i, j) Cross sections of E18.5 wt and *Gsh1/2^{-/-}* spinal cords at lumbar and thoracic levels (Fig. 54c, d, g, h, k, l) stained against NeuN (red) and Calbindin (green). (Fig. 54e-h) 25x magnifications of the dorsal horns are shown in a-d. (Fig. 54i-l) 25x magnifications of the dorsal funiculi are shown in a-d. (Fig. 54 a-h) *Gsh1/2^{-/-}* embryos lose lamina I and II. The big cells of lamina III are located in the most superficial laminae of *Gsh1/2^{-/-}* cords. (Fig. 54i-l) The dorsal funiculus of *Gsh1/2^{-/-}* spinal cords is truncated and has a V-shaped form.

The dorsal horn of the spinal cord is the primary receiving area of somatosensory information from the periphery. Sensory fibers enter the dorsal horn through the dorsal roots and terminate in the superficial laminae I-IV. *Gsh1/2^{-/-}* embryos exhibit a loss of lamina I and lamina II; therefore, several afferent fibers cannot project to their proper targets. To investigate whether these sensory fibers still innervate the dorsal horn of *Gsh1/2^{-/-}* spinal cords, I labeled primary cutaneous afferent fibers by antibody staining against TrkA (Huang et al., 1999). At E18.5 in wt embryos, TrkA⁺ afferents project into laminae I-II of the dorsal horn (Fig. 55a). Strikingly, very few TrkA⁺ afferents are detected within the

dorsal horn of *Gsh1/2^{-/-}* embryos and these afferent fibers innervate only a narrow band of dorsal horn neurons (Fig. 55b).

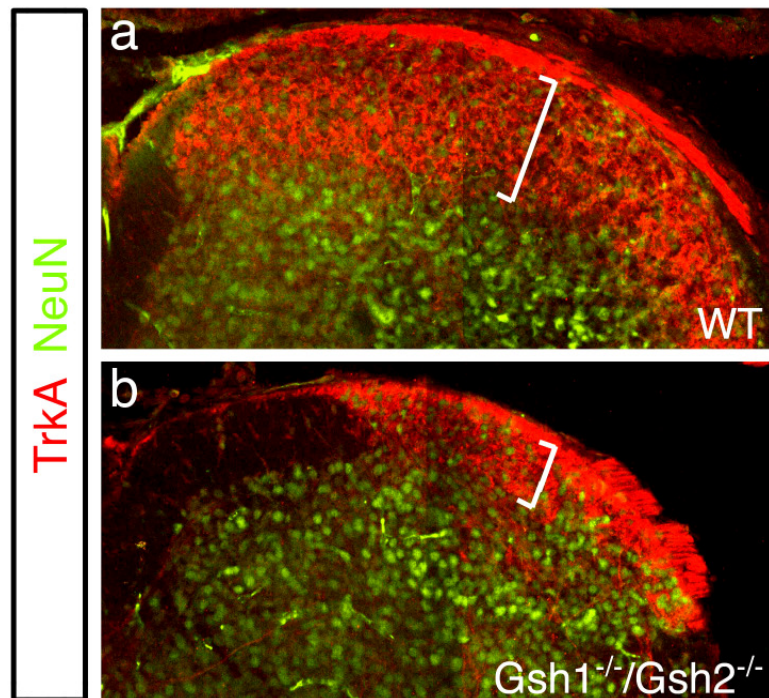


Figure 55: Comparison of afferent fibers entering the dorsal horn of E18.5 wt and *Gsh1/2^{-/-}* spinal cords. Primary afferent fibers entering the dorsal horn were labeled by staining cross sections of E18.5 wt and *Gsh1/2^{-/-}* spinal cords using antibodies against TrkA (red) and NeuN (green). (Fig. 55a, b) Only a few TrkA⁺ fibers innervate the dorsal horn in the absence of *Gsh1* and *Gsh2*.

To further analyze sensory afferent projections, I performed anterograde labeling of E18.5 wt and *Gsh1/2^{-/-}* DRGs by Dil injections. Projections to the dorsal horn were intensely labeled with Dil in both wt and *Gsh1/2^{-/-}* spinal cords (Fig. 56a, b), but *Gsh1/2^{-/-}* embryos exhibit alterations in the pattern of Dil labeling, whereby deep primary afferent fibers project more laterally instead of ventrally. Moreover, the primary afferent entry to the dorsal horn is compressed by the aberrantly shaped dorsal funiculus in the spinal cord of *Gsh1/2^{-/-}* embryos (see above) (Fig. 56b).

Together, these results indicate that *Gsh1/2^{-/-}* spinal cords exhibit strong projection defects of afferent sensory fibers in the dorsal horn.

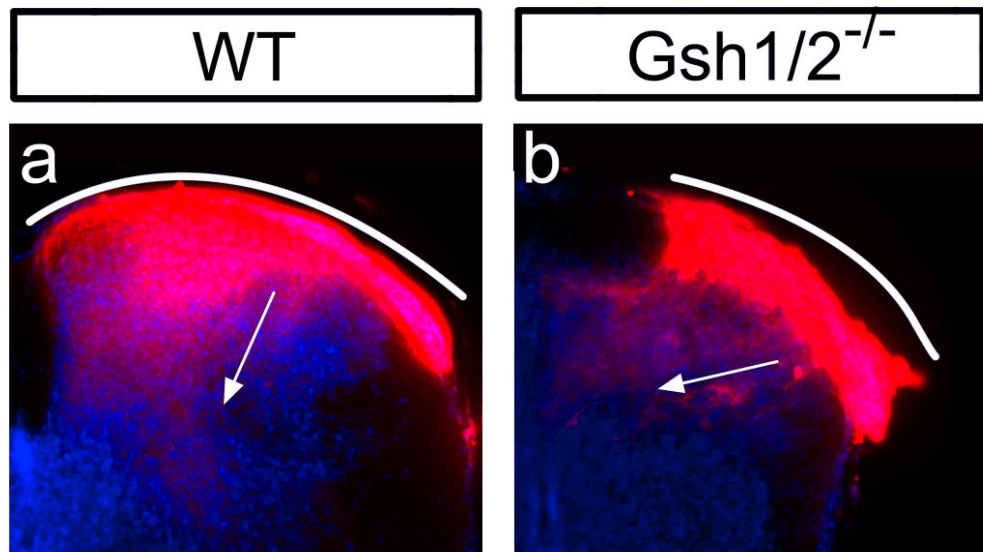


Figure 56: Dil labeling of primary afferents. DRGs of E18.5 wt and *Gsh1/2^{-/-}* were injected with liquid Dil and incubated for further seven days at RT prior to analysis. The afferent fibers labeled in the *Gsh1/2^{-/-}* dorsal horn project more laterally compared to wt littermates. The arrows symbolize the directions of afferent fibers. The white line marks the width of the dorsal horn.

4 Discussion

4.1 The role of Gsh1 and Gsh2 in patterning dorsal progenitors in the developing spinal cord

This study investigates how subsets of dorsal interneurons (dl) are specified during development of the spinal cord by focusing on transcriptional regulatory pathways in the progenitors of these interneurons. In this study, I determined the function that two homeodomain transcription factors, Gsh1 and Gsh2, play in directing neural cell fate in the dorsal half of the spinal cord. Prior to beginning this project, the molecular mechanisms that govern the specification of dorsal neurons and my analysis of the *Gsh2*^{-/-} mouse (Kriks, 2003) had suggested that this gene might play a role in patterning dorsal progenitors. However, while I was able to demonstrate a role for Gsh2 in the specification of early-born dl3 neurons (Kriks, 2003), the development of late-born neurons in the *Gsh2*^{-/-} spinal cord appeared to be normal. Moreover, *Gsh1*^{-/-} embryos show no disruption in dorsal spinal interneuron development. In defining the developmental expression profile of Gsh1 and Gsh2 in the dorsal spinal cord, I demonstrated that Gsh2 overlaps with Gsh1 in the progenitors of dl4 and dl5 neurons, and that both proteins continue to be expressed in the dorsal vz during the second wave of neurogenesis, during which two classes of late-born interneurons are generated. My studies, together with those of Gross et al., 2002 and Muller et al., 2002, indicate that during this second wave of neurogenesis two subsets of dlL neurons, the dlL_A and the dlL_B types, arise from a single progenitor domain that expresses both Gsh1 and Gsh2.

4.1.1 Gsh1 and Gsh2 are necessary for the specification of two types of early-born interneurons

4.1.1.1 Gsh1 and Gsh2 are obligate determinants for dl3 and dl5 neurons

The analysis of *Gsh2*^{-/-} embryos showed that *Gsh2* functions as an obligate determinant of a dl3 cell fate in the spinal cord (Kriks, 2003). In the absence of *Gsh2* almost all dl3 neurons are missing, coupled with a concomitant increase in dl2 neurons. The observation that dl4 and dl5 neurons develop normally in the *Gsh2*^{-/-} cord argues for a functional redundancy between *Gsh1* and *Gsh2* in the cord. Indeed, studies undertaken in the forebrain have shown that *Gsh1* and *Gsh2* function redundantly in the development of the ventral forebrain (Toresson and Campbell, 2001, Yun et al., 2001). The demonstration that dorsal interneurons develop normally in the spinal cord of mice lacking *Gsh1* supports the model, in which *Gsh1* and *Gsh2* function redundantly. Further evidence that *Gsh1* and *Gsh2* function as necessary, but redundant, determinants of dorsal interneuron identity have come from my analysis of *Gsh1/2*^{-/-} spinal cords. In these cords, dl5 neurons, in addition to dl3 neurons, are all but absent as evidenced by the complete loss of *Tlx3*- and *Lmx1b*-expressing cells, which mark dl3/dl5 and dl5 neuron populations, respectively. Neurons in the prospective dl5 domain express markers of dl4/dl6 neurons, such as *Lbx1*, *Pax2* and *Lhx1/5*. However, the exact fate of these prospective dl5 neurons is unclear, since *Ngn1*⁺/*Dbx2*⁺ dl6 progenitors do not expand dorsally in the *Gsh1/2*^{-/-} embryos, suggesting that these neurons do not adopt a dl6 cell fate. However, given that there is a reduction in the number of *Lbx1*⁺ cells in the *Gsh1/2*^{-/-} cord it is possible that the dl5 neurons, rather than being respecified, are lost in the *Gsh1/2*^{-/-} embryos.

My findings do, however, suggest that dl4 neurons are able to differentiate in the absence of *Gsh1/2*. It therefore appears that *Gsh1/2* are only required for the correct specification of dl3 and dl5 neurons. It has been suggested that dl4 neurons might represent a “ground state” for the dorsal spinal cord. Nonetheless, an additional factor (or factors) that is (are) independent of *Gsh1/2* function could function as a critical determinant of dl4 identity. One such factor is the bHLH transcription factor *Ptf1a*. *Ptf1a* is expressed exclusively in newborn dl4 interneuron progenitors at E10.0-E11.0, and mice lacking *Ptf1a*

exhibit a complete loss of dl4 neurons (Glasgow et al., 2005). Interestingly, the expression of Ptf1a is unchanged in the spinal cord of *Gsh1/2*^{-/-} embryos, which explains the proper specification of dl4 neurons in these mice. The observation that Ptf1a expression does not expand ventrally in the *Gsh1/2*^{-/-} spinal cord also provides further evidence that dl5 neurons are not respecified as dl4 neurons.

4.1.1.2 Cross-repressive interactions between homeodomain transcription factors do not operate in dorsal spinal progenitors

An important mechanistic question that arises is, how do Gsh1 and Gsh2 regulate the development of these two types of early-born interneurons? One possibility is that Gsh1/2 function as early patterning factors, establishing a progenitor domain that gives rise to dl3-dl5 neurons by repressing the expression of other early patterning genes that promote alternative fates. This mechanism is similar to the one that has been proposed to operate in both, the ventral spinal cord and the ventral neuroectoderm of *Drosophila*. In ventral spinal cord progenitors, different combinations of homeodomain proteins are expressed in each of the five progenitor domains. Many of these HD proteins have the ability to cross-repress each other in a pairwise fashion, and these cross-repressive interactions establish five distinct non-overlapping progenitor domains, each giving rise to different types of neurons (Briscoe et al., 2000; Goulding and Lamar, 2000). It is also known that Ind, the *Drosophila* homolog of Gsh1/2, functions in a similar manner in the ventral neuroectoderm of *Drosophila* (Weiss et al., 1998). The nervous system of *Drosophila* develops from neuroblasts, which are arrayed in three dorso-ventral columns; i.e. a dorsal, an intermediate and a ventral column. Neuroblasts in the dorsal column express the homeodomain protein Msh (muscle segment homeobox) (D'Allessio and Frasch, 1996; Isshiki et al., 1997), whereas the ventral column neuroblasts express Vnd (ventral nervous defective) (Jimenez et al., 1995; Mellerick and Nirenberg, 1995). The *Drosophila* homolog of Gsh1/2, Ind (intermediate neuroblast defective), is expressed in between Msh and Vnd, within the intermediate neuroblast column. Its expression abuts the Msh expression domain dorsally and the Vnd domain ventrally. As in the ventral mouse neural tube the sharp boundaries between these homeodomain proteins are

established through cross-repressive interactions. *Vnd* represses *Ind* expression in the ventral neuroblast column, thereby establishing the ventral boundary of *Ind*. *Ind* represses expression of *Msh*, thus establishing the ventral expression limit of *Msh*. In the absence of *Vnd*, *Ind* expands ventrally, encompassing the *Vnd* expression domain. On the other hand, in *Ind*^{-/-} embryos, *Msh*, as well as *achaete*, a proneural gene, which is also expressed in the dorsal column, expands ventrally (Weiss et al., 1998). However, *Ind* does not expand dorsally in the absence of *Msh*, suggesting that a different factor establishes the dorsal boundary of *Ind*. This DV patterning appears to be conserved in vertebrates, as homologs of *Msh*, *Ind* and *Vnd* exist in the mouse spinal cord. *Nkx2.1* and *Nkx2.2* are the vertebrate homologs of *Vnd* and are expressed in the ventral ventricular zone of the mouse spinal cord similar to *Vnd* in *Drosophila* (Holland et al., 1998). The vertebrate counterparts of *Msh* are *Msx1*, *Msx2* and *Msx3* (Wang et al., 1996; Ramos and Robert, 2005). In response to signals from the roof plate, Class A precursors (dl1-dl3 progenitors) express the homeodomain transcription factor *Msx1*. *Msx2* expression is restricted to the dorsal midline, while *Msx3* is expressed in dl1-dl5 progenitors. In view of their expression patterns, *Msx1* is the gene that would most likely function as a determinant of dl1-dl3 interneuron identity. As with *Ind* expression in *Drosophila*, the expression of *Gsh1/2* marks a dorso-intermediate region of the spinal cord. However, *Msx1* expression overlaps with *Gsh2* in dl3 progenitors and shares its ventral boundary with the dorsal boundary of *Gsh1*. While my data reveal some similarities in the expression patterns of *Gsh1/2* and *Ind* in the developing vertebrate and *Drosophila* nervous systems, respectively, it also suggests that a different regulatory mechanism operates in the dorsal half of the spinal cord. If cross-repression between the *Msx* class and the *Gsh* class of homeodomain proteins is involved in establishing the boundary between BMP-dependent Class A neurons and Class B neurons, which are independent from roof plate derived signals, *Msx1* would expand ventrally in the absence of *Gsh1/2*. However, this is not observed and *Msx1* expression remains restricted to dl1-3 Class A progenitors.

While the invertebrate/vertebrate homologs *Vnd/Nkx*, *Ind/Gsh* and *Msh/Msx* are expressed in a similar pattern along the DV axis, an additional progenitor domain is present in the vertebrate spinal cord. This fourth progenitor domain is characterized by the expression of *Dbx1* and *Dbx2* (Fjose et al, 1994; Pierani et al., 2001). These *Dbx*⁺ progenitors are located between the *Gsh1/2*⁺

domain and ventral progenitors that express genes of the Nkx family of homeodomain transcription factors. Thus, based on the expression of different classes of homeodomain transcription factors, it appears that the early vertebrate neural tube is broadly comprised of four DV progenitor territories. Although a *Dbx* gene homolog is present in *Drosophila* (J. Skeath, pers. comm.), its expression in the developing ventral cord appears to be restricted to distinct subsets of neuroblasts and postmitotic neurons. In the vertebrate neural tube, *Dbx2* functions as a Class 1 gene and its ventral expression limit is regulated by repression through Nkx6.1 (Vallstedt et al., 2001). *Gsh1/2* and *Dbx2* share a boundary between dl5 and dl6 progenitors. However, this boundary is unchanged in the *Gsh1/2*^{-/-} spinal cord indicating that cross-repression between *Gsh1/2* and *Dbx2* plays no role in establishing the dl5/6 progenitor boundary.

Thus, it appears that while some DV patterning activities of these homeodomain transcription factors have been conserved between invertebrates and vertebrates, their expression patterns have diverged, as have the regulatory interactions that determine their expression in CNS progenitors. The failure to find any evidence that cross-repressive interactions between *Gsh1/2* and other homeodomain transcription factors expressed in dorsally and ventrally adjacent progenitor domains suggests that a different mechanism of progenitor cell specification may operate in the dorsal half of the embryonic spinal cord.

4.1.1.3 Gsh1/2 function in regulating the expression of bHLH factors, which are the primary determinants of dorsal interneuron fate

Although no changes were observed in the expression of a number of HD proteins in dorsal interneuron progenitors when *Gsh1/2* are absent, there are marked changes in the expression of the proneural bHLH proteins, *Ngn1*, *Ngn2* and *Mash1* (see Fig. 31). These transcription factors function not only as generic proneural factors, but also as determinants of cell type identity. Not only does *Ngn1* expand ventrally in the absence of *Gsh2*, encompassing presumptive dl3 progenitors and sharing a boundary with *Gsh1* (Kriks, 2003), but in the absence of both *Gsh1* and *Gsh2*, *Ngn1* expands even more ventrally, encompassing the complete dl3-5 precursor domains, in addition to its endogenous dl2 and dl6 progenitor domains. My data suggest that this ventral expansion of *Ngn1* expression leads to the strong reduction of *Mash1* expression in dl3-5 progenitors. In turn, these findings also indicate that *Gsh1* and *Gsh2* function by restricting the spatial expression of proneural bHLH transcription factors. This raises the possibility that these proneural genes are the primary determinants of neuronal cell fate in the dorsal half of the spinal cord. Support for this hypothesis also comes from LOF analysis for several bHLH proteins. For example, the bHLH transcription factor *Math1* is expressed in the dl1 progenitor domain, where it is necessary for dl1 cell identity (Bermingham et al., 2001). In the absence of *Math1*, dl1 neurons fail to develop, and there is a dorsal expansion of *Ngn1/2*, which leads to an increase in the number of dl2 neurons (Gowan et al., 2001). Gowan and colleagues have also reported that the neural tube of *Ngn1/2*^{-/-} embryos exhibit the opposite phenotype, in which more dl1 neurons are produced at the expense of dl2 neurons. This cell fate switch from a dl2 to dl1 identity is accompanied by the ventral expansion of the *Math1* expression domain, such that it now encompasses presumptive dl2 precursors (Gowan et al., 2001). In this study, I have found that *Mash1* is necessary for the proper specification of dl3 neurons. *Mash1*^{-/-} mice develop fewer dl3 neurons and there is a concomitant increase in dl2 neurons. Once again, this switch in cell fate appears to be due to the ventral expansion of *Ngn1*. There is also a concomitant reduction in *Gsh2* expression in the presumptive dl3 progenitor domain at E10.5 when *Mash1* is absent. However, by E11.5, *Ngn1* expression is once again restricted to dl2

progenitors and *Gsh2* expression is upregulated in dl3 precursors.

Mash1 is also an obligate determinant for dl5 neuron development, as mice lacking *Mash1* do not develop dl5 neurons (see Fig. 15). Once again, in the *Gsh1/2*^{-/-} cord, *Mash1* expression is strongly reduced, accompanied by a ventral expansion of *Ngn1*. These findings are also consistent with a model in which *Gsh1/2* regulate dorsal cell fate by restricting the expression of *Ngn1* in differentiating dorsal progenitors. It also suggests a feedback regulation between *Mash1* and *Gsh1/2*, which is interesting, given that they share the same expression domain in the dorsal half of the neural tube.

Further support for a model in which proneural bHLH factors are the primary determinants of a distinct cell fate comes from GOF analyses. For example, overexpression of *Math1* and *Ngn1/2* in the chick neural tube leads to an induction of dl1 and dl2 neurons, respectively (Gowan et al., 2001). *Mash1* misexpression in the chick spinal cord also results in a dramatic upregulation of dl3 neurons (see Fig. 17, Nakada et al., 2004), although the increase in dl5 neurons is less obvious. Taken together, these LOF and GOF analyses provide evidence for a model, where the bHLH transcription factors *Math1*, *Ngn1/2* and *Mash1* function as primary determinants of dorsal interneuron development. Furthermore, they explain the phenotypes seen in *Gsh2*^{-/-} and *Gsh1/2*^{-/-} spinal cords. *Gsh1* and *Gsh2* restrict the expression of *Ngn1* to dl2 and dl6 progenitors. In the absence of these two homeodomain transcription factors, *Ngn1* expands, resulting in the loss of dl3 and dl5 neurons. This repression of *Ngn1* by *Gsh1/2* expression takes place independently from *Mash1*, as overexpression of *Gsh2* does not induce *Mash1*. My conclusion that *Ngn1* is able to repress *Mash1* expression is based on two observations: First, *Gsh1/2*^{-/-} embryos in which *Ngn1* expands ventrally, exhibit a dramatic downregulation in the level of *Mash1* expression. Second, overexpression of *Ngn1* in the chick neural tube strongly represses *Mash1* expression.

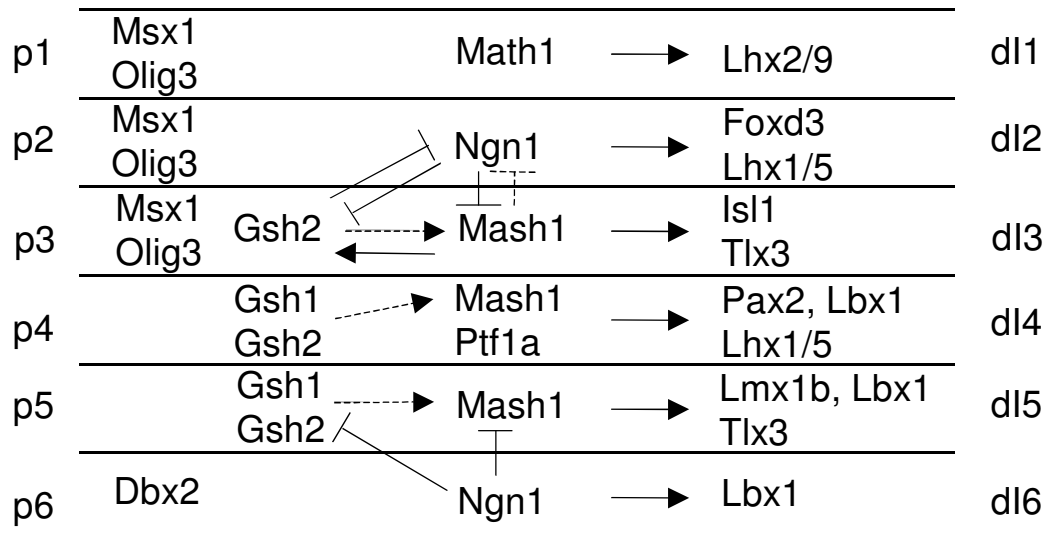


Figure 57. Schematic of the genetic interactions between Gsh1, Gsh2, Ngn1 and Mash1 during the early phase of dorsal interneuron specification. Arrows symbolize an induction, lines signify a repression. Solid lines represent direct effects, whereas dashed lines are indirect interactions.

4.1.2 **Gsh1/2 and Mash1 play a role in the specification of late-born neurons**

My results show that Gsh1/2 continue to be expressed in the progenitor domain of late-born neurons, where they are necessary for proper development of excitatory dIL_B neurons. In mice lacking *Gsh1/2*, these neurons are respecified as inhibitory dIL_A neurons. Mash1, which is also expressed in the dIL progenitor domain, is co-expressed with Gsh1/2 in many cells. However, in contrast to what is seen at earlier times, *Mash1*^{-/-} mice exhibit the opposite phenotype to that observed in *Gsh1/2*^{-/-} spinal cords. During this late phase of neurogenesis, a strong reduction in inhibitory dIL_A neuron cell numbers and a concomitant increase in excitatory dIL_B neurons is seen in the *Mash1*^{-/-} spinal cord. This late function of Mash1 differs from its function during the early wave of neurogenesis where Mash1 functions in concert with Gsh1/2 to specify excitatory neuron development. Mash1 function is required for the expression of the bHLH protein Ptf1a during the second, but not first wave of neurogenesis. At the time I was undertaking these studies, Glasgow et al. (2006) reported that Ptf1a is expressed in dIL progenitors and that it is required for the specification of Pax2⁺ dIL_A neurons. Mice lacking *Ptf1a* do not develop inhibitory dIL_A neurons, with all dIL neurons instead developing as excitatory Tlx3⁺ dIL_B cells. It therefore appears that Mash1 functions upstream of Ptf1a and the loss of Ptf1a expression in the *Mash1*^{-/-} cord may be the underlying reason for the loss of these inhibitory dIL_A neurons. By overexpressing *Ptf1a* in the chick spinal cord, I confirmed that Ptf1a is an important factor for dIL_A neuron development. Misexpression of *Ptf1a* in E6 chick neural tubes leads to both, a marked decrease in Tlx3-expressing dIL_B neurons and an upregulation of Pax2⁺ dIL_A in the svz on the electroporated half of the spinal cord.

My conclusion that *Ptf1a* might act downstream of *Mash1* is also supported by the expression patterns of Mash1 and Ptf1a at E12.5. Double-labeling with cell cycle markers indicates that Ptf1a is expressed in dIL progenitors, which are in the process of withdrawing from the cell cycle. In contrast, Mash1 is expressed in dividing progenitors, indicating that temporally it lies upstream of Ptf1a.

Interestingly, my data suggest that Ptf1a function is only necessary in the presence of Gsh1/2. When *Gsh1* and *Gsh2* are both absent, Ptf1a expression

is downregulated. This is most likely due to the reduction in Mash1 expression that occurs in the *Gsh1/2*^{-/-} cord. Despite the loss of Ptf1a, almost all of the late-born Lbx1⁺ neurons differentiate as Pax2⁺ dIL_A neurons in the *Gsh1/2*^{-/-} spinal cord. This leads me to conclude that the primary role of Ptf1a in differentiating dIL neurons is to repress Gsh1/2 function. I propose that Gsh1/2, which are necessary for dIL_B neuron differentiation, bias dIL neurons to an excitatory dIL_B fate. These excitatory dIL_B neurons express Tlx3, which is also known to repress Pax2, an obligate determinate of the inhibitory phenotype in dIL_A neurons (Cheng et al., 2004). Therefore, in order for dIL neurons to adopt a dIL_A fate, Tlx3 expression needs to be blocked, and this is achieved in part by activating the expression of Ptf1a in presumptive dIL_A cells.

4.2 Mash1 acts cell-autonomously as well as non-cell-autonomously in the specification of late-born neurons

The changes in the regulatory interactions between Gsh1/2, Mash1 and Ptf1a that govern the differentiation of neurons in the dorsal cord is striking and raise the question as to what underlies these changes. During the early phase of spinal cord development, inhibitory and excitatory neurons arise predominantly from distinct domains. With respect to the dorsal spinal cord, dl3 and dl5 neurons develop as excitatory glutamatergic cell types, whereas dl4 neurons activate an inhibitory differentiation program. However, at later developmental times, both of these cell types arise from a common progenitor domain (Gross et al., 2002; Muller et al., 2002). The observation that the loss of *Mash1* and *Gsh1/2* lead to largely opposite shifts in the relative numbers of dIL_A and dIL_B neurons is also consistent with these dIL precursors being bipotential. Furthermore, a recent study by Wildner et al. (2006) has shown that dIL_A and dIL_B neurons often arise from a common progenitor. My data suggests that Mash1 plays a key role in determining the choice between these dIL fates by functioning in both, a cell-autonomous manner and a non-cell autonomous manner. This Mash1 activity enables the co-generation of two classes of neurons from a single progenitor domain.

Mash1 functions autonomously in prospective dIL_A neurons, where it is required for the expression of Ptf1a. In experiments where *Mash1* was overexpressed in E6 chick spinal cords, I observed that Mash1 represses a dIL_B

cell fate, most likely by upregulating *Ptf1a* expression in these cells. Nonetheless, it appears that Mash1 by itself is not able to induce a dIL_A cell fate, and other yet to be identified factors may cooperate with Mash1 to execute the cell autonomous functions of Mash1. Interestingly, when a repressor form of Mash1, which comprises the *Mash1* bHLH domain fused to the repressor domain of *Engrailed* (EnR) (Smith and Jaynes, 1996), is electroporated into E6 chick spinal cords, precocious expression of Pax2 is seen in the vz of the electroporated side of the spinal cord. These ectopic Pax2-expressing cells are double-labeled with GFP, indicating that Mash1 induces a dIL_A cell fate in a cell autonomous manner. This precocious induction of Pax2 is only observed with the repressor form of Mash1.

The evidence to date also suggests that Mash1 functions in a non-cell autonomous manner by upregulating Dll1 expression and activating Notch signaling in dIL precursors. Previous studies in *Xenopus* have shown that Xash3, the *Xenopus* homolog of Mash1, is a strong activator of the Notch signaling pathway (Chitnis et al., 1996). Furthermore, *Mash1* null embryos show reduced expression of *Dll1* and NICD in dIL progenitors (see Fig. 48). More importantly, reduction of dIL_B neurons in the spinal cord of *Dll1*^{hypo/-} embryos that exhibit reduced Dll1-dependent signaling, provide further evidence that Notch signaling contributes to the specification of late-born neurons. In these mutant embryos, dIL_B cell numbers are preferentially decreased, accompanied by a reduction in the levels of activated Notch signaling. This is consistent with a model in which cells that are the recipients of high Notch signaling, i.e. the cells that express high NICD are biased toward a dIL_B cell fate. In support of this model, when *Dll1* is ectopically expressed in a salt-and-pepper fashion in dIL progenitors, the number of Tlx3-expressing dIL_B neurons is increased (see Fig. 53). Moreover, these ectopic Tlx3⁺ cells do not co-label with GFP, suggesting that Dll1 induces dIL_B neurons in a non-cell autonomous manner by upregulating NICD in adjacent cells. In contrast, widespread misexpression of *Dll1* in the chick spinal cord leads to a marked repression of dIL_B neurons. This can be accounted for by Dll1 acting in a cell autonomous manner to block Notch signaling. This effect has been observed in a number of situations where Dll1 is expressed at high levels (C. Kintner, pers. communication, Lai et al., 2004).

Another piece of evidence indicating Notch signaling either promotes, or is required for, dIL_B differentiation comes from analysis of mice that lack Presenilin-1, a protein required for Delta-dependent cleavage of Notch and the

generation of NICD, the intracellular mediator of Notch signaling. The spinal cords of *Psen-1^{-/-}* embryos show reduced Notch signaling, which is coupled to a reduction in the number of dIL_B neurons. From these data, I would like to propose a model in which the dIL cells that express high levels of Mash1 and Dll1 develop as dIL_A neurons, while those that express high levels of NICD develop as dIL_B neurons. In this model, Mash1 induces Ptf1a cell-autonomously, which, in turn, represses Gsh1/2 function. Mash1 also activates Notch signaling in surrounding cells. Notch represses Ptf1a function (Esni et al., 2004) and consequently may block the activity or expression of Ptf1a in presumptive dIL_B neurons. This model predicts that Notch signaling is not necessary for the generation of dIL_B neurons when Ptf1a is absent. This appears to be the case, as dIL_B neuron generation is not impaired in the *Mash1^{-/-}* spinal cord.

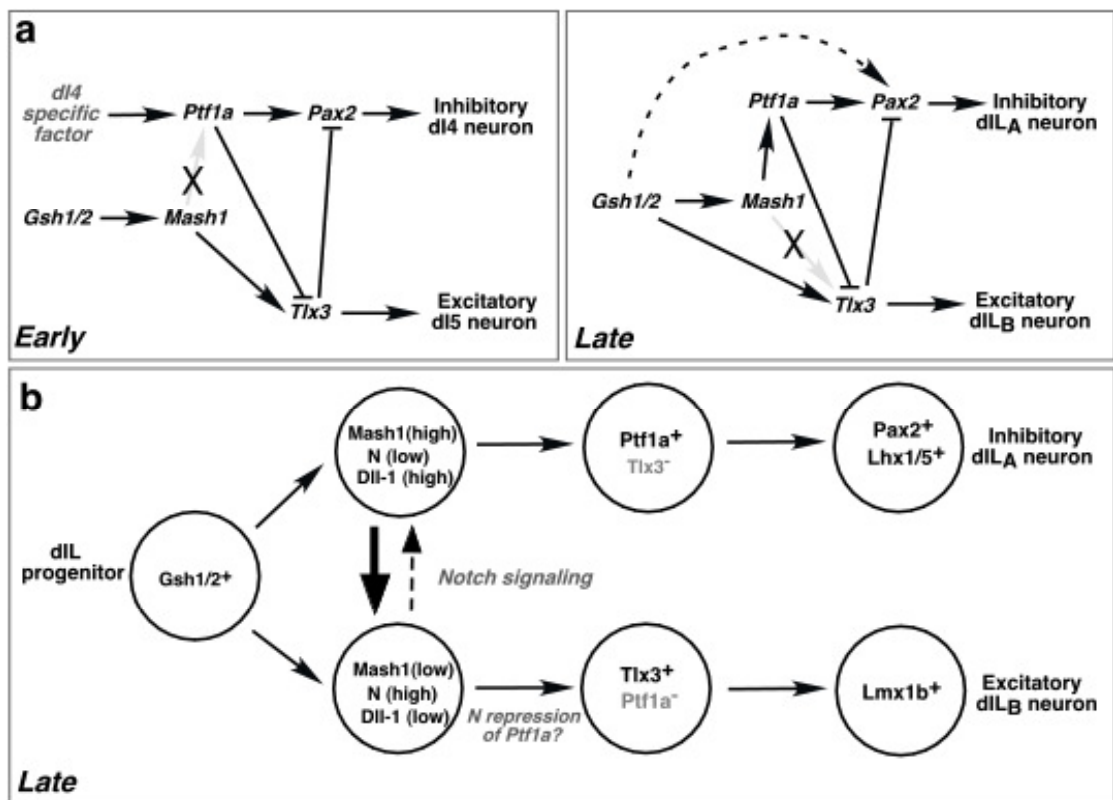


Figure 58. Schematic summary of the genetic interactions controlling inhibitory and excitatory cell fate specification in the dorsal spinal cord. (Fig. 58a) A transcriptional network that controls dorsal sensory neuron cell fate. (Left) At early stages (E10.5-11.5), Mash1 expression is maintained at high levels in dI5 progenitors by Gsh1/2. Mash1 in turn induces Tlx3 to promote the differentiation of excitatory dI5 neurons. Ptf1a is expressed in dI4 progenitors, where its expression is independent of Gsh1/2 and Mash1 (grey arrow). Ptf1a specifies dI4 neurons by inducing Pax2

and blocking *Tlx3* expression. (Right) At late stages (E12.5-13.5), *Mash1* positively regulates the expression of *Ptf1a*, which in turn antagonizes *Gsh1/2* by blocking *Tlx3* and induces inhibitory dLL_A neurons. At this time *Mash1* is no longer required for *Tlx3* expression (grey arrow). *Tlx3* expression is, however, dependent upon *Gsh1/2*. When *Gsh1/2* are absent, dLL cells adopt a dLL_A cell fate. These dLL_A neurons express *Pax2* and differentiate as inhibitory neurons (dashed line). (Fig. 58b) Model for specification of dLL_A and dLL_B neurons. *Gsh1/2* biases cells toward a dLL_B fate. The *Gsh1/2*-dependent activation of *Mash1* in a subset of dLL neuron precursor induces *Ptf1a* and *Pax2*. These prospective dLL_A precursors express high levels of *Dll1*, thereby activating Notch signaling in adjacent dLL_B progenitors. dLL_B progenitors express low *Dll1* and *Mash1*. Notch signaling in dLL_B progenitors may block *Ptf1a* function and expression, leading to the upregulation of *Tlx3* in these cells. Notch mediated lateral inhibition refines the choice between dLL_A and dLL_B fates resulting in the generation of excitatory and inhibitory neurons in a “salt and pepper” fashion from the dLL domain. $Pax2^+$ dLL_A cells differentiate into inhibitory sensory interneurons, whereas $Lmx1b^+/Tlx3^+$ cells develop as excitatory sensory interneurons.

One of the questions that arise is whether there might be other situations in which *Mash1*-dependent Notch signaling regulates the choice between neuronal cell fates. The generation of V2 interneurons in the ventral spinal cord is another example where *Mash1* is involved in the specification of a subpopulation of interneurons, which arise as two intermingled populations from the same progenitor domain. V2 interneurons comprise two molecularly distinct subtypes, the V2a and the V2b subpopulations. Both of these V2 interneuron subtypes arise in an intermingled fashion, similar to late-born dLL_A and dLL_B neurons.

Within the p2 progenitor domain, *Mash1* is expressed together with the winged-helix/forkhead transcription factor *Foxn4* in a subset of V2 progenitors, where both act cooperatively to specify V2b interneurons (Li et al., 2005). In both, the *Mash1*^{-/-} and the *Foxn4*^{-/-} spinal cord, V2b neurons fail to develop, instead these cells acquire a V2a cell fate. Consistent with the loss-of-function analysis, co-electroporation of *Mash1* and *Foxn4* together into chick spinal cords results in an upregulation of V2b neurons. Interestingly, although *Mash1* and *Foxn4* act cooperatively in the specification of V2b neurons, they both have distinct activities on their own, as is seen when either *Mash1* or *Foxn4* are misexpressed alone (Li et al., 2005). Overexpression of either *Mash1* or *Foxn4* alone results in a decrease in V2b neurons. When *Mash1* and *Foxn4* are co-electroporated, V2b numbers are increased.

This study reveals a number of interesting parallels in the roles of Mash1 in generating two classes of neurons from a common progenitor pool. In both instances, Mash1 acts as a specification factor, biasing cells toward one of two possible fates. Moreover, in both instances, the fate that Mash1 promotes is that of an inhibitory neuronal phenotype (see Fig. 37, G. Lanuza, unpublished observations). Also, Mash1 appears to act synergistically with another factor, Foxn4 in the case of V2 neurons, and an as yet unidentified factor in the case of dLL neurons. Although Li et al. (2005) did not show any direct evidence for the involvement of Notch signaling in the choice between V2a and V2b fates, their data is consistent with the hypothesis that Notch playing a role in the specification of V2 interneurons downstream of Mash1.

4.3 Changes between early and late neurogenesis in the spinal cord

A key finding of this study is the observation that Mash1 functions together with Gsh1/2 in specifying two early populations of excitatory dorsal interneurons, whereas Mash1 and Gsh1/2 have opposing roles during the late phase of dorsal neurogenesis. In an attempt to address what triggers this change in Mash1 function, I overexpressed a transcriptional activator form of *Mash1* (Mash1bHLH-VP16), as well as a transcriptional repressor form of *Mash1* (Mash1bHLH-EnR), allowing me to test the hypothesis that a change in the transcriptional activity of Mash1 may underlie this change in functionality. The misexpression analysis of the Mash1bHLH-VP16 construct at E3 confirmed previous studies (Nakada et al., 2004), which have shown that when Mash1 functions as a transcriptional activator it mimics the activity of full-length-Mash1. This is consistent with Mash1 acting as a transcriptional activator in specifying early-born dorsal interneurons.

During the late phase of neurogenesis, misexpression of either Mash1 alone or Mash1bHLH-VP16 has little effect on the relative generation of dLL_A and dLL_B neurons. This, coupled with the observation that expression of Mash1bHLH-EnR leads to the precocious expression of Pax2 in the ventricular zone (see Fig. 42), suggests that another factor might cooperate with Mash1 during the late phase of dorsal interneuron differentiation and alter Mash1 activity. However, the

nature of this factor is unclear. It is known that tissue-specific (Class II) bHLH proteins, including Mash1, form heterodimers with ubiquitously expressed (Class I) bHLH proteins such as E12 and E47 (Cabrera et al., 1991; Johnson et al., 1992). These protein-protein interactions are mediated by the Helix-Loop-Helix domain (Ellenberger et al., 1994). However, residues that do not participate in dimerization have been shown to confer cell type specification properties on Mash1 (Nakada et al., 2004). This suggests that Mash1 may interact directly with other nuclear factors via these residues. Unlike E12 and E47, which are expressed ubiquitously, these factors may interact with Mash1 in a context- or DNA sequence- dependent manner. In addition to studies showing Mash1 cooperates with Foxn4 to specify V2b progenitors (Li et al., 2005), expression studies in the dorsal neural tube are also consistent with Mash1 functioning in a context dependent manner. For example, Mash1 induces Isl1-expressing dI3 neurons predominantly in more dorsal regions of the spinal cord, whereas Lmx1b⁺ dI5 neurons are ectopically induced close to the endogenous dI5 domain. This suggests the presence of different co-factors in each of these domains. Indeed, Muller et al. (2004) have shown that Mash1 and Olig3 cooperate to specify Isl1⁺ dI3 neurons. But, different co-factors may also be expressed at different developmental times, which would explain how one bHLH protein has different functions at different times, such as the change in Mash1 function during early versus late neurogenesis.

Besides E-proteins, transcription factors of the Hes family interact physically with bHLH proteins in *Drosophila* and antagonize their function by recruiting the co-repressor Groucho (Giagtzoglou et al., 2003). However, it needs to be confirmed if this interaction is conserved in vertebrates.

Another key difference between the early and late phases of dorsal neurogenesis is the level of activated Notch in dorsal progenitors. While Notch signaling, as indicated by immunostaining against NICD, is seen in a mosaic pattern in dIL progenitors, NICD is virtually undetectable in the progenitors of early-born neurons. Consequently, while high NICD signaling is required for late neurogenesis, the specification of early dorsal neurons is uncoupled from this pathway. Interestingly, Dll1 is highly expressed at E10.5- E11.5 in the dorsal vz. The observation that Notch1, Notch2 and Notch 3 are expressed only at low levels in the dorsal ventricular zone at this time (Lindsell et al., 1996) may account for the attenuated Notch activity in the dorsal vz at this time. Further confirmation that

Notch signaling does not play a significant role at this time comes from Rumiko Mizuguchi's analysis of the *Presenilin-1*^{-/-} spinal cord. In this analysis, only minor changes in early neural specification were noted in the dorsal spinal cord.

4.4 Relationship between early-born versus late born sensory neurons

An important issue that arises from this study is the relationship between early-born dI4/dI5 neurons and the late-born dIL_A/dIL_B neurons. Both, these early and late cell types appear to have equivalent transcription factor profiles and neurotransmitter phenotypes. Also, all four populations migrate and settle in the dorsal horn proper, where sensory interneurons are located. dI4 and dIL_A neurons are inhibitory and express Pax2 and Lhx1/5, whereas excitatory dI5 and dIL_B neurons both express Lmx1b and Tlx3, suggesting that the late-born dIL cells represent an expansion of early-born dI4 and dI5 neuron populations. A possible explanation for this expansion could be the need for increased somatosensory discrimination in terrestrial vertebrates, compared to their aquatic counterparts. Teleost fish and amphibian tadpoles such as *Xenopus* have relatively small and simple dorsal horns, compared to terrestrial or avian vertebrates. One hypothesis for how this evolutionary problem was solved was to "duplicate" or expand the two classes of excitatory/inhibitory neurons that normally populate the dorsal horn, namely the dI4 and dI5 neurons. By expanding these two populations, the same repertoire of transcriptional determinants was used; however, one critical problem needed to be overcome in order for this to occur: Whereas, early-born neurons develop from dorso-ventral distinct progenitor populations, at later times these progenitor populations are no longer segregated. Mash1 plays a critical role in generating two different cell types from a single progenitor. I propose that late-born precursor cells express the homeodomain proteins Gsh1/2, which bias cells towards an excitatory fate. Therefore, it is necessary that Gsh1/2 function is repressed in a subset of them, allowing them to adopt an inhibitory cell fate. Mash1 fulfills this requirement by helping direct Ptf1a and Dll1 expression to dIL_A precursors. This asymmetrical expression of Dll1 in turn activates Notch, thus blocking the activity of Mash1 in dIL_B precursors and ensuring that they do not express Ptf1a, a key determinant of inhibitory dI4/dIL_A cell fate.

4.5 Comparison of Gsh1 and Gsh2 function in the spinal cord and telencephalon

Gsh1 and Gsh2 are expressed in other areas of the CNS. The role of both genes has been studied extensively in the forebrain, where they are involved in establishing the corticostriatal boundary. Their function is required for the proper specification of the proliferative cells in the ganglionic eminences (GEs) (Toresson et al., 2000; Yun et al., 2001) that give rise to the striatum and inhibitory cortical neurons. Ventral progenitors of the lateral ganglionic eminences (LGE) express Gsh2, whereas cortical progenitors in the adjacent dorsal domain express Pax6. The tight boundary between the dorsal and ventral telencephalic progenitors is maintained by cross-repressive interactions between Gsh2 and Pax6. This differs from the spinal cord, where Gsh2 and Pax6 are not expressed in a strictly complementary manner. Instead, Pax6 is broadly expressed in spinal cord progenitors, overlapping with Gsh1 and Gsh2 in dl3-dl5 progenitors (Kriks, 2003).

Interestingly, the bHLH factors Mash1 and Ngn1/2 show a similar expression profile to Gsh2 and Pax6 with respect to their expression in the developing telencephalon and spinal cord. The Gsh2-expressing cells in the LGE are also Mash1 positive, whereas the Pax6-expressing domain in the dorsal telencephalon is positive for Ngn1 and Ngn2. The expression profiles for Gsh1 and Gsh2 are also comparable in the developing spinal cord and telencephalon, with Gsh1 having a more restricted domain of expression in both structures (Toresson and Campbell, 2001; this study). In the developing ventral telencephalon, Gsh2 is highly expressed in both the medial ganglionic eminence (MGE) and LGE, whereas functional redundancy between Gsh1 and Gsh2 is suggested by the increased loss of striatal cell types in the forebrain of *Gsh1/2*^{-/-} embryos compared to either *Gsh* single mutant. The loss of striatal cell types is accompanied by the ectopic generation of cortical progenitors in the ventral telencephalon of *Gsh1/2*^{-/-} embryos, which is not observed in either *Gsh1* or *Gsh2* single mutants (Toresson and Campbell, 2001; Yun et al., 2003). Gsh1 and Gsh2 therefore have overlapping and parallel functions in both the telencephalon and the spinal cord where they specify different dorso-ventral progenitor domains.

The comparable expression patterns of Mash1, Gsh1/2 and Ngn1 in the spinal cord and ventral telencephalon (see above) suggest that Mash1 might

function in a similar manner in both regions of the CNS. Indeed, similar to its role in specifying inhibitory dIL_A neurons in the spinal cord, Mash1 is necessary for the generation of inhibitory interneurons generated in the GE, which then migrate tangentially to their final location in the neocortex. The absence of *Mash1* results in a loss of these GABAergic interneurons due to a loss of their progenitors in the ventral telencephalon (Casarosa et al., 1999). However, since inhibitory neurons in the telencephalon arise from a different domain (ventral telencephalon) than excitatory neurons (dorsal telencephalon), the role of Mash1 may be patterning rather than specification. Similar to the role of Mash1 in the spinal cord, Mash1 functions both cell-autonomously and non-cell autonomously to specify GABAergic interneurons in the telencephalon (Yun et al., 2002). Its function is required cell autonomously for the generation of early-born GABAergic interneurons, as evidenced by their loss when *Mash1* is absent. Mash1 also functions non-cell autonomously by upregulating Notch signaling in neighboring cells. In the *Mash1*^{-/-} telencephalon, Dll1 and Hes5 expression are reduced, similar to what Rumiko Mizuguchi found in the spinal cord of *Mash1*^{-/-} embryos. However, the role of Notch signaling in the ventral telencephalon is to mediate the temporal control of neurogenesis based on the observation by Yun et al. (2002) that in the absence of Notch signaling early-born progenitors mature prematurely to late-born progenitors. This function is different from the spinal cord, where Notch activity biases cells towards an excitatory cell fate.

4.6 Concluding remarks

While the issue of how progenitors are specified in the ventral neural tube has been studied in some detail, we still know very little about the mechanisms that specify dorsal progenitor identity. For instance, it was not known what role, if any, homeodomain transcription factors that are expressed in subsets of dorsal progenitors play in patterning/specifying dorsal progenitors. It was also unclear how these homeodomain transcription factors function. This doctoral thesis addresses these issues by defining the regulatory interactions between the Gsh class of homeodomain transcription factors and the proneural bHLH genes Mash1 and Ngn1 in the dorsal neural tube. In addition to demonstrating important roles for Gsh1 and Gsh2 in specifying dorsal progenitor identity, these findings provide evidence that the regulatory mechanisms that pattern dorsal progenitors differ from those operating in the ventral neural tube. This study provides important insights into the mechanisms that specify dorsal interneurons, which contribute to somatosensory circuits in the spinal cord.

This work also provides a major advance in our understanding of how neuronal cell types in the dorsal horn of the spinal cord are specified. These cell types are essential for sensory processing and although they play a critical role in pain pathways, we still know very little as to how they develop. Secondly, the experiments in this study allow us for the first time to construct a comprehensive unified model that outlines the genetic interactions that generate the two major classes of sensory interneurons that form the dorsal horn. This model incorporates not only those transcription factors previously found to play a role in dorsal neuron specification (e.g. Lbx1, Pax2, Tlx3, Ptf1a), but also additional transcription factors, including Gsh1, Gsh2 and Mash1, as well as the Notch signaling pathway. More importantly, this model outlines for the first time, and in detail, the genetic interactions by which postmitotic determination factors become restricted to subsets of dorsal interneurons.

We still know very little about how neuronal cell diversity and specialization occurs, particularly at later times in development when the early spatial patterning programs that generate different generic classes of neurons are no longer operating. While previous studies have shown that Notch regulates the choice between glial and neuronal fates in the vertebrate CNS, the role that Notch signaling plays in generating different neuronal fates in vertebrate development is

less clear. In this study, I show how Notch signaling is incorporated into the transcriptional program that determines excitatory versus inhibitory interneuron cell fates in the dorsal spinal cord. As such, this study is among the first to demonstrate genetically how a differential cell fate choice is executed between bipotential neuron progenitors.

4 Summary

This work examines the function of two homeodomain proteins, Gsh1 and Gsh2, in the specification of dorsal interneurons during the development of the spinal cord, as well as their interactions with other proteins that regulate their expression and function.

Gsh1 and Gsh2 are expressed in progenitors of dl3, dl4 and dl5 neurons, where they are necessary factors for the specification of two types of early-born excitatory neurons. In their absence, dl3 and dl5 neurons fail to develop; however, dl4 neurons are generated independently of Gsh1/2. The bHLH transcription factor Mash1 is co-expressed with Gsh1/2 in dl3-dl5 progenitors. At E10.5 and E11.5, *Mash1*^{-/-} embryos exhibit a similar phenotype to that seen in *Gsh1/2*^{-/-} embryos, with a reduction/loss of dl3 and dl5 neurons. This indicates that Mash1 and Gsh1/2 function cooperatively during the early wave of neurogenesis (E10-E11.5). During this developmental period, Gsh1 and Gsh2 function by repressing Ngn1 and Ngn2 expression, thereby maintaining Mash1 expression in the intermediate region of the spinal ventricular zone, which is the primary determinant of dl3 and dl5 cell fate. Gsh1 and Gsh2 continue to be expressed during a second wave of neurogenesis (E12-E13.5), when two types of dorsal interneurons (dIL) are generated from a single progenitor domain. These interneurons comprise inhibitory dIL_A neurons and excitatory dIL_B neurons and populate the dorsal horn of the spinal cord. During this second wave of neurogenesis, Gsh1/2 are necessary determinants of excitatory dIL_B neuron generation. Interestingly, the function of Mash1, which is co-expressed with Gsh1/2 in dIL progenitors, changes, compared to its function during early-born neuron generation. Mash1 opposes Gsh1/2 function in differentiating dIL cells, and is now necessary for the specification of inhibitory dIL_A neurons. Mash1 has two roles in the generation of dIL neurons; it activates the expression of the bHLH transcription factor Ptf1a in a cell-autonomous manner, which antagonizes Gsh1/2 function in prospective dIL_A neurons. Mash1 also activates Notch signaling in a non-cell autonomous manner by upregulating the expression of Notch ligand Delta1. This Notch signaling biases these cells towards a dIL_B fate.

Taken together, these findings identify Gsh1/2, Mash1 and Mash1-dependent Notch signaling as early key determinants of inhibitory versus excitatory cell fate in the dorsal spinal cord.

5 References

- Altman, J. and Bayer, S. A.** (1984). The development of the rat spinal cord. *Adv Anat Embryol Cell Biol* **85**, 1-164.
- Bai, C. B., Auerbach, W., Lee, J. S., Stephen, D. and Joyner, A. L.** (2002). Gli2, but not Gli1, is required for initial Shh signaling and ectopic activation of the Shh pathway. *Development* **129**, 4753-61.
- Bang, A. G., Papalopulu, N., Goulding, M. D. and Kintner, C.** (1999). Expression of Pax-3 in the lateral neural plate is dependent on a Wnt-mediated signal from posterior nonaxial mesoderm. *Dev Biol* **212**, 366-80.
- Bang, A. G., Papalopulu, N., Kintner, C. and Goulding, M. D.** (1997). Expression of Pax-3 is initiated in the early neural plate by posteriorizing signals produced by the organizer and by posterior non-axial mesoderm. *Development* **124**, 2075-85.
- Bermingham, N. A., Hassan, B. A., Wang, V. Y., Fernandez, M., Banfi, S., Bellen, H. J., Fritsch, B. and Zoghbi, H. Y.** (2001). Proprioceptor pathway development is dependent on Math1. *Neuron* **30**, 411-22.
- Bertrand, N., Castro, D. S. and Guillemot, F.** (2002). Proneural genes and the specification of neural cell types. *Nat Rev Neurosci* **3**, 517-30.
- Blumberg, B., Bolado, J., Jr., Moreno, T. A., Kintner, C., Evans, R. M. and Papalopulu, N.** (1997). An essential role for retinoid signaling in anteroposterior neural patterning. *Development* **124**, 373-9.
- Brichta, A. M. and Grant, G.** (1985). Cytoarchitectural organization of the spinal cord. In *The Rat Nervous System*, vol. 2 (ed. G. Paxinos), 293-301. Sydney: Academic Press.

- Briscoe, J., Sussel, L., Serup, P., Hartigan-O'Connor, D., Jessell, T. M., Rubenstein, J. L. and Ericson, J.** (1999). Homeobox gene Nkx2.2 and specification of neuronal identity by graded Sonic hedgehog signalling. *Nature* **398**, 622-7.
- Briscoe, J., Pierani, A., Jessell, T. M. and Ericson, J.** (2000). A homeodomain protein code specifies progenitor cell identity and neuronal fate in the ventral neural tube. *Cell* **101**, 435-45.
- Cabrera, C. V. and Alonso, M. C.** (1991). Transcriptional activation by heterodimers of the achaete-scute and daughterless gene products of *Drosophila*. *Embo J* **10**, 2965-73.
- Campos-Ortega, J. A.** (1994). Genetic mechanisms of early neurogenesis in *Drosophila melanogaster*. *J Physiol Paris* **88**, 111-22.
- Casarosa, S., Fode, C. and Guillemot, F.** (1999). Mash1 regulates neurogenesis in the ventral telencephalon. *Development* **126**, 525-34.
- Caspary, T. and Anderson, K. V.** (2003). Patterning cell types in the dorsal spinal cord: what the mouse mutants say. *Nat Rev Neurosci* **4**, 289-97.
- Chang, C. and Hemmati-Brivanlou, A.** (1998). Neural crest induction by Xwnt7B in *Xenopus*. *Dev Biol* **194**, 129-34.
- Chen, C. H., von Kessler, D. P., Park, W., Wang, B., Ma, Y. and Beachy, P. A.** (1999). Nuclear trafficking of Cubitus interruptus in the transcriptional regulation of Hedgehog target gene expression. *Cell* **98**, 305-16.
- Chen, Z. F., Rebelo, S., White, F., Malmberg, A. B., Baba, H., Lima, D., Woolf, C. J., Basbaum, A. I. and Anderson, D. J.** (2001). The paired homeodomain protein DRG11 is required for the projection of cutaneous sensory afferent fibers to the dorsal spinal cord. *Neuron* **31**, 59-73.

- Cheng, L., Arata, A., Mizuguchi, R., Qian, Y., Karunaratne, A., Gray, P. A., Arata, S., Shirasawa, S., Bouchard, M., Luo, P. et al.** (2004). Tlx3 and Tlx1 are post-mitotic selector genes determining glutamatergic over GABAergic cell fates. *Nat Neurosci* **7**, 510-7.
- Cheng, L., Samad, O. A., Xu, Y., Mizuguchi, R., Luo, P., Shirasawa, S., Goulding, M. and Ma, Q.** (2005). Lbx1 and Tlx3 are opposing switches in determining GABAergic versus glutamatergic transmitter phenotypes. *Nat Neurosci* **8**, 1510-5.
- Chesnutt, C., Burrus, L. W., Brown, A. M. and Niswander, L.** (2004). Coordinate regulation of neural tube patterning and proliferation by TGFbeta and WNT activity. *Dev Biol* **274**, 334-47.
- Chiang, C., Litingtung, Y., Lee, E., Young, K. E., Corden, J. L., Westphal, H. and Beachy, P. A.** (1996). Cyclopia and defective axial patterning in mice lacking Sonic hedgehog gene function. *Nature* **383**, 407-13.
- Chitnis, A. and Kintner, C.** (1996). Sensitivity of proneural genes to lateral inhibition affects the pattern of primary neurons in *Xenopus* embryos. *Development* **122**, 2295-301.
- Chizhikov, V. V. and Millen, K. J.** (2004a). Control of roof plate formation by Lmx1a in the developing spinal cord. *Development* **131**, 2693-705.
- Chizhikov, V. V. and Millen, K. J.** (2004b). Mechanisms of roof plate formation in the vertebrate CNS. *Nat Rev Neurosci* **5**, 808-12.
- Corbin, J. G., Gaiano, N., Machold, R. P., Langston, A. and Fishell, G.** (2000). The Gsh2 homeodomain gene controls multiple aspects of telencephalic development. *Development* **127**, 5007-20.
- Cornell, R. A. and Ohlen, T. V.** (2000). Vnd/nkx, ind/gsh, and msh/msx: conserved regulators of dorsoventral neural patterning? *Curr Opin Neurobiol* **10**, 63-71.

- Cox, W. G. and Hemmati-Brivanlou, A.** (1995). Caudalization of neural fate by tissue recombination and bFGF. *Development* **121**, 4349-58.
- D'Alessio, M. and Frasch, M.** (1996). msh may play a conserved role in dorsoventral patterning of the neuroectoderm and mesoderm. *Mech Dev* **58**, 217-31.
- De Calisto, J., Araya, C., Marchant, L., Riaz, C. F. and Mayor, R.** (2005). Essential role of non-canonical Wnt signalling in neural crest migration. *Development* **132**, 2587-97.
- Doniach, T.** (1995). Basic FGF as an inducer of anteroposterior neural pattern. *Cell* **83**, 1067-70.
- Dottori, M., Gross, M. K., Labosky, P. and Goulding, M.** (2001). The winged-helix transcription factor *Foxd3* suppresses interneuron differentiation and promotes neural crest cell fate. *Development* **128**, 4127-38.
- Ellenberger, T., Fass, D., Arnaud, M. and Harrison, S. C.** (1994). Crystal structure of transcription factor E47: E-box recognition by a basic region helix-loop-helix dimer. *Genes Dev* **8**, 970-80.
- Ericson, J., Morton, S., Kawakami, A., Roelink, H. and Jessell, T. M.** (1996). Two critical periods of Sonic Hedgehog signaling required for the specification of motor neuron identity. *Cell* **87**, 661-73.
- Ericson, J., Briscoe, J., Rashbass, P., van Heyningen, V. and Jessell, T. M.** (1997a). Graded sonic hedgehog signaling and the specification of cell fate in the ventral neural tube. *Cold Spring Harb Symp Quant Biol* **62**, 451-66.
- Ericson, J., Rashbass, P., Schedl, A., Brenner-Morton, S., Kawakami, A., van Heyningen, V., Jessell, T. M. and Briscoe, J.** (1997b). Pax6 controls progenitor cell identity and neuronal fate in response to graded Shh signaling. *Cell* **90**, 169-80.

- Erlander, M. G., Tillakaratne, N. J., Feldblum, S., Patel, N. and Tobin, A. J.** (1991). Two genes encode distinct glutamate decarboxylases. *Neuron* **7**, 91-100.
- Esni, F., Ghosh, B., Biankin, A. V., Lin, J. W., Albert, M. A., Yu, X., MacDonald, R. J., Civin, C. I., Real, F. X., Pack, M. A. et al.** (2004). Notch inhibits Ptf1 function and acinar cell differentiation in developing mouse and zebrafish pancreas. *Development* **131**, 4213-24.
- Fjose, A., Izpisua-Belmonte, J. C., Fromental-Ramain, C. and Duboule, D.** (1994). Expression of the zebrafish gene *hlx-1* in the prechordal plate and during CNS development. *Development* **120**, 71-81.
- Freneau, R. T., Jr., Troyer, M. D., Pahner, I., Nygaard, G. O., Tran, C. H., Reimer, R. J., Bellocchio, E. E., Fortin, D., Storm-Mathisen, J. and Edwards, R. H.** (2001). The expression of vesicular glutamate transporters defines two classes of excitatory synapse. *Neuron* **31**, 247-60.
- Gaiano, N., Nye, J. S. and Fishell, G.** (2000). Radial glial identity is promoted by Notch1 signaling in the murine forebrain. *Neuron* **26**, 395-404.
- Gerdes, J., Lemke, H., Baisch, H., Wacker, H. H., Schwab, U. and Stein, H.** (1984). Cell cycle analysis of a cell proliferation-associated human nuclear antigen defined by the monoclonal antibody Ki-67. *J Immunol* **133**, 1710-5.
- Giagtzoglou, N., Alifragis, P., Koumbanakis, K. A. and Delidakis, C.** (2003). Two modes of recruitment of E(spl) repressors onto target genes. *Development* **130**, 259-70.
- Gillespie, P. G. and Walker, R. G.** (2001). Molecular basis of mechanosensory transduction. *Nature* **413**, 194-202.
- Glasgow, S. M., Henke, R. M., Macdonald, R. J., Wright, C. V. and Johnson, J. E.** (2005). Ptf1a determines GABAergic over glutamatergic neuronal cell fate in the spinal cord dorsal horn. *Development* **132**, 5461-9.

- Goulding, M. D., Chalepakis, G., Deutsch, U., Erselius, J. R. and Gruss, P.** (1991). Pax-3, a novel murine DNA binding protein expressed during early neurogenesis. *Embo J* **10**, 1135-47.
- Goulding, M. and Lamar, E.** (2000). Neuronal patterning: Making stripes in the spinal cord. *Curr Biol* **10**, R565-8.
- Goulding, M., Lanuza, G., Sapir, T. and Narayan, S.** (2002). The formation of sensorimotor circuits. *Curr Opin Neurobiol* **12**, 508-15.
- Gowan, K., Helms, A. W., Hunsaker, T. L., Collisson, T., Ebert, P. J., Odom, R. and Johnson, J. E.** (2001). Crossinhibitory activities of Ngn1 and Math1 allow specification of distinct dorsal interneurons. *Neuron* **31**, 219-32.
- Gross, M. K., Dottori, M. and Goulding, M.** (2002). Lbx1 specifies somatosensory association interneurons in the dorsal spinal cord. *Neuron* **34**, 535-49.
- Guillemot, F., Lo, L. C., Johnson, J. E., Auerbach, A., Anderson, D. J. and Joyner, A. L.** (1993). Mammalian achaete-scute homolog 1 is required for the early development of olfactory and autonomic neurons. *Cell* **75**, 463-76.
- Hamburger, V. und Hamilton, H. L.** (1951). A series of normal stages in the development of the chick embryo. *J Morph* **88**:49-92.
- Helms, A. W. and Johnson, J. E.** (2003). Specification of dorsal spinal cord interneurons. *Curr Opin Neurobiol* **13**, 42-9.
- Hemmati-Brivanlou, A., Kelly, O. G. and Melton, D. A.** (1994). Follistatin, an antagonist of activin, is expressed in the Spemann organizer and displays direct neuralizing activity. *Cell* **77**, 283-95.

- Hendzel, M. J., Wei, Y., Mancini, M. A., Van Hooser, A., Ranalli, T., Brinkley, B. R., Bazett-Jones, D. P. and Allis, C. D.** (1997). Mitosis-specific phosphorylation of histone H3 initiates primarily within pericentromeric heterochromatin during G2 and spreads in an ordered fashion coincident with mitotic chromosome condensation. *Chromosoma* **106**, 348-60.
- Hirsch, M.R., Tiveron, M.C., Guillemot, F., Brunet, J.F., Goidis, C.** (1998) Control of noradrenergic differentiation and Phox2a expression by MASH1 in the central and peripheral nervous system. *Development* **125**, 599-608.
- Holland, L. Z., Venkatesh, T. V., Gorlin, A., Bodmer, R. and Holland, N. D.** (1998). Characterization and developmental expression of AmphiNk2-2, an NK2 class homeobox gene from Amphioxus. (Phylum Chordata; Subphylum Cephalochordata). *Dev Genes Evol* **208**, 100-5.
- Hoshino, M., Nakamura, S., Mori, K., Kawauchi, T., Terao, M., Nishimura, Y. V., Fukuda, A., Fuse, T., Matsuo, N., Sone, M. et al.** (2005). Ptf1a, a bHLH transcriptional gene, defines GABAergic neuronal fates in cerebellum. *Neuron* **47**, 201-13.
- Hsieh-Li, H. M., Witte, D. P., Szucsik, J. C., Weinstein, M., Li, H. and Potter, S. S.** (1995). Gsh-2, a murine homeobox gene expressed in the developing brain. *Mech Dev* **50**, 177-86.
- Huang, E. J., Wilkinson, G. A., Farinas, I., Backus, C., Zang, K., Wong, S. L. and Reichardt, L. F.** (1999). Expression of Trk receptors in the developing mouse trigeminal ganglion: in vivo evidence for NT-3 activation of TrkA and TrkB in addition to TrkC. *Development* **126**, 2191-203.
- Hui, C. C., Slusarski, D., Platt, K. A., Holmgren, R. and Joyner, A. L.** (1994). Expression of three mouse homologs of the Drosophila segment polarity gene cubitus interruptus, Gli, Gli-2, and Gli-3, in ectoderm- and mesoderm-derived tissues suggests multiple roles during postimplantation development. *Dev Biol* **162**, 402-13.

- Hynes, M., Stone, D. M., Dowd, M., Pitts-Meek, S., Goddard, A., Gurney, A. and Rosenthal, A.** (1997). Control of cell pattern in the neural tube by the zinc finger transcription factor and oncogene Gli-1. *Neuron* **19**, 15-26.
- Isshiki, T., Takeichi, M. and Nose, A.** (1997). The role of the msh homeobox gene during Drosophila neurogenesis: implication for the dorsoventral specification of the neuroectoderm. *Development* **124**, 3099-109.
- Jessell, T. M.** (2000). Neuronal specification in the spinal cord: inductive signals and transcriptional codes. *Nat Rev Genet* **1**, 20-9.
- Jimenez, F., Martin-Morris, L. E., Velasco, L., Chu, H., Sierra, J., Rosen, D. R. and White, K.** (1995). vnd, a gene required for early neurogenesis of Drosophila, encodes a homeodomain protein. *Embo J* **14**, 3487-95.
- John, A., Wildner, H. and Britsch, S.** (2005). The homeodomain transcription factor Gbx1 identifies a subpopulation of late-born GABAergic interneurons in the developing dorsal spinal cord. *Dev Dyn* **234**, 767-71.
- Johnson, J. E., Birren, S. J., Saito, T. and Anderson, D. J.** (1992). DNA binding and transcriptional regulatory activity of mammalian achaete-scute homologous (MASH) proteins revealed by interaction with a muscle-specific enhancer. *Proc Natl Acad Sci U S A* **89**, 3596-600.
- Julius, D. and Basbaum, A. I.** (2001). Molecular mechanisms of nociception. *Nature* **413**, 203-10.
- Kageyama, R., Ohtsuka, T., Hatakeyama, J., Ohsawa, R.** (2005) Roles of bHLH genes in neural stem cell differentiation. *Exp Cell Res* **306**, 343-8.
- Kaneko, T. and Fujiyama, F.** (2002). Complementary distribution of vesicular glutamate transporters in the central nervous system. *Neurosci Res* **42**, 243-50.
- Keller, R.** (2002). Shaping the vertebrate body plan by polarized embryonic cell movements. *Science* **298**, 1950-4.

- Kessel, M., Balling, R. and Gruss, P.** (1990). Variations of cervical vertebrae after expression of a Hox-1.1 transgene in mice. *Cell* **61**, 301-8.
- Kintner, C.** (2002). Neurogenesis in embryos and in adult neural stem cells. *J Neurosci* **22**, 639-43.
- Knecht, A. K. and Bronner-Fraser, M.** (2002). Induction of the neural crest: a multigene process. *Nat Rev Genet* **3**, 453-61.
- Knust, E.** (1994). Cell fate choice during early neurogenesis in *Drosophila melanogaster*. *Perspect Dev Neurobiol* **2**, 141-9.
- Kopan, R.** (2002). Notch: a membrane-bound transcription factor. *J Cell Sci* **115**, 1095-7.
- Kriks, S.** (2003). Frühe Charakterisierung dorsaler Interneurone. *University of Göttingen/ The Salk Institute of Biological Studies*.
- LaBonne, C. and Bronner-Fraser, M.** (1998). Neural crest induction in *Xenopus*: evidence for a two-signal model. *Development* **125**, 2403-14.
- Lai, E. C.** (2004). Notch signaling: control of cell communication and cell fate. *Development* **131**, 965-73.
- Lanuza, G. M., Gosgnach, S., Pierani, A., Jessell, T. M. and Goulding, M.** (2004). Genetic identification of spinal interneurons that coordinate left-right locomotor activity necessary for walking movements. *Neuron* **42**, 375-86.
- Le Douarin, N. M.** (1990). Cell lineage segregation during neural crest ontogeny. *Proc Natl Acad Sci U S A* **87**, 1119-23.
- Lee, K. J., Mendelsohn, M. and Jessell, T. M.** (1998). Neuronal patterning by BMPs: a requirement for GDF7 in the generation of a discrete class of commissural interneurons in the mouse spinal cord. *Genes Dev* **12**, 3394-407.

- Lee, K. J. and Jessell, T. M.** (1999). The specification of dorsal cell fates in the vertebrate central nervous system. *Annu Rev Neurosci* **22**, 261-94.
- Lee, K. J., Dietrich, P. and Jessell, T. M.** (2000). Genetic ablation reveals that the roof plate is essential for dorsal interneuron specification. *Nature* **403**, 734-40.
- Li, H., Zeitler, P. S., Valerius, M. T., Small, K. and Potter, S. S.** (1996). Gsh-1, an orphan Hox gene, is required for normal pituitary development. *Embo J* **15**, 714-24.
- Li, S., Misra, K., Matise, M. P. and Xiang, M.** (2005). Foxn4 acts synergistically with Mash1 to specify subtype identity of V2 interneurons in the spinal cord. *Proc Natl Acad Sci U S A* **102**, 10688-93.
- Liem, K. F., Jr., Tremml, G., Roelink, H. and Jessell, T. M.** (1995). Dorsal differentiation of neural plate cells induced by BMP-mediated signals from epidermal ectoderm. *Cell* **82**, 969-79.
- Liem, K. F., Jr., Tremml, G. and Jessell, T. M.** (1997). A role for the roof plate and its resident TGFbeta-related proteins in neuronal patterning in the dorsal spinal cord. *Cell* **91**, 127-38.
- Lindsell, C. E., Boulter, J., diSibio, G., Gossler, A. and Weinmaster, G.** (1996). Expression patterns of Jagged, Delta1, Notch1, Notch2, and Notch3 genes identify ligand-receptor pairs that may function in neural development. *Mol Cell Neurosci* **8**, 14-27.
- Liu, J. P., Laufer, E. and Jessell, T. M.** (2001). Assigning the positional identity of spinal motor neurons: rostrocaudal patterning of Hox-c expression by FGFs, Gdf11, and retinoids. *Neuron* **32**, 997-1012.
- Louvi, A. and Artavanis-Tsakonas, S.** (2006). Notch signalling in vertebrate neural development. *Nat Rev Neurosci* **7**, 93-102.

- Lufkin, T., Dierich, A., LeMeur, M., Mark, M. and Chambon, P.** (1991). Disruption of the Hox-1.6 homeobox gene results in defects in a region corresponding to its rostral domain of expression. *Cell* **66**, 1105-19.
- Ma, Q., Fode, C., Guillemot, F. and Anderson, D. J.** (1999). Neurogenin1 and neurogenin2 control two distinct waves of neurogenesis in developing dorsal root ganglia. *Genes Dev* **13**, 1717-28.
- Mayor, R., Morgan, R. and Sargent, M. G.** (1995). Induction of the prospective neural crest of Xenopus. *Development* **121**, 767-77.
- Mayor, R., Guerrero, N. and Martinez, C.** (1997). Role of FGF and noggin in neural crest induction. *Dev Biol* **189**, 1-12.
- McGinnis, W. and Krumlauf, R.** (1992). Homeobox genes and axial patterning. *Cell* **68**, 283-302.
- McGrew, L. L., Lai, C. J. and Moon, R. T.** (1995). Specification of the anteroposterior neural axis through synergistic interaction of the Wnt signaling cascade with noggin and follistatin. *Dev Biol* **172**, 337-42.
- McIntire, S. L., Reimer, R. J., Schuske, K., Edwards, R. H. and Jorgensen, E. M.** (1997). Identification and characterization of the vesicular GABA transporter. *Nature* **389**, 870-6.
- Mellerick, D. M. and Nirenberg, M.** (1995). Dorsal-ventral patterning genes restrict NK-2 homeobox gene expression to the ventral half of the central nervous system of Drosophila embryos. *Dev Biol* **171**, 306-16.
- Mizuguchi, R., Sugimori, M., Takebayashi, H., Kosako, H., Nagao, M., Yoshida, S., Nabeshima, Y., Shimamura, K. and Nakafuku, M.** (2001). Combinatorial roles of olig2 and neurogenin2 in the coordinated induction of pan-neuronal and subtype-specific properties of motoneurons. *Neuron* **31**, 757-71.

- Monsoro-Burq, A. H., Wang, E. and Harland, R.** (2005). Msx1 and Pax3 cooperate to mediate FGF8 and WNT signals during *Xenopus* neural crest induction. *Dev Cell* **8**, 167-78.
- Morrison, S. J., Perez, S. E., Qiao, Z., Verdi, J. M., Hicks, C., Weinmaster, G. and Anderson, D. J.** (2000). Transient Notch activation initiates an irreversible switch from neurogenesis to gliogenesis by neural crest stem cells. *Cell* **101**, 499-510.
- Muhr, J., Jessell, T. M. and Edlund, T.** (1997). Assignment of early caudal identity to neural plate cells by a signal from caudal paraxial mesoderm. *Neuron* **19**, 487-502.
- Muhr, J., Andersson, E., Persson, M., Jessell, T. M. and Ericson, J.** (2001). Groucho-mediated transcriptional repression establishes progenitor cell pattern and neuronal fate in the ventral neural tube. *Cell* **104**, 861-73.
- Muller, T., Brohmann, H., Pierani, A., Heppenstall, P. A., Lewin, G. R., Jessell, T. M. and Birchmeier, C.** (2002). The homeodomain factor *Ibx1* distinguishes two major programs of neuronal differentiation in the dorsal spinal cord. *Neuron* **34**, 551-62.
- Muller, T., Anlag, K., Wildner, H., Britsch, S., Treier, M. and Birchmeier, C.** (2005). The bHLH factor *Olig3* coordinates the specification of dorsal neurons in the spinal cord. *Genes Dev* **19**, 733-43.
- Muroyama, Y., Fujihara, M., Ikeya, M., Kondoh, H. and Takada, S.** (2002). Wnt signaling plays an essential role in neuronal specification of the dorsal spinal cord. *Genes Dev* **16**, 548-53.
- Nakada, Y., Hunsaker, T. L., Henke, R. M. and Johnson, J. E.** (2004). Distinct domains within *Mash1* and *Math1* are required for function in neuronal differentiation versus neuronal cell-type specification. *Development* **131**, 1319-30.

- Nieto, M., Schuurmans, C., Britz, O. and Guillemot, F.** (2001). Neural bHLH genes control the neuronal versus glial fate decision in cortical progenitors. *Neuron* **29**, 401-13.
- Nieuwkoop, P. D.** (1952). Activation and organization of the central nervous system in amphibians I. Induction and activation. *J. Exp. Zool* **120**, 1-32.
- Novitsch, B. G., Chen, A. I. and Jessell, T. M.** (2001). Coordinate regulation of motor neuron subtype identity and pan-neuronal properties by the bHLH repressor Olig2. *Neuron* **31**, 773-89.
- Park, H. L., Bai, C., Platt, K. A., Matise, M. P., Beeghly, A., Hui, C. C., Nakashima, M. and Joyner, A. L.** (2000). Mouse Gli1 mutants are viable but have defects in SHH signaling in combination with a Gli2 mutation. *Development* **127**, 1593-605.
- Parras, C. M., Schuurmans, C., Scardigli, R., Kim, J., Anderson, D. J. and Guillemot, F.** (2002). Divergent functions of the proneural genes Mash1 and Ngn2 in the specification of neuronal subtype identity. *Genes Dev* **16**, 324-38.
- Persson, M., Stamatakis, D., te Welscher, P., Andersson, E., Bose, J., Ruther, U., Ericson, J. and Briscoe, J.** (2002). Dorsal-ventral patterning of the spinal cord requires Gli3 transcriptional repressor activity. *Genes Dev* **16**, 2865-78.
- Pierani, A., Moran-Rivard, L., Sunshine, M. J., Littman, D. R., Goulding, M. and Jessell, T. M.** (2001). Control of interneuron fate in the developing spinal cord by the progenitor homeodomain protein Dbx1. *Neuron* **29**, 367-84.
- Placzek, M., Yamada, T., Tessier-Lavigne, M., Jessell, T. and Dodd, J.** (1991). Control of dorsoventral pattern in vertebrate neural development: induction and polarizing properties of the floor plate. *Development Suppl* **2**, 105-22.

- Ramos, C. and Robert, B.** (2005). msh/Msx gene family in neural development. *Trends Genet* **21**, 624-32.
- Rexed, B.** (1952). The cytoarchitectonic organization of the spinal cord in the cat. *J Comp Neurol* **96**, 414-95.
- Roelink, H., Porter, J. A., Chiang, C., Tanabe, Y., Chang, D. T., Beachy, P. A. and Jessell, T. M.** (1995). Floor plate and motor neuron induction by different concentrations of the amino-terminal cleavage product of sonic hedgehog autoproteolysis. *Cell* **81**, 445-55.
- Ruiz i Altaba, A.** (1998). Combinatorial Gli gene function in floor plate and neuronal inductions by Sonic hedgehog. *Development* **125**, 2203-12.
- Saint-Jeannet, J. P., He, X., Varmus, H. E. and Dawid, I. B.** (1997). Regulation of dorsal fate in the neuraxis by Wnt-1 and Wnt-3a. *Proc Natl Acad Sci U S A* **94**, 13713-8.
- Sasai, Y., Lu, B., Steinbeisser, H., Geissert, D., Gont, L. K. and De Robertis, E. M.** (1994). Xenopus chordin: a novel dorsalizing factor activated by organizer-specific homeobox genes. *Cell* **79**, 779-90.
- Sato, T., Sasai, N. and Sasai, Y.** (2005). Neural crest determination by co-activation of Pax3 and Zic1 genes in Xenopus ectoderm. *Development* **132**, 2355-63.
- Schoenwolf, G. C. and Smith, J. L.** (1990). Mechanisms of neurulation: traditional viewpoint and recent advances. *Development* **109**, 243-70.
- Singh, G., Kaur, S., Stock, J. L., Jenkins, N. A., Gilbert, D. J., Copeland, N. G. and Potter, S. S.** (1991). Identification of 10 murine homeobox genes. *Proc Natl Acad Sci U S A* **88**, 10706-10.
- Small, K. M. and Potter, S. S.** (1993). Homeotic transformations and limb defects in Hox A11 mutant mice. *Genes Dev* **7**, 2318-28.

- Schmidt, R. F. and Thews, G.** (1983) In: *Human Physiology: Motor systems*, Springer-Verlag, 81-110.
- Smith, S. T. and Jaynes, J. B.** (1996). A conserved region of engrailed, shared among all en-, gsc-, Nk1-, Nk2- and msh-class homeoproteins, mediates active transcriptional repression in vivo. *Development* **122**, 3141-50.
- Smith, W. C. and Harland, R. M.** (1992). Expression cloning of noggin, a new dorsalizing factor localized to the Spemann organizer in *Xenopus* embryos. *Cell* **70**, 829-40.
- Spemann, H. and Mangold, H.** (1924). Ueber Induktion von Embryonalanlagen durch Implantation artfremder Organisatoren. *Roux's Arch. Dev. Biol.* **100**, 599-638.
- Sun, Y., Nadal-Vicens, M., Misono, S., Lin, M. Z., Zubiaga, A., Hua, X., Fan, G. and Greenberg, M. E.** (2001). Neurogenin promotes neurogenesis and inhibits glial differentiation by independent mechanisms. *Cell* **104**, 365-76.
- Szucsik, J. C., Witte, D. P., Li, H., Pixley, S. K., Small, K. M. and Potter, S. S.** (1997). Altered forebrain and hindbrain development in mice mutant for the Gsh-2 homeobox gene. *Dev Biol* **191**, 230-42.
- Timmer, J., Chesnutt, C. and Niswander, L.** (2005). The activin signaling pathway promotes differentiation of dl3 interneurons in the spinal neural tube. *Dev Biol* **285**, 1-10.
- Timmer, J. R., Wang, C. and Niswander, L.** (2002). BMP signaling patterns the dorsal and intermediate neural tube via regulation of homeobox and helix-loop-helix transcription factors. *Development* **129**, 2459-72.
- Tomita, K., Moriyoshi, K., Nakanishi, S., Guillemot, F. and Kageyama, R.** (2000). Mammalian achaete-scute and atonal homologs regulate neuronal versus glial fate determination in the central nervous system. *Embo J* **19**, 5460-72.

- Toresson, H., Potter, S. S. and Campbell, K.** (2000). Genetic control of dorsal-ventral identity in the telencephalon: opposing roles for Pax6 and Gsh2. *Development* **127**, 4361-71.
- Toresson, H. and Campbell, K.** (2001). A role for Gsh1 in the developing striatum and olfactory bulb of Gsh2 mutant mice. *Development* **128**, 4769-80.
- Triezenberg, S. J., Kingsbury, R. C. and McKnight, S. L.** (1988). Functional dissection of VP16, the trans-activator of herpes simplex virus immediate early gene expression. *Genes Dev* **2**, 718-29.
- Valerius, M. T., Li, H., Stock, J. L., Weinstein, M., Kaur, S., Singh, G. and Potter, S. S.** (1995). Gsh-1: a novel murine homeobox gene expressed in the central nervous system. *Dev Dyn* **203**, 337-51.
- Vallstedt, A., Muhr, J., Pattyn, A., Pierani, A., Mendelsohn, M., Sander, M., Jessell, T. M. and Ericson, J.** (2001). Different levels of repressor activity assign redundant and specific roles to Nkx6 genes in motor neuron and interneuron specification. *Neuron* **31**, 743-55.
- van Straaten, H. W., Hekking, J. W., Beursgens, J. P., Terwindt-Rouwenhorst, E. and Drukker, J.** (1989). Effect of the notochord on proliferation and differentiation in the neural tube of the chick embryo. *Development* **107**, 793-803.
- von Ohlen, T. and Doe, C. Q.** (2000). Convergence of dorsal, dpp, and egr signaling pathways subdivides the drosophila neuroectoderm into three dorsal-ventral columns. *Dev Biol* **224**, 362-72.
- Wang, W., Chen, X., Xu, H. and Lufkin, T.** (1996). Msx3: a novel murine homologue of the Drosophila msh homeobox gene restricted to the dorsal embryonic central nervous system. *Mech Dev* **58**, 203-15.

- Waters, S. T., Wilson, C. P. and Lewandoski, M.** (2003). Cloning and embryonic expression analysis of the mouse *Gbx1* gene. *Gene Expr Patterns* **3**, 313-7.
- Weiss, J. B., Von Ohlen, T., Mellerick, D. M., Dressler, G., Doe, C. Q. and Scott, M. P.** (1998). Dorsoventral patterning in the *Drosophila* central nervous system: the intermediate neuroblasts defective homeobox gene specifies intermediate column identity. *Genes Dev* **12**, 3591-602.
- Wildner, H., Muller, T., Cho, S. H., Brohl, D., Cepko, C. L., Guillemot, F. and Birchmeier, C.** (2006). dILA neurons in the dorsal spinal cord are the product of terminal and non-terminal asymmetric progenitor cell divisions, and require Mash1 for their development. *Development* **133**, 2105-13.
- Willis, W. D. & Coggeshall, R. E.** (1991) In: *Sensory mechanisms of the spinal cord* (Plenum, New York).
- Wilson, P. A. and Hemmati-Brivanlou, A.** (1995). Induction of epidermis and inhibition of neural fate by Bmp-4. *Nature* **376**, 331-3.
- Wine-Lee, L., Ahn, K. J., Richardson, R. D., Mishina, Y., Lyons, K. M. and Crenshaw, E. B., 3rd.** (2004). Signaling through BMP type 1 receptors is required for development of interneuron cell types in the dorsal spinal cord. *Development* **131**, 5393-403.
- Yamada, T., Placzek, M., Tanaka, H., Dodd, J. and Jessell, T. M.** (1991). Control of cell pattern in the developing nervous system: polarizing activity of the floor plate and notochord. *Cell* **64**, 635-47.
- Yun, K., Potter, S. and Rubenstein, J. L.** (2001). Gsh2 and Pax6 play complementary roles in dorsoventral patterning of the mammalian telencephalon. *Development* **128**, 193-205.

- Yun, K., Fischman, S., Johnson, J., Hrabe de Angelis, M., Weinmaster, G. and Rubenstein, J. L.** (2002). Modulation of the notch signaling by Mash1 and Dlx1/2 regulates sequential specification and differentiation of progenitor cell types in the subcortical telencephalon. *Development* **129**, 5029-40.
- Yun, K., Garel, S., Fischman, S., Rubenstein, J.L.** (2003) Patterning of the lateral ganglionic eminence by the Gsh1 and Gsh2 homeobox genes regulates striatal and olfactory bulb histogenesis and the growth of axons through the basal ganglia. *J Comp Neurol* **461**, 151-65.
- Zimmerman, L. B., De Jesus-Escobar, J. M. and Harland, R. M.** (1996). The Spemann organizer signal noggin binds and inactivates bone morphogenetic protein 4. *Cell* **86**, 599-606.

7 Appendix

7.1 Primer sequences

All primer sequences are listed in 5' → 3'- orientation.

7.1.1 Primers used for genotyping of KO mice

Gsh1: WT: OL *Gsh1* WTs: GCACCGCAAGGCTGCAAGTGCTCTT
OL *Gsh1* WTas: ATACCATGTGAGACAGTTCTCTCTGCTAG
KO: OL *Gsh1* KOs: AGCGTCGTGATTAGCGATGATGAACCA
OL *Gsh1* KOas: TCCAGTTTCACTAATGACACAAAC

Gsh2: WT: OL *Gsh2* WTs: CAAGGGTTGTCAAGTAGAGTGG
OL *Gsh2* WTas: CTTACGCGACGGTTCTGAAAC
KO: Neos: CAAGATGGATTGCACGCAGG
Neoas: CGATGTTTCGCTTGGTGGTC

Mash1: WT: OL *Mash1* WTs: CTCCGGGAGCATGTCCCCAA
OL *Mash1* WTas:CCAGGACTCAATACGCAGGG
KO: Neos: CAAGATGGATTGCACGCAGG
Neoas: CGATGTTTCGCTTGGTGGTC

Psen1: WT: OL *Psen1* WTs: ACCTCAGCTGTTTGTCCCGG
OL *Psen1* WTas:GCACGAGACTAGTGAGACGTG
KO: Neos: CAAGATGGATTGCACGCAGG
Neoas: CGATGTTTCGCTTGGTGGTC

s=sense, as=antisense

7.1.2 Vector-specific primers

pBluescript SK: T3: ATTAACCCTCACTAAAGG
T7: GCTAGTTATTGCTCAGCGG

pIRES-EGFP: OL pIRES-EGFP (5'): TTCTTTTTCCTACAGCTCCTG

7.1.3 Primers for cloning

Cloning of Ngn1-full-length cDNA

Ngn1 sense: TAGGAATTCCAGTAAGTGCGCTTCGAAGG
EcoRI

Ngn1 antisense: TAGGGATCCCTAGTGGTATGGGATGAAACA
BamHI

Cloning of Ptf1a-full-length cDNA

Ptf1a A sense: TAGCCGCGGCACGAGGGAGGGGCTGAG
SacII

Ptf1a A antisense: CTCGCCAGGATCCCCAAAGGCGGTGG
BamHI

Ptf1a B sense: CCACCGCCTTTGGGGGATCCTGGCGAG
BamHI

Ptf1a B antisense: TAGGGATCCCGATGTGAGCTGTCTCAGGAC
BamHI

7.2 Sequences of cloned cDNAs

7.2.1 Ngn1 sequence

NM_010896	165	CAGTAAGTGC	224
Ngn1-pIRES-EGFP	29		88
NM_010896	225	CTGCAAGATGCCTGCCCTTTGGAGACCTGCATCTCTGATCTCGACTGCTCCAGCAGCAA	284
Ngn1-pIRES-EGFP	89	CTGCAAGATGCCTGCCCTTTGGAGACCTGCATCTCTGATCTCGACTGCTCCAGCAGCAA	148
NM_010896	285	CAGCAGCAGCGACCTGTCCAGCTTCCTCACCGACGAGGAGGACTGTGCCAGGCTACAGCC	344
Ngn1-pIRES-EGFP	149	CAGCAGCAGCGACCTGTCCAGCTTCCTCACCGACGAGGAGGACTGTGCCAGGCTACAGCC	208
NM_010896	345	CCTAGCCTCCACCTCGGGGTGTCCGTGCCAGCCGGAGAGCGCTCCCGCCCTCTCCGG	404
Ngn1-pIRES-EGFP	209	CCTAGCCTCCACCTCGGGGTGTCCGTGCCAGCCGGAGAGCGCTCCCGCCCTCTCCGG	268
NM_010896	405	GGCATCGAATGTTCCCGGTGCCAGGACGAAAGAGCAGGAACGGCGGAGGCGGCGAGGTCG	464
Ngn1-pIRES-EGFP	269	GGCATCGAATGTTCCCGGTGCCAGGACGAAAGAGCAGGAACGGCGGAGGCGGCGAGGTCG	328
NM_010896	465	CGCTCGGGTGC	524
Ngn1-pIRES-EGFP	329	CGCTCGGGTGC	388
NM_010896	525	CAACGATCGCGAGCGCAACCGCATGCACAACCTCAACGCTGCGCTGGACGCCTTGCGCAG	584
Ngn1-pIRES-EGFP	389	CAACGATCGCGAGCGCAACCGCATGCACAACCTCAACGCTGCGCTGGACGCCTTGCGCAG	448
NM_010896	585	CGTGCTGCCCTCGTTCCCCGACGACACCAAGCTCACCAAGATTGAGACGCTGCGCTTCGC	644
Ngn1-pIRES-EGFP	449	CGTGCTGCCCTCGTTCCCCGACGACACCAAGCTCACCAAGATTGAGACGCTGCGCTTCGC	508
NM_010896	645	CTACAACCTACATCTGGGCCCTGGCTGAGACACTGGCCTGGCAGATCAAGGGCTCCCCGG	704
Ngn1-pIRES-EGFP	509	CTACAACCTACATCTGGGCCCTGGCTGAGACACTGGCCTGGCAGATCAAGGGCTCCCCGG	568
NM_010896	705	GGGCAGTGCCCGGGAGCGCCTCCTGCCTCCGAGTGTGTCCCCTGTCTGCCCGGGCCCC	764
Ngn1-pIRES-EGFP	569	GGGCAGTGCCCGGGAGCGCCTCCTGCCTCCGAGTGTGTCCCCTGTCTGCCCGGGCCCC	628
NM_010896	765	GAGCCCGGCCAGCGACACTGAGTCCTGGGGTTCGGGGCCGCTGCCTCCCCCTGCGCCAC	824
Ngn1-pIRES-EGFP	629	GAGCCCGGCCAGCGACACTGAGTCCTGGGGTTCGGGGCCGCTGCCTCCCCCTGCGCCAC	688
NM_010896	825	TGTGGCATCACCACCTCTCTGACCCAGTAGTCCCTCGGCTTCAGAAGACTTCACCTATGG	884
Ngn1-pIRES-EGFP	689	TGTGGCATCACCACCTCTCTGACCCAGTAGTCCCTCGGCTTCAGAAGACTTCACCTATGG	748
NM_010896	885	CCCGGGCGATCCCCTTTTCTCCTTTCTGGCCTGCCAAAGACCTGCTCCACACGACGCC	944
Ngn1-pIRES-EGFP	749	CCCGGGCGATCCCCTTTTCTCCTTTCTGGCCTGCCAAAGACCTGCTCCACACGACGCC	808
NM_010896	945	CTGTTTCATCCCATACCACTAGG	967
Ngn1-pIRES-EGFP	809	CTGTTTCATCCCATACCACTAGG	831

The arrow marks the start codon, and the line marks the stop codon.

7.2.2 Ptf1a sequence

AF298116	223	CATGGACGCCGTACTCCTGGAGCACTTCCCCGGGGCCTGGACACCTTCCCATCCCCTTA	282
Ptf1a-pIRES -EGFP	61	 CATGGACGCCGTACTCCTGGAGCACTTCCCCGGGGCCTGGACACCTTCCCATCCCCTTA	120
AF298116	283	CTTTGATGAGGAAGATTCTTCACCAGCAGTCTCTCGGGACCCGCTGGAGGACAGCGA	342
Ptf1a-pIRES -EGFP	121	 CTTTGATGAGGAAGATTCTTCACCAGCAGTCTCTCGGGACCCGCTGGAGGACAGCGA	180
AF298116	343	CGAGCTGCTGGGGACGAGCAAGCAGAAGTAGAGTTCTCAGCCACCAGCTACACGAATA	402
Ptf1a-pIRES -EGFP	181	 CGAGCTGCTGGGGACGAGCAAGCAGAAGTAGAGTTCTCAGCCACCAGCTACACGAATA	240
AF298116	403	CTGCTACCGCGACGGGGCGTGCCTGCTGCTGCAACCCGCGCCCTCGGCCGCCCGCACGC	462
Ptf1a-pIRES -EGFP	241	 CTGCTACCGCGACGGGGCGTGCCTGCTGCTGCAACCCGCGCCCTCGGCCGCCCGCACGC	300
AF298116	463	GCTCGCCCCGCCCTTTGGGGGATCCTGGCGAGCCCGAGGACAACGTCAGCTATTGCTG	522
Ptf1a-pIRES -EGFP	301	 GCTCGCCCCGCCCTTTGGGGGATCCTGGCGAGCCCGAGGACAACGTCAGCTATTGCTG	360
AF298116	523	CGATGCAGGGGCTCCTCTCGTGCCTTCCCCTACTCGCCTGGCTCACCGCCCTCGTGCCT	582
Ptf1a-pIRES -EGFP	361	 CGATGCAGGGGCTCCTCTCGTGCCTTCCCCTACTCGCCTGGCTCACCGCCCTCGTGCCT	420
AF298116	583	CGCCTACCCGTGTGCCGCGGTGCTGTCCCCCGGTGCGCGGCTCGGTGGTTGAACGGGGC	642
Ptf1a-pIRES -EGFP	421	 CGCCTACCCGTGTGCCGCGGTGCTGTCCCCCGGTGCGCGGCTCGGTGGTTGAACGGGGC	480
AF298116	643	TGCGGCAGCGCGGCAGCAAGGCGGCGGACGCGTGCCTCCGAGGCGGAGCTGCAGCA	702
Ptf1a-pIRES -EGFP	481	 TGCGGCAGCGCGGCAGCAAGGCGGCGGACGCGTGCCTCCGAGGCGGAGCTGCAGCA	540
AF298116	703	GCTGCGACAAGCCGCTAATGTGCGAGAGCGGCGCGCATGCAGTCCATCAACGACGCCCT	762
Ptf1a-pIRES -EGFP	541	 GCTGCGACAAGCCGCTAATGTGCGAGAGCGGCGCGCATGCAGTCCATCAACGACGCCCT	600
AF298116	763	CGAGGGGCTGCGTTTCGCACATCCCCACGCTACCCTACGAAAAGCGCCTCTCCAAAGTAGA	822
Ptf1a-pIRES -EGFP	601	 CGAGGGGCTGCGTTTCGCACATCCCCACGCTACCCTACGAAAAGCGCCTCTCCAAAGTAGA	660
AF298116	823	CACGCTGCGCTTGGCCATAGGCTACATTAACCTCCTCAGCGAGCTGGTGAAGCCGACCT	882
Ptf1a-pIRES -EGFP	661	 CACGCTGCGCTTGGCCATAGGCTACATTAACCTCCTCAGCGAGCTGGTGAAGCCGACCT	720
AF298116	883	GCCGCTGCGCGGAGTGGCGAGGTGGTTGCGGGGCCAGGTGGCAGCCGGCACCTCGG	942
Ptf1a-pIRES -EGFP	721	 GCCGCTGCGCGGAGTGGCGAGGTGGTTGCGGGGCCAGGTGGCAGCCGGCACCTCGG	780
AF298116	943	AGAGGACAGTCCCGGTAACCAGGCCAGAGGTTATCATCTGCCATCGAGGCACCCGTTT	1001
Ptf1a-pIRES -EGFP	781	 AGAGGACAGTCCCGGTAACCAGGCCAGAGGTTATCATCTGCCATCGAGGCACCCGTTT	840
AF298116	1002	CACCCTCCCCAGTGACCCGGATTATGGTCTCCCTCCTTTCAGGGCACTCTCTTTCCT	1061
Ptf1a-pIRES -EGFP	841	 CACCCTCCCCAGTGACCCGGATTATGGTCTCCCTCCTTTCAGGGCACTCTCTTTCCT	900
AF298116	1062	GGACTGATGAAAAACAGCTCAAAGAACAAAATATCATCCGTACAGCTAAAGTGTGGACCC	1121
Ptf1a-pIRES -EGFP	901	 GGACTGATGAAAAACAGCTCAAAGAACAAAATATCATCCGTACAGCTAAAGTGTGGACCC	959

The arrow marks the start codon.

8 Acknowledgements

I would like to thank Prof. Martyn Goulding for his encouragement, constant support and the opportunity to work on such an interesting project. It is a real pleasure to work for him. I am very thankful to have had the chance to experience such a wonderful research environment with him as my supervisor at the Salk Institute. Thanks for everything!

I am especially indebted to Prof. Michael Kessel for being my supervisor, for establishing the contact with Martyn and his constant support.

I am also very thankful to Prof. Sigrid Hoyer-Fender for taking over the Korreferat and for always being so helpful whenever I had a question.

Special thanks go to Guillermo Lanuza, for all our discussions, his great advice about my project and his friendship.

A big thanks goes to Rumiko Mizuguchi, who was such a wonderful collaborator in the lab.

I would also like to thank the rest of Goulding lab for providing such a great working atmosphere, for helping me whenever I needed help and for being good friends. Especially, I would like to thank here Andrea Pillai, Eric Geiman and Tommie Velasquez.

Furthermore, I would like to thank Rumiko Mizuguchi, Eric Geiman and Todd Kroll for their help with editing and proof reading my thesis.

Finally, I would like to thank Alex Sternin, Siobhan Caesar and Todd Kroll for the great times I had outside the lab.

Lebenslauf

Persönliche Daten:

Name: Sonja Kriks
Geburtsdatum: 16.01.1977
Geburtsort: Hameln
Nationalität: deutsch

Schulbildung:

1983-1987 Grundschule Sünteltal, Hameln
1987-1989 Orientierungstufe Nord, Hameln
1989-1996 Albert-Einstein-Gymnasium Hameln
Juli 1996 Abitur

Ausbildung:

1996-1998 Ausbildung als Biologisch-Technische-Assistentin an der Rheinischen Akademie, Köln

Studium:

1998-2002 Studium der Biologie (Diplom) an der Georg-August-Universität Göttingen
2002-2003 Diplomarbeit, Titel:
"Frühe Charakterisierung dorsaler Interneurone"
Salk Institute For Biological Studies, USA
Abteilung Molecular Neurobiology, Prof. Martyn Goulding
Juni 2003 Diplom
2003- Promotionsstudiengang Biologie an der Georg-August-Universität Göttingen
Thema:
"Function and interaction of homeodomain proteins during development of the spinal cord"

Labortätigkeiten:

- 1998-2001 Studentische Hilfskraft
Max-Planck-Institut für Experimentelle Medizin,
Göttingen
Abteilung Molekulare Neuroendokrinologie
- 07/2001 - 08/2001 Studentische Hilfskraft
Max-Planck-Institut für Biophysikalische Chemie,
Göttingen
Abteilung Molekulare Zellbiologie

Publikationen:

Kriks S, Lanuza GM, Mizuguchi R, Nakafuku M, Goulding M. Gsh2 is required for the repression of Ngn1 and specification of dorsal interneuron fate in the spinal cord. (2005) *Development*, 132, 2991-3002.

Mizuguchi R*, **Kriks S***, Cordes R, Gossler A, Ma Q, Goulding M. Ascl1 and Gsh1/2 control inhibitory and excitatory cell fate in spinal sensory interneurons. (2006) *Nat Neurosci*, 9, 770-8. (***Joint-Erstautor**)